UNIVERSITAT POLITÈCNICA DE CATALUNYA
BARCELONATECH
Escola Superior d'Enginyeries Industrial,
Aeroespacial i Audiovisual de Terrassa

Ph.D. in Electronic Engineering

Development of textile capacitive sensor

Doctoral thesis by
Marc Martínez Estrada

Supervised by
Dr. Raúl Fernández García
Dr. Ignacio Gil Galí

Barcelona, November 2022

Acknowledgement

Me gustaría agradecer primero a mi tutor Prof. Raúl Fernández García por todo su apoyo y ayuda a lo largo de esta Tesis. Agradezco todas las explicaciones en detalle y conversaciones sobre teoría fundamental de la Electrónica, así como sobre el mundo académico e investigador. Gracias a él, creo que tengo más claro querer luchar por continuar mi aventura en la universidad como profesor e investigador, aun con todas las dificultades que eso conlleva.

También agradecer a mi co-tutor Prof. Ignacio Gil por todo su apoyo durante estos años de trabajo. Sus conocimientos de simulación electromagnética fueron de gran ayuda al inicio de la tesis y sus críticas constructivas me han ayudado a mejorar mucho en todos los aspectos. En concreto, a la hora de revisar los artículos publicados.

Agradecer al país en el que vivo, y que, gracias a mi esfuerzo, me ha permitido estudiar desde que empecé la universidad y hasta el día de hoy por todas las becas recibidas que han permitido a una persona como yo, llegar a día de hoy aquí.

Por nuestro laboratorio, han pasado varias personas durante estos 4 años, pero no puedo agradecer lo suficiente a Chengyang y a Mariam por todas esas horas de trabajo compartido, por esas charlas y discusiones, que nos han llevado a conseguir resultados maravillosos durante estos años. Pero no solo se ha quedado ahí, sino que me llevo dos grandes amigos para toda la vida.

Durante todo mi periodo universitario, fueron muchos los profesores que me han inspirado, pero si hay alguien de quien no me puedo olvidar es de la Prof. Nuria Salan. Ella es la que me provoco el amor que siento por los materiales y su aplicación y, en parte, tiene culpa de que hoy esté trabajando en este campo. Además, puedo decir que ha sido casi mi *madre* en la universidad por todo lo que me ha aportado y ayudado en lo personal. Le doy las gracias, aunque ello signifique que siempre esté en deuda con ella y me haga participar en muchos de sus planes.

Saliendo del mundo académico, puedo decir que he llegado aquí gracias a mis padres y mi familia. Durante toda la vida me han empujado a esforzarme y luchar por lo que quería. Ellos lo han dado todo por mí, aun cuando menos

teníamos, he sentido que lo tenía todo. Hoy no puedo más que sentirme orgulloso de poder devolverles de esta forma todo lo que me han aportado.

A mi novia Andrea, que apareció durante la ejecución de la tesis. Ella ha estado siempre apoyándome y dándome calma. Me ha incitado a seguir luchando y esforzarme por lo que quería. A día de hoy se ha ganado ser una de las personas más importantes de mi vida, y que me ha visto en momentos críticos y aun así ha sabido qué decirme.

Agradecer a todos y cada uno de mis amigos que han estado ahí y que me han escuchado en esos días más duros de la tesis. Especialmente, a Víctor L. ese chico que conocí la primera semana de universidad, cuando acababa de llegar a Barcelona y estaba solo. Él ha estado ahí siempre, me acompaño los días más duros de esta etapa y también en los mejores. Espero tenerle siempre en mi vida.

Pero si hay algún amigo al que le tengo que agradecer su apoyo es a Dani T. Él me acompaña desde que éramos unos niños y no se ha cansado nunca de recordarme lo que confía en mí y que sabe que haré algo grande. Si alguien ha estado siempre ahí, en los mejores pero sobretodo en los peores, que hemos vivido unos cuantos, ha sido él. Amigo, compañero de piso y de aventuras, espero que sigamos juntos durante muchos años, aunque te canse.

A todas estas personas, y al resto que no he podido añadir en estas líneas. Gracias de corazón.

Summary

Nowadays, the textile clothing industry is searching for new ways to add value to their products. Developments in textile sensors start to demonstrate their usability and possibilities when they are integrated on fabrics. The Internet of Things context pushes the companies to find new ways to obtain information from our surroundings to be able to actively react, in real-time, to the situation we are living in. For many years, the integration of sensors in textile has been regarded as inconvenient. The users do not feel comfortable to use it since the textile properties are modified.

In recent years, advancement in technology and integration of conductive materials into textile materials have provided that the researchers new opportunities to integrate sensors on fabrics. Conductive yarns produced following the textile processes results in a family of yarns which are soft, flexible and conductive. The conductive material is unnoticeable by sight which is very important for the final user feeling. These conductive yarns are being used to develop conductive fabrics or patterns that do not give the feeling of being a sensor or electrically conductive. The sensors play an important role to make our daily life more comfortable and easy. But due to their certain features, conventional sensors may not be a good fit for the applications in some fields. Textile sensors rise as a new alternative tool to address the shortcomings of the conventional sensors. Textile capacitive sensors could provide a new tool to introduce sensors in fields where it could not be done previously. The advantages of the textile capacitive sensors are flexibility, long area coverage and proximity to the measured stimulus.

The thesis is focused on the textile capacitive sensor development. The conductive materials, the effect of the materials on the sensor behaviour and the textile integration methods are covered over the course of the thesis. The textile capacitive sensor is based on the permittivity change detection, which could be either the substrate permittivity or the surroundings environment. Textile capacitive sensors are relevant because their flexibility is suitable for many daily tasks monitoring, some of them related to patients or dependent people.

The results obtained in this thesis extend the state of the art for the textile capacitive sensors. The produced textile sensors and applications

developed support the viability of the suggested technology.

En la actualidad, la industria de la moda está buscando nuevas formas de añadir valor a sus productos. El desarrollo en los sensores textiles integrados en los tejidos, empieza a demostrar su utilidad y posibilidades. El contexto actual de Internet de las cosas (IoT), está provocando que las compañías busquen nuevas formas de obtener información de nuestro alrededor, para así, poder reaccionar activamente, en tiempo real, a las situaciones que estamos viviendo. Durante años, la integración de sensores textiles ha sido rechazada, sobre todo por los posibles usuarios. Estos no se sentían cómodos usando tejidos con sensores integrados, debido a la modificación que estos provocaban en las propiedades de los mismos.

En los últimos años, los avances en los procesos tecnológicos y la integración de materiales conductores en los materiales textiles han provisto a los investigadores de nuevas oportunidades para poder integrar sensores en los tejidos. Los hilos conductores producidos mediante técnicas textiles resultan ser unos hilos suaves, flexibles y conductores. El material conductor pasa a ser indetectable visualmente, lo cual es muy importante para las sensaciones del usuario final. Estos hilos conductores son usados para desarrollar tejidos o patrones conductores que no dan la sensación de ser sensores o conductores de la electricidad. Los sensores juegan un papel muy importante a la hora de hacer nuestra vida diaria más fácil y cómoda. Pero, debido a una serie de características, los sensores convencionales no pueden ser usados en ciertas aplicaciones. Los sensores textiles aparecen como alternativa viable para responder a desventajas que pueden tener los sensores convencionales a la hora de ser integrados. Los sensores textiles pueden llegar a ser una opción para introducir sensores en nuevas aplicaciones, antes inexploradas. Las ventajas que aportan los sensores textiles son su flexibilidad, cobertura de un área amplia y la proximidad al estímulo medido.

La tesis se centra en el desarrollo de sensores textiles. Los materiales conductores, el efecto de los materiales en el comportamiento del sensor y los procesos de integración serán estudiados durante esta tesis. El sensor textil capacitivo se basa en la variación de la permitividad, la cual puede ser provocada por un cambio en dicha propiedad en el tejido o en las cercanías del sensor. El sensor textil capacitivo, gracias a su flexibilidad, podría llegar a ser relevante en aplicaciones de monitoreo diario, algunas de ellas relacionadas con personas dependientes o pacientes en hospitales.

Los resultados obtenidos a lo largo de esta tesis extienden el estado del arte de los sensores textiles capacitivos. Los sensores textiles producidos y las aplicaciones desarrolladas respaldan la viabilidad de la tecnología presentada.

Contents

List of Figures

List of Tables

Publications included in this thesis

Journal publications

- Martinez-Estrada, M., Moradi, B., Fernández-Garcia, R., & Gil, I. (2018). Impact of manufacturing variability and washing on embroidery textile sensors. Sensors (Switzerland), 18(11), 3824. https://doi.org/10.3390/s18113824

- Martínez-Estrada, M., Moradi, B., Fernández-Garcia, R., & Gil, I. (2019). Impact of conductive yarns on an embroidery textile moisture sensor. Sensors (Switzerland), 19(5), 1–10. https://doi.org/10.3390/s19051004

- Martínez-Estrada, M., Fernández-García, R., & Gil, I. (2021). Experimental analysis of fabric substrate on a moisture sensor. Journal of the Textile Institute, 112(6), 881–886. https://doi.org/10.1080/00405000.2020.1783781

- Marc, M. E., Ignacio, G., & Raul, F. G. (2021). A Smart Textile System to Detect Urine Leakage. IEEE Sensors Journal, 21(23), 26234–26242. https://doi.org/10.1109/JSEN.2021.3080824

- Martínez-Estrada, M., Ventura, H., Gil, I., & Fernández-García, R. (2022). A Full Textile Capacitive Woven Sensor. Advanced Materials Technologies, 2200284. https://doi.org/10.1002/ADMT.202200284

- Martínez-Estrada, Marc, Vuohijoki. Tiina, Poberznik. Anja, Shaikh. Asif, Virkki. Johanna, Gil. Ignacio, and Fernández-García. Raúl. (2022). A smart chair to monitor sitting posture by capacitive textile sensors. IEEE Sensors Journal **Submitted**

Conferences

- Martinez-Estrada, M., Moradi, B., Fernández-Garcia, R., & Gil, I. (2018). Embroidery Textile Moisture Sensor. Proceedings 2018, Vol. 2, Page 1057, 2(13), 1057. https://doi.org/10.3390/proceedings2131057
- Martinez-Estrada, M., Fernandez-Garcia, R., & Gil, I. (2020). A wearable system to detect urine leakage based on a textile sensor. FLEPS 2020 - IEEE International Conference on Flexible and Printable Sensors and Systems. https://doi.org/10.1109/FLEPS49123.2020.9239554
- Martínez-Estrada, Marc; Ventura, Heura; Gil, Ignacio; Fernández-García, R. (2022). Experimental abrasion analysis of textile capacitive sensor. 21st World Textile Conference, 1–4. https://doi.org/10.34658/9878366741751

Other publications of the author related but not included in this thesis

- Moradi, B., Martinez-Estrada, M., Fernandez-Garcia, R., & Gil, I. (2018). Wearable ring resonator antenna. Physica Status Solidi A. Applications and Materials Science (Print Edition), 215(23), 1800140–1800141. https://doi.org/10.1002/pssa.201800410

- Moradi, B., Martinez-Estrada, M., Fernandez-Garcia, R., & Gil, I. (2019). Study of double ring resonator embroidered wearable antennas for microwave applications. European Conference on Antennas and Propagation, 1. http://hdl.handle.net/2117/190210

- El Bakkali, M., Martinez-Estrada, M., Fernandez-Garcia, R., Gil, I., & El Mrabet, O. (2020). Effect of bending on a textile UHF-RFID tag antenna. European Conference on Antennas and Propagation, 1. https://doi.org/10.23919/EuCAP48036.2020.9135331

- El Gharbi, M., Martinez-Estrada, M., Fernandez-Garcia, R., Ahyoud, S., & Gil, I. (2020). A novel ultra-wide band wearable antenna under different bending conditions for electronic-textile applications. Journal of the Textile Institute, 1–7. https://doi.org/10.1080/00405000.2020.1762326

- El Gharbi, M., Martinez-Estrada, M., Fernandez-Garcia, R., & Gil, I. (2021). Determination of salinity and sugar concentration by means of a circular-ring monopole textile antenna-based sensor. IEEE Sensors Journal, 21(21), 23751–23760. https://doi.org/10.1109/JSEN.2021.3112777

- Martinez-Estrada, M., Gil, I., & Fernandez-Garcia, R. (2021). An alternative method to develop embroidery textile strain sensors. Textiles, 1(3), 504–512. https://doi.org/10.3390/textiles1030026

- Martinez-Estrada, M., Fernández-Garcia, R., Gil, I. (2019). Sensor resistivo de elongación (Patent No. P201930793).

Preface

The initial research on how to integrate conductive lines or devices into textiles were performed over the last decade of the 20th century. From then to now, the interest in smart textiles has been growing. Companies and researchers have been working around it with the objective of obtaining new textiles with added value and new functionalities. Although, smart textiles cover a wide variety of applications and utilities, nowadays textile sensors are one of the most valuable fields. The integration of sensor into the normal clothing provide new opportunities to monitor the environment around us and use the information acquired to act *smart* in our daily life. Society is taking a new paradigm where knowledge is the most added value that a product could have. Researchers are looking into the integration and development of textile sensors to substitute common electronic devices applied into wearable devices to improve the quality of the data, to reduce the impact for the user or to find new applications where conventional electronic devices could not be used. Textile sensor has many applications in diverse fields such as healthcare sensing, motion sensing, chemical sensing, physical sensing, environmental sensing, force sensing, etc.

This thesis aims to develop, analyse and test the performance of the textile capacitive sensors in detail. Even though, there are textile capacitive sensors developed in the literature, the present thesis intends to demonstrate how the capacitive textile sensors could be integrated using only textile methods providing solutions beyond the state of the art. It will be demonstrated how the textile industry is prepared to start producing textile sensors using the materials proposed, such as conductive yarns, produced by textile techniques and the machinery available. Different methodologies of integration are going to be analysed and how the sensor behaviour is affected by the materials used. With the methodology studied, textile sensor applications will be analysed to approve their workability and functionality. It is important to emphasise some characteristics that are essential for the development of the textile capacitive sensor such as flexibility, total integration over the textile, soft touch-feeling and resistant. The performance of developed textile capacitive sensors has been tested for two parameters humidity and presence detection, which are most widely demanded and used

applications of the textile sensors.

During the thesis, an international collaboration with the Intelligent Clothing Research Group from Tampere University (Finland) was carried out. The international collaboration consisted of a 3 months stay where a project was conducted between the thesis' author and researchers from Tampere University. A smart chair was developed and manufactured by the integration of the textile capacitive sensors presented during the thesis. As a result of this international collaboration with the Tampere University our research outcome is shared with scientific community with an internationally recognised paper.

This Ph.D. thesis is organised by following the guidelines according to the format **Compendium of articles**, meaning that the results presented along the document have been already published in international JCR journals and conference proceedings. The list of published Journal articles and conference proceedings over the course of thesis completion are recapped in Section **Publications included in this thesis**.

The thesis content is divided in 4 parts:

- Part 1 contains the Chapter 1 where review of the working principle of the capacitive sensors as well as most common integration methods are presented. Additionally, an analysis of most common structures is performed and comparative study on the capacitive textile sensors found in literature are conducted.

- Part 2 is the Methodology Section, which is formed by chapters from 2 to 6, where the steps that the capacitive textile sensor should have got over before starting the manufacturing process are exposed. The materials selection, geometry simulation and theoretical model are analysed to determine the desired characteristics of the sensor. In addition, the methodology to characterise the materials, sensor production and the behaviour of the sensor produced is explained in detail.

- Part 3 or Results Section contains the chapters from 7 to 10. Chapter 7 presents the Spice model of the sensor designed by the author. This model is used to find an adjustment of the interdigital capacitance value of the structure. Chapter 8 shows the capacitive textile sensor produced by means of embroidery technology. Along this chapter different tests are performed to demonstrate its workability. Furthermore, different materials for the conductive threads and textile substrates are used. The response of the sensor against humidity is analysed. The Chapter 9 contains the results of the capacitive textile sensor integrated by woven technology, which permits to introduce the conductive yarns and produce the sensor into the structure of the woven fabric. Measurement methods used previously, explained in Chapter 4, are revised due to the complexity of the circuits. To conclude

the section, Chapter 10 presents the applications developed during the thesis. The applications developed could be divided into two groups: humidity sensing and presence sensing.

- Finally, Part 4 contains the Chapter 11, where the main conclusions and results reported during the document are summed up. Some future work activities aligned with current research outcomes from this thesis work are proposed.

The work conducted during the realisation of this thesis, from 2018 to 2022, was carried out with in the group RFLEX (Radio Frequency Identification and Flexible Electronics), which is part of the Electronic Engineering department of the Universitat Politecnica de Catalunya (Campus de Terrasa). RFLEX is also associated with the INTEXTER (Instituto de Investigación Textil y Cooperación Industrial de Terrassa). The aim of the RFLEX group is to research, study and develop electronic wearables integrated into textiles. TThe research team recognised as a consolidated group by Catalan Government (AGAUR) focuses on both antennas and sensors research.

This work has been funded by the Catalan and Spanish governments through different projects and grants. We would like to highlight the following projects that permit the group to develop its research activities:

- Project TEC2016-79465-R by the Spanish Government. Title:*Integración electrónica en sustratos textiles para el desarrollo de tejidos inteligentes.*
- Project PID2021-124288OB-I00 by the Spanish Government. Title:*Sensores textiles para aplicaciones sanitarias*

Furthermore, this Ph.D. thesis has been supported by a predoctoral fellowship (2020-FI-B-00028) from the *Agència de Gestió d'Ajuts Universitaris i de Recerca* (AGAUR), by *Terrassa Universitària* Terrassa's Council and by the UPC Electronic Engineering Department.

Part I

Introduction

1

State of the art of textile capacitive sensors technology

This chapter provides a brief introduction to smart textiles so that the readers will be familiar with the basic concepts. Specifically, current state of art in capacitive textile sensors, and its working principles and various design approaches will be presented. Particularly, the capacitive textile sensors take the main role, which will be studied analysing the actual state of the technology, the working principle and design possibilities available.

1.1 Introduction

Nowadays, *textile sensors* is one of the smart textile areas that gather more research attention. These efforts have been motivated by the fabric surface availability where a sensor could provide additional functionality. Society is building up around the idea of a connected world or Internet of Things (IoT). Data collected in real-time is desired to obtain knowledge about the environment that surrounds us and textile sensors could be the key to acquire it.

Textile sensors implemented in the clothing industry or home clothing could provide the tool to obtain the desired data. As fabric covers the greater part of our body or home, the available surface to install the sensors

is unlimited. The requirement which the textile sensors need to accomplish is being unobtrusive. Touch-feeling is the most important drawback at the beginning of the technology and new processes permit to accomplish the touch requirement with a higher grade of integration. If the full integration is completed, the fabric will be perceived as enriched textile, avoiding the perception change of the fabric.

1.2 Capacitive sensors

A sensor is a device that receives a stimulus and responds with an electrical signal. The stimulus is referring to a physical phenomena which could be light intensity, heat, sound, force, moisture, pressure, distance, motion, chemical composition, among others. The sensor output is an electrical signal readable by the human which can be channelled, amplified and modified by human-made[1]. The case study focuses on the capacitive sensors, which corresponds to a type of sensors that produce the transformation from a physical phenomena to an electrical signal by means of the capacitance property.

Here are some of the main characteristics of the sensor as following;

- Sensitivity: The sensitivity of the sensors is defined as the slope of the output characteristic curve, or generally, the relation between the physical stimulus and the electrical signal.
- Stability: Referred to the degree to which sensor characteristics remain constant over the time.
- Accuracy: Property that mark the ability to provide a response close to the real value of the stimulus.
- Response time: Time needed for the sensor to respond to the stimulus.
- Hysteresis: Defined as a deviation of the sensor's response at a specified point of the stimulus when it is approached from the opposite direction, which referred to the design direction of work.
- Operating life: Lifetime of the sensor working.
- Stimulus range (span): Range of values from the physical phenomena that the sensor can respond with an output signal.
- Resolution: The smallest amount of a stimulus that can be sensed.
- Linearity: Deviation of the sensor response from a specified straight line. It can be found also as linearity error or non-linearity.

- Repeatability: Property that means the ability of the sensor to reproduce the same response as other of the same production set under identical conditions.

1.2.1 Working principle

Before getting into the working principle of the capacitive sensors, lets for introduce the basics of the capacitance concept. The capacitance is the ratio of electric charge stored (q) to a difference in electric potential (V) between two charged objects, defined in equation below.

$$C = \frac{q}{V} \tag{1.1}$$

The fixed ratio, C is called *capacitance*. Explained with a flat plates capacitor scheme in mind, which is shown in Figure 1.1, the capacitance value depends on the size of area and the spacing between the plates.

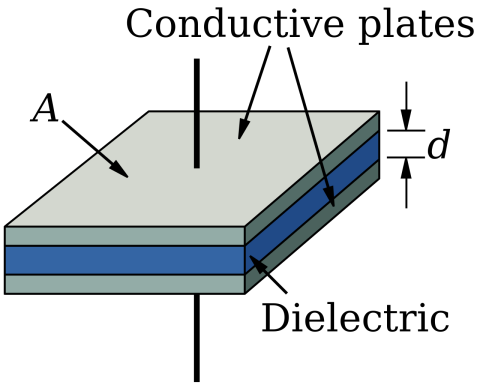

Figure 1.1: Two parallel plate capacitor scheme.

The capacitance of a flat capacitor can be found from:

$$C = \epsilon_0 \frac{A}{d} \tag{1.2}$$

Where A is the area of the flat plates and d the distance between them. The permittivity of the dielectric between the plates (air case) is represented by ϵ_0.

The working principle relies on the modification of the characteristics of the capacitive property by an external stimulus. Capacitive sensor's sensing ability depends on the geometry of the charged objects, the distance between charged elements and dielectric permittivity.

In this thesis, a capacitive sensor based on the permittivity change is chosen. The geometry and the distance between the shape chosen for the charged objects are maintained constant. To represent this fact, the capacitance of the sensor can be expressed by:

$$C = \epsilon_0 \kappa G \tag{1.3}$$

Where G is the geometric constant, ϵ_0 is the permittivity associated with the air and κ is the permittivity of the dielectric material between the geometrical shapes [1]. For instance, the capacitive sensors presented along this thesis react to every stimulus which produces an alteration in the dielectric constant that affects the capacitance.

Usually, the dependence between the stimulus and the permittivity alteration is not perfectly linear, but this can be attended by utilising some signal processing algorithms as well as mathematical algorithms.

1.3 Textile capacitive sensors

A textile capacitive sensor is defined as a capacitive sensor which has been implemented on a textile substrate with materials produced following the textile processes. It can be easy to confuse the textile capacitive sensor concept and identify a conventional electronic sensor attached to a fabric as it. But it is important to highlight that to acquire the textile sensor designation all the sensor components has to be implemented with textile materials and techniques. In addition, textile sensors resulted from this transformation should keep its initial characteristics almost unaltered.

Textile sensors are thought as an alternative to substitute conventional electronic sensor to take advantage of the textile characteristics. E.g. textile sensors could cover longer areas for lower prices, with respect to conventional electronic sensors that usually require multiple sensor deployment. This example is one of the wide variety of characteristics that could be used to make the most of some applications. Some relevant characteristics are flexibility, thickness, low profile, comfortable, low weight, technologies available to produce or to lower costs (due to the scalability of the processes).

The production process of the textile sensors determines the degree of integration achieved by the textile sensor. There are two technology options to build a textile sensor. One of the technologies can be defined as *Additive technology*, which is based on the addition of a material or substance to produce the textile sensor. Figure 1.2a shows an example of the integration classification. Embroidery technology, which is a well-known technology for the society, belongs to that group. The second technology refers to the processes where the sensors are built during the fabrication process of the textile. Figure 1.2b shows a structural integration sensor into a woven fabric. Woven technology is one example of this group. Different integration methods will be further explained in Section 1.4.

Textile capacitive sensors can be found in a wide variety of forms and structures. Most of the structures used in textile capacitive sensors are adaptations of the corresponding electronic sensors used in industry, Figure

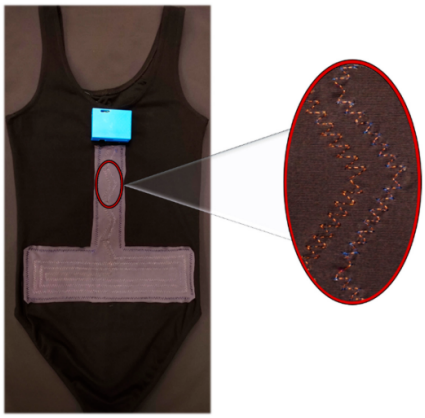

(a) Additive integration [2]

(b) Structural integration [3]

Figure 1.2: Classification of different integration methods

1.3 shows a textile version of a two plate capacitor. For force or pressure measurement, the most widely used structure to design the textile sensor is the two parallel plate capacitor. The structure is built by conductive textile or flexible material, which form the plates, with a dielectric material between them. But also, researchers work on different structures to answer to the application requirements. In depth explanation about structures is performed in section 1.5.

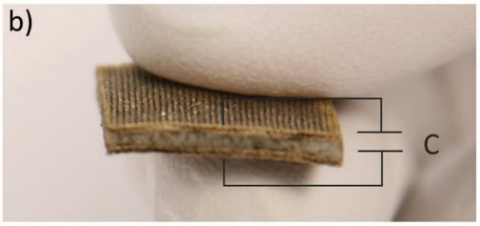

Figure 1.3: Textile 2 plates capacitor [4]

For textile capacitive sensors, independent of the structure used, there is always one surface which will make contact with the substance or the object to measure. Depending on the application, it is wanted, to have full contact between the sensor and the object/substance, partial or none contact, appearing a dielectric material between sensor and object/substance to measure. The situation is determined by the stimulus to measure and the aim of the data collected.

In the initial state of smart textile technologies, the conventional electronic components were installed over the textile and connected between them by conductive lines or cables. Nowadays, technological developments allow the researchers to focus on the integration of sensors directly on the

textiles by conductive yarns or materials. But, it is still necessary to connect them to PCBs.

1.4 Integration method

Parts of the characteristics of a textile sensor are consequence of the integration method used. The principal substrate should be a textile to be able to define a sensor as a textile sensor. During the process a conductive material is going to be integrated over or into any textile material that take part of the final fabric. As previously was mentioned, there are two groups of techniques to integrate a sensor in a fabric.

1.4.1 Additive technology

The additive technology was the first integration method used during the textile sensor research. At the beginning, some conventional electronic components were attached over the fabric and connected between them with conductive lines or yarns. An example of this can be observed in [5]. Two sensors made by a thin-film capacitor and a line-resistor are introduced between yarns during the woven process of the textile, which they can be seen in Figure 1.4.

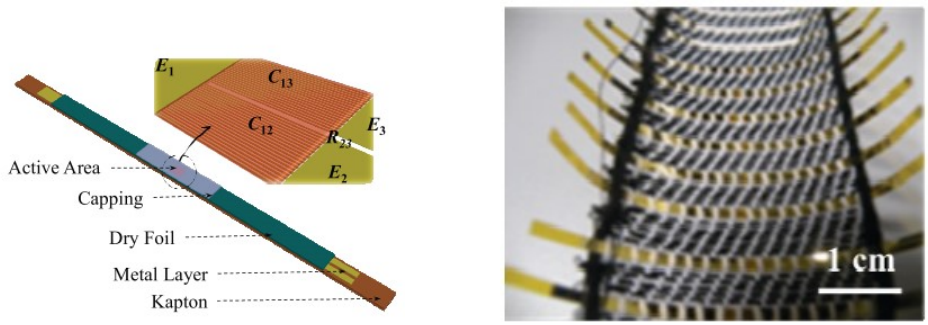

(a) Structure with both sensors integrated on a film

(b) Woven textile with several film integrated

Figure 1.4: Sensor film integrated into a woven textile [5]

At the present time additive technologies allow the sensor to be produced over the substrate with conductive materials. The natural textile additive technology is the embroidery method. This method consists in the disposition of an external yarn, which for a textile sensor should be a conductive yarn, in a substrate [6], the result can be observed in Figure 1.5. That external yarn joined to the substrate is considered part of the fabric from here on out. Embroidery touch feeling is also well-known by the society and is not a drawback to introduce sensors to daily clothes.

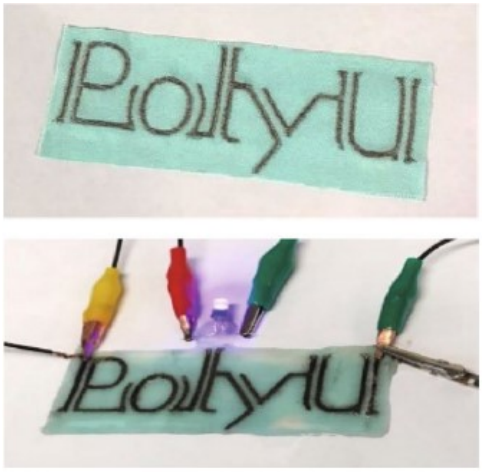

Figure 1.5: Embroidered sensor used as a circuit to light up a led[6]

The more innovative technologies involve deposition of conductive materials as conductive ink or coating textile materials with conductive materials. At an initial state, it was usual to produce yarns or textiles with a conductive coating, to be used in the production of these textile sensors. Furthermore, textile yarns with a conductive coating have been demonstrated as a good option to create textile sensor by embroidering or introducing the resulting yarns in the production process[7, 8]. An example of these references is shown in Figure 1.6.

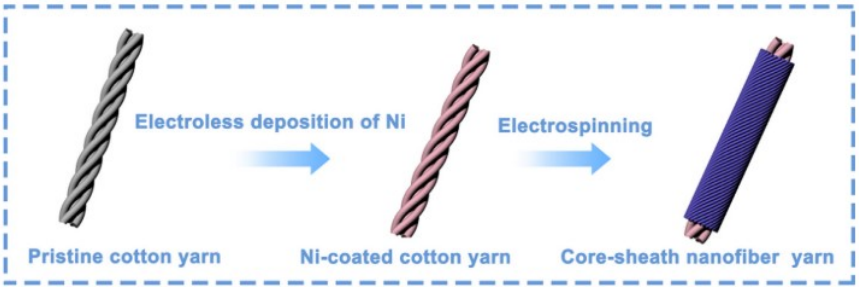

Figure 1.6: Conductive yarn produced by coating technique[7, 8]

Lastly, to produce textile sensors by printing with conductive ink over the textile substrate, two processes are observed. First, screen printing process was adapted to produce textile sensor. Screen printing technology is used by the textile industry to create clothes decorated with pictures or shapes. To create textile sensors, conductive ink is used during the process and the meshes used to dispose the ink as required are adapted to conductive ink requirements. As a result, conductive print is performed over textile substrate [9], results can be observed in Figure 1.7a. The second process, ink-

jet printing is a process well-known by electronic industry. It is considered as an adaptation of the fabrication process from the Printed Circuit Boards (PCB). In consequence, ink-jet printed structures over textile or flexible substrate are achieved [10]. Figure 1.7b shows the ink jet printed structures.

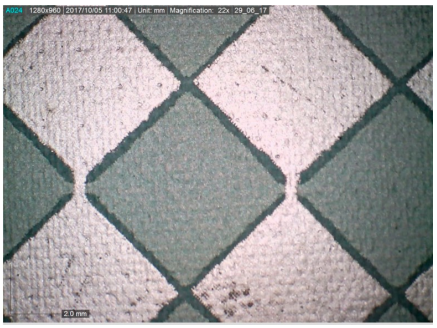

(a) Screen printing technology [9]

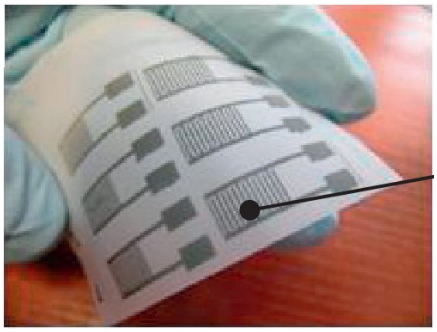

(b) Ink jet printing technology [10]

Figure 1.7: Sensors produced by the addition of conductive ink over a flexible substrate

1.4.2 Structural sensor

When the sensor is integrated or produced during the textile substrate manufacturing it can be referred as a fully integrated textile sensor. These sensors are integrated into the structure of the textile what makes them impossible to be separated from the substrate.

Usually, fully integrated textile sensors are manufactured with conductive yarns incorporated into woven or knitted technologies. During these processes, the structure of the sensor is constructed into the structure of the fabric. The development of the machinery needed in knitted and woven processes makes more viable the integration of these sensors. To produce a sensor with knitted process, one of the options is to introduce a conductive yarn following the knitted structure between the yarn loops[11], as it can be seen in Figure 1.8.

The woven process is more challenging when a sensor is constructed into the structure. Machinery used for large-scale productions could have limitations in the design of the sensor structure. For this reason, it is more convenient to use weaving machines controlled by a Jacquard, which is a system that allows to create unlimited weaving patterns. The jacquard system is an addition to a normal weaving loom, where every warp yarn position is controlled by a series of cables connected to a device situated over the weaving machine. Electrocardiogram(ECG) electrodes have been built in woven textiles and demonstrated their usability[3], the reference sample is presented in Figure 1.9. But for the moment, the sensor design

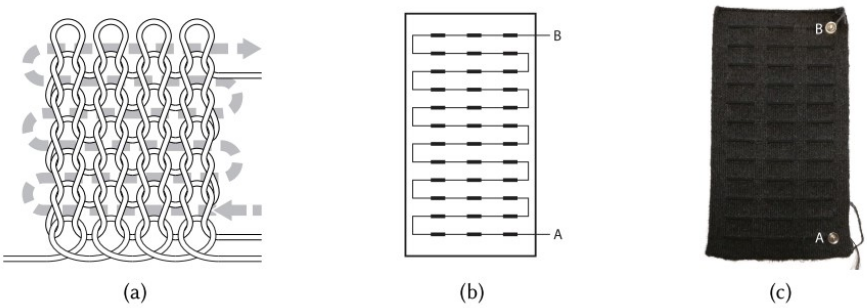

Figure 1.8: Scheme of a knitted sensor[11]

into woven structures are limited due to the technology development and cost of the machinery required.

Figure 1.9: ECG woven electrode[3]

1.5 Capacitor structure

The capacitor structure is an important factor for the stimulus which is desired to be measured. Capacitance textile sensors can be differentiated by two structure families: 3-D structures or 2-D structures.

3-D structures refer to the capacitor structures where the sensor is built in 3 dimensions. Size, width and height are important for the geometry of the sensor and the measurement method selected. The most representative structure is the 2 plate capacitor, which has been adapted to be built on textiles. The principle of the structure is maintained and these capacitors are built with 2 conductive plates or shapes, separated by a di-

electric material. This structure has many variations along the textile sensors production. Researchers have replicated that structure into the yarn structure [12] (Figure 1.10a), the textile structure [13] (Figure 1.10b) and also between yarns [14] (Figure 1.11a) or fabrics [4] (Figure 1.11b).

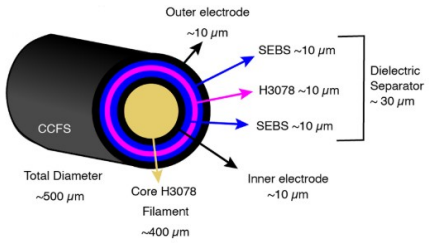

(a) Capacitor built in a yarn [12]

(b) Capacitor build in a textile [13]

Figure 1.10: Sensors produced by the addition of conductive ink over a flexible substrate

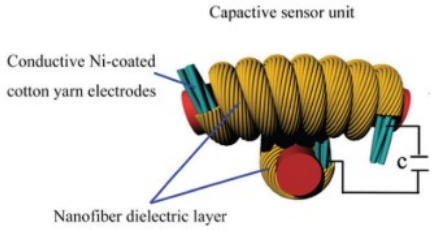

(a) Capacitor built between two yarns [14]

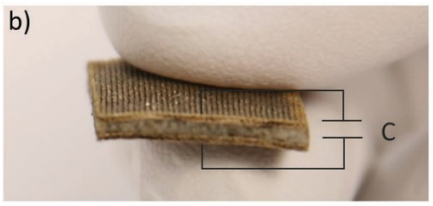

(b) Capacitor built between two fabrics [4]

Figure 1.11: Sensors produced by the addition of conductive ink over a flexible substrate

The plane structures or 2-D structures are built on textiles with conductive materials where the height of the geometry produced with conductive material is negligible. This group of sensors usually measures stimulus that alter the environment around the sensor. Some examples of these structures are the plane electrodes [15] and the interdigitated structures [16] presented in Figure 1.12.

1.5.1 Interdigital structure theory

Interdigital capacitance structure is worth to be mentioned specifically. This structure has been used for so long and studies of the behaviour and geometry can be found in the literature. Theoretically, the interdigital capacitance structure is expected to accomplish some requirements to follow the theoretical equations and model explained in [17]. Figure 1.13 shows the interdigital

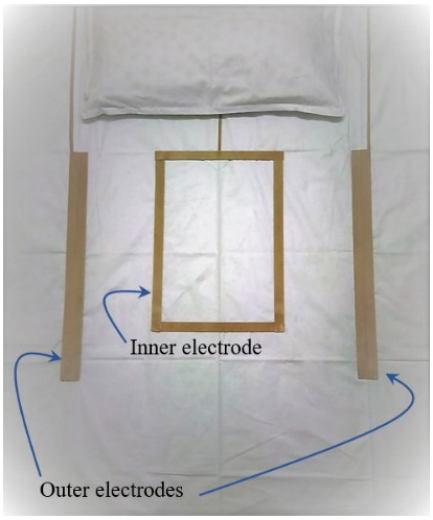

(a) Plane electrodes capacitor[15]

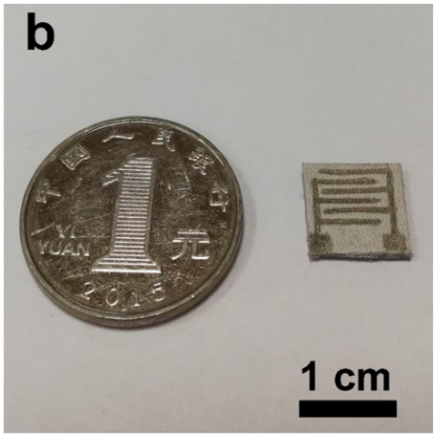

(b) Interdigital structure capacitor

Figure 1.12: 2-Dimensional capacitor[16]

structure model. It is formed by two electrodes, identified as input/output ports, from where fingers rise to almost reach the other electrode. These fingers are separated from the others by gaps with a dimension defined as G. The fingers have a thickness W and length L which are important for the capacitance of the structure.

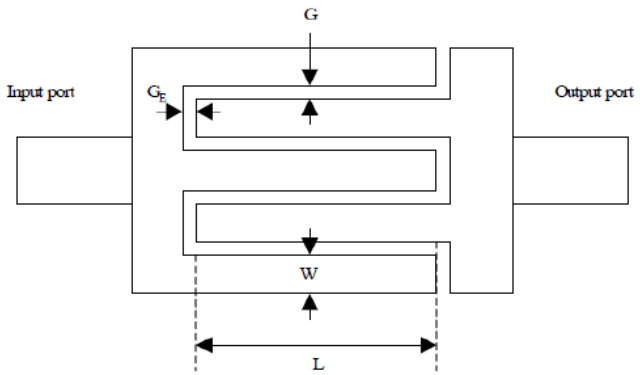

Figure 1.13: Interdigital structure referenced [17]

To be treated as a lumped element, the interdigital capacitor characteristic length should be relatively small to the circuit's operating wavelength. In this case, the interdigital structure is accompanied by a plane ground. Another hypothesis to take into account is the relation between the length of the fingers and the space between the fingers, which has to be relatively small regarding the length.

Once that conditions are fulfilled and the substrate is selected, the total capacitance of an interdigital structure is given by[17]:

$$C_{RH} = (\varepsilon_r + 1)l[(N-3)A_1 + A_2](pF) \tag{1.4}$$

$$A_1 = 4.409tanh[0.55\frac{h}{W}^{-0.45}]10^{-6}\,(\frac{pF}{\mu m}) \tag{1.5}$$

$$A_2 = 9.92tanh[0.52\frac{h}{W}^{-0.5}]10^{-6}\,(\frac{pF}{\mu m}) \tag{1.6}$$

Where:

$C_x = capacitance\ from\ textile\ sensor$
$\varepsilon_r = Permittivity\ of\ dielectric\ material$
$l = Length\ of\ fingers$
$N = Number\ of\ fingers$
$h = height\ of\ the\ substrate\ material$
$W = width\ of\ the\ conductor\ material$

A1 and A2 are necessary to represent the interior and exterior of the fingers along the interdigital capacitor structure. As it is observed in the Equation 1.4 gaps are not affecting the capacitance value of the structure due to the hypothesis done.

1.6 Textile capacitive sensor applications

Textile capacitive sensors have been applied in a wide variety of applications due to their adaptability. Along the years, and the development of the integration techniques exposed earlier in Section 1.4, the deployment of the textile sensors is growing in healthcare applications. The characteristics of the textile sensors which differentiates them from electronic based sensors, such as flexibility, lower impact and long area coverage, make them more suitable for healthcare and worth to develop. Applications could be divided depending on the working principle used to measure the external stimulus. However, some stimulus can be measured with more than once working principle. Therefore, each application is presented separately explaining the most relevant characteristics.

Strain capacitive textile sensor[4, 8, 12, 14, 16, 18–22] were the first textile sensors integrated over a textile substrate. Initially, they focus on the use of conductive elastic yarns where the strain suffered by the material could be measured by the variation of capacitance provoked by the geometric change. Also, conductive elastic textiles were produced after the development of the

textile manufacturing processes. Figure 1.14 shows an example of a textile strain sensor.

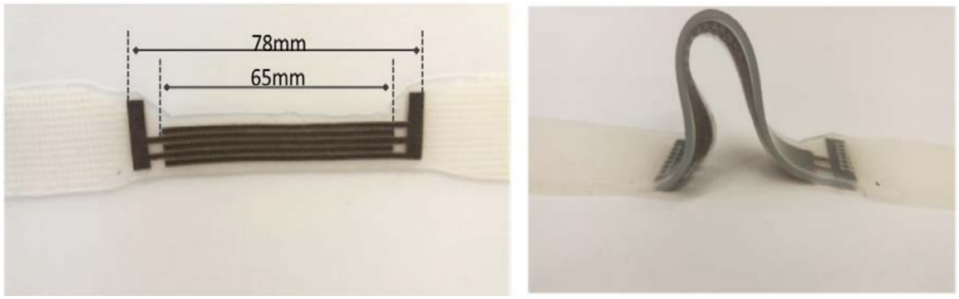

Figure 1.14: Interdigital soft-strain textile sensor[4]

Strain capacitance sensor demonstrated the functionality of conductive elastic material to measure strain in different applications. Developments are focused on the chemical research of new polymers which properties stand for more strain cycles.

Strain capacitance sensors are also used to measure angle[19, 23–25]. The objective is to be able to monitor the motion of joints, such as knee or fingers, to evaluate recovery times for injuries, which they are presented in Figure 1.15. In this work[19] it is demonstrated how the textile capacitive sensor presented could evaluate the angle that the finger joint takes.

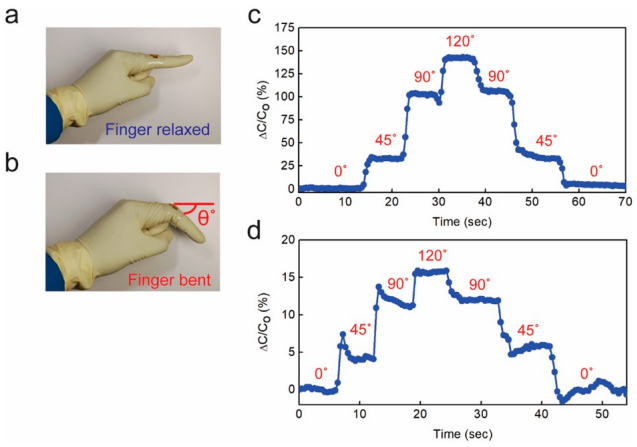

Figure 1.15: Strain sensor used to evaluate recovery from an injury[19]

Pressure capacitive sensors have been presented during the last years as one of the most promising textile sensors. The integration into textile substrates make possible to cover wider areas with a single sensor or to produce an array of sensors in the same area for similar cost. Pressures stimulus detection can be done by structural changes in the textile capacitor[4, 14,

21, 22, 26–32 or by the permittivity change of the dielectric material[13, 33, 34]. Detection of geometrical changes are commonly presented as two parallel plate capacitor disposition[31], Figure 1.16. In this work, a two parallel plate capacitor is produced with two conductive textiles, which are manufactured with conductive fibres, and a dielectric material separating them. The pressure is detected by the change of the distance between the conductive fabrics. Also is mentioned, that the sensor could measure the appearance of moisture or sweat by the variation of permittivity.

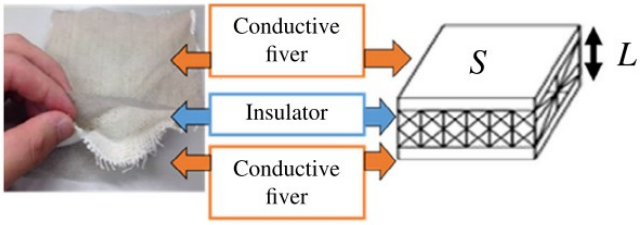

Figure 1.16: Pressure capacitive sensor[31]

An interesting particular application for the pressure/strain sensors is the integration of a textile sensor into the reinforcement of a composite to measure the deflection of the material piece[35], which is shown in Figure 1.17. Researchers explain that the integration of conventional electronic sensors into the composite structure have consequences for the structural properties. However, the integration of a textile capacitive sensor into the reinforcement does not affect the structural properties as well as permits to measure the forces applied to the sample piece.

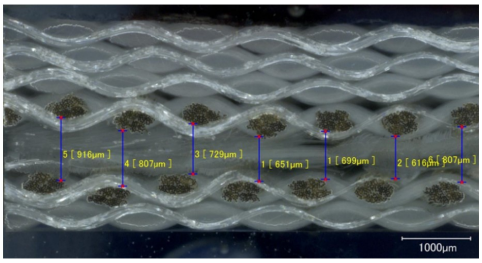

Figure 1.17: Textile sensor integrated into the reinforcement of a composite1.17

Another variety of pressure capacitive sensors, where the capacitance change is not only related with the distance change, but also permittivity change [33], is presented in Figure 1.18. In this work a two parallel capacitive textile sensor is presented. The remarkable characteristic is that the dielectric material between the fabrics is porous, which provides a better behaviour facing tensions and pressures along its lifecycle. This property

causes the permittivity variation when pressure is applied, because the difference of quantities of dielectric material and air between the fabrics.

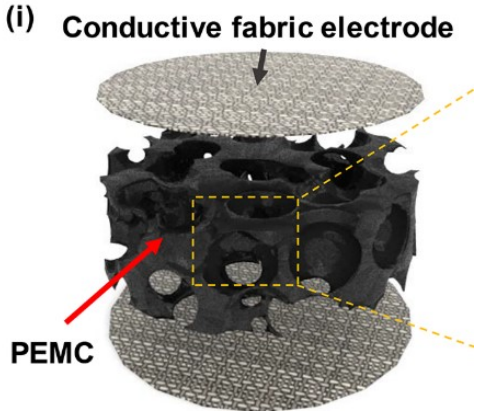

Figure 1.18: Textile capacitive sensor where the dielectric change in shape and properties[33]

Motion capacitive textile sensor[12, 14, 36–38] is a variant from strain, pressure and angle capacitive sensor. But motion sensors are focused on the correlation of that sensor information to more complex metrics related to the movement of the body. A perfect example of these motion sensor is presented in Figure 1.19. In [38], a motion sensor which is capable to measure the tension of the muscles and movement of the body joints as finger or elbow is presented. The researchers demonstrated the viability of e-skin design based on the textile presented and could be applied into robotics or prosthetics.

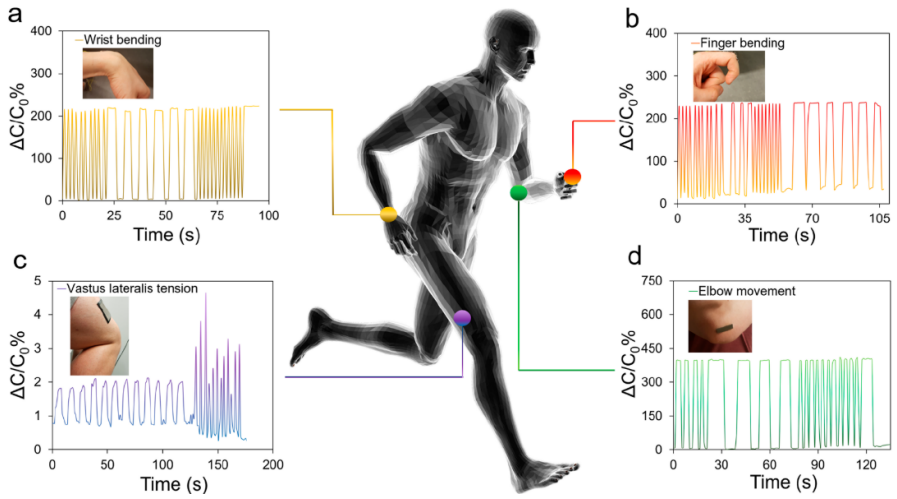

Figure 1.19: Different uses for the motion textile sensor. E-skin viability[38]

From here on out, the sensor presented measure stimulus which cause a dielectric permittivity change. The most important group of capacitive sensors measuring by means of permittivity change is the humidity sensors group. Textile capacitive humidity sensors are referred to the sensors that measure the quantity of water around them [5, 22, 39–43]. A textile humidity sensor can be built with two parallel conductive yarns introduced into a textile and measuring the capacitance between them, e. g. Figure 1.20 shows the capacitive sensor explained. In [43] is shown its workability, but the dependence of the measurement in two individual yarns is dangerous for the reliability of the sensor.

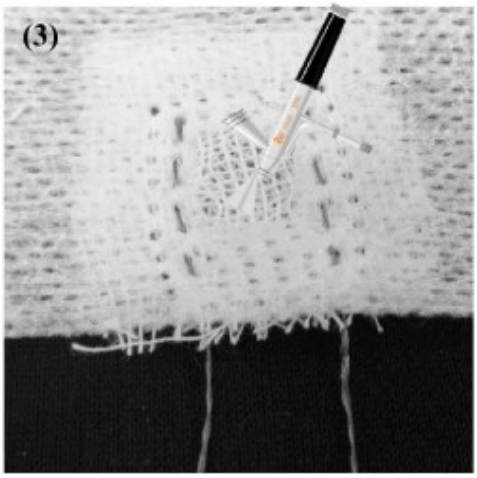

Figure 1.20: An humidity textile sensor produced by two conductive yarns[43]

A specific use for the humidity capacitance sensors is the breathing rate measurement [15, 23, 44]. The breath of a person contains multiple particles of liquid and other components which in contact with a textile capacitive sensor changes its permittivity[44]. In Figure 1.21 the sensor is presented. In this work, a textile capacitive sensor is used to control the breathing rate of a person into the mask. The data obtained by the sensor is enough to distinguish between apnea, normal breath and deep breath.

The next group of sensors is able to detect presence or touch by the contact or proximity of the human body that changes the permittivity around the sensor, modifying the capacitance[14, 27, 45, 46]. A finger approaching a capacitive textile sensor, produced by capacitive yarns, is detected with different levels of proximity [14]. The finger as its getting close to the capacitance formed by the crossed yarns, changes the permittivity around the capacitor. The closer you get, the more the more changes in permittivity. The working scheme is observed in Figure 1.22.

To conclude, textile capacitive sensors can be used as a chemical compo-

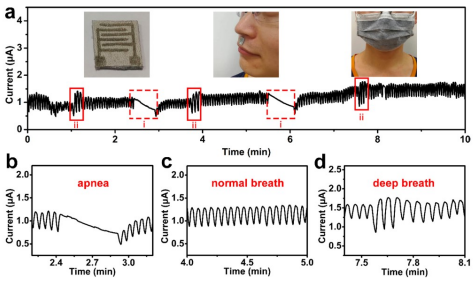

Figure 1.21: A textile capacitive sensor to control the breathing rate[44]

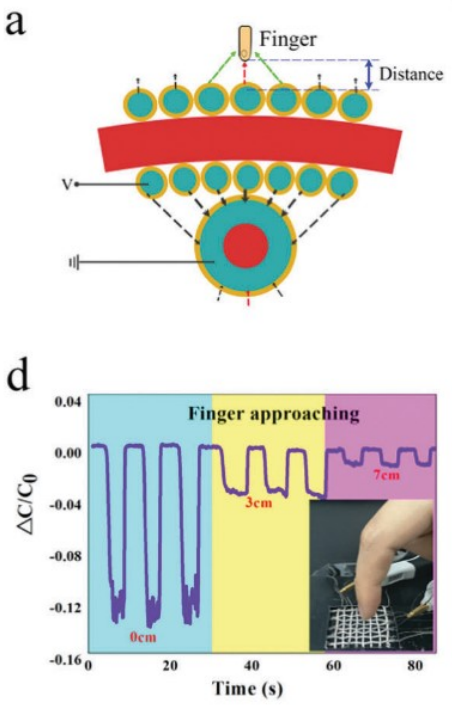

Figure 1.22: Proximity capacitive textile sensor[14]

sition sensors[5, 47, 48]. Blood classification, gas composition or sweat analysis are some examples of the applications that a textile capacitive sensor could carry out. Usually, these sensors are produced over flexible substrates, but the techniques used are compatible with textile sensor production. The textile chemical composition sensors share their structures with humidity textile sensors. To be able to distinguish the composition, the data processing should be further developed.

1.7 Reliability of textile capacitive sensors

During the process of definition of a product, one of the crucial steps to approve the product viability is the reliability validation. In addition, for textile capacitive sensors, it is an essential characteristic, which is used by every researcher to justify the substitution of an electronic sensor for a textile capacitive sensor. The researchers focus on the properties lost by textile capacitive sensors provoked by processes such as washing, corrosion or abrasion.

Washing reliability is the first research point that every textile sensor should pass before being applied in real world applications. The damage that washing could produce to textile capacitive sensor are physical and chemical. Conductive silver fibres used for the construction of Electrocardiography (ECG) electrodes are affected by washing cycles increasing their impedance[49]. In this work, a comparison between two electrodes shows that the electrodes which have covered the edges are less affected by the washing. The researchers support that after a certain number of flushes, the impedance remains relatively constant in the frequency range up to 5 kHz. Also, the impedance increase could be compensated by a calibration. A washing test performed over some piezoresistive sensors, which are produced with different conductive yarns composed of stainless steal fibres or copper fibres, [50] demonstrated that after each washing, for a total of ten cycles, the samples stitches of the sensor have no experienced damage and the sensors behaved similarly. Another work studied if the ECG electrodes are affected differently depending on the use of a washing net to keep them safe from the washing machine wall[51]. Results shown that the electrodes washed with net are being slightly affected by the washing under 50 cycles, compared to the electrodes without a net. The test finished when 150 cycles are performed, at this point it can be seen how the electrodes without net are affected double ($+720\Omega$) than the electrodes with net($+370\Omega$). Washing reliability is an important factor to evaluate if textile sensors could be used in our daily life. Reducing chemicals during washing, the number of washing cycles and the use of new conductive yarns produced by textile industry could reduce the impact of this process.

Corrosion reliability research is not taken into account as much as the importance it has. During washing cycles, corrosion appearance is expected. It was detected after 20 washing cycles by [49]. Further corrosion tests were performed by other researchers [52]. In this work, extensive corrosion tests were carried out to a silver coated synthetic textile and a cotton wool comprising silver wire. Immersions as described in DIN EN ISO 105-E04 and ISO 3160-2, as well as, artificial sweat during 4 hours, 24 hours and 7 days were done. The results evidenced that these materials did not suffer any considerable impedance changes after up to 7 days of immersion. The material chosen and the technique used to prepare the conductive textile

material take an important role in corrosion behaviour.

Lastly, abrasion reliability research point take importance when textile capacitive sensors are implemented in applications where long life cycles are expected. Textiles are exposed to abrasion in their normal use, which can be observed on clothes, upholstery and techniques fabrics. A sensor based on single-walled carbon nanotube (SWCNTs) and polyester/spandex fabric (PET/SP) was tested against abrasion degradation[53]. The results shown how the surface sensor kept intact after 30.000 cycles. In contrast, a comparison made between some textile sensor and garments conducted by the University of Otago, New Zeland[54] shown unacceptable abrasion effects where resistances on some conductive textiles increase after abrasion test between 60 to 100%. Abrasion reliability still has some disparity of results which are directly related to the process quality.

To sum up, to solve reliability problems and detect the technologies which reduce the impact of them are the key for textile capacitive sensor to take the leap to the society daily use. Research is important and still have much work to do. As society is leading towards IoT world where the sensors would be a big part of our life, textile sensors are expected to grow and develop to solve all the drawbacks that keep them out of the use. Plenty of applications could be benefited by the use of textile capacitive sensor such as reducing cost, decreasing the impact in the user, obtaining new applications, among others.

For that, the near future research will focus on the production technology adaptation to textile sensor integration and the exploration of application and new ways to deploy the textile sensor technology.

Part II

Methodology

2

Sensor structure

As it was previously discussed in Chapter 1, the geometry of the sensor and the working principle are the first parameters of the sensor which define its behaviour. There are wide variety of possible geometries, as it was previously discussed, but to design a textile capacitive sensor is desired that the sensor can be easy to integrate with different manufacturing methods. The idea is to demonstrate the flexibility of technology and provide a base to the industry, which is concerned to take a step forward and start to integrate textile sensor in their fabrics. For this reason, the interdigital structure has been chosen.

Interdigital structure is a well-known structure for electronic sensors. Also, interdigital structure permits to be integrated by more methods than others in the literature, as it is integrated in a plane surface as a 2-D structure. Other methodologies where a complex conductive yarn or two textile layers are needed, and this could be seen by the textile industry companies as a drawback due to the extra manufacture necessities. Extra necessities could result in redesigns of the production process, which companies are not willing to do them because of the cost associated with them.

Interdigital structure stands out over the other structures for being used as a humidity sensor[40], composition sensor(blood)[48] or gas sensor[55], but also for strain sensor[4] or building supercapacitors[56]. The versatility demonstrated by the structure provides enough reasons to choose the interdigital structure.

3

Textile materials

The objective of the thesis is to fully integrate a capacitive sensor into a textile substrate the materials used take important relevance along the work. Not only the fabric substrates are used, but also the conductive yarns are selected to produce the textile sensor.

The textile substrate chosen should satisfy certain requirements depending on the situations that are being used such as the substrates which are going to be embroidered, should have density enough to accept the sensor structure when is embroidered. Substrate materials will affect the initial capacitance value and the response value range of the sensor. This is provoked by their permittivity as a dielectric material and different behaviour against the environment, such as humidity. In order to provide wide range of possible applications, the substrate textile materials selected as options where cotton fabric, polyester fabric and mix cotton-polyester fabric. There is the possibility to find some textiles with low quantities of other materials mixed, but as the dielectric constants for every fabric are going to be measured, it is not relevant. Table 3.1 reflects the general properties of the substrates used throughout the thesis.

The second important material in the textile sensor production is the conductive yarn. Different types of conductive yarns are being used in this thesis work. Here, two of the most commonly used yarns in the textile market are chosen. The first kind of yarn is represented by a commercial Shieldex 117/17 dtex 2-ply, which is a polyamide multifilament yarn coated with pure silver 99%. The second type of yarn is commercial Bekaert yarns,

	Thickness (mm)	Weight(g/m^2)	Manufacture
Cotton (CO)	0,256	164	Woven
Med Cotton (MED)	0.306	197	Woven
Polyester (PES)	0.199	80	Woven
CO/PES	0,720	292	Woven/Knitted

Table 3.1: Substrate used to develop the textile capacitive sensor

which are produced by ring yarn method where conductive stainless steel fibres were mixed with cotton or polyester fibbers in different percentages. The following Table 3.2 describes their properties:

	Shieldex (PA-S)	Bekaert (PES-SS)	Bekaert (PES-SS)	Bekaert (CO-SS)
Conductor	-	40%wt	20%wt	20%wt
Density (tex)	11.7/2	20/2	20/2	20/2
Linear R(Ω/cm)	≤ 30	≤ 50	50-100	35-70
Type	Twisted multifil.	Ring yarn	Ring yarn	Ring yarn

Table 3.2: Properties for the yarns used to build the textile capacitive sensor

Some of the typical yarns used in our research are shown in Figure 3.1. The differences in aspect are noticeable. Shieldex yarn, which is made with a coating of silver, has a shiny colour. Meanwhile, Bekaert yarn aspect is similar to the common yarns used by the clothing industry.

(a) Shieldex coated yarn

(b) Bekaert ring yarns

Figure 3.1: Conductive yarns used

4

Simulation method

Simulation is required considering the necessity to obtain a viable model to foresee the static capacitance value for an interdigital structure. Also the possibility to simulate not only the conductive structure, but also the substrate material and its effects on the sensor behaviour. Simulation permits to set up every characteristic available for the textile capacitive sensor and expect a result as close as possible to reality.

But, first of all, the simulation method needs to be defined. As a platform to conduct the simulations, CST Studio is chosen. Over the course of this thesis, different version and release of CST Studio is used to conduct the simulations. The first simulations were performed with CST 2017, which version needs to be set up manually to obtain the impedance values. As the research progress, newer version of the CST is released and the CST was updated to CST 2020. With the newer version of the CST Studio, it became possible to obtain the impedance values directly without doing any other calculations. Lower Frequency solver mode in Frequency domain is chosen, which includes the electrostatic solver.

The parameters which CST studio required for the modelling of the sensor and to obtain the capacitance value for the interdigital sensor are:

- Geometric values; The structure should be defined completely in the simulation. Some parameters have high impact on the final results.
- Material composition; All the components of the sensor should be defined by their material.

- Material properties (conductive yarn or equivalent material and textile substrate); The essential properties are the permittivity of dielectric materials and conductivity of the line materials.

- Surround of the sensor during the measurement process.

The interdigital sensor structure can be modelled after all these requirements are defined. Figure 4.1 shows a snapshot of the simulated structure on CST Studio. The modelled structure has been designed by parametric values, so that it provides the flexibility to modify the structure easily. The potential terminals are defined in each pad of the interdigital sensor.

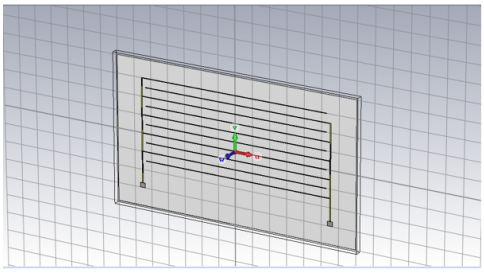

Figure 4.1: Snapshot of the simulated structure where their geometrical parameters are defined by variables

The Low Frequency Domain solver includes three different solver methods: magnetoquasistatic, electroquasistatic and fullwave. In this case, Electroquasistatic method is used to obtain the admittance matrix which contains the information needed to calculate the characteristic values for the simulated sensor. Figure 4.2 shows the admittance matrix obtained by CST Studio simulation.

```
Admittance Matrix (grounded) at frequency [       0.200 kHz](load system):

-----------------------------------------------------
Real part
=========

                   potential1        potential2

potential1        -1.055560e-09 S   -1.394819e-18 S
potential2        -1.394819e-18 S   -5.310588e-09 S


Imaginary part
==============

                   potential1        potential2

potential1         4.523308e-08 S   -1.671214e-08 S
potential2        -1.671214e-08 S    4.608633e-08 S
```

Figure 4.2: Admittance matrix obtained in CST Studio for 0.2 kHz

The capacitance can be calculated using the imaginary part of the admittance matrix, which can be defined as susceptance (B) found in *potential1-potential2* position in the imaginary part. The value is substituted in the equation:

$$C = \frac{B}{\omega} \tag{4.1}$$

Where ω is the angular frequency in radians/second. The capacitance value obtained from the CST Simulation using the susceptance value is shown in Figure 4.3.

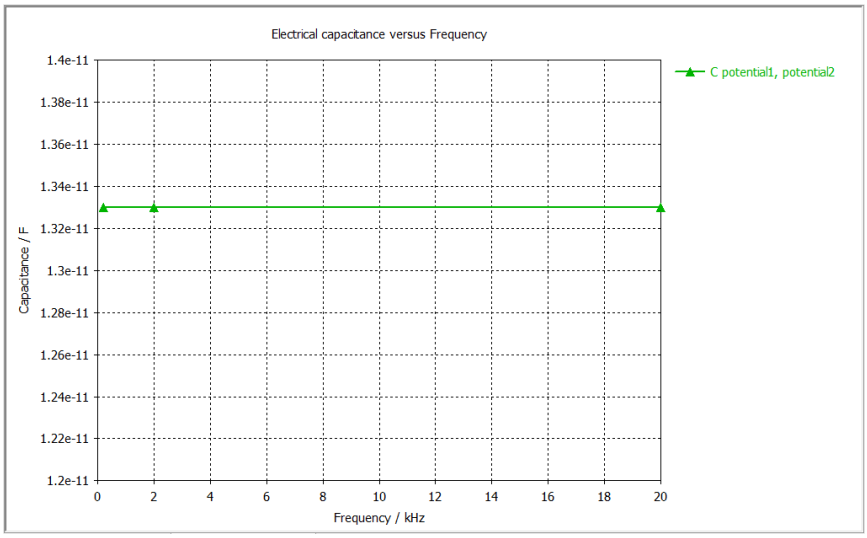

Figure 4.3: Capacitance value obtained from the CST Studio

As for Electroquasistatic result, CST Studio provides an unique capacitance value, which does not vary along the frequency range defined. If the capacitance value for a specific frequency is desired, the value has to be calculated by post-processing calculations.

5

Textile integration technology

5.1 Embroidering integration method

Embroidery is the craft technique used to decorate textiles performing drawings using a needle to apply yarns. This technique has been used for so long by people at home to craft by themselves decorations or other pattern in clothes. The embroidery machines have been developed, until nowadays that the market provides the opportunity to obtain more advanced machinery for personal use.

To embroider a complex structure, as the interdigital structure selected, where the geometry is decisive for the behaviour of the sensor, an embroidery machine controlled by a computer software is used. The machine used is a Singer Futura XL-550 (Singer Corporation, La Vergne, TN, USA), which is presented in Figure 5.1.

The first step to embroider a structure is the design preparation. In the present case, an interdigital structure was prepared to be embroidered, which was previously simulated. The structural layout has to be prepared for the Singer software to be read and send it to the embroidery machine. The simulated models (CST designs) are exported to a file format readable by the design embroidery software, which is called Easy Design EX4.0. It is important to maintain the size parameters in this step. The model file is imported by the embroidery design software and converted to a structure made

Figure 5.1: Embroidery machine Singer Futura XL-550

of stitches and yarn. The software permits the user to carefully adjust some textile properties for the embroidery structure such as the stitch pattern, the structural boundaries and yarn density. These parameters need to be adjusted carefully and taken into account because they are determining for the textile sensor behaviour, affecting the total resistance of the structure, the conductivity of the lines and the continuity of the line.

The stitch pattern selected for the interdigital structure is the satin fill mode, which provide an adjustable density of yarn for the structure and a continuous structure for the lines. An example of the satin stitch pattern is observed in Figure 5.2. The final embroidery design file is imported by the Singer communication software to the embroidery machine.

Figure 5.2: Textile capacitive sensor embroidered with satin stitch pattern with a 70% of pattern density.

The material preparation starts when the embroidery design is ready. At this point, the textile substrate is selected. It is important to select a textile substrate which density is medium or high. Low density textiles can be affected significantly by the embroidery process. The composition of the material could be selected depending on the application. This selection is studied and commented in the following sections. The yarn introduction in an embroidery process is performed from two sides. The upper yarn is the yarn introduced by the needle directly which comes from a reel disposed on the upper part of the machine. The bottom yarn, which is introduced from a bobbin disposed under the fabric, is trapped by the upper yarn.

The yarn introduction process is based on the movement of the needle. The needle moves through the textile with the upper yarn. When the upper yarn crosses the textile, the bottom yarn is introduced in the loop formed by the upper yarn, then the needle pulls the upper and bottom yarn creating a loop. This process is recognised as a single stitch, Figure 5.3 represents the movement, which replicated hundreds or thousands times results in the embroidery pattern. The yarns used during the process can be from different materials, but they must have similar linear density. For the textile capacitive sensor presented, the conductive yarn is introduced as the upper yarn, however, the bottom yarn used could be polyester or cotton common yarn.

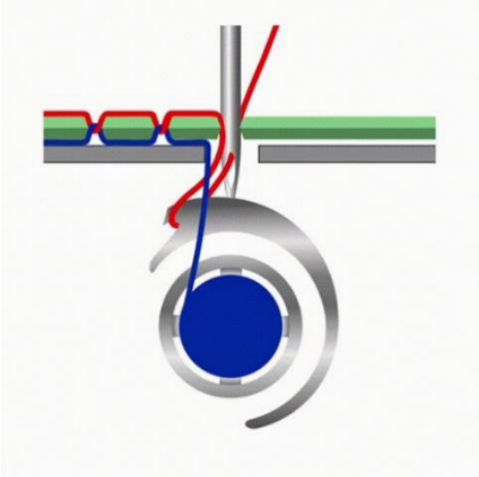

Figure 5.3: Embroidery scheme to explain the process. Red yarn represents the conductive yarn. Blue yarn could be a polyester or cotton yarn

The conductive yarns which are produced by a coating of a multifilament yarn need to be treated before the embroidery process. The yarn is coated also with a paraffin, which is lost during the process, to avoid the friction heat during the embroidery process which affects significantly to the yarn integrity.

Resulting from the embroidery manufacture process, a textile conductive embroidered sensor is obtained. The textile sensor should stand for a time, due to the static electricity remain as a consequence of the needle friction during the process. The static electricity effect could be observed during the measurements after the production.

5.2 Weaving integration method

The weaving process is the method used to manufacture a fabric through a sequential introduction of a horizontal yarn (weft yarn) between vertical yarns (warp yarns) that come from a beam. Warp beam is used to be prepared with 2000-6000 yarns disposed in parallel by groups. The process to place this amount of yarns has a high cost and the machinery used is specific. For this reason, there are a few companies that produce the warp beams and the great part of woven textile producers bought it.

To configure the structure of the final fabric, the warp yarns are moved up or down by a Jacquard system corresponding to the position required for the weave. Consecutively for each Jacquard position, a weft yarn is inserted between the warp yarns, causing the link between both when the Jacquard system changes the disposition of the warp yarns. After hundreds or thousands of movements as the one described, a woven fabric is produced. The weft yarns were prepared in a yarn rack and connected to one of the six introduction yarn systems that our weaving machine have. As it can be observed, Figure 5.4 shows the weaving process scheme.

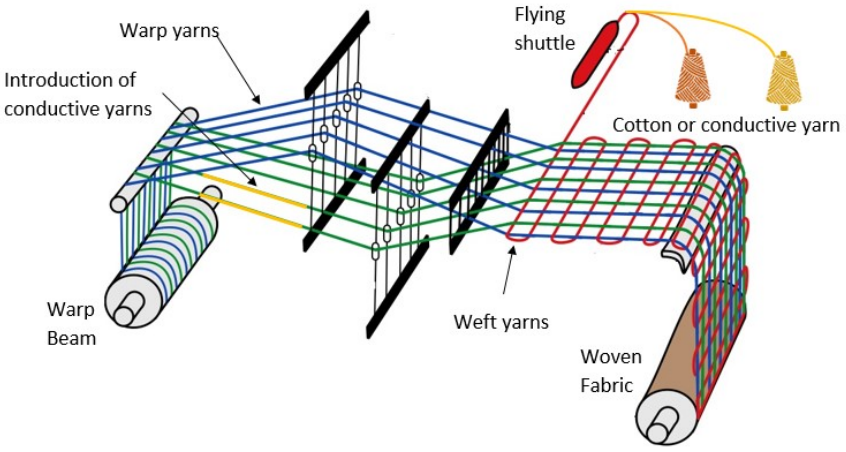

Figure 5.4: Weave process scheme

The method of the introduction of the weft yarn varies depending on the specific technology. In Figure 5.4, it can be observed as a flying shuttle,

which is a hand-made system. In the case of the Dornier LWV8/J weaving machine, an insertion by air pressure is used, the weaving machine moved by a Jacquard Staubli LX1600B can be observed in Figure 5.5.

Figure 5.5: Dornier LWV8/J weaving machine moved by a Jacquard Stäubli LX1600B

To weave the sensor, the conductive yarns should be introduced on the warp and weft. Preparing a new warp beam is unfeasible due to the cost and the machinery need. But manually, the process could be set up to overcome the situation. The warp yarns could be partially substituted by hand for conductive yarns for the length of the produced sensor. The process to substitute each yarn consists in cutting the initial yarn, which is in the beam, and knot a portion of conductive yarn between these both ends of yarn left which is represented as yellow yarns in the figure. This process is repeated for each yarn that needs to be conducted during the capacitance woven sensor production.

The resulting fabric from the process counts with 40 yarns cm-1 in warp direction, 26 yarns cm-1 in weft direction and a mass per surface of 292 g m-2.

It is important to highlight that a textile with a sensor integrated in its structure is obtained as a result of the methodology. This case, as it was explained during Section 1.4, is different from the embroidery methodology. The textile sensor integrated in the structure of the textile makes it undetectable by the touch and sight, if the colour of the conductive yarns are similar to the rest forming the fabric. These characteristics open a wide variety of applications where the user should not be conscious about the sensor.

6

Characterisation of the sensor properties

6.1 Permittivity characterisation of the substrates

Material permittivity is measured by a Microwave Frequency Q-Meter[**QWED**], as shown in Figure 6.1. The textile substrate is measured at room temperature. As the permittivity value in textiles is related also with the humidity trap on the material it would be studied and presented in the following section. To calculate the permittivity is necessary to provide to the Q-Meter software the thickness of the textiles. The thickness is measured by an Electronics Outside Micrometer (132-01-040A).

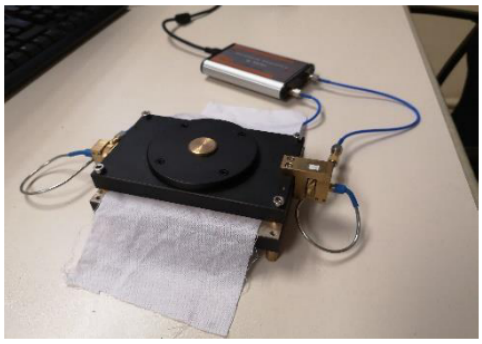

Figure 6.1: Microwave Frequency Q-Meter

The Q-Meter software provides the permittivity and the loss tangent of the material introduced.

6.2 Retained moisture measurement

The ability to retain moisture by the substrate is important to understand the sensor behaviour, due to the permittivity of the substrates are affected by the humidity. Every substrate ability to retain humidity needs to be analysed.

To perform the test a Humidity analyser MOC-63U is used, it is presented in Figure 6.2 This test consists in the introduction of a substrate sample into a chamber. The first step is to measure the weight of the sample at the starting point. Then, the environment is heated to 100^{o}C for a specific time. The weight of the sample is measured after applying temperature for this time to observe the difference from the initial point which is related directly to the quantity of water particles that the substrate trapped.

Figure 6.2: Humidity analyser MOC-63U

The value obtained is calculated by the difference in weight before and after the process, in percentage of weight. The higher is the value obtained, the higher capacity to retain water the substrate has.

6.3 Impedance measurement

To characterise the electric parameter of the textile capacitive sensor, a Rohde & Schwarz HM8118 LCR meter (Rohde & Schwarz, Munich, Germany) is used. The impedance module and phase are measured[57]. Figure 6.3 shows the image of the LCR meter used.

Figure 6.3: Image of the Rohde & Schwarz HM8118 LCR meter used

When a test object is connected, the impedance module and the corresponding phase angle, which corresponds to the phase between current and voltage, are determined. As this measurement values are frequency dependant, they are determined by means of an AC test signal of 1V. The accuracy is determined by the measurement range and the frequency. In the case of study the error is equal to 0.1% of the measurement and can reach values of 0.5% in frequencies which are higher than 100kHz. The LCR meter provides the possibility to obtain the capacitance, inductance and resistance values of the equivalent circuits, which can be series or parallel. These parameters are calculated internally from the impedance module and phase values.

Concerning the procedure follow for the connection of the sensor to the Rohde & Schwarz HM8118 LCR meter:

- First, the probes are connected in short circuit position to calibrate the LCR meter. The value observed during the connection is taken into account for the decision of calibrating.
- The probes are connected to the side electrodes of the interdigital sensor
- The sensor is maintained stretched to avoid movements during the measurement
- The values of impedance modulus and phase are observed on the LCR meter screen. By the switches, the frequency and the equivalent circuit can be selected to display the desired data.

The measurement of the LCR meter provides additional information regarding the structure. The LCR meter detects the equivalent circuit of the textile sensor, which should be a parallel circuit. In case that the LCR

meter detects that the sensor behaves as a series circuit, it would indicate that there is some shortcut on the structure.

At the moment that all the steps are followed and the sensor values are checked, the frequency swept measurements are collected by a LabView program and stored in an Excel file.

6.4 Capacitive measurement

The capacitance measurement could make us focus more on the permittivity change, and push aside the resistance component. This fact permits the user to not worry by parameters that do not affect directly the capacitance, as the temperature, when the sensor is working.

Two ways were opened during the research and define the different methods to obtain the capacitance value. The methods are distinguished depending the electric circuit used: alternate current (AC) or direct current (DC).

6.4.1 LCR Meter capacitance measurement

The first measurements of the capacitance value were obtained by the LCR Meter. The capacitance value is obtained in AC. As it was previously mentioned, the capacitance value of a sample is obtained by the LCR Meter using the impedance module and phase to calculate it, hence it is not measured directly.

As the capacitance value was obtained in AC, it means that is not going to match with electrostatic simulation or the spice model. To solve the miss-match, different methods to obtain the capacitance value in DC were prepared.

6.4.2 Charge-Discharge method

The first of the methods used to obtain the capacitive value in DC is the charge discharge method. This method consists in the connection of the capacitor to a DC circuit. The circuit prepared have a resistor (R) connected in series to the capacitor, between the power source and the capacitor. The current charges the capacitor in a specific amount of time. This time is measured and used to evaluate the capacitor value.

Figure 6.4 shows the set up prepared for the charge discharge method. The oscilloscope is connected to the power supply (grey cables) and to the capacitor connections (blue cables). Both signals are displayed in the oscilloscope screen which permit to evaluate the time that the capacitor spends until it arrives to the 63% of the Voltage.

The time of charge at 63% of the Voltage is called time constant (τ) which can be used to obtain the capacitive value of the sensor (C) by the following equation:

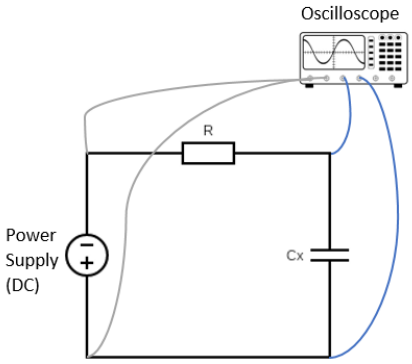

Figure 6.4: Set up for the charge discharge method

$$\tau = RC \tag{6.1}$$

Cycle count method

Using a similar DC circuit, a variant of the charge-discharge method is prepared. The cycle count methodology changes the point of view of the value associated with the sensor. The capacitance of the sensor is not obtained as in previous methods.

The method is defined as a *cycle count method* because the value obtained by the method corresponds to the number of cycles that a microcontroller needs to charge the capacitor. Two ports from a microcontroller are used. Send pin is the port where the voltage is set. Meanwhile, receive pin is the port where the voltage is measured. The cycle count example circuit is shown in Figure 6.5.

Both pins are connected with a resistor between them. The resistor value defines the resolution of the method, which is related with the amount of current going through the resistor. The capacitive sensor is connected to the receive pin, in order to be charged. The charged state of the capacitor is reached when in both pins, send pin and receive pin, the voltage is equal.

6.5 Humidity measurement process

The textile capacitive sensor behaviour against humidity is characterised to determine the possible applications where it can perform. To study the behaviour of the sensor a relative humidity test was designed to observe how the textile sensor responds to permittivity changes. These changes could be based on the textile substrate or the environment around it. Humidity test

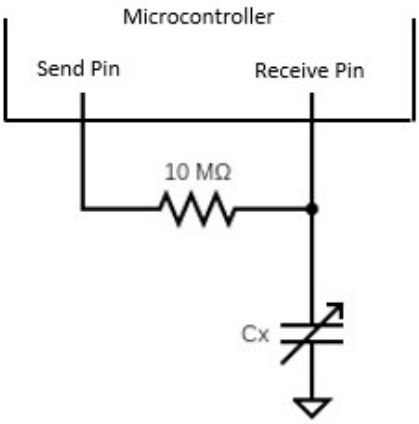

Figure 6.5: Measurement circuit for the cycle count method

was selected because its simplicity to reproduce the conditions and the wide variety of applications related directly with it.

To prepare the conditions to carry out a humidity test a CCK-25/48 Dycometal climatic chamber (Dycomental Equipos S.L., Viladecans, Spain) is used, it is shown in Figure 6.6. The climatic chamber allows to control the relative humidity and the temperature inside the chamber. The humidity control accuracy permits to select a percentage of relative humidity between 5% and 98%, meanwhile, the temperature can be set up between 5ºC and 90ºC.

Figure 6.6: Picture of the CCK-25/48 Dycometal climatic chamber used

The first group of sensors studied in the climatic chamber experiment a swept in relative humidity between 25% to 65%. The temperature is fixed during the test. The relative humidity value is increased by 5% point each step and it waits until its stable. Then the relative humidity is maintained for 5 minutes. At this point, the values for impedance module and phase

are taken.

Resulting from consecutively relative humidity swept test decisions are made. The most important decision taken is to increase the relative humidity range to cover more options. The final setup for the relative humidity test covers from 30% to 90% of relative humidity. Another decision made is to fix the temperature of the test at 20ºC, due to the low impact of the temperature on the results.

6.6 Washing process

The reliability of the textile sensor is an important characteristic of the final application, the washability of the textile sensor is tested. In order to analyse the impact of being washed, the electrical impedance of the textile sensor is measured after every washing cycle. The washing process is performed following the UNE-EN ISO 6330:2012. The regulations to perform a washing process are carefully explained in order to obtain decisive results. The soap used is a neutral ECE-Color Detergent ISO 105-C06 soap (Testgewebe Gmbh, Brüggen, Germany), which accomplishes every requirement needed. This kind of soap is used to avoid introducing more variables to the test, because it does not have any additional chemical such as softening. Another decision is taken following the regulation aforementioned is the machine selection. A Balay T5609 (BSH Electrodomesticos, Zaragoza, Spain) washing machine is used to perform the test, which was configured at 1000 rpm and 40ºC of temperature.

The sensors were introduced into a washing net to protect them. Additionally, 1kg of support fabric is used to simulate the inner conditions of a washing cycle. For the soap, a 1% by weight of clothes is introduced to perform the washing cycle.

6.7 Presence test procedure

The textile capacitive sensor presence behaviour is assessed. The presence is a stimulus which could be detected by the permittivity change on the surrounds of the textile capacitive sensor which makes viable to be able to measure with the textile sensor presented.

A first test to observe the behaviour of the textile capacitive sensor, when a person is over it, is designed. The idea is to test the reaction of the sensor at the moment when the person enters in contact with the surface of the textile. The test consists in a stand-up sitting cycle. The person sits down on the chair during 10 seconds, afterwards the person stands up and remains in that position 10 seconds. The cycle is repeated 4 times. The capacitance values of the sensor are taken continuously.

Additionally, the textile capacitive sensor behaviour when an object is placed over it, is studied. The textile capacitive sensor is tested disposing a bag over it with different weights. The object test repeats the cycle of the person, placing the object over the sensor for 10 seconds and retiring it for 10 seconds. The cycle is also repeated 4 times.

As the working principle of the sensor relies on the permittivity change produced by the surrounds of the sensor, the possibility to distinguish between a person and an object could give and added value to the technology.

6.8 Martindale test

The Martindale test consists on the abrasion of the textile sample to test against a normalised abrasive fabric. Figure 6.7 shows the Martindale machine. The aim of the Martindale test is to observe the behaviour of the fabric to the abrasion that could suffer during its lifetime. The regulation that has to be followed during the test is presented in UNE-EN ISO 12947.

The force applied during the movement of the abrasive fabric is determined by the fabric family. In the case of study, it is determined that the fabric corresponds to the upholstery fabric family. Then, the weight that should be applied for these fabric is 795±7g.

Figure 6.7: Martindale machine performing a test

The movement performed during the Martindale test by the abrasive fabric follows a Lissajous curve pattern. The test finishes when more than three yarns of the sample break or, for the woven capacitive sensors, if the electrical continuity is lost (i.e. resistance lower than 50Ω). The electrical conductivity is evaluated with a Multimeter Tenma 88 72-7730A after each Martindale evaluation step. Table 6.1 presents the different steps of the

Martindale test.

Interval (nº cycles)	**Martindale evaluation step (nº cycles)**
1.000-6.000	1.000
6.000-20.000	2.000
20.000-50.000	5.000
+50.000	10.000

Table 6.1: Frequency of Martindale evaluations steps

Part III

Results

7

Interdigital spice model

The interdigital structure presented in Section 1.5.1 has been modelled following the requirements that permit to fix some parameters, such as the space between the fingers. The model presented in [17] is not suitable for this work. It is due to the use of a ground plane and the hypothesis that the distance between fingers is always small enough to not be counted.

The interdigital structure used along the thesis is presented in Figure 7.1, where the parameters which define the behaviour of the structure are presented. The parameters which define the geometry are height(H), length(L), distance between fingers(d), distance between electrode and finger end(c), finger thickness(e) and number of fingers (n).

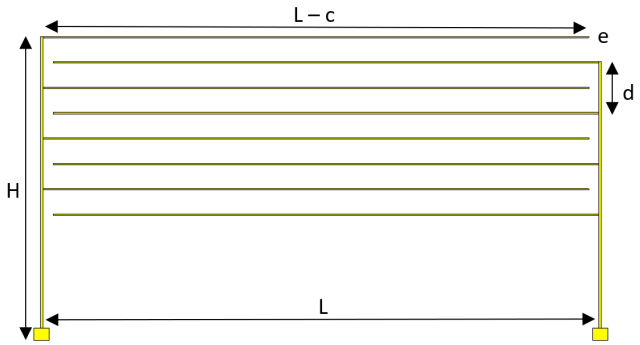

Figure 7.1: Interdigital structure with parameters depicted

A spice model for the interdigital structure presented is studied to predict the real value of the capacitive textile sensor. The simplified model will make the assumption that the total capacitance of the interdigital capacitance sensor is the summation of individual capacitances present between the fingers. However, the structure also contains a resistive component which is associated with the conductive material and the substrate. Figure 7.2 presents the equivalent impedances present along the structure.

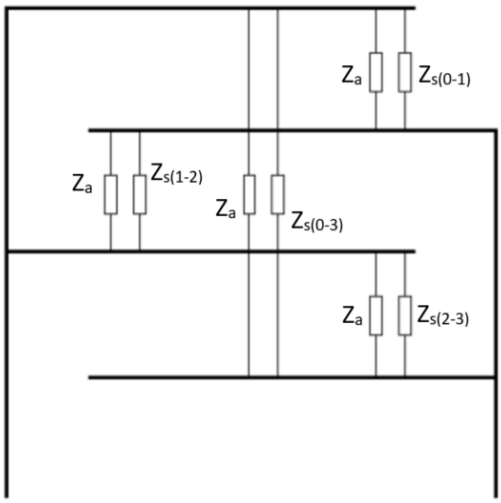

Figure 7.2: Spice model represented in a simple interdigital structure

Z_a refers to the equivalent impedance when the air is seen as the dielectric material of the structure and Z_s refers to the equivalent impedance when the substrate is treated as the dielectric material. The subscripts define the fingers which take part in the calculus from 0 to n-1, where n is the total number of fingers. The finger's end capacitance against the electrode is neglected because is relatively small to the rest of capacitances. The equations that describe the spice model, taken into account all the fingers are:

$$C_s = \sum_{k=0}^{k=n-1} C_{k,k+1} + \sum_{k=0}^{k=n-3} C_{k,k+3} \ldots + \sum_{k=0}^{k=n-x} C_{k,k+x} \tag{7.1}$$

$$C_a = \sum_{k=0}^{k=n-1} C_{k,k+1} + \sum_{k=0}^{k=n-3} C_{k,k+3} \ldots + \sum_{k=0}^{k=n-x} C_{k,k+x} \tag{7.2}$$

$$C_{spicemodel} = C_s + C_a \tag{7.3}$$

Where x is the total number of fingers minus one. The spice model takes into account important parameters of the interdigital structure as the distance between the fingers and air capacitances, which is not taken into account by theoretical interdigital models. As a result, the value predicts closely the capacitance value of the interdigital structure. The comparison of the spice model with the measured value is shown in Sections 8.2 and 9.2.

8

Embroidered capacitive textile sensor

8.1 Introduction

Chapter 8 presents a textile capacitive sensor produced by embroidery technique. The interdigital structure explained along the Sections 1.5 and 1.5.1 has been embroidered over a textile substrate. Considering the possibilities of application of the textile capacitive sensors, different materials for the substrate and the conductive yarns have been used. The sensor has been tested under humidity conditions to observe the behaviour of the sensor when a stimulus interacts with the sensor surface altering the dielectric constant of the surface. Finally, it is also presented the manufacturing variability which has been considered as one of the challenges of the smart textile production, specifically for textile sensor.

8.2 Comparison between spice model, EM model and measured model

In this section, a comparison between spice model, electromagnetic (EM) capacitance and textile sensor capacitance measured has been carried out along the project.

The interdigital structure embroidered and its geometry are presented in Figure 8.1

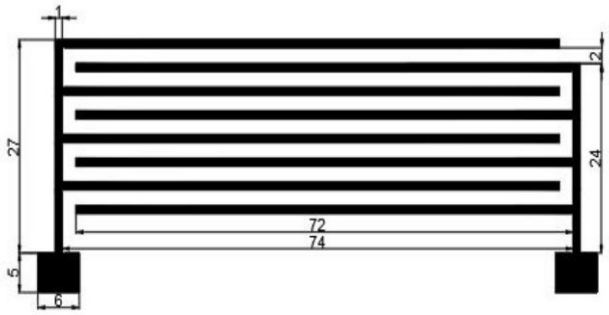

Figure 8.1: Interdigital structure with parameters depicted (in mm)

At the first moment, the textile capacitance value was measured by the LCR meter, which provides the measurement in AC. The nature of the capacitance value obtained did not permit us to compare with the electrostatic value (DC) obtained by the simulation. To obtain a measurement in DC of the textile capacitive sensor, a charge discharge measurement was carried out and the curve of charging was captured. The method used was previously explained in Section 6.4.2. The response of charging the textile capacitive sensor was captured and it is shown in Figure 8.2.

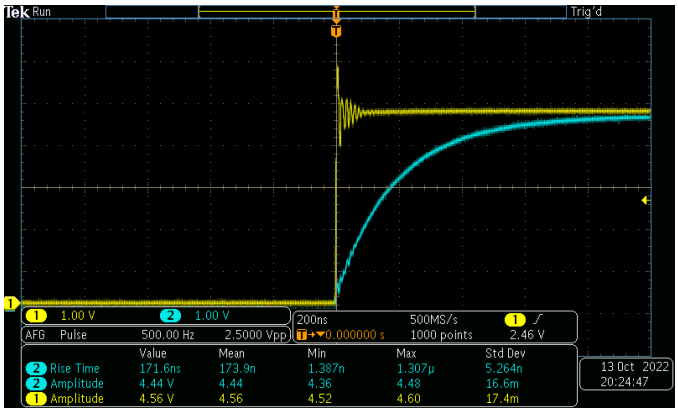

Figure 8.2: Measurement of the textile capacitive sensor. Oscilloscope screen captured

The measurement provides the value of 173 ns of charge time at 63% of voltage for the embroidered sensor. This time value permits to evaluate the capacitance value by the equation:

$$\tau = RC \tag{8.1}$$

Where the R is the series resistance of the circuit, which in the case of

the study was $10k\Omega$. Using the equation, the capacitance value for the embroidered sensor is 17.3 pF. It has to be mentioned that the measurement cables have a 3 pF of parasitic capacitance. Then, the capacitance value used for the comparison corresponding to the measurement is 14.3 pF.

Previously to the production process, the simulation of the structure was done. The capacitance value obtained in CST studio for the embroidered sensor is 15.3 pF.

Also, the capacitance values using the spice model presented in Section 7 are calculated. The parameters of number of fingers, the distance between the fingers and dimensions are substituted in the equation to obtain the capacitance value of 15.4 pF for the embroidered sensor.

Values for spice model, simulation model and measurement value are presented in Table 8.1

	Spice model	**EM model**	**Measured value**
Embroidered	15.4 pF	15.3 pF	14.3 pF

Table 8.1: Capacitance values for the embroidered sensor

The values of capacitance of the sensor are very close to each other. The spice model, which was prepared to take into account the distances between fingers, is matching perfectly. Comparing the capacitance value between spice model, simulation and embroidered sensor measured, it is observed how the measured value has a 1 pF of difference against the others. This difference could be related to slight differences in the parameters when it was measured or that the physical structure of the sensor is not matching perfectly with the simulated or spice model. However, it could be said that the values match between them and the spice model and EM model can be accepted.

8.3 Embroidery textile moisture sensor

In this Section a summary of the results reported and published in Paper A are provided.

8.3.1 Introduction

The first textile capacitive sensor is prepared to be produced by embroidery technique. The sensor interdigital structure has been simulated and calculated theoretically to obtain the expected capacitance range. The aim of the first embroidery textile capacitive sensor is to observe how the sensor response to the humidity. The embroidered sensors behaviour at environ-

mental conditions is studied. Also, the embroidered sensor capacitance value caused by a geometrical change is compared with simulation values.

The embroidered sensor is produced following the embroidery process explained at the beginning of this chapter. The conductive yarn used is the Shieldex conductive yarn. Shieldex conductive yarn properties are explained in Section 3 on Table 3.2. The substrate material chosen is a woven cotton fabric with a thickness of 0.43 mm. The permittivity is also measured for the substrate obtaining a value of 1.9.

The embroidered textile sensors are introduced in the climatic chamber individually and the impedance values, module and phase, are gathered for a frequency between 20 Hz and 20 kHz. The climatic chamber is set up at its initial point with a temperature of 20^{o}C and a relative humidity of 25%. The temperature remained constant during the test procedure, meanwhile the humidity is increased in 5% steps. To increase the relative humidity a stable value of humidity is kept during 5 minutes to secure the sensor measurement.

8.3.2 Measurements of the sensor

Both sensors tested are presented in Figure 8.3. As it is observed, both sensors maintain every geometric value equal unless the length, which is increased 3 times from the short sensor to design the long sensor.

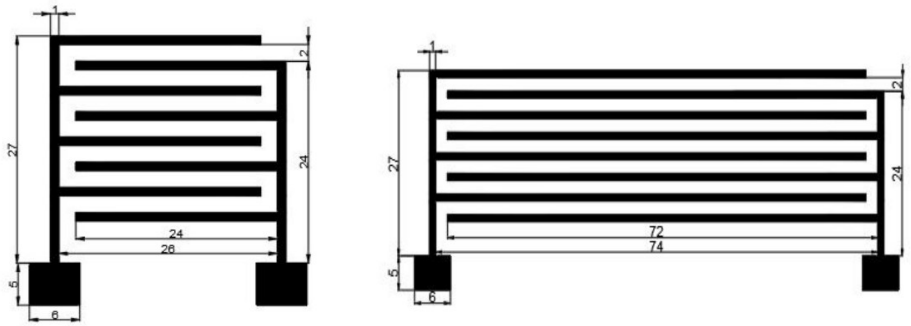

Figure 8.3: Interdigital sensor structure presented in two sizes (in mm). a) short sensor b)long sensor

Figure 8.4 shows the impedance values gathered during the humidity test for both textile sensor configurations. The graph shows how the impedance module of both sensors is reduced when the relative humidity percentage increases, which confirms at first view the functionality of the proposed structure as a moisture sensor. The phase impedance defines the behaviour

of the embroidered sensor, which the behaviour denotes at a low relative humidity percentage that the sensor has a capacitive behaviour.

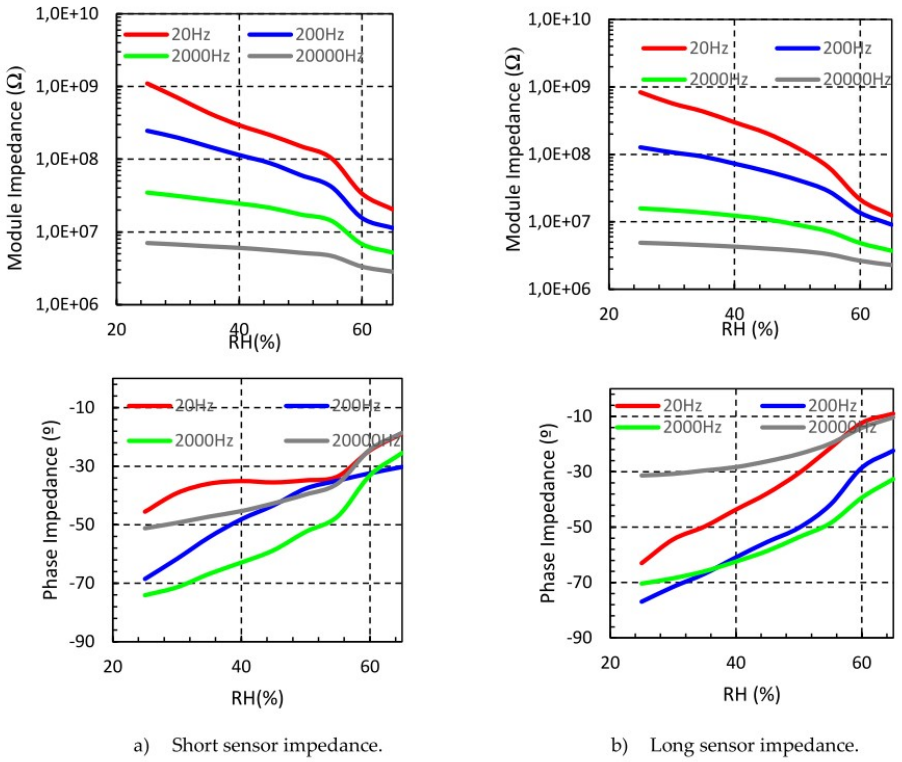

a) Short sensor impedance. b) Long sensor impedance.

Figure 8.4: Impedance values gathered during humidity test for a) short sensor b)long sensor

Moreover, when the relative humidity is increased the sensor behaviour tends to be resistive, as a consequence of the hydrophilic property of the cotton woven substrate. Hydrophilic property provokes an increase of the dielectric permittivity. As a result, the reactance part of the impedance is reduced which decreases the value of the sensor impedance module at higher moisture values.

Both embroidered sensor configurations have similar behaviour against relative humidity. However, as expected due to the simulations done before the embroidery process, the impedance of the longer sensor (Figure 8.4b) is lower than the short sensor impedance (Figure 8.4a) for every frequency measured. As an example, at a test signal of 20Hz from 25% to 65%, the short sensor impedance modulus decreases from $1.1G\Omega$ to $20.4M\Omega$, whereas, for the long sensor decreases from $0.83G\Omega$ to $12.5M\Omega$. During the test, it is noticed that impedance values at lower frequencies are too high for being measured by a portable device, even if that device is designed specifically

for this reason.

After the analysis of the data collected at different frequencies, it is found out that in 2kHz range the impedance values gathered are more appropriate for a wearable device. The embroidered sensor behaviour at 2kHz is analysed in depth, which leads to identify the behaviour as an RC parallel lumped model, where both R and C are moisture dependent, Figure 8.5.

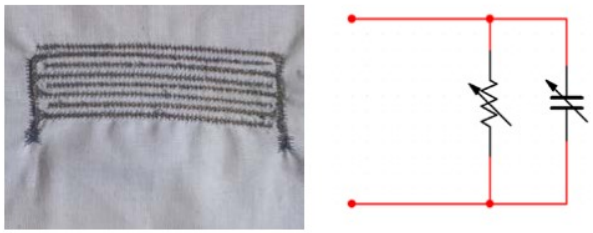

Figure 8.5: Sensor and modelled circuit RC parallel

Parallel resistance and parallel capacitance are calculated from the impedance modulus and phase by the following equations:

$$\frac{1}{Z_p} = \frac{1}{R_p} + j\omega C_p; \quad \omega = 2\pi f \tag{8.2}$$

$$|Z_p| = \frac{1}{\sqrt{(\frac{1}{R_p})^2 + (\omega C_p)^2}} \tag{8.3}$$

$$\theta = \tan^{-1}(-\omega C_p R_p) \tag{8.4}$$

Where Z_p and θ are the impedance modulus and phase obtained by the LCR meter and f is the frequency at which it is measured. The impedance values obtained at 2 kHz are converted into parallel resistance and capacitance to be represented as observed in Figure 8.6.

The graph shows how the resistance values for both sensors decrease when humidity increases. The opposite is observed for the capacitance, which increases when the relative humidity increases due to the permittivity change in the substrate and around the sensor. It is observed a sensitivity change around 55% of relative humidity for both sensors, but it is more significant for the short sensor. The capacitance values during the moisture swept increases from 1.45 pF to 8.84 pF for the short sensor and 3.13 pF to 19.40 pF for the long sensor.

Something interesting to point out is that the relation between the capacitance value for the initial relative humidity state from both sensors is 3, which is the value that was multiplied by the length to set up different configurations at the beginning of the experiment. The relation observed obeys the theoretical equation presented in Section 1.5.1 used as a reference during the thesis.

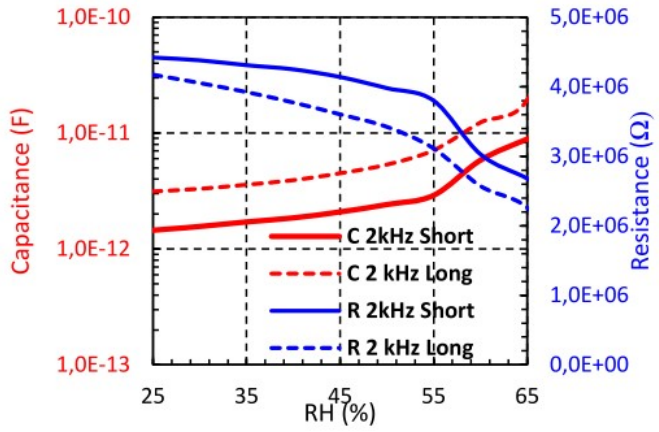

Figure 8.6: Measurement obtained for resistance and capacitance values in parallel circuit

8.4 Impact of manufacturing variability and washing on embroidery textile sensors

In this Section a summary of the results reported and published in Paper B are provided.

8.4.1 Introduction

Taking into account the previous results, the embroidered capacitive sensor is prepared to study the impact of the manufacturing variability and how the sensor responds to the washing process. To prepare the sensor, a size must be selected from the first test results. Taking into account the capacitance values of the sensors, the long sensor is selected from the previous paper, Figure 8.3b. Ten samples are embroidered following the same manufacturing process.

The sensor is measured in a frequency range from 20Hz to 20kHz. For each frequency value, the sensor is measured between 25% and %65 of relative humidity, meanwhile the temperature remained constant at 20^{o}C.

8.4.2 Manufacturing variability results

In this analysis, to evaluate the repeatability of the embroidered sensor, is necessary to select a group of data to work with. In this case, the 200Hz frequency measurements are selected.

The impedance values from ten samples are analysed together to obtain different variability information. The variability data is shown in Figure 8.7. It is shown the module and phase impedance at 200Hz. The red line represents the average measured impedance with a 95% confidence interval

error and black continuous line depicts the linear regression for the average values. A dotted line and a dashed line are added to represent the linear regression for the maximum and minimum deviations of the values. The data shows a linear dependence behaviour with the moisture for the module and phase impedance. The regression index R^2 is higher that 0.95 for every regression.

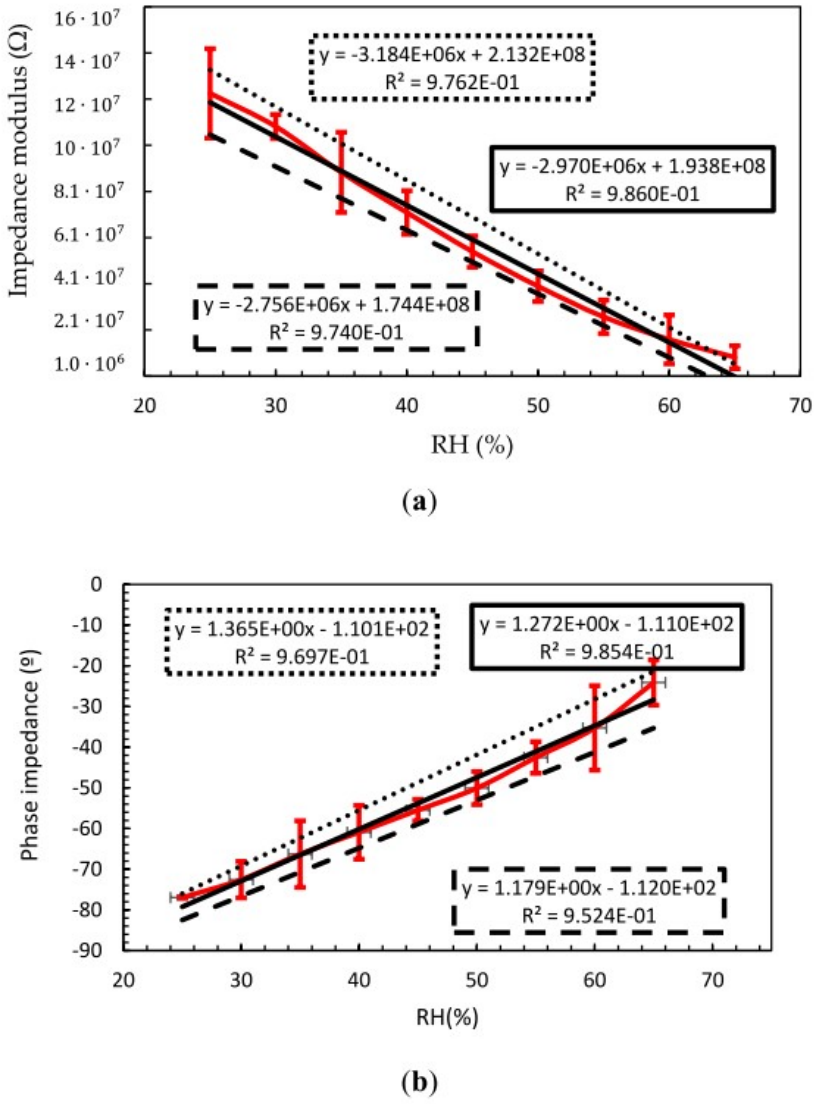

Figure 8.7: Impedance values for repeatability and dispersion error study

However the sensor static characteristics shows variations, due to the manufacturing process variability, the sensor usability remains. The values

of dispersion measured for sensitivity and zero shifts are depicted in Table 8.2. Particularly, the sensitivity of the sensor impedance module has a value of $2.97M\Omega/\%\text{RH} \pm 7\%$, meanwhile the average zero shift is $193.8M\Omega \pm 10\%$. The value of the sensor impedance phase achieves a sensitivity value of $1.272^{\text{o}}/\%\text{RH} \pm 7.3\%$ and the zero shift a value of $111^{\text{o}} \pm 0.9\%$

Impedance modulus				Impedance phase			
	min	mean	max		min	mean	max
Sensitivity $(\frac{M\Omega}{\%RH})$	-3.184	-2.97	-2.756	Sensitivity $(\frac{M\Omega}{\%RH})$	1.179	1.272	1.365
Zero shift $(M\Omega)$	174.4	193.8	213.2	Zero shift $(M\Omega)$	-112	-111	-110

Table 8.2: Sensor impedance properties with process variability for 95% interval of confidence

From the values of dispersion, the expected error on module and phase impedance due to manufacturing variability are determined. The results are shown on Figure 8.8. A maximum error lower than 6% on the moisture measurement is obtained. It is noticed that the error decreased when the moisture increased for the impedance modulus. For the phase error it occurs the opposite, the error increases when the humidity increases.

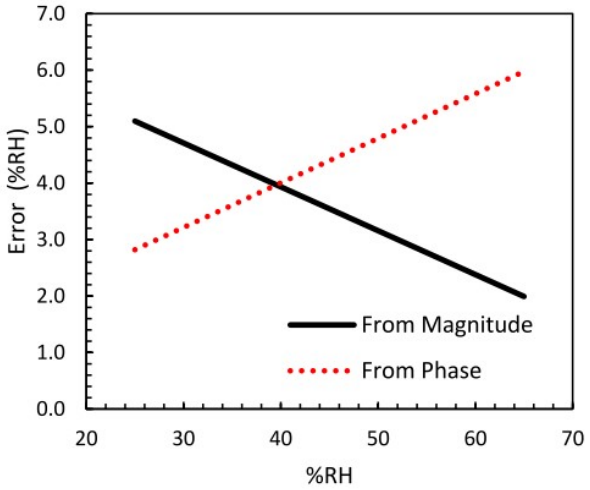

Figure 8.8: Dispersion values for module and phase impedance

According to the behaviour observed, the relative humidity could be measured by the phase impedance under the 40% of relative humidity. For higher values of moisture, impedance modulus should be used. This measurement set up could reduce the measurement error up to 4%.

8.4.3 Washing cycles analysis

Concerning to assure the success of the textile capacitive sensor in real applications, they should guarantee their functionality after the washing process. The embroidered sensor electrical behaviour is evaluated after following a washing cycle, as the previously mentioned. In Figure 8.9 the sensor impedance module and phase data taken along the washing test are presented. The red and black continuous line correspond to the impedance modulus and phase before any washing cycle and its linear regression for each case. After carrying out one conventional washing cycle the values are represented by a dash-dot line. For the second washing cycle data group, a dash-line is used. The linear regression for each group is also represented by its corresponding equation.

The graph shows how after being washed, the impedance module increased for all moisture values, whereas the impedance phase is reduced. This behaviour change points out that after a washing cycle the capacitance behaviour of the proposed sensor decreased, due to an increase of the resistance. When the second washing cycle is done, it is observed how the behaviour change less than the observed previously.

Table 8.3 summarises the impact of washing cycles on embroidered sensor behaviour. It has been observed a clear difference before and after washing the sensor. After the first washing, impedance module sensitivity is reduced by 14.1%, meanwhile, the zero drift has been shifted just 1%. However, after the second washing cycle, only an additional 7.8% of reduction is observed, which represents a reduction of 20.8% with regard to unwashed samples. With respect to the impedance phase, almost no differences were observed between one or two washings. After washing the sensitivity is reduced between 18–19% and the offset about 2% in both cases. It is observed how the first washing cycle affects significantly more than the second cycle. This fact could be explained by the presence of a treatment over the substrate which it disappears with the washing cycles or the lost in the weight of the samples, which is equivalent to the lost of conductive material. After the second washing cycle, the samples are weighted and it is determined that great part of the behaviour change is associated with the treatment lost.

	Impedance modulus				Impedance phase			
Z	Sensitivity ($\frac{M\Omega}{\%RH}$)	Δ S%	Zero shift ($M\Omega$)	Δ Zs%	Sensitivity $\frac{\phi}{\%RH}$	Δ S%	Zero shift (ϕ)	Δ Zs%
No-wash	-2.97		194		1.272		-111.04	
1 wash	-2.55	-14.1	196	1.03	1.029	-19.1	-112.94	1.71
2 wash	-2.35	-20.8	186	4.12	1.041	-18.1	-114.24	2.88

Table 8.3: Relation between the parameters measured and the relative humidity

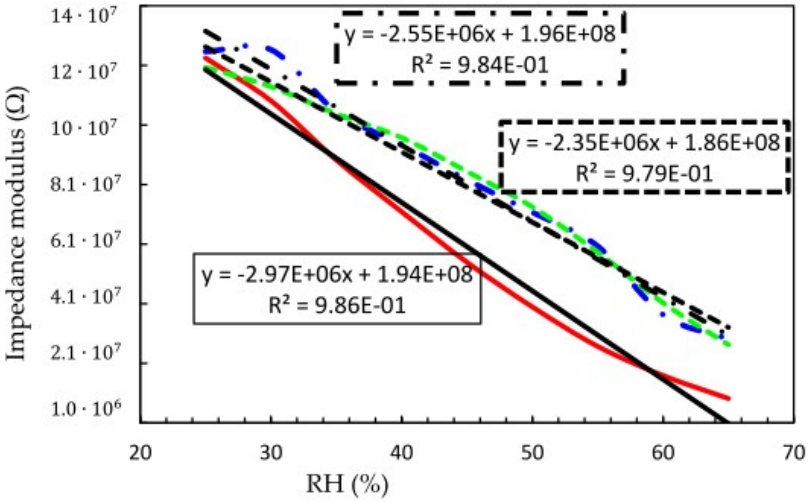

(a) Module impedance.

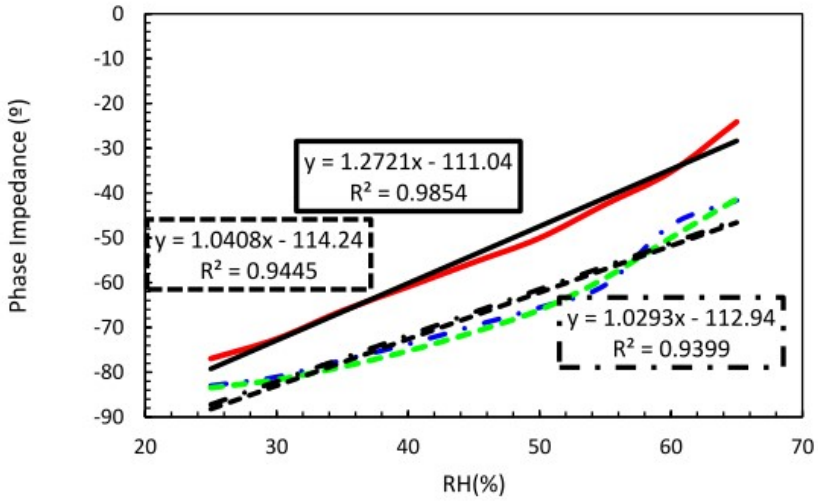

Figure 8.9: Impedance module and phase compared before and after washing cycles

The most common textile treatment is the antibacterial treatment, which is done to prepare the textile surface to guarantee integrity of the fabric during the distribution and storage. This chemical treatment modifies the dielectric properties of the material.

8.5 Impact of conductive yarns on an embroidery textile moisture sensor

In this Section a summary of the results reported and published in Paper C are provided.

8.5.1 Introduction

At this point of the research, the embroidered capacitive sensor has demonstrated its usability. The dependence of the impedance modulus and phase with moisture makes it suitable for being used as a moisture sensor, but also, to further research the use of the sensor to other applications where the permittivity change provides an opportunity to measure the physical stimulus. The embroidered capacitive sensor geometry is maintained in this work. Two embroidered sensors are produced with each conductive yarn. The sizes of each sensor have been presented already in Section 8.3.

However, the behaviour of the sensor is expected to be dependant on the material that composes it. Conductive yarns possibilities are wide nowadays in the market. More and more companies are launching new conductive yarns produced with different textiles techniques, which as mentioned before, could provide special characteristics to the conductive yarns that differentiate them from others. How could a conductive yarn change the behaviour of the sensor or how the conductive material integrated during yarn manufacture process could affect the sensor, are the questions which are going to be answered with this paper. To focus on the behaviour changes due to the yarn properties, the fabric substrate is maintained between different sensors embroidered with different yarns.

8.5.2 Yarn preparation

To evaluate conductive yarns effects in the embroidered capacitive sensor behaviour, three different conductive yarns are prepared. First, the Shieldex yarn used in previous works. This yarn is a 117/17 dtex 2-ply made with a silver coating over a polyamide filaments. Secondly, two ring yarn made by Bekaert which composition is, on one hand a polyester fiber yarn with stainless steel fibers mixed, distributed in 80-20% in weight. On the other hand a cotton fibber yarn with stainless steel fibers on it distributed in the same percentages, 80-20% in weight. Properties for the yarns used were previously presented in Section 3.

The differences in the manufacturing process of the yarns are noticeable in their properties. To highlight more the differences, images taken by the microscope are shown in Figure 8.10. These images should help to compare the behaviours.

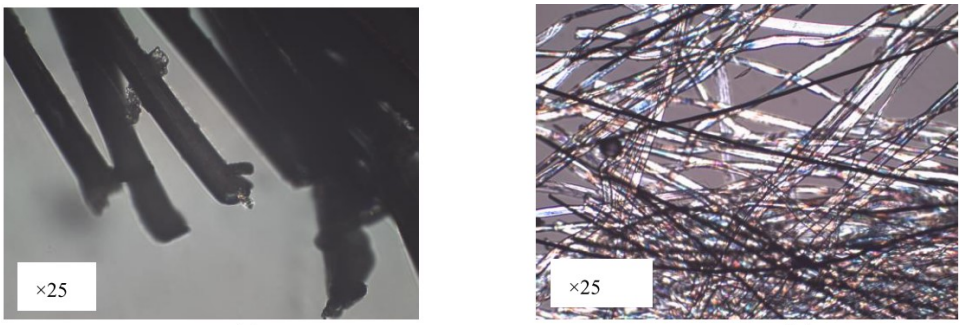

(a) (b)

Figure 8.10: Microscope image of the used conductive yarns (a) Shieldex: this yarn is made of polyamide (PA) (inner) coated with pure silver (outer); (b) Bekaert: This yarn is made by mixing fibbers (white fibbers) of cotton with stainless steel (black fibbers)

The microscope images depict the differences between the yarn structures. On Shieldex yarn the surface of the filaments is coated with silver, which can be observed as an uniform layer. In the meantime, the Bekaert yarn is a mixture of polyester/cotton fibbers as the main material with stainless steel (black fibbers) mixed on it. It can be observed how these fibbers are smaller than Shieldex's filaments, which can result in more micro spaces between them. The fibber disposition for the Bekaert yarns make them softer than Shieldex yarn, which could be an important advantage for the sensors when they are integrated into clothes or fabrics in direct contact with human skin.

8.5.3 Behaviour test discussion

The sensors embroidered have been tested into the climatic chamber as the previous test shown. The conditions for the test are maintained over the works to be more accurate with the behaviour comparison. Then results for frequencies between 20Hz and 20kHz are expected in a 30-65% relative humidity swept at 20^{o}C.

Shieldex yarns are the first to be tested. Figure 8.11 shows the behaviour of the two embroidered sensor configurations. As it is expected the impedance modulus of the sensor is reduced when the environmental moisture increases, also is observed for both configurations how the impedance phase increases when the relative humidity in the chamber increases. The capacitance behaviour of the sensor is reduced by the humidity, becoming almost purely resistive. This change is also being explained before, but to remind it, the hydrophilic behaviour of the cotton fabric absorbs humidity provoking a change in the dielectric permittivity, which is increased. As a result the capacitance of the system increases, decreasing the impedance

total modulus.

Long and short sensors show similar behaviour when the relative humidity increases. However, the impedance of the long sensor is lower than the impedance of the short sensor. Due to the higher capacitance in longer sensor. Particularly, at 20Hz test signal the short sensor decreases from $0.7G\Omega$ to $20.4M\Omega$, whereas, for the long sensor decreases from $0.57G\Omega$ to $12.5M\Omega$ during the relative humidity swept between 30-65%.

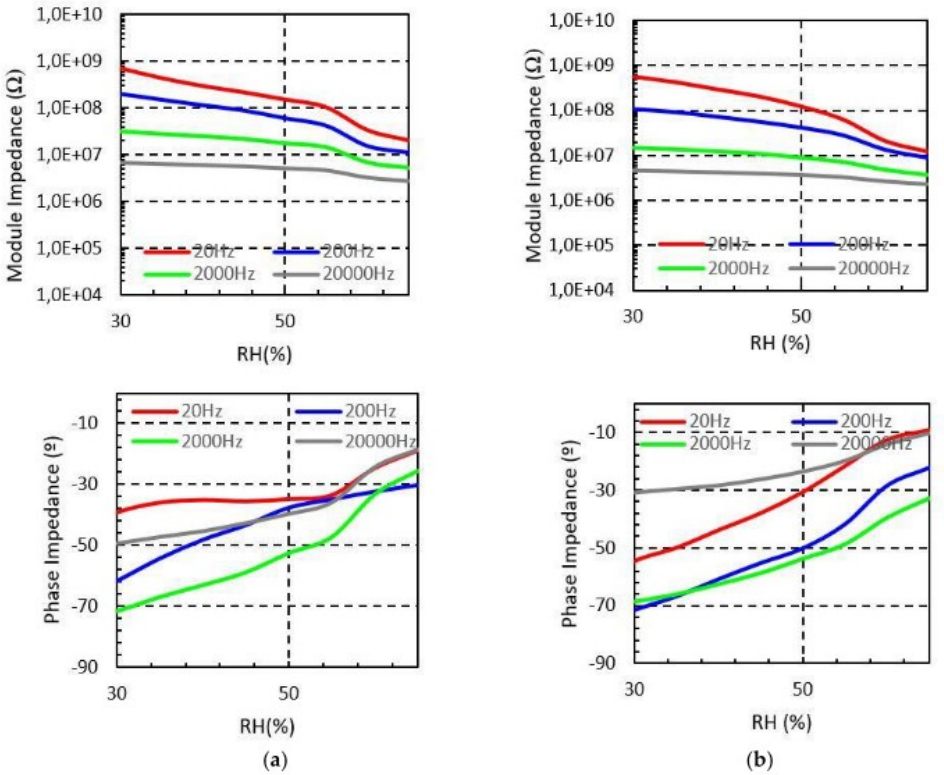

Figure 8.11: Measured Shieldex sensors impedance from 30% to 65% RH at different frequencies (T = 20°C). (a) Short sensor impedance (b) Long sensor impedance

Figures 8.12 and 8.13 show the impedance measurement of the sensor embroidered by Bekaert yarns. Generally, both Bekaert yarns have the same behaviour and their modulus impedance is reduced when moisture increases. Also measured phase impedance increases when moisture makes it so. However, both PES-SS and CO-SS show a significant impedance module reduction compared with the sensors built with Shieldex yarns, and this is reproduced in all cases studied. Specifically, for PES-SS the impedance modulus decreases from $0.12G\Omega$ to $0.92M\Omega$, although, for the long sensor decreases from $27M\Omega$ to $0.37M\Omega$. For the CO-SS case, the impedance modulus de-

creases from $0.13G\Omega$ to $4.2M\Omega$, whereas, for the long sensor decreases from $23.7G\Omega$ to $0.37M\Omega$.

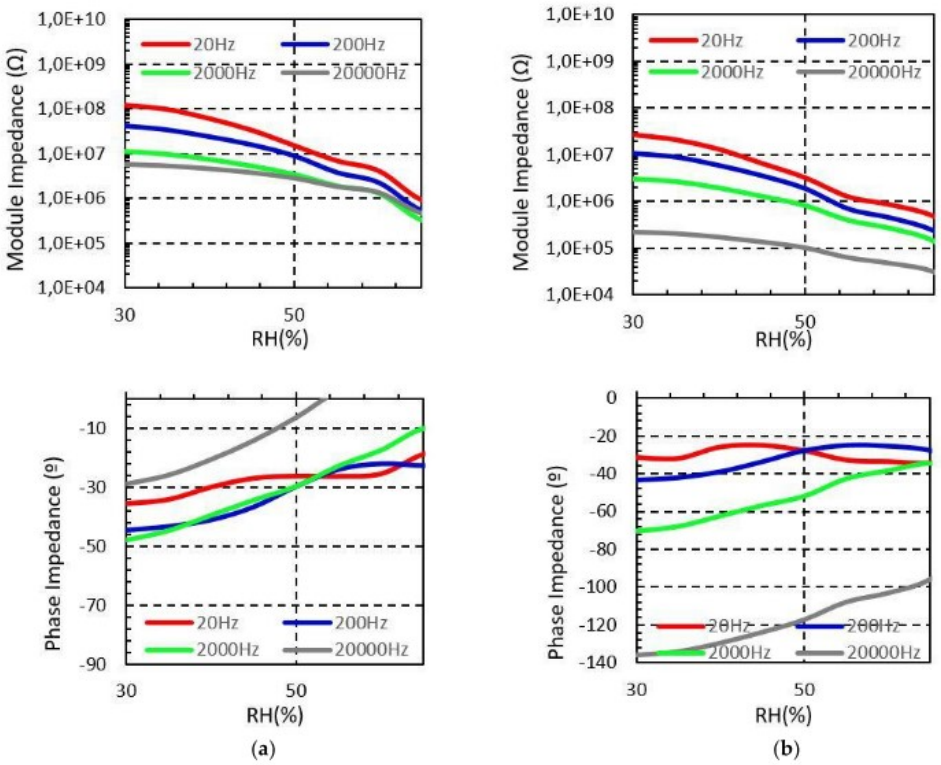

Figure 8.12: Measured Bekaert (PES-SS) sensors impedance from 30% to 65% RH at different frequencies (T = 20°C). (a) Short sensor impedance (b) Long sensor impedance

The explanation for these impedance differences between Shieldex and Bekaert yarns is based on the electrical conductivity of the yarn, and how it is being affected by the moisture. Non-conductive materials present on the yarn should not have any significant impact on this behaviour, but when the presence of humidity is higher, these materials could absorb more moisture, affecting the electrical properties of the conductive materials mixed with them.

To compare ranges, which should be suitable for a wearable device to measure, impedance measured values at 2kHz are presented in Table 8.4. Here it could be observed more easy that, for the same size parameters, sensors embroidered with Bekaert yarn had almost three times less impedance modulus than the Shieldex sensors. The differences are directly related to the structure. Bekaert yarns, which are made by mixed fibbers in ring yarn process, are more sensitive to humidity. These yarns are able to retain more humidity on their surface, between fibbers, what affects directly to their

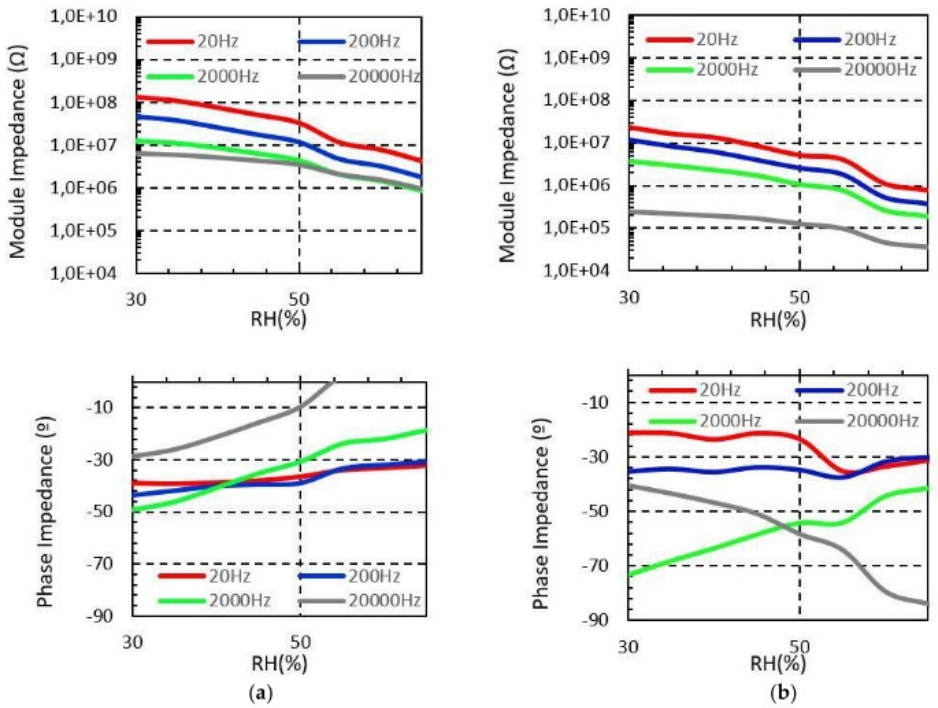

Figure 8.13: Measured Bekaert (CO-SS) sensors impedance from 30% to 65% RH at different frequencies (T = 20 °C). (a) Short sensor impedance (b) Long sensor impedance.

electrical properties having an impact on the final impedance values. It is observed than it is not only the values at the beginning of the experiment, but also the values when the humidity increases.

Sensor	Shieldex	Bekaert(PES-SS)	Bekaert(CO-SS)
Short	$31.2 - 5.18M\Omega$	$11.3 - 0.32M\Omega$	$12.6 - 0.85M\Omega$
Long	$14.8 - 3.71M\Omega$	$2.98 - 0.14M\Omega$	$3.62 - 0.19M\Omega$

Table 8.4: Measured sensors module impedance range at 2 kHz.

In order to complete the analysis, as it has been done in other works, the electrical model associated with the behaviour of the sensors is also studied. The RC parallel lumped model is presented for every different built sensor. Again, the resistance and capacitance in parallel are dependant with the moisture swept.

From Figure 8.14 to Figure 8.16, the R and C dependence for the sensor embroidered with Bekaert and Shieldex yarn at 2kHz is shown. Each figure contains short and long sensor represented by continuous and dash line,

respectively.

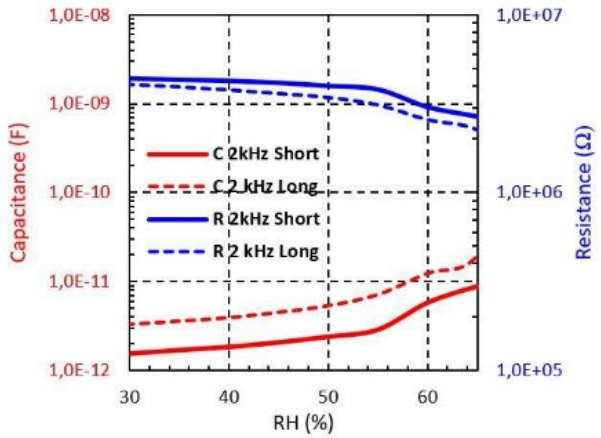

Figure 8.14: Measured Shieldex sensors resistance and capacitance in parallel from 30% to 65% RH at different frequencies

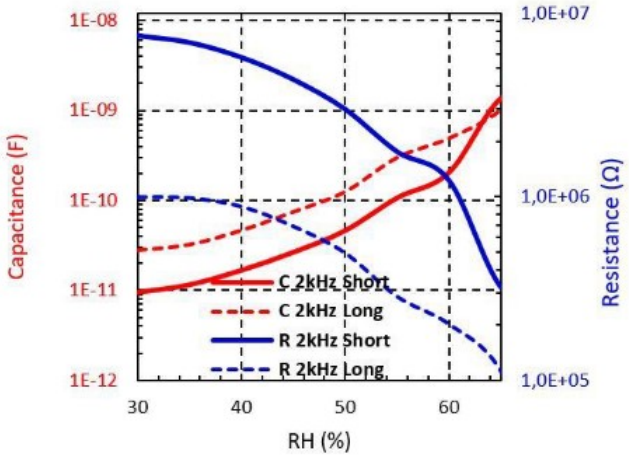

Figure 8.15: Measured Bekaert (PES-SS) sensors resistance and capacitance in parallel from 30% to 65% RH at different frequencies

The general behaviour is maintained in all the sensors, demonstrating that the moisture affects the sensors in similar form. When moisture levels are increased, the capacitance of the sensor is increased with it. But the resistance decreases, due to the conductivity increase, in all cases studied. It should be pointed out that the sensitivity shown by the yarns is higher when Bekaert yarns are observed, compared with Shieldex yarn. The higher sensitivity is associated with the impact that the moisture has on the electrical properties of the yarn, which made the sensor to develop their values

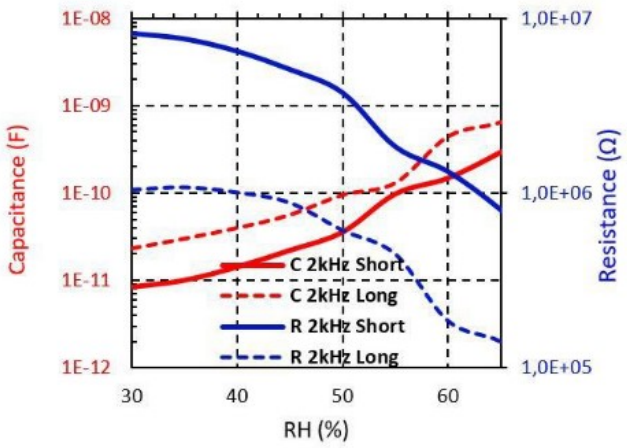

Figure 8.16: Measured Bekaert (CO-SS) sensors resistance and capacitance in parallel from 30% to 65% RH at different frequencies

obtaining wider ranges than previous sensors built by Shieldex yarn. The sensitivity increase provides more levels of measurement between relative humidity steps, which could provide higher accuracy when the sensors were calibrated.

Resistance and capacitance values for every sensor are presented in Tables 8.5 and 8.6. The Bekaert yarns have a larger range of parallel resistance value than the Shieldex sensors. Also, the Bekaert sensor initial resistance is higher due to the yarn resistance. However, between the Bekaert yarns it is not observed a relevant difference provoked by the non-conductive material.

Individually, the resistance of Shieldex short sensor is reduced about 39%, whereas for Bekaert PES-SS and Bekaert CO-SS the reduction achieves 95.7% and 90.2%, respectively, when the moisture is swept from 30% to 65% (Table 8.5). For the moisture range studied, the capacitance increases about one order of magnitude ($\times 10$) for Shieldex yarn and about two orders of magnitude ($\times 100$) for Bekaert PES-SS and Bekaert CO-SS (Table 8.6). This key fact points out that Bekaert yarns are more sensitive to develop moisture sensors, increasing the overall sensor sensitivity.

These different behaviours depending on the conductive yarn used could provide properties to the final sensor application. Depending on the sensitivity needed, the conductive yarn could be selected to fit the use expected. Also, the behaviour could be related to the manufacturer process, hence, the design of a conductive yarn could be performed more precisely to respond the necessities of the textile sensor. As an example, ring yarns provide a higher effective surface for the moisture to be trapped.

	Shieldex	**Bekaert(PES-SS)**	**Bekaert(CO-SS)**
Short	$4.42 - 2.68M\Omega$	$7.57 - 0.32M\Omega$	$8.22 - 0.8M\Omega$
Long	$4.17 - 2.26M\Omega$	$0.99 - 0.11M\Omega$	$1.04 - 0.14M\Omega$

Table 8.5: Measured sensors parallel resistances ranges at 2 kHz.

	Shieldex	**Bekaert(PES-SS)**	**Bekaert(CO-SS)**
Short	1.56-8.84pF	9.48pF-1.37nF	8.37pF-0.29nF
Long	3.3-19.4pF	28.3pF-1.02nF	23pF-0.65nF

Table 8.6: Measured sensors parallel capacitances ranges at 2 kHz.

8.6 Experimental analysis of fabric substrate on a moisture sensor

In this Section a summary of the results reported and published in Paper D are provided.

8.6.1 Introduction

After the analysis of the effect of different conductive yarns in the textile capacitive sensor behaviour, a decision is made. It is necessary to study the effect of the textile substrate material in the behaviour of the textile sensor. The yarn percentage in weight against the rest of the textile material which composes the textile sensor is relatively low. Hence, it is expected that the textile substrate material has more impact on the behaviour of the sensor than the conductive yarns.

The structure to be embroidered is maintained from previous works. At this stage where there are some parameters changing, maintain the structure is important to be able to compare results where the differences observed will be provoked by the properties changed, decreasing the risk of obtaining perturbed conclusions.

8.6.2 Substrate methodology

The interdigital structure is prepared to be embroidered over three different substrates, two cotton substrates and one polyester substrate. These substrates are chosen because they are the most common materials used to produce fabrics in the industry at the present time. The conductive yarn used is maintained constant, at this time a commercial Shieldex 117/17 2-ply is used to embroider the capacitive sensors.

The characterisation of the substrates is performed previously in the behaviour test. The most important properties of the substrate materials are shown in Table 8.7. The substrate permittivity and loss tangent are

measured by means of a Microwave Frequency Q-Meter. Also, the fabric absorption is evaluated by the Humidity analyser MOC-63U. Both methodologies are explained in Section 6.

	Thickness (mm)	**Permittivity**	**Loss tan**	Moisture (Weight%)
Cotton (CO)	0,256	1,87	0,0750	5,96%
Med Cotton (MED)	0,306	2,02	0,0671	8,02%
Polyester (PES)	0,199	1,5	0,0189	2,23%

Table 8.7: Substrate properties measured for the behaviour analysis.

The results of the retained moisture in every substrate show that cotton fabric retains a 6% of weight as humidity and polyester retains a 2.2%. The results obtained demonstrates that cotton and polyester yarns which compose the substrates react in different ways to the moisture in the air. In fact, cotton is more affected by the humidity change, due to its hydrophilic nature, which could be observed when the substrate is able to keep more moisture at ambient conditions.

One point to take into account is the presence of treatments on the surface of the textiles, as previously seen when the washability of the sensor was studied. For the samples prepared to be studied regarding the substrate materials, only the medical cotton is treated with an antibacterial treatment. This treatment is the main difference between the cotton fabric and the medical cotton.

8.6.3 Behaviour comparison regarding the substrate material

During the study of the substrate material some conditions on the test are changed. The objective of these changes is to obtain more information from every measurement done. In this case the frequency signal measured is extended till 200kHz. Also the relative humidity range is expanded, from 65% to 80% in its upper limit. The humidity range expansion provides extra knowledge about the behaviour change when the humidity increases.

The behaviour of the substrates in frequency is shown in Figure 8.17 and 8.18. These figures show the shift in frequency at 40% and 80% of relative humidity. The representation of the shift in frequency could provide information about the electrical model of the sensor. It is observed how the capacitive sensor response in frequency is affected by the substrate material and the relative humidity. At 40% of relative humidity is observed how the impedance module decreases as the frequency increases. The trend observed shows the different behaviour depending on the material substrate. Medical cotton (MED) impedance module varies from $6.6M\Omega$ to $29k\Omega$, standard cotton (CO) varies from $176M\Omega$ to $40k\Omega$ and polyester (PES) varies from $1.19G\Omega$ to $41k\Omega$.

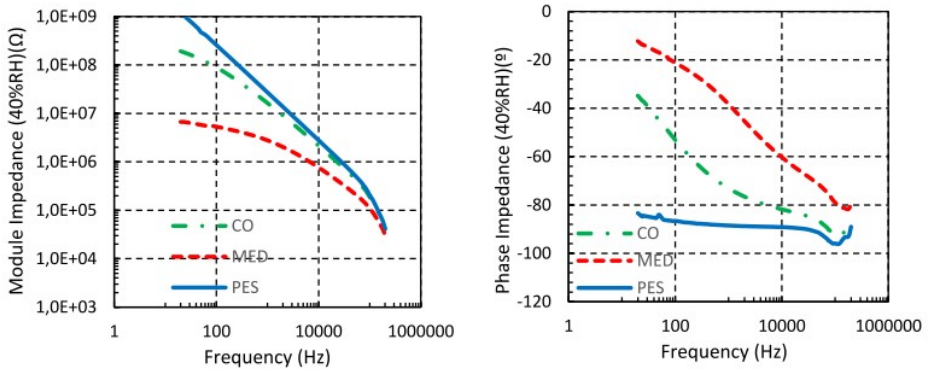

Figure 8.17: Experimental frequency response of sensor impedance at 40 %RH

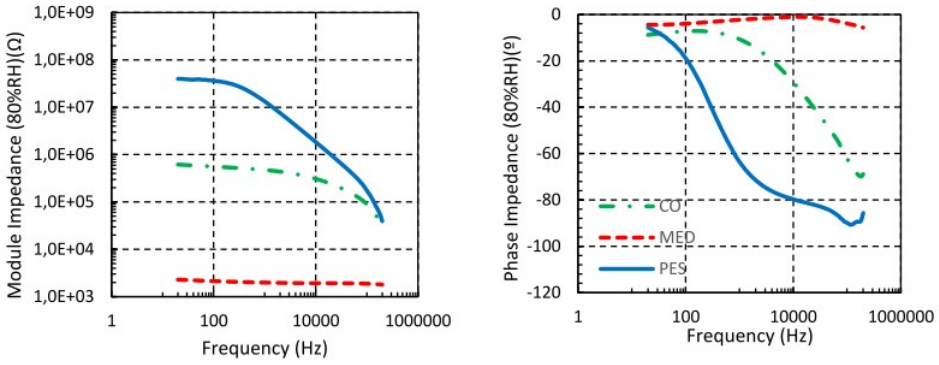

Figure 8.18: Experimental frequency response of sensor impedance at 80 %RH

At lower frequencies ($\leq 100Hz$) the MED substrate behaves mainly as a resistance, which is observed in its phase impedance value (-20º). Its impedance modulus has the lower slope between the substrates. Whereas, the PES substrate has a capacitance behaviour and the higher slope in its impedance module. It is observed how the impedance of the substrate that has lower permittivity and lower absorption of moisture is the one that has the more significant capacitance component.

The sensor behaviour became very similar at higher frequencies, where it is observed in the module impedance with the collapsing of the lines and the impedance phase tendency to -90%

When the moisture arrives to the 80% of relative humidity the behaviour of the sensors has been changed clearly. The substrate that most variation experiments is the MED substrate. MED substrate impedance modulus is almost constantly through the frequency shift, remaining around $2k\Omega$.

The impedance phase also is maintained, which value was around 0^{o}. The behaviour is resistive at this point for the sensor embroidered in MED substrate. In contrast, the PES and CO sensors worked as a resistive-capacitive (RC) circuit. The impedance modulus values for the PES substrate go from $39M\Omega$ to $60k\Omega$ and from $609k\Omega$ to $20k\Omega$ for the CO substrate. Also, it is observed how both of these substrates impedance phase start at low frequency with resistive behaviour and as the frequency increases, their behaviour trend is capacitive.

The MED substrate behaviour responds to a high conductivity when the moisture is present on the surface. The chemical treatment that the substrate has is known to be antibacterial, which is achieved by increasing the conductivity of the substrate that prevents bacteria to develop. This treatment decreases the parasitic resistivity, which makes it more affected by the moisture than others. The PES substrate case matchs with the expectations created by the textile properties. As an hydrophobic material is less affected by moisture, due to there are less water particles added to the surface which changes less the values between different states of humidity compared with other substrates.

To analyse the behaviour when a humidity swept is performed, the different behaviour of the sensors at 2kHz of the test signal is selected to be represented in a graph. In Figure 8.19, the module and phase impedance for every sensor in the study is shown. The moisture is changed between 30-80% of relative humidity. Experimental errors are depicted in the graph. The behaviour, in broad terms, is very similar. Their module impedance decreases when humidity increases, whereas the phase impedance increases when the moisture increases.

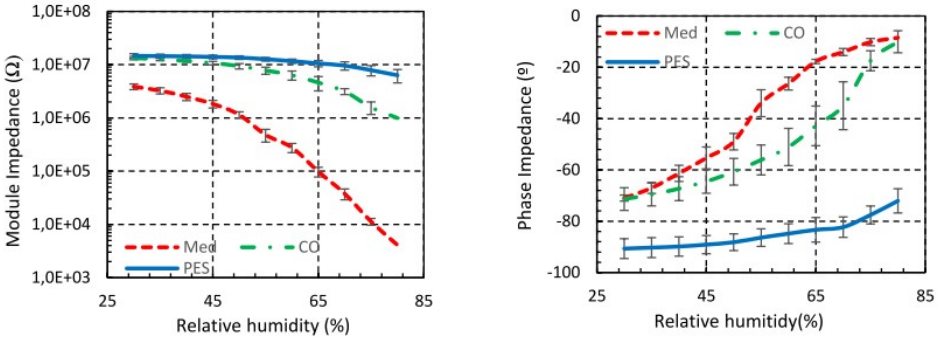

Figure 8.19: Measured impedance along relative humidity at 2 kHz

Specifically, the impedance module ranges from $13.3M\Omega$ to $0.99M\Omega$ on CO and from $3.86M\Omega$ to $4k\Omega$ on MED denotes how the impedance module is affected significantly by the moisture. In contrast PES substrate has the shortest range of values when the humidity range is covered, moving from

$14.7M\Omega$ to $6.33M\Omega$. In phase impedance is appreciated how cotton based substrates (CO and MED) suffers a reduction from -70º to -10º, but for PES substrate the capacitive nature is maintained during the humidity shift with values between -72 and -90º. The results denote the affection of the cotton substrates against humidity provokes the sensor built over them to have wider impedance module ranges and a complete shift in their phase values. As a result the final behaviour, at higher relative humidity states, is resistive. For the PES substrate case the module impedance decreases with a softer slope, and phase impedance is hardly affected, maintaining its capacitive behaviour.

From the repeatability errors in the graph, the PES substrate sensor also obtains lower error values than both cotton substrates, which results in higher repeatability.

As in previous analyses, the parallel RC circuit is also obtained and shown in Figure 8.20. The values are obtained for the same humidity ranges at 2kHz. As it is deduced from the impedance, resistance values decrease as the humidity increases, due to the increase in the effective conductivity of the dielectric. Produced by the water particles on the textile surface. The capacitance values are increased by the relative humidity. Therefore, the hydrophilic properties of the material define the electric sensor behaviour. PES substrate, that is defined as mainly capacitive, has values of capacitance lower than 10pF along the humidity shift. However, both cotton substrates at lower moisture values, where the behaviour is capacitive, have capacitive values of 7 and 12pF for CO and MED, respectively. At higher moisture values the behaviour of cotton substrate sensor is mainly resistive, due to the increase of the capacitance, with a value up to $450k\Omega$ and $1.9k\Omega$ for CO and MED.

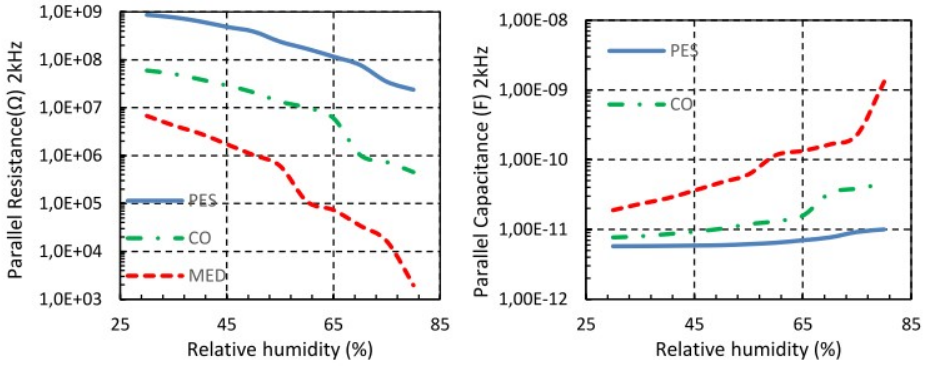

Figure 8.20: Measured equivalent circuit for the sensor at 2 kHz

In order to clarify the experiment results, the relative permittivity has been characterised. It is known that the capacitance is related directly with

the real part of the permittivity. Figure 8.21 shows the measured relative permittivity for each substrate along a small swept of relative humidity.

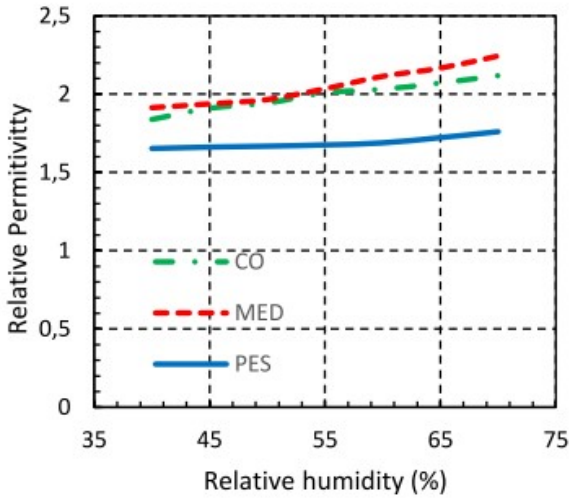

Figure 8.21: Relative permittivity measured for each substrate

It is observed how the permittivity values of the materials are affected by the moisture changes, increasing the permittivity values. Cotton substrates permittivity are similar, 1.83 and 1.91 at 40% for CO and MED. These values are increased a 15.4 and 15.2% during the relative humidity increasing. PES substrate permittivity is 1.63 at 40% of relative humidity, and after the swept is only being increased a 6.6%, which corresponds almost to a half part of the amount increased by the cotton substrates. If the permittivity change values are compared with the increase in capacitance experienced by the sensors, which are a 491% for the MED capacitance sensor, a 288% for the CO capacitance sensor and a 32% for the PES capacitance sensor, it can be deduced that the capacitance shift can not be only attributed to the dielectric permittivity over the substrate surface. Capacitance shift can be affected by the geometric changes or permittivity changes in the environment around the sensor. But something that can be observed is that the material less affected by the humidity is the one whose permittivity is less affected too.

8.7 Conclusions

When it comes to textile sensor integration, embroidery is likely to be the first technique to take into account. Embroidery is one of the most extended integration methods, due to the general knowledge, the fast prototyping, low cost to initiate and low cost machinery. Nowadays, CAD designs are

easy to import to embroidery machine software and convert the files into machine stitches. The conditions exposed make embroidery the best integration technique to begin the smart textile journey. In this chapter, the working principle of textile capacitive sensor to measure humidity, the study of conductive yarns and the effect of the substrate materials on the sensor behaviour, are reported.

Concerning textile capacitive sensors, their usability have been demonstrated by the results obtained for the humidity measurement. The embroidered capacitive sensor could be used in a wide range of frequency signal. The studies indicate that if the desired characteristic to measure from the sensor is the impedance, the optimal range is around 2kHz. At this signal value, the impedance module and phase acquired are in a range that a wearable device could work with. The variability error obtained during the comparison of the sensors produced is a 6%. This value could be reduced to a 4% if during the measurement, two different values are used for different ranges, i.e., for values lower than 40% RH the impedance modulus is used exclusively, but for higher humidity values, the phase impedance develops adjust more with the relative humidity value. Some non-conclusive washing tests are performed, but it is detected that chemical treatments used to store the fabrics affect the behaviour of the proposed sensor. During the behaviour analysis, the embroidered capacitive sensor is found to behave as an RC parallel, where both characteristics (R and C) are dependant with the moisture.

Conductive yarns where studied and how they affect the behaviour of the sensor. The yarns produced by ring yarn methods, which is the production process to produce the common yarns used in clothes, showed more sensitivity to moisture than coated yarns. The Bekaert behaviour could be explained by the effective surface, where the water particles could be trapped. Also, the materials that compose the yarns affect slightly the behaviour of the sensor. In addition, yarns produced with ring yarn method result in a better touch feeling when embroidered than the coated filament yarns.

When the substrate material effect on the sensor behaviour is studied, it is found that the material that composes the substrate is the parameter that affects more significantly the behaviour of the sensor. Water absorption of a material is related directly to the moisture change in its permittivity, and as a consequence, the capacitance. Capacitance changes could be not only due to the permittivity change in the substrate, but also with little dimensional changes in the structure of the permittivity of the surrounding area. Impedance behaviour transforms from capacitive to resistive when a higher level of moisture is reached, but for polyester substrate the impedance maintains its capacitive behaviour in all the moisture levels.

To sum up, the conclusions obtained from the different studies performed during the embroidery technique evaluation show that the substrate material

is the parameter that defines the great part of the behaviour of the capacitive sensor. The behaviour change due to the materials provides versatility to the sensor. Materials used to build the embroidered capacitive sensor will be chosen following the requirements of the future application where the sensor is being used.

9

Woven Capacitive textile sensor

9.1 Introduction

Chapter 9 presents a textile capacitive sensor produced by weaving techniques. The results from Chapter 8, where an embroidered capacitive sensor is used to detect relative humidity and the behaviour characterisation depending on the materials that compose the sensor, provide a base to go beyond in the integration method. Woven technology implies that the sensor could be produced in large scale production, increasing the number of applications where it can be used. This methodology transforms the sensor from being produced over a textile fabric already produced to produce the sensor during the textile substrate manufacture process. As a result of this methodology change, the textile sensor obtained is integrated along the substrate structure, making the sensor indistinguishable by touch.

The conductive yarn selection turns into one of the most relevant requirements. The yarn should resist the weave process, which implies strength and resistance, but also be soft enough to be unnoticeable. The woven sensor has been tested under relative humidity swept to compare the results with embroidered sensor. The aim is to demonstrate that the structure is suitable for being woven and the results are maintained or improved.

9.2 Comparison between spice model, EM model and measured model

In this section, the comparison of the spice model, EM model and the woven capacitive sensor measured are presented. The section follows the same procedure done in Section 8.2. The interdigital woven structure and the geometry parameters are shown in Figure 9.1

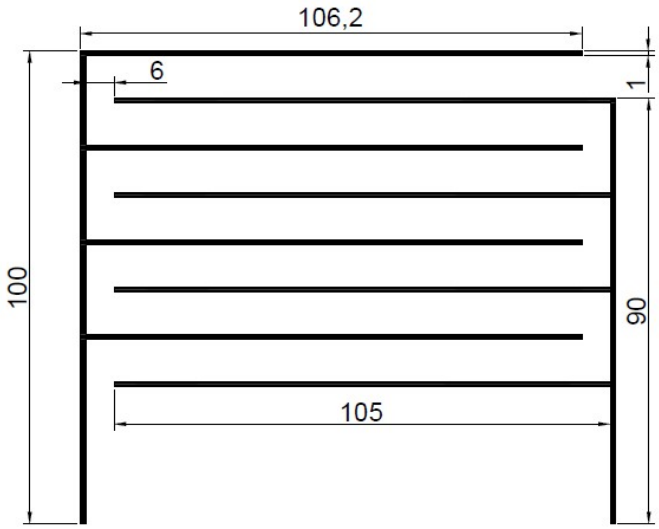

Figure 9.1: Interdigital woven structure with parameters depicted (in mm)

The sensor is connected to the DC circuit prepared for the charge discharge method. The measurement is prepared to be observed on the oscilloscope. The response of charging the woven capacitive sensor was captured and Figure 9.2 shows the response time.

The measurement provides the value of 155ns of charge time at 63% of Voltage for woven sensor. Using the equation, also shown in Section 8.2, the capacitance value for the woven capacitive sensor is calculated using the number of fingers and geometric parameters shown in Figure 9.1. The result is 15.5 pF, which results in 12.5 pF when the parasitic capacitance of the oscilloscope cables is removed.

The simulation of the woven structure performed previously to the manufacture process shows an electrostatic capacitance of 13.4pF

To complete the values to compare, the capacitance value using the spice model presented in Section 7 is calculated. A capacitive value 10.2pF is obtained for the woven sensor.

Values for spice model, simulation model and measurement value are presented in Table 9.1

The capacitance values for the woven structure match with slight differ-

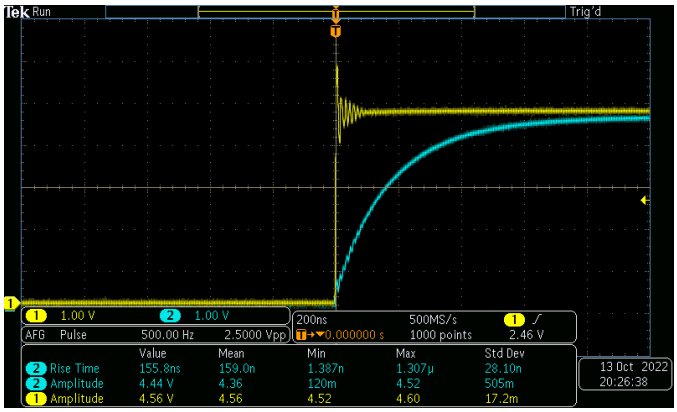

Figure 9.2: Measurement of the woven capacitive sensor. Oscilloscope screen captured

	Spice model	**EM model**	**Measured value**
Woven	10.2pF	13.4pF	12.5pF

Table 9.1: Capacitance values for the woven sensor

ences. The bigger difference is observed in the spice model. It could mean that some of the hypothesis taken along the modelling is not fitting perfectly when the geometry grows. However, the capacitance values between model and woven sensor measured are experiencing the same shift experienced in the previous comparison. The reason could be some miss-match between some of the parameters configured in the simulation, as the permittivity or the with of the conductor, which are parameters hard to maintain constant. Results demonstrate that spice model and simulation predicts correctly the value obtained in the real measurement for the woven capacitive sensor.

9.3 A Full Textile Capacitive Woven Sensor

In this Section, a summary of the results reported and published in Paper E are provided.

Using the methodology explained in Section 5.2 two woven capacitive sensors are obtained as a result. In order to obtain the different sensors, two conductive yarns are used. One of them is a commercial Shieldex 117/17 2-ply(S), which was produced with a silver 99% coating covering a polyamide filament. The second yarn used is a Bekaert 20/2 Tex (B) polyester mixed with stainless steel fibbers with a proportion of 60/40%, respectively, which was produced by ring yarn procedure. The yarns have different properties; On one hand, Shieldex yarn has more tensile resistance and lower electrical

resistance. On the other hand, Bekaert yarn is more comfortable and lighter. Properties of conductive yarns are presented in Section 3.

Regarding the manufacture process of the sensors with Shieldex yarn, 12 individual yarns of the warp are substituted by Shieldex conductive yarns. These yarns formed two vertical lines along the woven fabric, which lines connected the different horizontal lines or fingers. Afterwards, Shieldex conductive yarn is introduced on the weft system to proceed with the weave process of the fabric. The same methodology is performed with the Bekaert yarn. As a result, two types of sensors are obtained. Sensors produced with warp and weft yarn from Shieldex which are referred as USTS, and sensors made with warp and weft yarn from Bekaert which are referred as UBTB.

In Figure 9.3 both sensors are shown. It is necessary to remark again that, the conductive yarns integrated with weave methodology take part into the structure of the fabric, making them unnoticeable. In Figure 9.3, the conductive yarns can be detected due to the difference in colour. But if the colour of the yarns were the same or similar, it would be impossible to detect the sensor by sight.

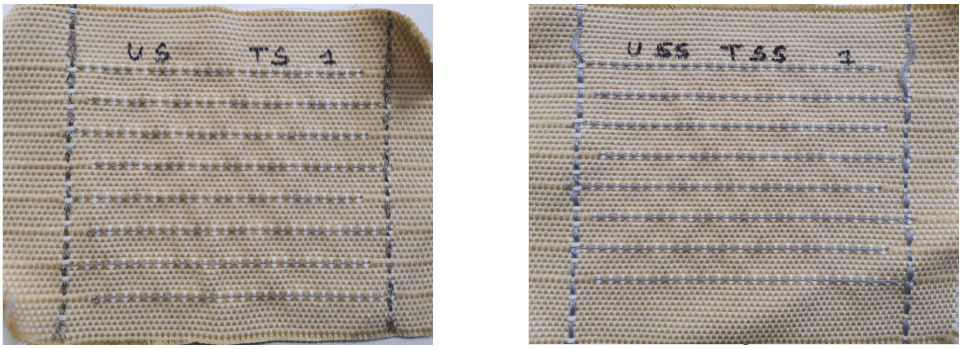

(a) USTS (b) UBTB

Figure 9.3: Textile woven sensor

9.3.1 Humidity test characterisation

The woven capacitive sensor behaviour is studied when the humidity test done with all the sensors produced previously is performed. The humidity test is modified for these sensors to cover the more relative humidity range. At this time the range is increased, starting from 30% to 95% of relative humidity. The capacitance values are taken for frequency values from 20Hz to 20kHz.

The ranges of capacitance values along the relative humidity swept at 20Hz were from 9.74pF to 2.31μF for the sensor produced with Shieldex yarn (USTS) and from 11.9pF to 0.3μF for the sensor produced with Bekaert yarn (UBTB). When capacitance values are studied and during the preparation of

the graphs, it is observed that when the capacitance values for every sensor where scaled in logarithmic scale to observe all the range in the same graph, the values are close to a linear behaviour.

It is decided to apply a logarithmic scale to the capacitive values to be able to study the linearity of the capacitance values. The values represented in Figure 9.4 and 9.5 respond to the following equation.

$$log_{10}(C) = aHR + b \tag{9.1}$$

where C refers to the capacitance values in Farads and HR refers to the relative humidity value on percentage.

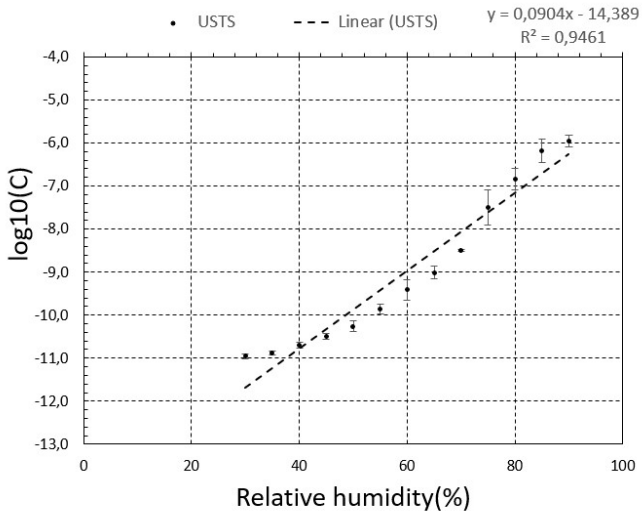

Figure 9.4: Behaviour of USTS woven sensor. Dots denote the average value and vertical line dispersion value

Linear regression is evaluated for each group of sensors and can be found on the Figures 9.4 and 9.5. Values from linear regression are related to the equation presented previously. Parameters of the equations are exposed in Table 9.2.

	Linear Regression	R^2
USTS	0,0904·HR-14,389	0,9461
UBTB	0,0794·HR-13,92	0,9539

Table 9.2: Properties for the yarns tested

The evaluation of the linear regression from both groups provides the sensitivity for each sensor studied, equivalent to the slope of the linear regression. UBTB shows a lower slope and its R^2 is higher which determines

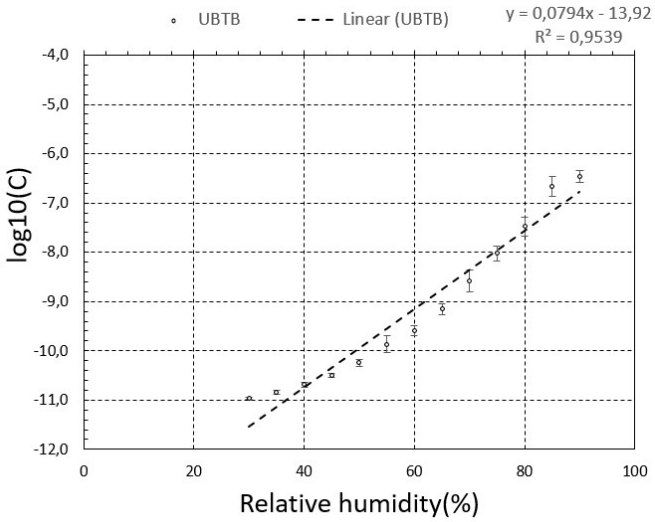

Figure 9.5: Behaviour of UBTB woven sensor. Dots denote the average value and vertical line dispersion value

UBTB as more linear than USTS. Even if, the values from the USTS sensor are not far from the UBTB quality.

The graphs shown in Figure 9.4 and 9.5 also contain the dispersion values for every capacitance value measured. Although, it is observed how the dispersion value is low in the majority of points along both sensor graphs. But both sensors have a high dispersion zone. USTS has the highest dispersion at 75% and 85% of relative humidity, the standard deviation values are 4.3% to 5.5% respectively. Being the highest standard deviation point on 75% of relative humidity with a value of 5.5%. Instead, UBTB standard deviation values are more stable and reduced. There are not as big differences as for USTS values. The highest standard deviation values are on 80% and 85% of relative humidity with a value of 2.5% and 2.9%, respectively, regarding the average value.

The differences between both sensor groups could be explained by the properties of the conductive yarns. On one hand, the Shieldex sensors sensitivity is higher, due to the silver conductivity ($62 * 10^6 Sm^-1$) which is higher than the stainless steal conductivity ($[1.28 - 1.32] * 10^6 Sm^-1$) and also, silver has lower resistivity. On the other hand, UBTB has a lower standard deviation than USTS. The fact could be explained by the production methodology used to manufacture Bekaert yarn (ring yarn methodology), which is more compatible with woven production process.

When the weaving sensors were produced the expectations were high. It is expected that sensora produced by woven technology not only are prepared to be large scale produced, but also to have less standard deviation between

different samples. For this fact, data acquired in previous test shown in Chapter 8 are compared with woven capacitive sensor data in Table 9.3

	Sensitivity $log(C)(RH)^{-}1$	**Standard deviation** average(%)	**Improvement** %
Embroidery	0.0736	2.1	-
Weaving	0.0904	1.34	36.2%

Table 9.3: Comparison between technologies

The comparison presents the woven sensors as an improvement to the embroidered sensors. On average, embroidered sensors present a 2.1% of standard deviation, considering all the sensor produced by this technology. Meanwhile, woven sensor has a 1.34% of a standard deviation on average. As a conclusion, the weaving process produce sensors with higher repeatability and less dispersion. Also the sensitivity of the sensors have been improved from embroidering to weaving a 36%.

A comparison with other humidity sensor found in the literature and previous works is done in Table 9.4. As it can be observed, woven technology perform as well as the other technologies and sensors. Woven capacitive sensor has been distinguished by higher repeatability, better aspect and low touch impact over the rest of the textile sensors presented. The woven textile sensor provides better capacitance values to be able to prepare a model which provides the relative humidity value.

	Sensitivity $log(Z)(RH)^{-}1$	**Working Range** %RH	**Size** HxW(mm)	**Integration Technology**
This work	0.0673	30-90	100x106.2	woven
[**43**]	0.0559	20-90	4.25x4.25	drop-coated
[**58**]	0.0535	25-80	27x74	embroidered
[**59**]	0.0804	40-90	150x220	embroidered

Table 9.4: Comparison with other interdigital humidity sensor. In this case the impedance sensitivity is used to be able to compare with other sensors.

9.3.2 Presence test characterisation

The presence test results are presented and analysed. The section intend to demonstrate the ability of the woven capacitive sensor to detect human presence. As it was explained in Section 6.7, capacitance values of the woven sensor are taken during the standing-up and sitting cycle. The idea is to observe two possible states: occupied state when the person is sat down over the sensor and void state when the person is stand up.

Figure 9.6 shows the capacity shifts results of the presence test for both woven sensor, USTS and UBTB, which are represented as a continuous and

dash line. The Y-axis values are calculated by

$$\Delta C(\%) = \frac{C_f - C_0}{C_0} \tag{9.2}$$

Where C_f is the measured capacitance value and C_0 is the initial capacitance value.

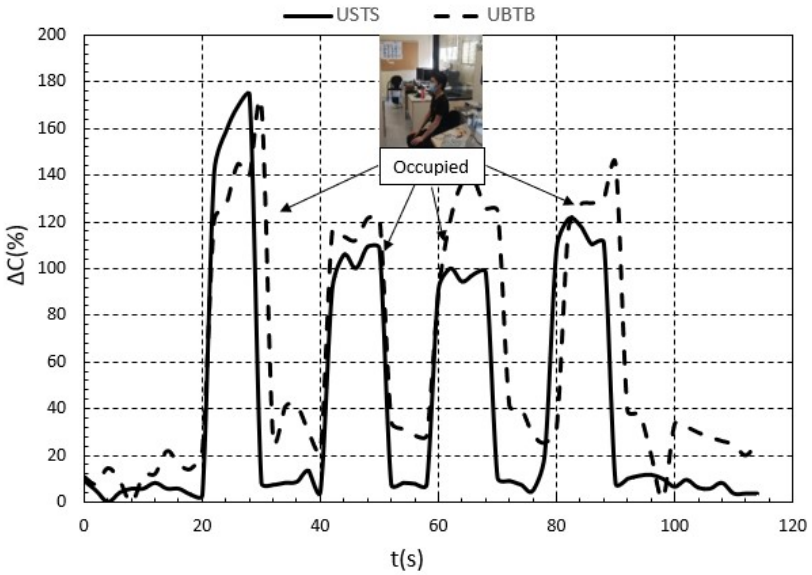

Figure 9.6: Capacity shift, in percentage, during presence detector test

As it can be observed, the response of the woven sensors when the person is sitting over the sensor is notable. The capacitance maintains its value during the sitting situation until the person got up, instantly the capacitance value decreases abruptly to the initial values. Initial or void state values for USTS starts at 0-15% of capacitance variation. When the person sit down over the sensor the capacitance values increase until a 100-170% of capacitance variation. The UBTB sensor behaviour is equal to the USTS during the presence test, having a 0-15% capacitance variation during the void state and increasing that value until 120-170% when the sensor is occupied by a person sat.

The results demonstrate that the sensor response is able to distinguish between void and occupied state. Following test consist in the detection of a heavy object on the top of the sensor. Specifically, a bag with 4,6,10 and 15kg is placed over the sensor. The results can be seen on Figure 9.7.

The capacitance values obtained during the object cycle showed a maximum increase of 20% of capacitance variation, which is similar to void state values. The capacitance values did not respond to the bag being placed

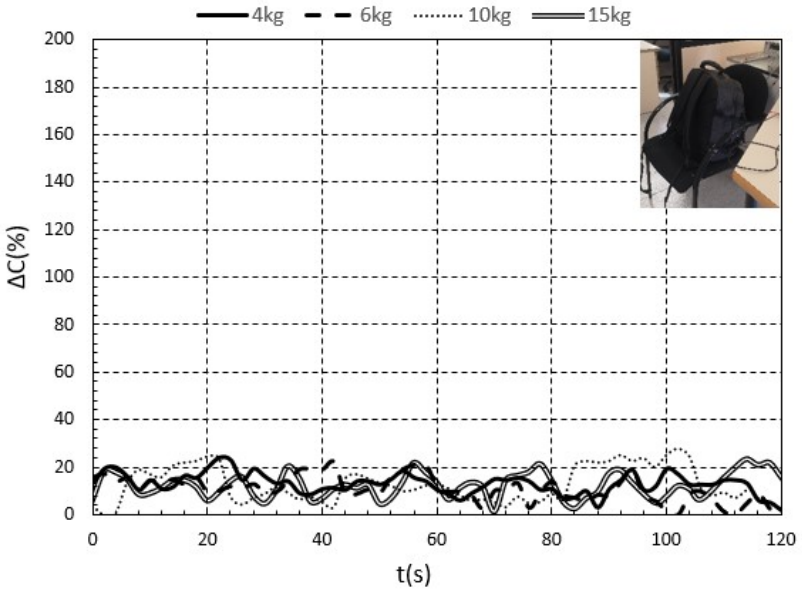

Figure 9.7: Capacity shift, in percentage, during load test

over the sensor, and remain between 15-20% of capacitance variation during the test performance. The results are similar for all load cases, which not provide any additional information for different load values. The study's conclusion points out that the variation during the bag cycle could be due to the bag material, which predictably, had a different permittivity value. These results permit to highlight the ability of the sensor to distinguish between a person and an object, due to the permittivity differences of the materials that compose the detected substance.

Both sensors present an interesting behaviour when presence test is performed, demonstrating their functionality as a presence sensor and opening the door to new applications opportunities.

9.4 Abrasion test

In this Section, a summary of the results reported and published in Paper F are provided.

An important factor in textile properties is the abrasion response of a fabric. Also, if the woven capacitive sensor is expected to perform properly in upholstery uses, the abrasion response of the sensor should be studied. To measure the impact of the abrasion over the sensor surface a Martindale test is performed over the manufactured woven sensors. The set up of the test was previously explained in Section 6.8.

Three different samples are prepared for the test. The non-conductive

substrates sample, the woven sensor manufactured with Bekaert yarn and the woven sensor produced with Shieldex yarn. Samples prepared on the test holders are observed in Figure 9.8

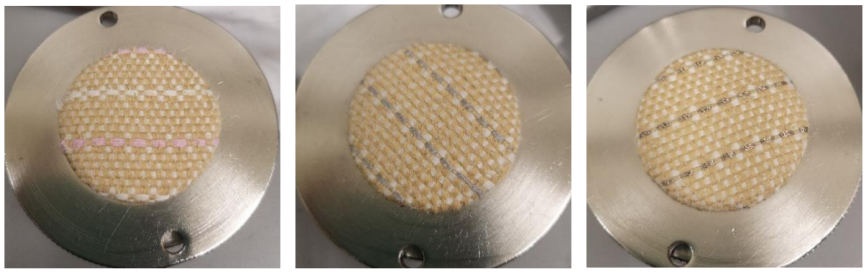

a) b) c)

Figure 9.8: Samples initial state. a) non-conductive sample b) Bekaert c) Shieldex

During the interval up to 6.000 cycles, the samples did not show any alteration. Electrical properties remain unaltered and physical aspect did not have signs of wear out. Further steps are performed, when the 20.000 cycle interval is completed some wear out effects are observed in samples (Figure 9.9). It is important to point out that the sample which is more affected is the non-conductive sample. The electrical properties are not being affected at this interval.

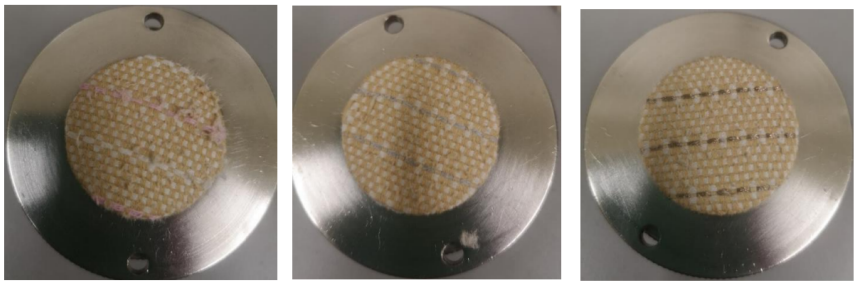

a) b) c)

Figure 9.9: Samples after 20.000 cycles. a) non-conductive sample b) Bekaert c) Shieldex

At the third cycle interval, which is up to 35.000 cycles, the conductive samples did not lose the continuity. However, when 40.000 cycles are finished the electrical continuity is lost. Figure 9.10 shows the sample states at this interval mentioned. The signs of wear out are important at this point, pilling is observed all over the fabric surface. Broken yarns are observed in non-conductive sample, but they are still not observed in both sensor fabrics.

For both electrical samples, the conductivity is decreased due to the

a) b) c)

Figure 9.10: Samples after 40.000 cycles. a) non-conductive sample b) Bekaert c) Shieldex

abrasion. However, this reduction on the electrical conductivity is not uniform on the samples. In Bekaert the resistance increases from 16 Ω/cm up to 120 Ω/cm whereas in Shieldex it increases from 0.7 Ω/cm up to 200 Ω/cm. Results are summarised in Table 9.5.

	Bekaert		**Shieldex**	
	Initial	**35k cycles**	**Initial**	**35k cycles**
Resistance Ω/cm	16	≤120	0.7	≤200

Table 9.5: Comparison between electrical properties before and after the Martindale test

The resistance rise is due to the lost of conductivity material for each yarn, Bekaert yarn lost some stainless steel fibres during the abrasion test. Meanwhile Shieldex yarn coating has been affected by the abrasion decreasing the quantity of silver in the filament surface.

9.5 Conclusions

At the moment that a textile sensor is preparing for large scale production the first step or check that must be fulfilled is to be woven. Weaving technology is the process method which is capable to produce more fabric meters in less time. But the process is limited by pattern availability and conductive materials integration. In this chapter the adaptability of the embroidered sensor design is studied.

The woven capacitive sensor, which is integrated into the structure of the woven fabric, is produced. Two yarns are used to observe the properties for each configuration of materials. Different yarns are not affecting so much the electrical properties of the overall sensor. But properties, as the repeatability, are slightly better on Bekaert yarn sensor. Several comparison

with the embroidered sensors measuring humidity levels are done, and it is concluded that woven capacitive sensor has similar behaviour but lower deviation error between different produced sensors.

Textile properties are less affected when the sensor is integrated into the structure, for example the sensor is unnoticeable by touch feeling. Ring yarns also respond better to the weaving process.

Abrasion effects on the woven capacitive sensor are acceptable for upholstery applications. Also, it is demonstrated that the abrasion resistance is improved by the conductive yarns used to produce the sensor. The textile properties not only are not affected negatively, but in abrasion case they are improved by the use of these conductive yarns.

The woven capacitive sensor has been tested detecting presence and it has been demonstrated that is capable to identify between void and occupied states. Furthermore, the woven sensor does not react significantly when a bag is placed over the sensor, which permits to distinguish between an object and a human. The new application tested opens a new path to develop presence sensors.

10

Applications for capacitive textile sensor

10.1 Introduction

During the works and tests developing the textile capacitive sensors, some cases of use show up. The experiments performed in previous chapters were done with the aim to demonstrate the usability of the textile capacitive sensors. Also, the different integration techniques were studied which integration methods characteristics provide information to select a path to develop different applications.

At embroidered textile sensors, the easiness of integration and the cost, suggest applications where the sensor is integrated on clothes which are not directly in contact with the body or uses where the cost of production could be a drawback for the development. Touch feeling of embroidery patterns is well-known by society, but if the user knows that the embroidered pattern also contains a *sensor* they could be concerned. Society is still unwilling to new technologies which they do not know.

A woven textile sensor was developed as a response to embroidered sensor drawbacks. Results demonstrate that it was a correct decision. The woven sensor physical properties improve the embroidered sensor properties, specially the touch feeling. Making the sensor unnoticeable and providing the opportunity to apply it in applications where direct contact with the body happen.

Taken the conclusions and results from previous chapters, several textile capacitive sensor applications are developed. The following sections present the applications developed and how the sensor performs.

10.2 A smart textile system to detect urine leakage

In this Section a summary of the results reported and published in Paper G are provided.

10.2.1 Introduction

Urine leakage, enuresis and similar diseases provoked by moisture are problems with high social impact and economic cost. Urine leakage is an affection that can suffer up to 33% of patients in health centres, such as hospitals, nursing homes, among others. Moreover, the urine leakage has not directly an impact on the patients' health, but associated consequences to the constant contact of skin with moisture. Infections or injuries are some of these consequences that could be avoided. Despite the fact that the methodology followed to reduce the appearance of these circumstances is the use of diapers, long time between substitutions of the wet diaper could produce injuries or infections. The root problem is the long time exposure to soak materials, diapers or sheets. As a response, nurses or caregivers, who work at hospitals or retirement homes, must check periodically diapers and sheets for every patient to reduce the period when the patient is in close contact with high levels of moisture.

The urine leakage detection requires a sensor fully integrated to have a low impact in user comfort. The usability of the sensor increases if the complete system could be installed without affecting the daily life of the patient. Also, these requirements may help medical staff to use the system without concerns or fear. Moreover, the integration could be carried out on bed clothes or underwear, providing real-time information about the humidity around the area. The information about moisture provided could help to take actions in an active way, affecting the patient only when required, avoiding the unnecessary checks.

As the PCB cannot be integrated in textile, to guarantee the wearability and usability, it should be as small as possible. The size of the electronics needed would be smaller than a buckle belt, which includes the battery. In order to be attached in any place of the bed structure or on the waistline.

A system is prepared to read the humidity values on a bed sheet and on underwear and send the data to be visualised by the nurses or caregivers.

10.2.2 System architecture

The system architecture, which takes the humidity values from the sensor and communicate them, is based on a textile sensor node, a gateway and a remote server. The scheme architecture is shown in Figure 10.1 Each part of the system has a specific task to conduct. The textile sensor node is in charge of obtaining the values of humidity of its surrounds and wireless transmitting them through the gateway. The data is configured to be saved in a database. It could be configured to be sent by WiFi (internet connection) or Bluetooth, but the internet connection which is present in the installations is the best network to use, as it provides more read range than Bluetooth. The remote server is prepared to be able to read the database and visualise the data for the caregivers and nurses.

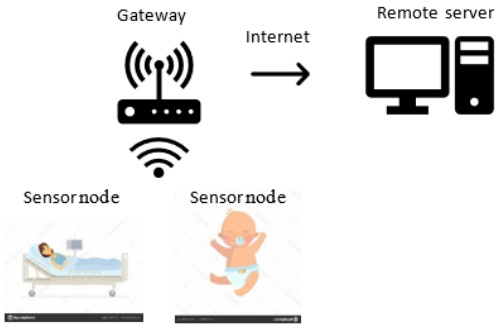

Figure 10.1: System architecture

The developed system provides real-time data collection and should give the mechanism to the hospital or nursing home staff to control multiple nodes at the same time permitting them to take actions actively.

10.2.3 Sensor node

The core of the wearable system is the textile sensor. The sensor used for the application presented follows the lines presented along this thesis document. The sensor is an interdigital structure, embroidered over a textile substrate. The moisture provokes a shift in its substrate properties, specifically in capacitance values. The textile sensor needs an unit control (UC) to measure the capacitance value from the interdigital structure and transmits the values obtained by means of a wireless connection. The UC contains a battery to have autonomy, but it is prepared depending on the time needed. The aim is to achieve a system able to obtain the data and send it with the minimum size.

Textile moisture sensor

The textile capacitive sensor is built as it was explained in Chapter 8. But some considerations need to be explained, as the capacitance value of the sensor is given by the dimensions of the pattern (geometrical properties) and material properties (dielectric permittivity), the first step is to design the interdigital structure to embroider in each situation. As the textile sensor is prepared to be used in an underwear and a bedsheet, two different sizes need to be designed. The area of measurement for both situations should cover approximately the zone where the humidity could appear without trespassing the available substrate size. For the bed sheet, the sensor is embroidered covering the body standard width centred, which is where the urine leakage is expected and risk zone where sores are more common. In the underwear the location is placed where the urine is dropped in the diaper and where the diaper extracts the moisture and the sensor would detect it. As it was explained in Section 4 CST Studio simulation is performed to determine an approximation of the capacitance value and make sure that the textile sensor could be measured by the UC. Figure 10.2 shows the design parameters which are modified to prepare the sensor, which are defined as height(H), length (L), distance between lines(d), distance between vertical and horizontal lines(c), line thickness(e) and pair of fingers (n). Dimensions for both sensors are presented in Table 10.1.

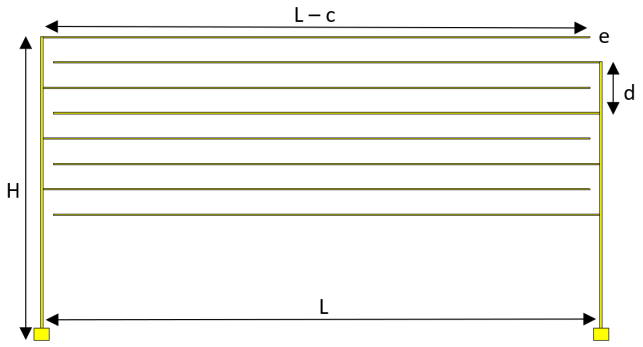

Figure 10.2: Sensor design on CST Studio between

	H(mm)	**L**(mm)	**d**(mm)	**c**(mm)	**e**(mm)	**n**
Underwear	30	69	2	2	1	4
Sheet	150	220	8	4	2	4

Table 10.1: Dimensions of sensors presented

The yarn used in both cases is the Shieldex yarn that has been used previously. The yarn is made by 17 filaments of polyamide coated with

pure silver. To connect the sensor to the UC, snaps are installed in both integrated sensors. On the sheet they are installed in one of the borders, meanwhile for the underwear are installed on the waist.

Finally, both sensors are embroidered on respective substrates. The underwear is produced by mixed cotton-polyester yarns, meanwhile for the bed sheet is composed by pure cotton yarns, very similar to the sheets used at hospitals. The substrate compositions are important for the analysis of the behaviour, because, as it has already demonstrated, substrates are the key parameter for the sensor tendency and sensitivity. These parameters are also affected by chemical treatments that could be done over the substrates. Both examples of textile embroidered sensor are observed on Figures 10.3 and 10.4

Figure 10.3: Underwear embroidered

Unit control

The UC is based on the microcontroller SAM D21 family provided by Microchip and wireless interface NINA-W10 from u-Blox which provides WiFi and Bluetooth connectivity. Other of the main characteristics of the microcontroller are low-power, 32-bit Cortex-M0+ MCU with Advanced Analog to Digital Converter (ADC) and Pulse Witdh Modulator (PWM).

The location of the UC depends on the application. When the system is installed for the measurement of moisture in a bed, the device is being attached to the bottom face of the bed, where one of the borders of the sheet is placed. For the bed case, the battery is not needed for the UC power supply, which could be provided by an external power source such as the other hospital devices which are close to every bed used for the patient

Figure 10.4: Sensor embroidered on a sheet

monitoring. As the UC is placed under the bed, it can be connected as well without any inconvenience to the patient comfort and safety. In the underwear case, the application implies the variability and a battery is needed. The battery and the UC conform a unit which is designed to be an isolated box. The microcontroller selected has low power options to decrease at the minimum the power consumption of the system.

The microcontroller used on the system consumes 40 mA, without any low power set up, during the WiFi connection. On the measurements it might consume until 80 mA. The 80 mA consumption lasts less than 1 second. Considering these consumption's, the battery necessary to feed the UC could spend 80 mAh, if it is measuring every second. It could be decreased to hardly 40 mAh if the measurements are done in a large space of time. If the measurement is taken every 2 seconds and takes into account 5 seconds preparing the communication, the sensor will consume 60mAh. It means that with a 1200 mAh battery, which size is similar to a buckle belt, the sensor will have a 20 hours of battery life. Despite the fact that consumption is high, it is necessary to take into account that low power strategies have not been applied in this application yet.

Implementation of charge-discharge method

The methodology to measure the capacitance on the application must be adapted to fulfil the requirements. The capacitance from the sensor is measured by the microcontroller's ADC and its wide range implies two different

measurement circuits. To measure the capacitance a two circuits charge-discharge method is designed. The process of the charge discharge method was previously explained in Section 6.4.2. Figure 10.5 present the connection diagram used to measure each range that the textile capacitive sensor could have.

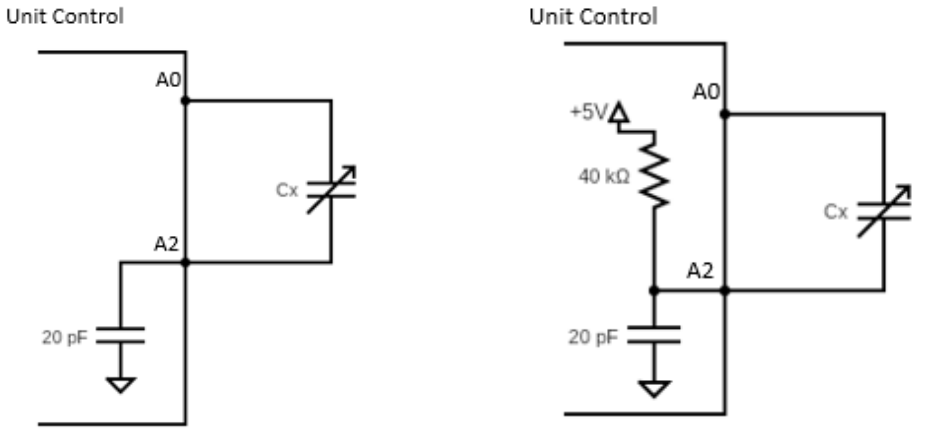

(a) Circuit on pF measurement range

(b) Circuit on nF or uF measurement range

Figure 10.5: Measurement circuits of the textile sensor value

To begin the measurement and verify that the sensor is uncharged, both terminals are connected to 0V. Hereafter, A0 terminal is set at 5V for the first measurement circuit. The voltage at A0 charges Cx (textile sensor) and a 20 pF capacitance, which is internally connected to the pin. The first measurement circuit can be observed in Figure 10.5a. When Cx is fully charged the voltage at A2 is measured and the Cx value can be obtained by means of the equation:

$$C_x = \frac{V_{out}}{V_{in} - V_{out}} C_{int} \tag{10.1}$$

Where:

$C_x = capacitance\ from\ textile\ sensor$
$V_{out} = Voltage\ on\ A2$
$V_{in} = Voltage\ on\ A0$
$C_{int} = internal\ capacitance\ in\ pin\ A2\ (20\,pF)$

If the voltage value at A2 terminal reaches 4,8V it means that the Cx

$\gg$ 20pF, then a different measurement circuit should be used to obtain the capacitive value of the sensor. The circuit necessary to measure the capacitance at this point is shown on Figure 10.5b. The A2 pin is configured as an input, where a pull-up resistance is set up, and A0 pin is set at 0V. Cx starts to charge when both pins are configured, and a timer counts the time till the Cx is charged. When it is finished, the Cx value is calculated by the equation.

$$C_x = \frac{-t/R}{ln(1 - \frac{V_{out}}{5})} \tag{10.2}$$

Where:

$C_x = capacitance\ from\ textile\ sensor$
$V_{out} = Voltage\ on\ A2$
$R = Pull - up\ resistance\ (40k\Omega)$
$t = chargetime$

Both measurement circuits and methods cover the entire range of values that the textile capacitive sensor could take.

Data management

When the capacitance value is obtained, it is saved on the UC and transmitted by wireless communication to the gateway by means of HTTP protocol. The complete micro routine is depicted in Figure 10.6. The time in which the procedure is completed is about 1,5 seconds, which is needed to guarantee the charge and discharge of the capacitance for the whole range.

10.2.4 Remote server

Data transmitted by the sensor node is stored in the remote server. Information received is saved in a specific database for every sensor node. Real-time visualisation is prepared with an user interface to be as clear as possible. To develop the database and the web server, XAMPP software was chosen. This software includes the operations to create a HTTP Apache web server and a MySQL database. The software is intuitive, easy to implement and with a large community behind that gives support and provides enough information to easily build it. The control panel for XAMPP is shown in Figure 10.7

The database developed can be seen in Figure 10.8The structure consists of three data fields: id, raw data and time stamp. The *id* identifies the sensor node from where is the data arriving. The *raw data* stores the capacitance value obtained from the sensor and the *time stamp* marks once the measurement was done. The sensor id is previously registered on the

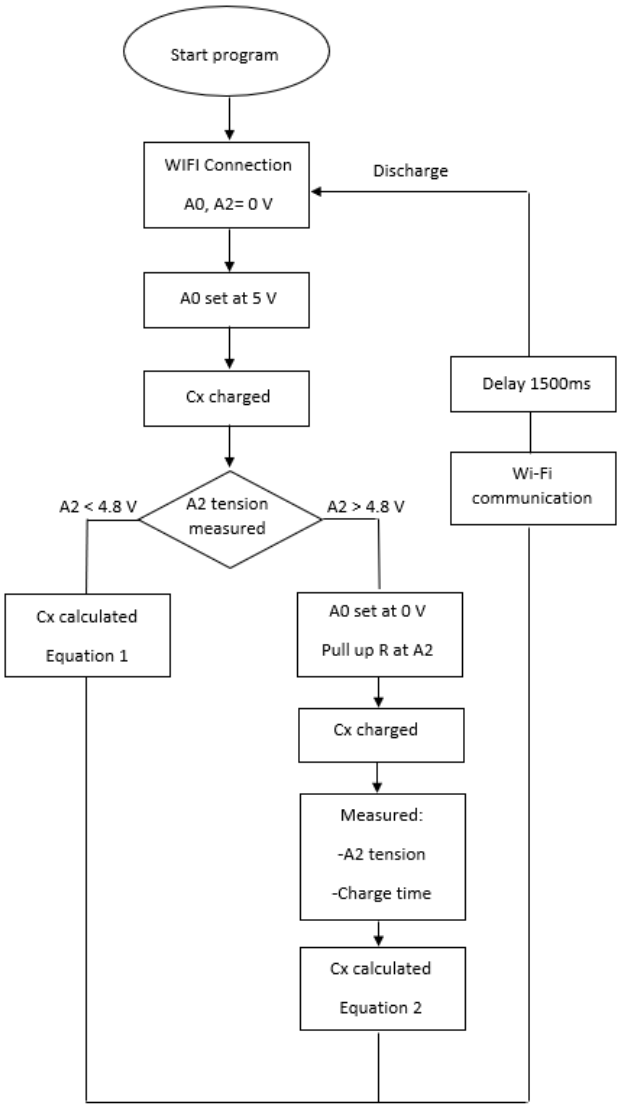

Figure 10.6: Routines to calculate capacitance

database to guarantee write permissions to the UC data. The database and the protocol defined for the UC are prepared to admit new data fields such as battery life time. Database information provides the opportunity to take actions actively and be conscious of the exact time of the urine leakage.

The graphic user interface (GUI), which has been developed with Grafana, is observed in Figure 10.9. Grafana is an open source software, which can be used as a web application, selected due to its compatibility with MySQL database. Grafana tools permits to connect with the database immediately.

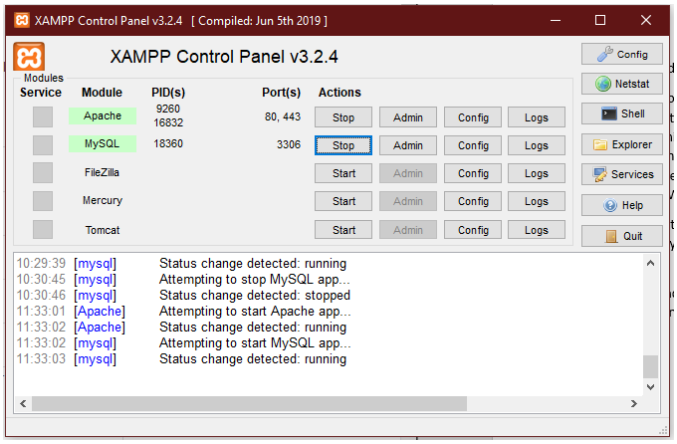

Figure 10.7: XAMPP control panel

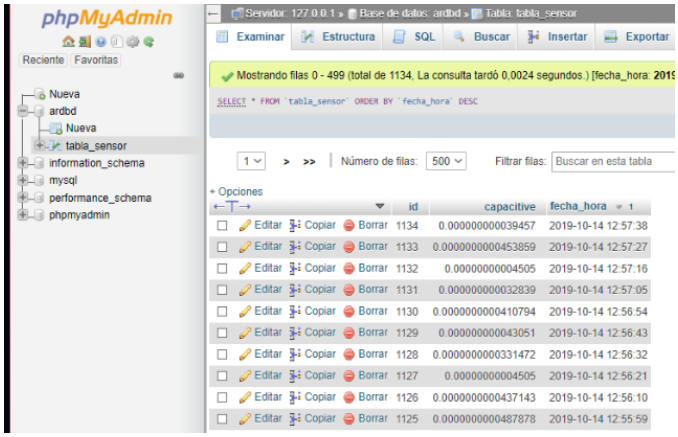

Figure 10.8: Database table filled by the board

The visualisation of the capacitance values are prepared to be shown in a graph where abscissa axis represents the measurement time stamp and ordinate axis the measure textile sensor capacitance. An example of sensor response is observed in Figure 10.9. The response observed corresponds to a moisture swept form 40% of relative humidity(RH) up to moisture saturation of the sensor. Slightly changes are observed in the graph during the swept from 40% to 70%, which are presented in logarithmic scale in order to observe all the range. When the moisture enters in contact with the sensor, the capacitance values suddenly increases. The values provide a valuable information of the moment where the moisture enter in contact with the sensor and which could be used by staff from hospitals and nursing homes.

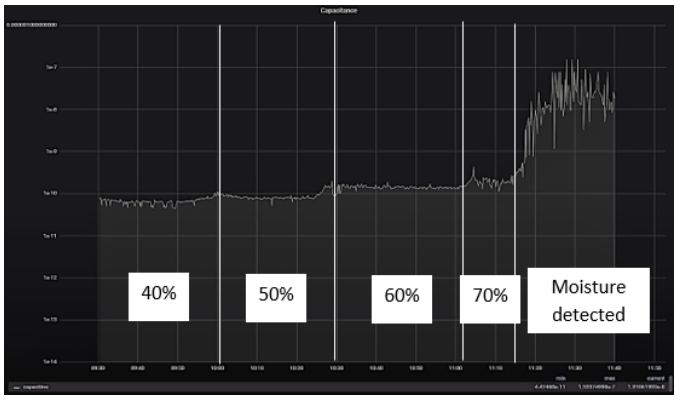

Figure 10.9: Example of Grafana graph. Y-axis depicts the capacitance measured. X-axis, the time when the value has been taken.

10.2.5 System in action

The system is tested under two different situations for every textile sensor prepared. One of the situations consists of the comparison between the charge discharge method and the Rohde & Schwarz HM8118 LCR meter measurements. To compare both measured values the sensor is introduced in the CCK-25/48 Dycometal climatic chamber. The sensor is prepared on a holder, an placed into the climatic chamber connected once to the LCR and, afterwards to the UC. The climatic chamber parameters, such as temperature and relative humidity, are controlled by a LabView program. The second test consists on the leakage detection trying to simulate a real case. In this case, each test has some specific parameters, but, in general, a diaper for every case is disposed over the sensor and a leakage is simulated over it. The quantity of water dropped will depend on the case.

Underwear

The embroidered sensor integrated on an underwear is characterised. On Figure 10.10 a swept from 30% to 80% of relative humidity is shown. The permittivity change provoked by the increase of moisture in the environment and over the substrate surface when moisture is absorbed, affects directly to the capacitance value. The graph shows the measurement results for the LCR meter and the Unit Control (charge/discharge method). Capacitance values for 30% are about 10pF and it reaches about 10nF for 80% RH. Both measurement values are slightly different, due to the different nature of the values. The charge discharge method is measured in direct current and an LCR is measured in alternate current at low frequency. Despite the different values, they do not have any impact on the system functionality, because the system needs to focus on a reached threshold.

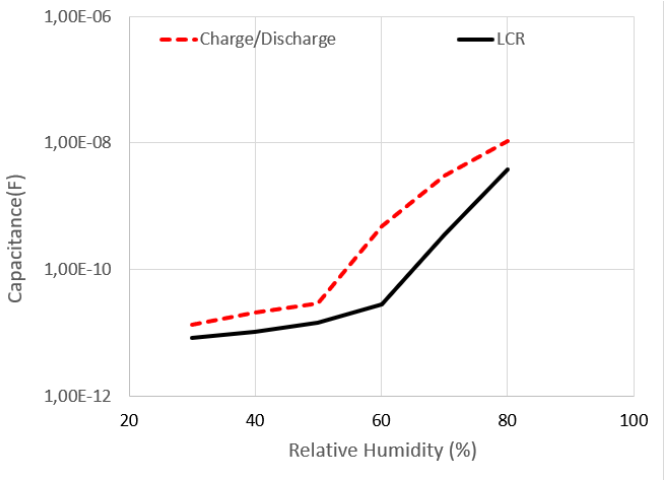

Figure 10.10: Sensor on underwear measured with LCR meter and Charge/discharge method from 30% RH to 80% RH

The results obtained from the comparison permit to follow the next step and test the system behaviour to detect a leakage from a diaper. The test is due as a real situation, where measurements were visualised from the GUI presented. The diaper was placed inside the underwear with the sensor area oriented along the diaper, which covers as much surface as it can.

To simulate the miction of a baby or child, 80 to 100 ml are prepared. The diaper selected characteristics indicate that it is able to absorb till 240 ml without giving the user a wet feeling. The sensor is connected and data is received. After 600 seconds, 100 ml of water are poured into the diaper to simulate a urine leakage. As it is observed in Figure 10.11 once the urine leakage is produced, the sensor capacitance value is increased at the moment. The fact means that the diaper absorption traps the water poured into the absorbent material and this material starts to expel moisture to the outside of the diaper, which is the main process that gives a dry feeling to the user.

The outer part of the diaper starts to have moisture because of that flow from the inside. It is observed how the value of the sensor increases significantly from 37 pF to $149\mu F$ in less than 120 seconds. Notice that before pouring the water, the sensor value was the environmental relative humidity value, which corresponds to about 55% according to the previous sensor characterisation by charge/discharge method. At this moment the diaper is removed, as it was expected to happen in a real time situation. The recovery time is also measured, and the capacitance value reach 126 pF in 600 seconds. The sensor capacitance value does not recover the original value, which can be treated as hysteresis, which is caused by hydrophilic behaviour of the cotton. But as the detection value is far from that point, the capacitance value is accepted as recovered to use it again.

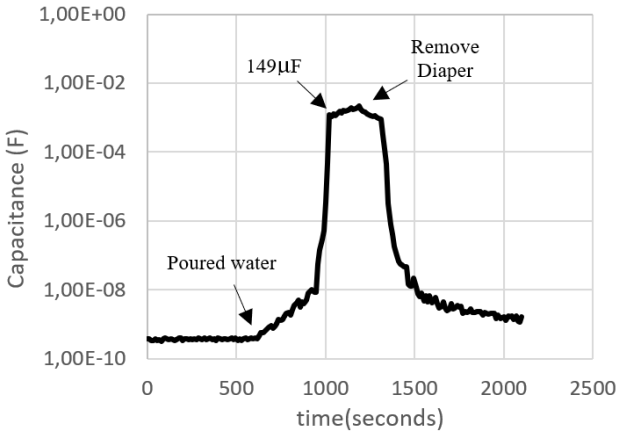

Figure 10.11: Sensor capacitance evolution when 100 mL of water are poured on the diaper

Cotton Sheets

For this case, the sensor size has been increased, in order to increase the are of detection. In Figure 10.12 sensor values obtained by different methodologies are compared. As it was done with the underwear case, LCR meter values and charge/discharge values are presented in the same graph. A swept of 40-90% RH is performed. The capacitance value for 40% RH is about 250-300pF and it reaches up to $20\mu F$ for 90% RH. Although the behaviour along the relative humidity swept is different between the methods, it is necessary to remember that both capacitance values have different natures, the values measured on wet/dry situations are close to each other. Again, the proposed system can be used to detect wet conditions and urine leakage appearance.

Figure 10.13 the measured capacitance with the complete system is shown for a adult diaper. Adult diaper can absorb almost 10 time more moisture than a baby diaper. The miction volume of an adult is between 250-750ml. To reproduce a real time situation 750ml of water were poured in the diaper placed over the sensor. The pouring quantity is also close to the limit absorption as previously done in the other case. As it is shown in the graph, after the pouring, a slight change in the capacitance from 280pF to 500pF is detected. The adult diaper does not expel the moisture as it was seen on the baby diaper. After 600 seconds the capacitance of the sensor changes abruptly up to $320\mu F$. The moisture is detected when a real leakage from the diaper occurred, as the adult diaper has a layer to avoid diffusion of the moisture in vapour. Once the diaper is retired, the sheet starts to dry and the sensor recovers its initial capacitance value.

For both textile capacitive sensors used in the system the sensitivity and

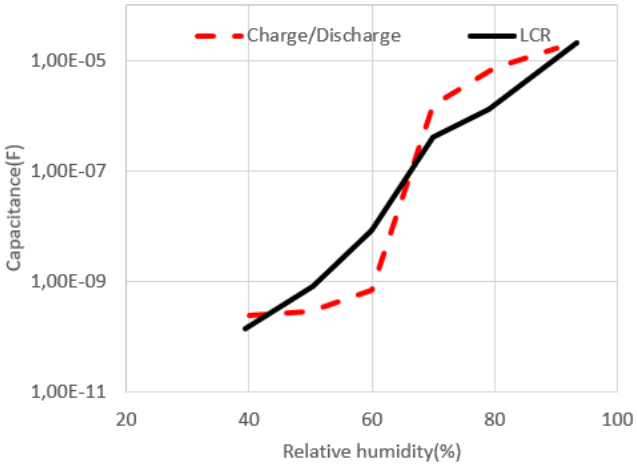

Figure 10.12: Sensor on a sheet measured with LCR meter and Charge/discharge method from 40% RH to 90% RH

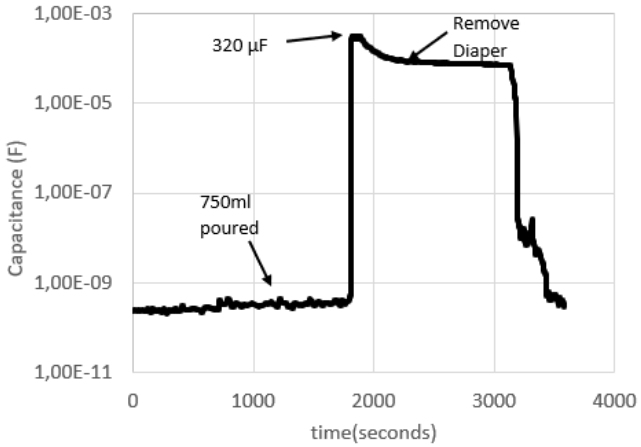

Figure 10.13: Sensor on a sheet capacitance evolution when 100 mL of water are poured on the diaper

linearity were studied obtaining the values shown in Table 10.2

	e(mm)	**d**(mm)	**Sensitivity**(Z)/%RH	**Linearity** R^2
Underwear	1	2	-0.034	0.8759
Sheet	2	8	-0.0804	0.9875

Table 10.2: Sensitivity and linearity for the sensor in each application

10.3 A smart chair to monitor sitting posture by capacitive textile sensors.

In this Section a summary of the results reported and published in Paper H are provided.

10.3.1 Introduction

During the woven capacitive sensor test, a new application for the textile capacitive sensor was found. The presence detection was demonstrated during the test performed to the woven capacitive sensor. A 3 months stay was done at Tampere University, Finland, where, they are currently working on smart textiles. They have several open projects that they are currently working on. One of these projects plan to design smart furniture which can interact with the users by integrating textile sensors on it.

A smart chair to monitor the gesture was started to be designed. As the initial results from the capacitive sensor detecting presence were though to be a binary response, pressure detection was not considered.

The great part of the jobs tend to be office work, where prolonged static sitting positions are repeated for several days. These sedentary occupations present health risk for developing musculoskeletal disorders, cardiovascular, metabolic and cognitive issues. For these reason, it was prepared to introduce sensors in one of the components of the workstations, the office chair. Adjusting the chair set up to an ergonomic optimal positioning and follow it during the session, may reduce musculoskeletal risks for pain and discomfort of the lower back, elbows, fingers and legs.

An ergonomic position is not the only requirement to avoid the issues mentioned, the movement of the person is also needed. A dynamic or active sitting is also needed, where sitting positions change during time to avoid long periods with the same gesture.

Ergonomic office chairs have been designed to help people to achieve optimal posture. They have been designed to be adjustable in shape, height, armrests, reclining backrest and additional lumbar spine supports. But users are not used to adjust the chair for themselves. A feedback system integrated into the chair may help to tackle this issue and guide the users towards a more optimal sitting posture.

The ergonomic chairs are commonly covered with textile, which provides a substrate to integrate the textile capacitive sensors. Being so close to the body, the sensors provide a direct sensing, which could not be provided by other sensors.

The feedback system needs also a microcontroller to obtain the values from the textile capacitive sensors. The data from the sensor is analysed and organised to be stored. The information could be sent to a database or visualised in real time. The idea would be to create a software that uses the

information from the sensor to notify the person sat when they are having a bad position, when they need to move or when they need to stand up. The final system is designed as a tool for companies to promote their workers' health, but also could be used by hospitals or nursing homes, or even being installed on wheelchairs.

10.3.2 Office chair preparation

The sitting behaviour is studied to identify the optimal places where the sensor should be. The data from the sensor should be enough to determine the position taken by the person, and from here to decide if an action is needed. The sensor distribution on an office chair is shown on Figure 10.14. The sensor positions are spots where the user contact defines the gesture.

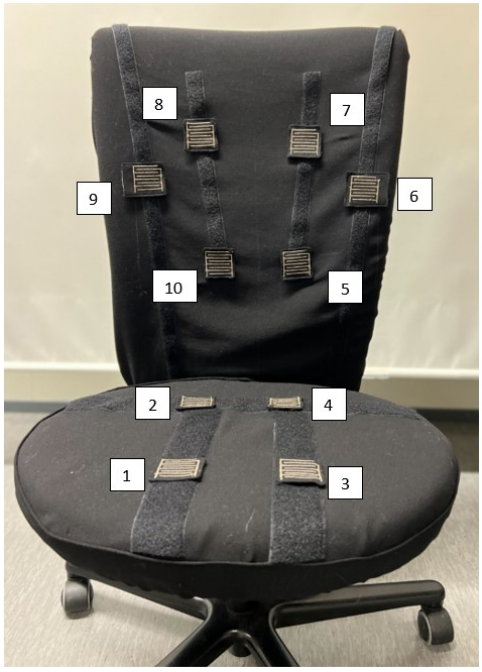

Figure 10.14: Smart chair with sensor distribution and number identification

The locations identified are: i) bilaterally on the lower back (to promote straight posture with the hips as close to the backrest of chair as possible); ii) bilaterally on the upper back just beneath the shoulder blades to promote the user's proximity with the backrest of the chair and to prevent slumped sitting and forward lean posture; iii) bilaterally on the sides of the mid-back to prevent excessive leaning to the side; and iv) bilaterally on the buttocks and on the back of the thighs to ensure contact with the seat and to discourage crossing the legs or not centred positions.

The textile sensor is prepared by embroidery technique, due to the fast

prototyping and low cost. The yarn used is a Shieldex 110/34 dtex 2-ply, which was the yarn supplied by the Tampere University. Dimensions and structure of the interdigital textile sensor are shown in Figure 10.15. The size designed accomplishes the requirement of detection of proximity and covers the desired zone. Bigger sensor could not provide the accuracy desired to distinguish between positions. The substrate chosen was a 100% wool crepe fabric, which is an elastic material commonly use to create covers.

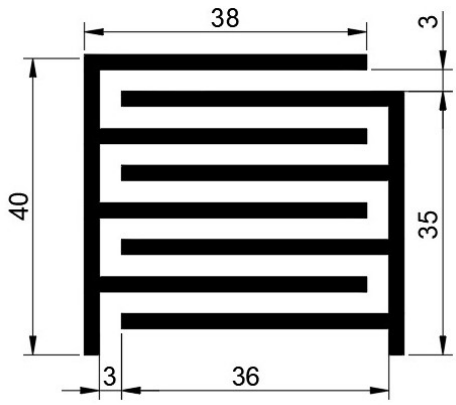

Figure 10.15: Interdigitated sensor geometry (dimensions in mm)

The prototype was built over an office chair without armrests. The chair was covered with the substrate with some Velcro lines attached. The idea of the Velcro lines is to have the opportunity of replacing the sensors for the position test in case some location must be modified. Embroidered capacitive sensors were sewn individually to a piece of Velcro (opposite to the Velcro lines in the chair). An individual sensor is presented in Figure 10.16

Figure 10.16: Ready-made sensor from both sides

10.3.3 Implementation of the cycle count method

Two parts are explained in this section. The measurement procedure during the test and the steps followed by the volunteers and positions taken.

Figure 10.17 shows the circuit designed for every sensor placed on the Smart Chair. The cycle count method was explained previously in Section 6.4.2.

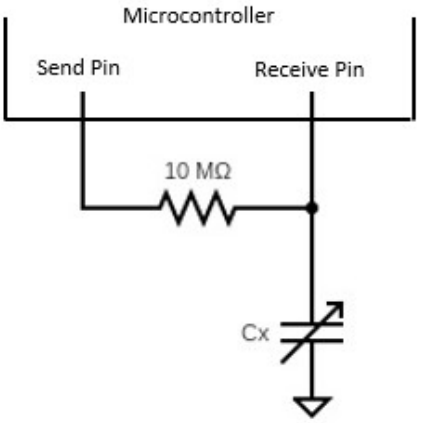

Figure 10.17: Measurement circuit of each individual sensor

For this implementation, two microcontroller pins are required as a send and receive pin. Send pin is the port where the 5V tension is set up. Receive pin is the port where the tension value is compared with the send pin constantly. These microcontroller pins are connected with a resistance between them. In the circuit used, the resistance value is $10M\Omega$, because it was the value that provides the desired behaviour. The resistance could be set up between $100k\Omega\Omega$ to $50M\Omega$, which defines the resolution of the method. The sensor is connected on the receive pin, as it is shown in Figure 10.17.

The measurement process starts setting up a 5V tension on the send pin. Then, the current goes through the resistance, the higher is the resistance, the lower is the current. The unknown capacitance (capacitive sensor) starts to be charged due to the current that flows through the resistance. The voltage is measured in the receive pin and compared with the tension set up in send pin. In the meantime that there is no match between both voltages, the software counts every cycle done. When the capacitor is fully charged, the voltage in both pins are equal, then, the program stops counting cycles. The number of cycles counted is used to indicate the sensor value. The microcontroller provides a vector with the values of every sensor connected to it, following the receive pin order of the sensor measured.

During the measurements, it is observed that the cycle count process

provides information about different levels depending on body proximity. As the capacitive sensor working principle relies on the permittivity change around it, during the presence detection the sensor is measuring the proximity of the body to it. Hence, when there is more pressure between the body and the chair surface, the clothes from the volunteer are pressed. The pressure reduces the distance between their body and the sensor, causing an increase in the number of cycles. But this fact has a limit, which is the cloth limit to be pressed. Different levels observed during tests are presented in Table 10.3

	Surrounding detection	**Contact**	**Close contact** (pressure)	**Higher contact** (pressure)
Cycle count	± 500	± 1000	± 1500	± 2000

Table 10.3: Levels of activation of the sensor depending on the cycle count.

The level that indicates contact between sensor and body of the volunteer is marked in each individual graph by a red dash line.

10.3.4 Positions measured by the feedback system

For the test procedure followed by the volunteers, all measurements are taken in office settings. Each participant is asked to adjust the office chair once they are sat on it. They are asked to verify that feet are in contact with the floor and buttock area is located as close to the backrest as possible. The positions are requested to be done exaggerated, to observe more differences between the data values. At this point, the sensor locations are checked to match with every corresponding participant's physical marker. The process prepared consists on the 8 most common positions taken or expected, which are presented in Figure 10.18. The positions selected include the optimal ergonomic sitting position, crossed leg, lean the back to sides, leaning back and detachment from the backrest.

Five volunteers have been tested to compare different sitting behaviour when similar positions are taken. The aim is to be able to see the gesture that the volunteers are taken.

To refer to each sensor, a number is associated with each one, The numbers are presented in previous image in Figure 10.14. Sensors from 1 to 4 are the seat sensors, 1 and 3 are front sensors and 2 and 4 back seat sensors. Sensors from 5 to 10 are distributed on the backrest. Low back sensors are 5 and 10, middle back sensors are 6 and 9 and high back sensors are 7 and 8.

The first of the positions and the reference position for the entire study is the ergonomic posture. The ergonomic position should not provoke any

Figure 10.18: Measured sitting positions during the smart chair test

disorder risk or tension all over the body. Data from the volunteers sitting in that positions is shown in Figure 10.19

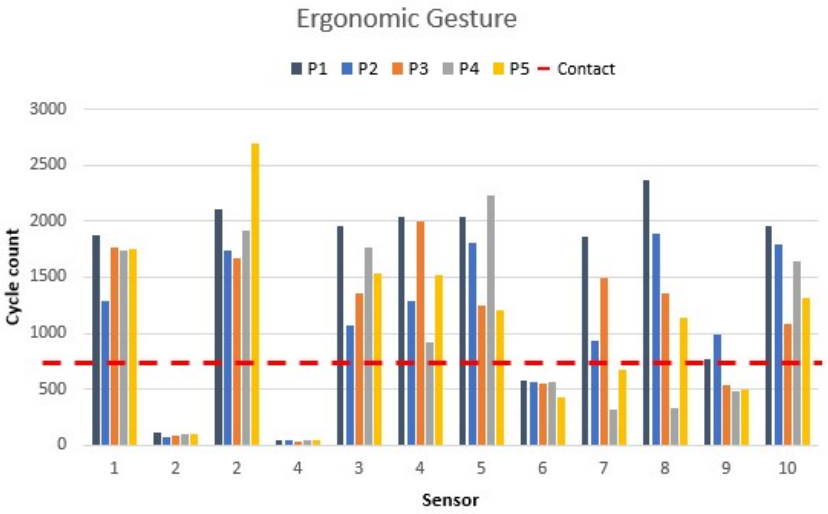

Figure 10.19: The ergonomic posture sensor values as shown in Figure 10.18a

Every sensor on the seat acquires a value higher than 1000 when the ergonomic position is taken by the participants. The backrest sensors are activated depending if the back of the participant is close enough to the sensor. The majority of the participants, except one, perform the ergonomic gesture correctly. Middle back sensor should not be activated which means that the participant is centred on the chair. The values of these sensors are not 0, because they are detecting the body close to them but not in contact. Participant 4 did not activate high back sensor (7 and 8) which indicates that their back curvature did not permit them to be close enough.

The sensor values show asymmetrical distribution for the participants 2,4 and 5 to the right. The differences observed for the sensor values were calculated as $\Delta S = (S2 - S4)$ and the results are accepted as the difference of pressure done. Participant 2 had a $\Delta S = 456$, participant 4 had a $\Delta S = 152$ and participant 5 had a $\Delta S = 1170$. Another participant, in that case participant 3, showed and asymmetrical position to the left, indicated by the negative result, $\Delta S = -325$

Next step is to analyse the sensors values when one leg is crossed, for each leg case. This position is usually taken by workers to provide distension from their bodies. Participants crossed first their right leg. Figure 10.20 shows right leg crossed data

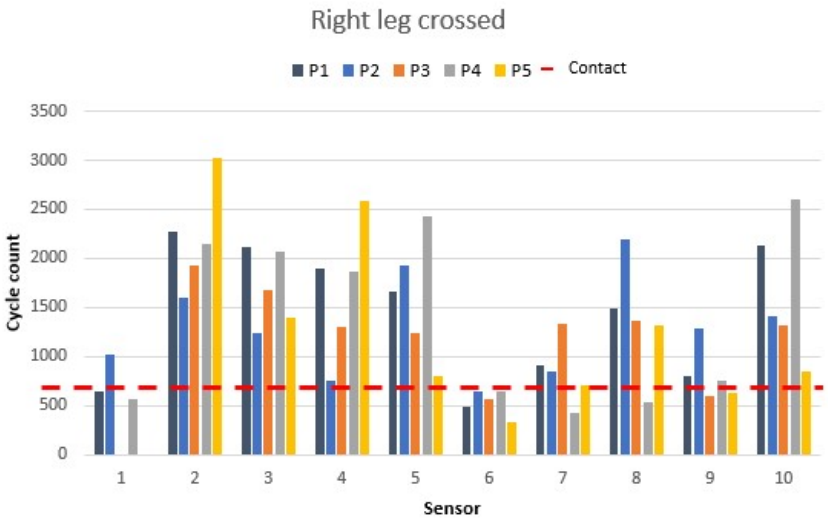

Figure 10.20: Right leg crossed sensor values as shown in Figure 10.18b

Sensor 1 is expected to have values close to 0 during this position test. Four participants, but participant 2, matched the condition described and showed activation exclusively in sensor 3, from the front seat sensors. Participant 2 increased the pressure in sensor 8 and 9, which correspond to the right side upper and middle back. The values could describe a difficult to

take the position or a discomfort on it. Participant 4 held all the pressure provoked from the movement on the right low back sensor(10). Participants are asked to cross the left leg, values resulting from the movement are depicted in Figure 10.21

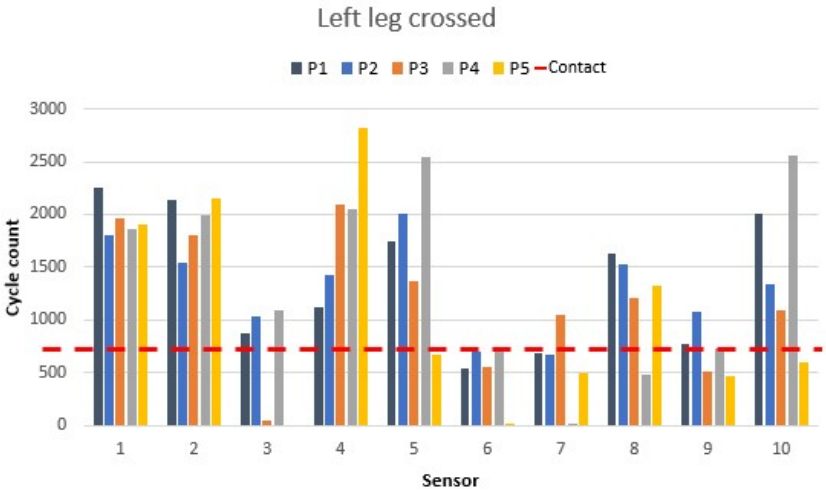

Figure 10.21: Left leg crossed sensor values as shown in Figure 10.18c

The noticeable change is provoked by the leg change, and corresponds to the values expected. Values from sensor 1 and 3 are changed and take the value that the other sensor had in previous position. But participants 1, 2 and 3 shows that the flexibility on their left leg do not let them to take the position correctly and avoid some detection, they had values close to 500. The back seat sensors take higher values when the leg that correspond to the side is crossed, due to the pressure. Similar effect is observed in backrest sensor, which exchange values between sides from one test to another.

The feedback system demonstrates to detect how the leg crossed affects the sitting position and the pressure distribution.

The following posture is performed by workers when they are doing task under pressure. The tension provokes a detaching of the back from the backrest leaning to the table or the screen they are working on. Figure 10.22 shows the position values.

The movement affects the values observed in high back sensors(7 and 8) and middle sensors (6 and 9) which are deactivated. Low back sensor (5 and 10) values depend on the detachment of every person. In that case participants 1, 2 and 3 maintain their lower back in contact with the backrest. Seat sensors did not experiment any change.

Sitting on the edge position could be taken by workers who expect to finish the task in a short period of time and get up again. Figure 10.23 shows the values for that position

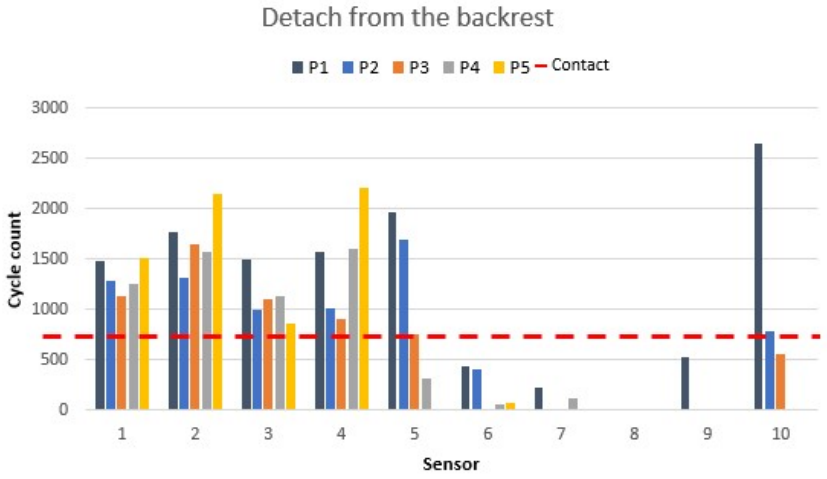

Figure 10.22: Detach from the backrest sensor values as shown in Figure 10.18d

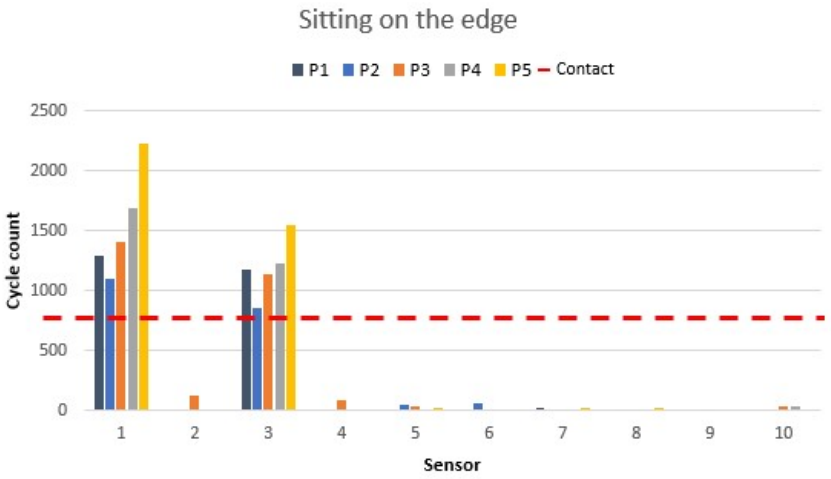

Figure 10.23: Sitting on the edge of the chair sensor values as shown in Figure 10.18e

The results obtained by the sensor clearly identify all participant only activate the front seat sensors. The position discussed should be avoided. A timer could be set in the software to play an alarm if the position is maintained from a long period of time.

Next positions tested are previous moments to a fall of the chair or also, if the position taken by the user is very asymmetrical. Figure 10.24 shows the leaning right position values.

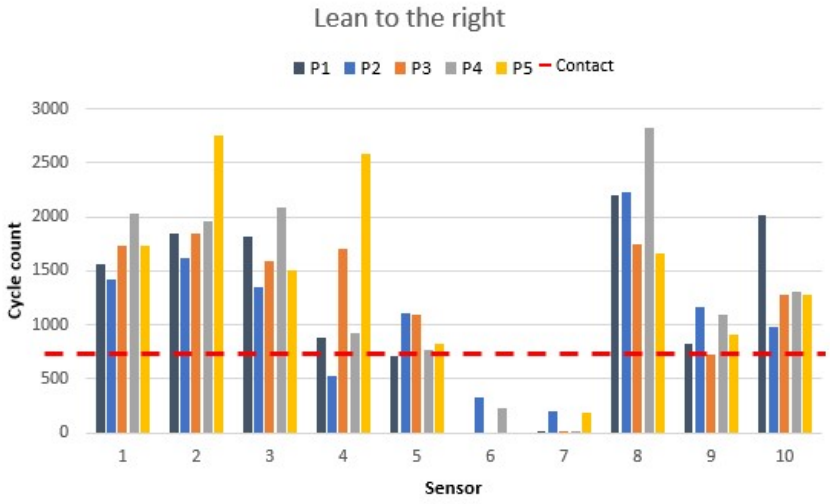

Figure 10.24: Right leaning sensor values as shown in Figure 10.18f

When participants leaned to the right sensors 6 and 7 were deactivated. Value from the sensor 9, which corresponds right middle backrest is activated reaching its higher value during the test. Sensor 8, right higher backrest, increase its value due to the pressure applied on it. The position is clearly differentiated from the others. Participants change the position and leaned to the left. The values of the leaning change are depicted in Figure 10.25.

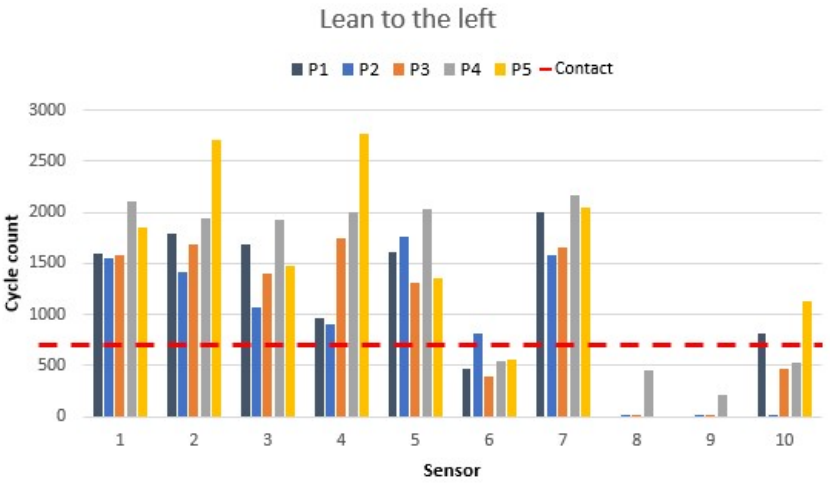

Figure 10.25: Left leaning sensor values as shown in Figure 10.18g

Sensors 8 and 9, previously activated are deactivated by the leaning. Sensors 6 and 7, the opposite sensors, are now activated. Sensor 10 and

5, which corresponds to lower backrest, exchange values when the leaning change is done. Seat sensors are not experiencing any value change, due to the participants only leaning their backs. For both leaning situations detection is demonstrated. Leaning detection could be more useful in other smart chair applications, such as a wheelchair, where people with mobility disorders need to be monitored to avoid harm. Also in real-time situation values from the seat are going to change. Alarm could be played if every right/left side sensor deactivate or activate at the same time.

The last position analysed is usually adopted by tired persons in office chairs. The lower back is detached from the backrest by a movement to the from performed by the hips. The back is curved due to the movement and normally the legs are stretched. The sensor values for the position taken by participants is shown in Figure 10.26.

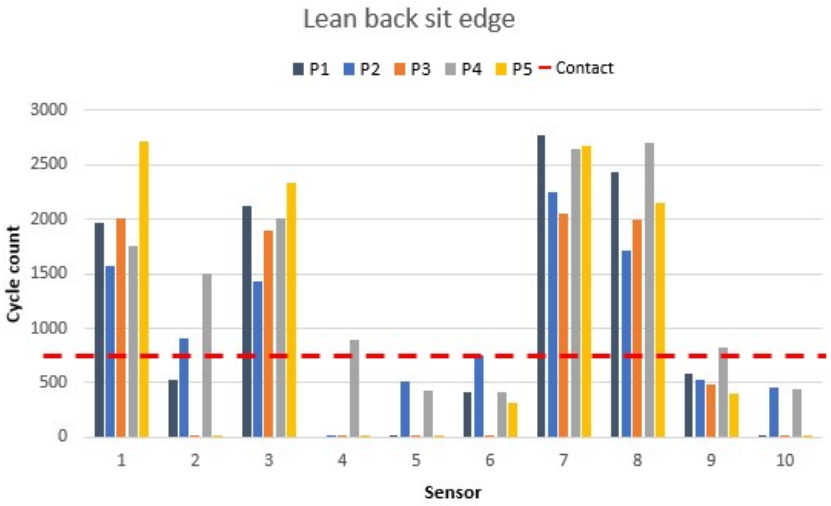

Figure 10.26: Left leaning sensor values as shown in Figure 10.18h

Sensor activated are 1 and 3, from the front seat, and 7 and 8, from the high backrest. The other sensor are deactivated or detecting body close to it, but normally lower than contact value. The values from the sensor activated reach their higher value, which means that pressure is higher than any other position.

The feedback system demonstrates its functionality. The chair permits the differentiation of the positions taken by the participants and definition of alarms could be prepared to avoid risk situations. It is observed that the measurement methodology provides different level of activation for the sensors, which are being defined as proximity, contact, close contact and high pressure. The feedback system is presented as a tool to correct the position, detect asymmetrical gesture or monitor the movement behaviour of the worker or user. The information could be used to prevent any kind of

musculoskeletal disorders or pains while sitting for long periods. These part of the feedback system is developed on the software. Also the results showed that these system could be used in other circumstances as a wheelchair to monitor person with reduced mobility.

Part IV

Conclusions

11

Conclusions and Future Work

11.1 Conclusions

In this thesis, it has been analysed, designed and tested a textile capacitive sensor based on the permittivity change working principle produced with different textile processes as embroidery and weaving. These different integration methods, textile materials used and different applications proposed have been reported in six JCR articles during the thesis period.

The first 3 parts of the thesis expresses the studies and research conducted and in this final part conclusions and future work will be presented.. Preface section exposed the motivations and the objectives of the thesis.

An overview of the actual state of the art of the textile capacitive sensors, different working principles, integration methods and applications is conducted on Chapter 1, which is found in Part 1 where, capacitive sensors and their most important characteristics are presented. In this section, the working principles available for a capacitive sensor are explained and their main differences are treated. Textile capacitive sensors are presented. Their main characteristics and requirements to be defined as a textile sensor are clearly presented. The classification by their integration method, structure and by its working principle are revised. The chapter finishes with an application review of the textile capacitive sensors and the actual state of the reliability.

Modelling materials (substrates or conductive yarns) and experimental requirements are carried out in Part 2. Out of all available structures, Interdigital structure is chosen since it could be built in a single layer. Structure analysis was performed, which consists of a theoretical revision of the structure, following with a simulation process of the structure. The results of the process point out the most important parameters of the structure . Textiles materials review show the wide variety of design options that textile sensors have at the present. Conductive yarns produced by common textile processes are available and have been demonstrated as one of the best options in the actual market.

Part 3 presents the results carried out in the thesis. The contents are presented divided into proper chapters depending on the most important characteristic.

In Chapter 7, the Spice model of the structure is designed. The equation obtained was used to predict the capacitance value of the structure for different integrating methods or applications.

In Chapter 8 the integration of the capacitive sensor over a textile substrate is performed by embroidery technique. The methodology of the embroidering process is presented and reviewed. Every decision during the process is properly explained. The initial measurement method is presented, which is the impedance module and phase measurement. Humidity has been chosen, between the stimulus that affect the permittivity, as the one to be measured with the embroidered textile sensor presented, because of the availability of options to prepare test situations. Humidity test is performed on the sensor to observe the behaviour. Firstly, the embroidered sensor is tested to demonstrate its functionality and the ability to detect different levels of relative humidity. The embroidered capacitive sensor demonstrates the ability exposed and some additional test, as the washing cycle or repeatability results were done. The results showed that the sensor behaviour is affected by the treatments that fabrics have to protect them from the storage situation. Other results point out that the maximum dispersion error experienced by a sensor at a specific relative humidity was a 6% which it is an acceptable range for a integration technology which such a low cost and performed by a standard machine. Due to its behaviour, impedance sensor could be visualised as a parallel RC circuit where both of the parameters are affected by humidity changes. Additional performance tests are conducted on sensors with various conductive yarns and substrate materials. The conductive yarns modify the behaviour of the sensor provoked mainly, by the yarn surface and the ability of it to retain or store water. However, the substrate materials have been demonstrated as the variable that affect more the behaviour of the textile capacitive sensor. The substrate could provide a lower sensitivity to the sensor, maintaining the shorter range , or the opposite, where the sensor has a wider operating range which need several circuits to be measured by a designed device. These behaviours provide

more design option to measure the humidity such as resulting on a binary response sensor or a relative humidity percentage sensor.

Next, Chapter 9 describes the process to integrate a sensor structure in a woven fabric. The integration was prepared from the adaptation of the embroidery pattern into a weave pattern. Some changes to the interdigital pattern have to be done in order to achieve the woven capacitive sensor. The behaviour of the woven capacitive sensors are tested against humidity, but the initial relative humidity range is increased for them. The woven sensor response was surprising, specially the dispersion error identified which was less than the error presented by embroidered sensor. Repeatability was a characteristic that improves when the weave technology was applied. This fact opens the door to applications which need large scale production, which was considered as a drawback in textile sensors. Companies and researchers are concerned by poor large-scale developments in textile sensor field, which stops the applicability of the discovered new technologies. A new application possibility was faced during one of the humidity test performed to characterise the sensor. Presence detection is possible with the woven capacitive sensor and some tests were carried out to demonstrate its functionality. Presence detection sensor was able to distinguish void or occupied seats while accurately identifying whether it is a person or an object.

Finally, in Chapter 10 application of developed capacitive sensors for two real cases are presented. The system to detect urine leakage by the integration of a textile sensor into a underwear or a bed sheet are presented. These sensors could be implemented as a wearable unit or as an additional device for hospitals. The system detects the urine leakage by capacitance value of the textile sensor which changes abruptly. The real time data obtained from the sensors are relayed through wireless communication technologies such as WiFi, Bluetooth or Zigbee to the nurses or caregivers so that necessary actions can be taken. In the other application, it is used the ability of the sensor to detect presence. The textile sensor, integrated over an office chair, is capable of reading the sitting position. The results demonstrated that sensor can detect the sitting position of the person and relays this information to the user such that any readjustments are needed. The available data could be used to address and resolve the issues such as falling or leaning. The experiments shown that sensors performed well for these specific applications and the usage of these sensors could be extended for various fields by simply making some software and hardware adjustments.

Overall, the thesis demonstrates the functionality of textile capacitive sensors for effective humidity and presence detection and accurate measurement. Textile capacitive sensor versatility could respond several applications where the stimulus to measure affects the permittivity of the substrate or environment. Requirements for a specific application could be fulfilled by the integration method, the conductive yarns and the substrate material. Also, the cost of production is an advantage because textile materials availability

and manufacturing cost are lower than electronic systems and procedures. It is expected that the outcome of the research activities conducted in this thesis will serve a baseline to develop new algorithms and sensor systems as well as leading for new research ideas.

11.2 Future works

The following research activities in line with the study in this thesis could be carried out as a future work:

- To study the impact of the printing technology over the textiles integration methods, which could provide higher accuracy in lines and electrodes.
- To develop an interface between textile capacitive sensor and the microcontroller to be easy movable.
- To investigate the effect of washing and abrasion on conductive yarns and on the substrate is suggested.
- To integrate and develop the bed textile sensor to detect humidity, as it has been demonstrated that market has interest on it
- To develop and adapt the presence detection sensor to be integrated into automotive car seats.

Bibliography

[1] Jacob Fraden. *Handbook of modern sensors: Physics, designs, and applications*. Fifth edit. Springer International Publishing, 2016, pp. 1–758. ISBN: 9783319193038. DOI: 10.1007/978-3-319-19303-8.

[2] Astrid García Patiño, Mahta Khoshnam, and Carlo Menon. "Wearable device to monitor back movements using an inductive textile sensor". In: *Sensors (Switzerland)* 20.3 (2020), pp. 5–8. ISSN: 14248220. DOI: 10.3390/s20030905.

[3] Tomohiro Kuroda, Hideya Takahashi, and Atsuji Masuda. "Woven electronic textiles". In: *Wearable Sensors* (2021), pp. 249–275. DOI: 10.1016/b978-0-12-819246-7.00009-7.

[4] Ozgur Atalay. "Textile-based, interdigital, capacitive, soft-strain sensor for wearable applications". In: *Materials* (2018). ISSN: 19961944. DOI: 10.3390/ma11050768.

[5] C. Atamana et al. "Humidity and temperature sensors on plastic foil for textile integration". In: *Procedia Engineering*. Vol. 25. 2011, pp. 136–139. DOI: 10.1016/j.proeng.2011.12.034.

[6] Jianfeng Wen, Bingang Xu, and Jinyun Zhou. "Toward Flexible and Wearable Embroidered Supercapacitors from Cobalt Phosphides-Decorated Conductive Fibers". In: *Nano-Micro Letters* 11.1 (2019). ISSN: 21505551. DOI: 10.1007/s40820-019-0321-x.

[7] Kun Qi et al. "Core-sheath nanofiber yarn for textile pressure sensor with high pressure sensitivity and spatial tactile acuity". In: *Journal of Colloid and Interface Science* 561 (2020), pp. 93–103. ISSN: 10957103. DOI: 10.1016/j.jcis.2019.11.059. URL: https://doi.org/10.1016/j.jcis.2019.11.059.

[8] Sejin Choi et al. "Fabrication of capacitive yarn torsion sensors based on an electrospinning coating method". In: *Polymer International* 68.11 (2019), pp. 1921–1927. ISSN: 10970126. DOI: 10.1002/pi.5902.

[9] Josue Ferri et al. "A wearable textile 2D touchpad sensor based on screen-printing technology". In: *Materials* 10.12 (2017). ISSN: 19961944. DOI: 10.3390/ma10121450.

[10] Jerzy Weremczuk, Grzegorz Tarapata, and Ryszard Jachowicz. "Humidity Sensor Printed on Textile with Use of Ink-Jet Technology". In: *Procedia Engineering* 47 (2012), pp. 1366–1369. ISSN: 1877-7058. DOI: 10.1016/J.PROENG.2012.09.410.

[11] Richard Vallett et al. "Toward Accurate Sensing with Knitted Fabric: Applications and Technical Considerations". In: *Proceedings of the ACM on Human-Computer Interaction* 4.EICS (2020). ISSN: 25730142. DOI: 10.1145/3394981.

[12] Wanhayoi Geng, Tyler J. Cuthbert, and Carlo Menon. "Conductive Thermoplastic Elastomer Composite Capacitive Strain Sensors and Their Application in a Wearable Device for Quantitative Joint Angle Prediction". In: *ACS Applied Polymer Materials* 3.1 (2021), pp. 122–129. ISSN: 26376105. DOI: 10.1021/acsapm.0c00708.

[13] Ronghui Wu et al. "All-Textile Electronic Skin Enabled by Highly Elastic Spacer Fabric and Conductive Fibers". In: *ACS Applied Materials and Interfaces* 11.36 (2019), pp. 33336–33346. ISSN: 19448252. DOI: 10.1021/acsami.9b10928.

[14] Xiaolu You et al. "Stretchable capacitive fabric electronic skin woven by electrospun nanofiber coated yarns for detecting tactile and multimodal mechanical stimuli". In: *Journal of Materials Chemistry C* 6.47 (2018), pp. 12981–12991. ISSN: 20507526. DOI: 10.1039/C8TC03631D.

[15] Lakshmi Areekath et al. "An Electric-Field Based Breathing Rate Monitor". In: *2018 IEEE International Symposium on Medical Measurements and Applications (MeMeA)*. Rome, Italy: 2018 IEEE International Symposium on Medical Measurements and Applications (MeMeA), 2018. ISBN: 9781538633922. DOI: 10.1109/MeMeA.2018.8438780.

[16] Kiyo T Fujimoto et al. "Aerosol jet printed capacitive strain gauge for soft structural materials". In: *npj Flexible Electronics* 4.1 (2020). ISSN: 23974621. DOI: 10.1038/s41528-020-00095-4. URL: http://dx.doi.org/10.1038/s41528-020-00095-4.

[17] Manjunath Reddy H V Beeresha R S, A M Khan. "Design and Optimization of Interdigited Capacitors". In: *International Journal of Research in Engineering and Technology* 05.21 (2016), pp. 273–277.

[18] Jinglong Xu et al. "A graphite nanoplatelet-based highly sensitive flexible strain sensor". In: *Carbon* 166 (2020), pp. 316–327. ISSN: 00086223. DOI: 10.1016/j.carbon.2020.05.042. URL: https://doi.org/10.1016/j.carbon.2020.05.042.

[19] Roda Nur et al. "A Highly Sensitive Capacitive-type Strain Sensor Using Wrinkled Ultrathin Gold Films". In: *Nano Letters* 18.9 (2018), pp. 5610–5617. ISSN: 15306992. DOI: 10.1021/acs.nanolett.8b02088.

[20] Longteng Yu et al. "Dual-Core Capacitive Microfiber Sensor for Smart Textile Applications". In: *ACS Applied Materials and Interfaces* 11.36 (2019), pp. 33347–33355. ISSN: 19448252. DOI: 10.1021/acsami.9b10937.

[21] Qi Zhang et al. "A low-cost and highly integrated sensing insole for plantar pressure measurement". In: *Sensing and Bio-Sensing Research* 26.September (2019), p. 100298. ISSN: 22141804. DOI: 10.1016/j.sbsr.2019.100298. URL: https://doi.org/10.1016/j.sbsr.2019.100298.

[22] Talha Agcayazi et al. "Fully-Textile Seam-Line Sensors for Facile Textile Integration and Tunable Multi-Modal Sensing of Pressure, Humidity, and Wetness". In: *Advanced Materials Technologies* 5.8 (2020), pp. 1–15. ISSN: 2365709X. DOI: 10.1002/admt.202000155.

[23] Liming Chen et al. "Textile-Based Capacitive Sensor for Physical Rehabilitation via Surface Topological Modification". In: *ACS Nano* 14.7 (2020), pp. 8191–8201. ISSN: 1936086X. DOI: 10.1021/acsnano.0c01643.

[24] Qi Zhang et al. "Textile-Only Capacitive Sensors with a Lockstitch Structure for Facile Integration in Any Areas of a Fabric". In: *ACS Sensors* 5.6 (2020), pp. 1535–1540. ISSN: 23793694. DOI: 10.1021/acssensors.0c00210.

[25] Jian-Feng Wu et al. "Human Limb Motion Detection with Novel Flexible Capacitive Angle Sensor Based on Conductive Textile". In: *Electronics* 7.9 (2018), p. 192. ISSN: 2079-9292. DOI: 10.3390/electronics7090192.

[26] Changwon Wang, Young Kim, and Se Dong Min. "Soft-material-based smart insoles for a gait monitoring system". In: *Materials* 11.12 (2018), pp. 1–14. ISSN: 19961944. DOI: 10.3390/ma11122435.

[27] Se Dong Min et al. "Development of A Textile Capacitive Proximity Sensor and Gait Monitoring System for Smart Healthcare". In: *Journal of Medical Systems* (2018). ISSN: 1573689X. DOI: 10.1007/s10916-018-0928-3.

[28] Kyobin Keum et al. "Highly sensitive textile-based capacitive pressure sensors using PVDF-HFP/ionic liquid composite films". In: *Sensors (Switzerland)* 21.2 (2021), pp. 1–11. ISSN: 14248220. DOI: 10.3390/s21020442.

[29] Siming Li et al. "Highly Sensitive and Flexible Capacitive Pressure Sensor Enhanced by Weaving of Pyramidal Concavities Staggered in Honeycomb Matrix". In: *IEEE Sensors Journal* 20.23 (2020), pp. 14436–14443. ISSN: 15581748. DOI: 10.1109/JSEN.2020.3008474.

[30] Min Fu et al. "A Highly Sensitive, Reliable, and High-Temperature-Resistant Flexible Pressure Sensor Based on Ceramic Nanofibers". In: *Advanced Science* 7.17 (2020), pp. 1–8. ISSN: 21983844. DOI: 10.1002/advs.202000258.

[31] Yuri Tsuda, Masato Odagaki, and Yasuhito Kondo. "Development of a sensor with a conductive textile for detecting decubitus ulcers". In: *IEEJ Transactions on Electrical and Electronic Engineering* 15.7 (2020), pp. 1065–1069. ISSN: 19314981. DOI: 10.1002/tee.23151.

[32] Guanzheng Wu et al. "Fabrication of capacitive pressure sensor with extraordinary sensitivity and wide sensing range using PAM/BIS/GO nanocomposite hydrogel and conductive fabric". In: *Composites Part A: Applied Science and Manufacturing* 145.March (2021), p. 106373. ISSN: 1359835X. DOI: 10.1016/j.compositesa.2021.106373. URL: https://doi.org/10.1016/j.compositesa.2021.106373.

[33] Jungrak Choi et al. "Synergetic Effect of Porous Elastomer and Percolation of Carbon Nanotube Filler toward High Performance Capacitive Pressure Sensors". In: *ACS Applied Materials and Interfaces* 12.1 (2020), pp. 1698–1706. ISSN: 19448252. DOI: 10.1021/acsami.9b20097.

[34] Xufeng Zhou et al. "A fiber-shaped light-emitting pressure sensor for visualized dynamic monitoring". In: *Journal of Materials Chemistry C* 8.3 (2020), pp. 935–942. ISSN: 20507526. DOI: 10.1039/c9tc05653j.

[35] Paul Hofmann et al. "Utilization of the textile reinforcements of fiber reinforced plastics as sensor for condition monitoring". In: *Composites Part A: Applied Science and Manufacturing* 126.August (2019), p. 105603. ISSN: 1359835X. DOI: 10.1016/j.compositesa.2019.105603. URL: https://doi.org/10.1016/j.compositesa.2019.105603.

[36] Stanislav Bobovych et al. "RestEaZe: Low-power accurate sleep monitoring using a wearable multi-sensor ankle band". In: *Smart Health* 16.February (2020), p. 100113. ISSN: 23526483. DOI: 10.1016/j.smhl.2020.100113. URL: https://doi.org/10.1016/j.smhl.2020.100113.

[37] Chi Cuong Vu and Jooyong Kim. "Highly elastic capacitive pressure sensor based on smart textiles for full-range human motion monitoring". In: *Sensors and Actuators, A: Physical* 314 (2020), p. 112029. ISSN: 09244247. DOI: 10.1016/j.sna.2020.112029. URL: https://doi.org/10.1016/j.sna.2020.112029.

[38] Jarkko Tolvanen et al. "Stretchable Sensors with Tunability and Single Stimuli-Responsiveness through Resistivity Switching under Compressive Stress". In: *ACS Applied Materials and Interfaces* 12.12 (2020), pp. 14433–14442. ISSN: 19448252. DOI: 10.1021/acsami.0c00023.

[39] Reza Razmand et al. "A Graphene Oxide-Based Humidity Sensor for Wearable Electronic". In: *ICEE 2019 - 27th Iranian Conference on Electrical Engineering* (2019), pp. 423–426. DOI: 10.1109/IranianCEE.2019.8786557.

[40] R. Alrammouz et al. "Highly porous and flexible capacitive humidity sensor based on self-assembled graphene oxide sheets on a paper substrate". In: *Sensors and Actuators, B: Chemical* 298.July (2019), p. 126892. ISSN: 09254005. DOI: 10.1016/j.snb.2019.126892. URL: https://doi.org/10.1016/j.snb.2019.126892.

[41] Thomas Grethe et al. "Textile humidity sensors". In: *Symposium on Design, Test, Integration and Packaging of MEMS/MOEMS, DTIP 2018* (2018), pp. 1–3. DOI: 10.1109/DTIP.2018.8394188.

[42] Yamei Wang et al. "High-Sensitivity Wearable and Flexible Humidity Sensor Based on Graphene Oxide/Non-Woven Fabric for Respiration Monitoring". In: *Langmuir* 36.32 (2020), pp. 9443–9448. ISSN: 15205827. DOI: 10.1021/acs.langmuir.0c01315.

[43] Pi Guey Su and Chun Fu Chang. "Fabrication and electrical and humidity-sensing properties of a flexible and stretchable textile humidity sensor". In: *Journal of the Taiwan Institute of Chemical Engineers* 87 (2018), pp. 36–43. ISSN: 18761070. DOI: 10.1016/j.jtice.2018.03.050. URL: https://doi.org/10.1016/j.jtice.2018.03.050.

[44] Ruijie Xie et al. "Wearable Leather-Based Electronics for Respiration Monitoring". In: *ACS Applied Bio Materials* 2.4 (2019), pp. 1427–1431. ISSN: 25766422. DOI: 10.1021/acsabm.9b00082.

[45] Talha Agcayazi, Yigit Menguc, and Shawn Reese. "Skin in the Game: A Tunable Interface-Quality Sensor for Human-Coupled Accessories". In: *IEEE Sensors Letters* 4.9 (2020). ISSN: 24751472. DOI: 10.1109/LSENS.2020.3011864.

[46] Tae Young Choi et al. "Stretchable, Transparent, and Stretch-Unresponsive Capacitive Touch Sensor Array with Selectively Patterned Silver Nanowires/Reduced Graphene Oxide Electrodes". In: *ACS Applied Materials and Interfaces* 9.21 (2017), pp. 18022–18030. ISSN: 19448252. DOI: 10.1021/acsami.6b16716.

[47] Ashlesha Bhide, Sriram Muthukumar, and Shalini Prasad. "CLASP (Continuous lifestyle awareness through sweat platform): A novel sensor for simultaneous detection of alcohol and glucose from passive perspired sweat". In: *Biosensors and Bioelectronics* 117.June (2018), pp. 537–545. ISSN: 18734235. DOI: 10.1016/j.bios.2018.06.065. URL: https://doi.org/10.1016/j.bios.2018.06.065.

[48] Adnan Mujahid, Stephan Aigner, and Franz L. Dickert. "Micro-structured interdigital capacitors with synthetic antibody receptors for ABO blood-group typing: Dedicated to Prof. Dr. Reinhard Niessner and Prof. Dr. Dietmar Knopp on the occasion of their 65th birthday". In: *Sensors and Actuators, B: Chemical* 242 (2017), pp. 378–383. ISSN: 09254005. DOI: 10.1016/j.snb.2016.11.056. URL: http://dx.doi.org/10.1016/j.snb.2016.11.056.

[49] Elena Hadzhigenova et al. "Experimental Investigation of Washing Effects on the Properties of Textile Electrodes". In: *43rd International Spring Seminar on Electronics Technology (ISSE)*. 2020, pp. 3–8. ISBN: 9781728167732. DOI: 10.1109/ISSE49702.2020.9120885.

[50] Nauman Ali Choudhry et al. "Design, Development and Characterization of Textile Stitch-Based Piezoresistive Sensors for Wearable Monitoring". In: *IEEE Sensors Journal* 20.18 (2020), pp. 10485–10494. ISSN: 15581748. DOI: 10.1109/JSEN.2020.2994264.

[51] Yayoi Tetsuou Tsukada et al. "Validation of wearable textile electrodes for ECG monitoring". In: *Heart and Vessels* 34.7 (2019), pp. 1203–1211. ISSN: 16152573. DOI: 10.1007/s00380-019-01347-8. URL: https://doi.org/10.1007/s00380-019-01347-8.

[52] P. Fiedler et al. "Impedance pneumography using textile electrodes". In: *Proceedings of the Annual International Conference of the IEEE Engineering in Medicine and Biology Society, EMBS* (2012), pp. 1606–1609. ISSN: 1557170X. DOI: 10.1109/EMBC.2012.6346252.

[53] Chi Cuong Vu and Jooyong Kim. "Human motion recognition using SWCNT textile sensor and fuzzy inference system based smart wearable". In: *Sensors and Actuators, A: Physical* 283 (2018), pp. 263–272. ISSN: 09244247. DOI: 10.1016/j.sna.2018.10.005. URL: https://doi.org/10.1016/j.sna.2018.10.005.

[54] Sophie Wilson and Raechel Laing. "Fabrics and garments as sensors: A research update". In: *Sensors (Switzerland)* 19.16 (2019), pp. 1–35. ISSN: 14248220. DOI: 10.3390/s19163570.

[55] C. Ataman et al. "A robust platform for textile integrated gas sensors". In: *Sensors and Actuators, B: Chemical* 177 (2013), pp. 1053–1061. ISSN: 09254005. DOI: 10.1016/j.snb.2012.11.099.

[56] Soongeun Kwon et al. "Scalable fabrication of inkless, transfer-printed graphene-based textile microsupercapacitors with high rate capabilities". In: *Journal of Power Sources* 481.September 2020 (2021), p. 228939. ISSN: 03787753. DOI: 10.1016/j.jpowsour.2020.228939. URL: https://doi.org/10.1016/j.jpowsour.2020.228939.

[57] RohdeSchwarz. *RS®HM8118 Programmable LCR-Bridge Benutzerhandbuch User Manual*. Tech. rep. 2015, p. 76.

[58] Marc Martínez-Estrada et al. "Impact of conductive yarns on an embroidery textile moisture sensor". In: *Sensors (Switzerland)* 19.5 (2019), pp. 1–10. ISSN: 14248220. DOI: 10.3390/s19051004.

[59] Martinez Estrada Marc, Gil Ignacio, and Fernandez Garcia Raul. "A Smart Textile System to Detect Urine Leakage". In: *IEEE Sensors Journal* 21.23 (2021), pp. 26234–26242. ISSN: 15581748. DOI: 10.1109/JSEN.2021.3080824.

Part V

Appendix

Paper A

Martinez-Estrada, M., Moradi, B., Fernández-Garcia, R., & Gil, I. (2018). Embroidery Textile Moisture Sensor. Proceedings 2018, Vol. 2, Page 1057, 2(13), 1057. https://doi.org/10.3390/proceedings2131057

proceedings

MDPI

Proceedings

Embroidery Textile Moisture Sensor †

Marc Martinez-Estrada, Bahareh Moradi, Raúl Fernández-Garcia * and Ignacio Gil

Department of Electronic Engineering, Universitat Politècnica de Catalunya, 08222 Terrassa, Spain; marc.martinez-estrada@upc.edu (M.M.-E.); bahareh.moradi@upc.edu (B.M.); ignasi.gil@upc.edu (I.G.)

* Correspondence: raul.fernandez-garcia@upc.edu

† Presented at the Eurosensors 2018 Conference, Graz, Austria, 9–12 September 2018.

Published: 21 November 2018

Abstract: In this work, two embroidered textile moisture sensors are presented. The sensors are based on a capacitive interdigitated structure embroidered on a cotton substrate with an embroidery conductor yarn composed by 99% pure silver plated nylon yarn 140/17 dtex. In order to evaluate the sensor sensitivity, the impedance of the sensor has been measured by means of a LCR meter from 20 Hz to 20 kHz on a climatic chamber with a sweep of the relative humidity from 25% to 65% at 20 °C. The experimental results show a clear and controllable dependence of the sensor impedance with the relative humidity. Therefore, this dependence points out the usefulness of the proposed sensor to develop wearable applications on health and fitness scope.

Keywords: sensor; e-textile; embroidery; moisture

1. Introduction

Embroidery has been revealed as the most effective technique to implement wearable sensors. This fact is due to the availability of the manufacturing technology (industrial embroidery machines), efficient exploitation of the expensive specialized conductive threads and repeatability of geometries and layouts [1]. These wearable sensors are suitable for application fields such as health monitoring, physical training, emergency rescue service and law-enforcement [2]. In particular, the integration of flexible, lightweight and comfortable designs allows the deployment of wearable solutions [3]. In the last years, a great effort has been focused in designing new sensors included in garments for healthcare applications [4].

In this work, an embroidered textile sensor in order to measure the moisture is presented. A full characterization and modelling has been carried out. The remainder of the paper is organized as follows. Section 2 describes the Material and methods, the textile sensor layout and implementation as well as the measurement set-up. In Section 3 the experimental results are shown and discussed. Finally, in Section 4 the conclusions are summarized.

2. Materials and Methods

The proposed moisture sensor is based on a capacitive embroidered interdigitated structurewhose dimensions are depicted in Figure 1. A commercial Shieldex 117/17 dtex 2-ply has been chosen as a conductive yarn in order to embroider the interdigitated structures on a high hygroscope substrate. Specifically, a cotton substrate with a thickness (h) of 0.43 mm has been chosen. A Singer Futura XL-550 embroidery machine with a satin fill stitch pattern has been selected in order to achieve a homogeneous yarn distribution over the sensor surface.

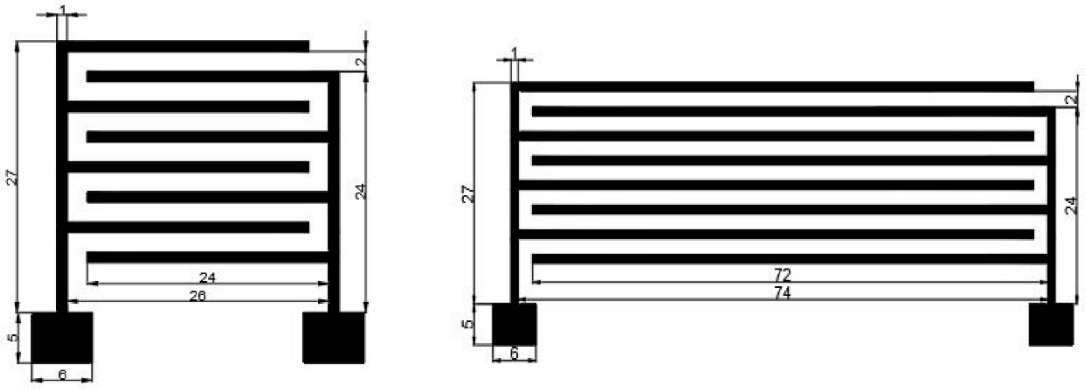

Figure 1. Layout and dimension detail of the proposed moisture sensor (in mm): (**a**) short sensor; (**b**) long sensor. The bottom squares correspond to the characterization pads.

In order to characterize the sensor behavior, the device has been tested ina CCK-25/48 Dycometal climatic chamber and the sensor impedance has been measured by means of an external Rohde & Schwarz HM8118 LCR meter. An image of the experimental setup and embroidered short sensor are shown in Figure 2.

The sensors impedances have been measured from 20 Hz to 20 kHz in a 25% to 65% of relative humidity environment, meanwhile the temperature has remained constant at 20 °C.

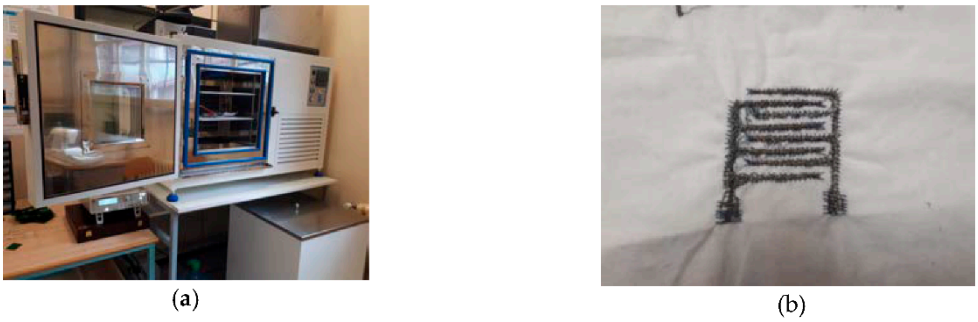

Figure 2. Image of the experimental setup. (**a**) climatic chamber, (**b**) embroidered short sensor

3. Results and Discussion

Figure 3 shows the measured sensor impedance when the moisture is swept from 25% to 65% for four different test frequencies. It is observed that the impedance module of sensor is reduced when the environmental moisture increases, which confirms the functionality of the proposed structure as a moisture sensor. The measured phase impedance of the sensor denotes that for low relative humidity the sensor has a capacitive behavior, as expected. Moreover, for higher relative humidity concentration the sensor tends to be resistive. The reason of this behavior is the hydrophilic property of the cotton. Indeed, when the relative humidity increases, the cotton substrate absorbs water and the electrical permittivity of the substrate increases. As a result, the impedance of the sensor is reduced.

Long and short sensor shows similar behavior with the relative moisture. However, as it is expected, the impedance of the longer sensor (Figure 3b) is lower than the impedance of the short device (Figure 3a). In particular, for the 20 Hz test signal, the short sensor impedance decreases from 1.1 GΩ to 20.4 MΩ when the moisture increases from 25% to 65%, whereas, for long sensor device it decreases from 0.83 GΩ 10 12.5 MΩ for the same moisture range.

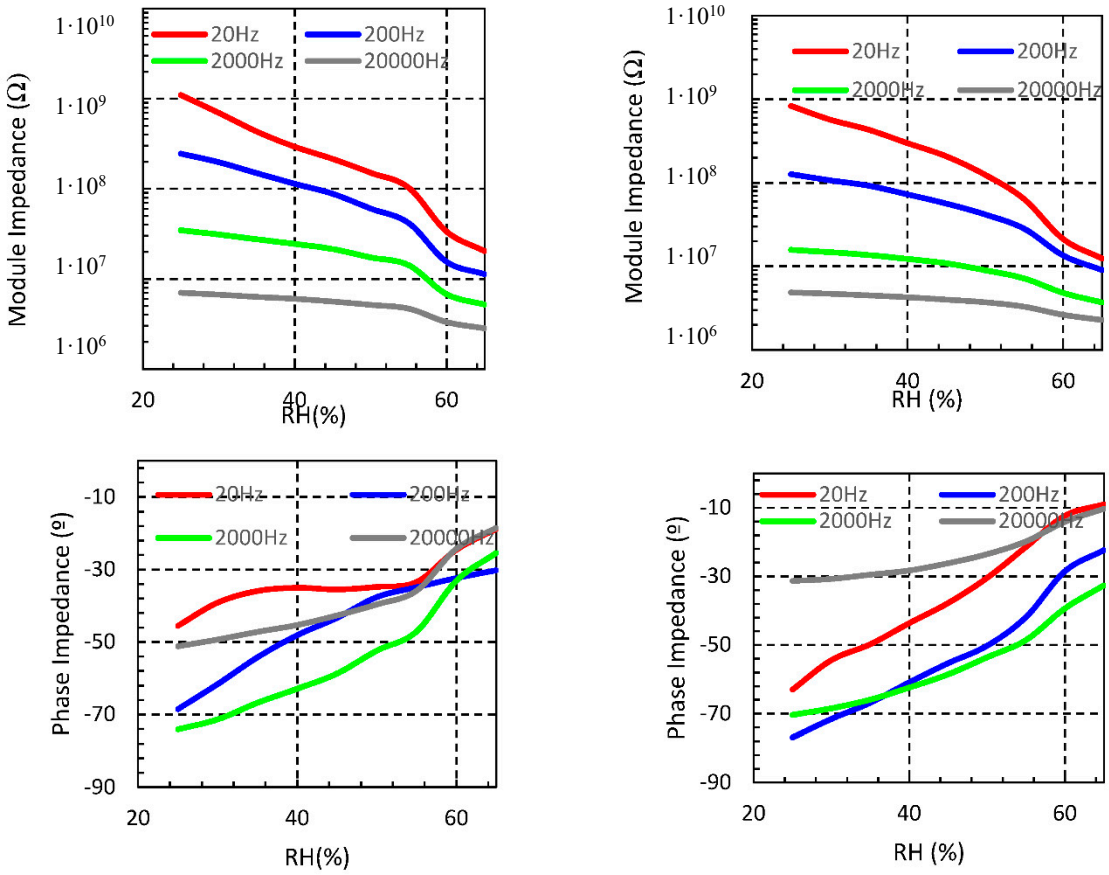

a) Short sensor impedance. b) Long sensor impedance.

Figure 3. Measured sensors impedance from 25% to 65% RH at different frequencies (T = 20 °C).

It should be noticed that the obtained impedance values at the low frequency range are too high in order to develop a portable device based on the proposed sensor. These wearable devices are typically based on a single integrated circuit, such as the AD5933 impedance converter [5] (Texas Instruments, Dallas, USA). Nevertheless, using the proposed sensor in the range of kHz allows obtaining impedances in the range of a MΩ. In these cases, the impedance values that can be measured with this integrated circuits.

If we focus on the electronic performance according to the behavior of the proposed sensors at 2 kHz, they can be modelled as a RC parallel lumped model (Figure 4b), where the R and C values are moisture dependent.

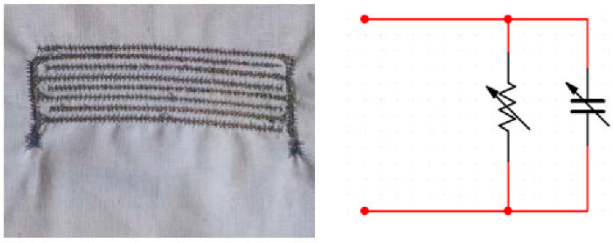

a) b)

Figure 4. Proposed long sensor (**a**) physical implementation (**b**) Electrical model.

In Figure 5 the R and C dependence from 25% to 65% RH at 2 kHz is shown for both short and long sensor. It can be observed than when the moisture level increases the capacitance is increased, whereas the resistance is reduced in both sensors. It should be pointed out that both sensors show a

similar trend with the moisture impact, with a clear sensitivity change around 55% RH. Despite, the short sensor has a lower capacitance and higher resistance value, due to his physical dimensions. In fact, the capacitance increases from 1.45 pF to 8.84 pF for the short sensor and from 3.13 pF to 19.40 pF for the long sensor. Meanwhile, the resistance decreases from 4.42 MΩ to 2.68 MΩ and from 4.17 MΩ to 2.26 MΩ for the short and long sensor, respectively.

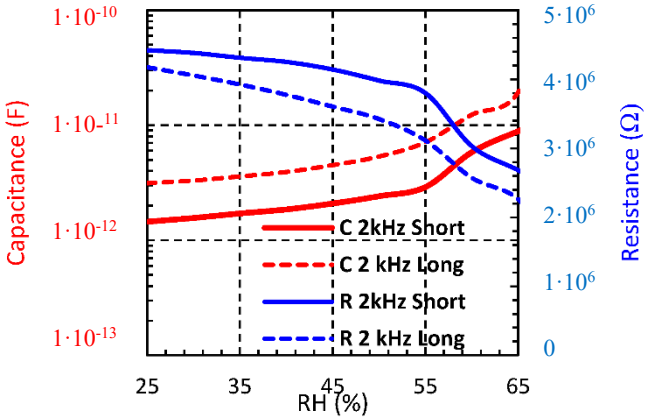

Figure 5. Measured sensors impedance from 25% to 65% RH at different frequencies.

4. Conclusions

In this work two interdigitated embroidered textile sensors have been proposed and characterized. The sensors have been embroidered over a cotton substrate with a commercial Shieldex 117/17 dtex 2 yarn. The measured results show that the proposed sensors can be modelled by means of a RC parallel lumped circuit, where the R and C value are moisture dependent. These preliminary results demonstrate experimentally the usefulness of the proposed sensors at the kHz range to develop wearable application over textiles materials for health and fitness applications, such as the sweating measurement.

Acknowledgments: This work was supported by the Spanish-MINECO Project TEC2016-79465-R.

Conflicts of Interest: The authors declare no conflict of interest.

References

1. Castano, L.M.; Flatau, A.B. Smart Fabric Sensors and E-Textile Technologies: A Review. *Smart Mater. Struct.* **2014**, *23*, 053001.
2. Tartare, G.; Zeng, X.; Koehl, L. Development of a Wearable System for Monitoring the Firefighter's Physiological State. In Proceedings of the 2018 IEEE Industrial Cyber-Physical Systems (ICPS), St. Petersburg, Russia, 15–18 May 2018; pp. 561–566.
3. Saenz-Cogollo, J.; Pau, M.; Fraboni, B.; Bonfiglio, A. Pressure Mapping Mat for Tele-Home Care Applications. *Sensors* **2016**, *16*, 365.
4. Bouwstra, S.; Chen, W.; Feijs, L.; Oetomo, S.B. Smart Jacket Design for Neonatal Monitoring with Wearable Sensors. In Proceedings of the 2009 Sixth International Workshop on Wearable and Implantable Body Sensor Networks, Berkeley, CA, USA, 3–5 June 2009; pp. 162–167.
5. Devices, A. AD5933 1 MSPS, 12-Bit Impedance Converter, Network Analyzer. Available online: http://www.analog.com/media/en/technical-documentation/data-sheets/AD5933.pdf (accessed on 15 May 2018)

© 2018 by the authors. Licensee MDPI, Basel, Switzerland. This article is an open access article distributed under the terms and conditions of the Creative Commons Attribution (CC BY) license (http://creativecommons.org/licenses/by/4.0/).

Paper B

Martinez-Estrada, M., Moradi, B., Fernández-Garcia, R., & Gil, I. (2018). Impact of manufacturing variability and washing on embroidery textile sensors. Sensors (Switzerland), 18(11), 3824. https://doi.org/10.3390/s18113824

sensors

MDPI

Article

Impact of Manufacturing Variability and Washing on Embroidery Textile Sensors

Marc Martinez-Estrada, Bahareh Moradi, Raúl Fernández-Garcia * and Ignacio Gil

Department of Electronic Engineering, Universitat Politècnica de Catalunya, 08222 Terrassa, Spain; marc.martinez.estrada@upc.edu (M.M.-E.); bahareh.moradi@upc.edu (B.M.); ignasi.gil@upc.edu (I.G.)

* Correspondence: raul.fernandez-garcia@upc.edu; Tel.: +34-937-398-089

Received: 17 October 2018; Accepted: 6 November 2018; Published: 8 November 2018

Abstract: In this work, an embroidered textile moisture sensor is presented. The sensor is based on a capacitive interdigitated structure embroidered on a cotton substrate with an embroidery conductor yarn composed of 99% pure silver plated nylon yarn 140/17 dtex. In order to evaluate the sensor sensitivity, the impedance of the sensor has been measured by means of a impedance meter (LCR) from 20 Hz to 20 kHz in a climatic chamber with a sweep of the relative humidity from 25% to 65% at 20 °C. The experimental results show a clear and controllable dependence of the sensor impedance with the relative humidity. Moreover, the reproducibility of the sensor performance subject to the manufacturing process variability and washing process is also evaluated. The results show that the manufacturing variability introduces a moisture measurement error up to 4%. The washing process impact on the sensor behavior after applying the first washing cycle implies a sensitivity reduction higher than 14%. Despite these effects, the textile sensor keeps its functionality and can be reused in standard conditions. Therefore, these properties point out the usefulness of the proposed sensor to develop wearable applications within the health and fitness scope including when the user needs to have a life cycle longer than one-time use.

Keywords: sensor; e-textile; embroidery; moisture; conductive yarn

1. Introduction

Textiles have been revealed as a natural and convenient substrate choice in the development of wearable electronic applications due to the fact that humans have been covering our body with fabrics for thousands of years [1]. This fact, together with the rapid miniaturization of electronic components and the development of new materials is allowing for the integration of electronic functionalities on fabrics, using well known textile manufacturing techniques, such as weaving knitting, embroidery, etc. [2]. Among the techniques, embroidery has been revealed as the most effective technique to implement wearable electronics due to the availability of the manufacturing technology and the flexibility of the technologies to make different geometries and layouts over the textiles [3]. Among the different embroidery e-textile applications, in the last years, a great effort has been focused on designing new e-textile sensors that are included in garments [4]. Many of the studies are focused on fields such as health monitoring [5], physical training [6], emergency rescue service, and law-enforcement [7].

Previous literature mainly reports on single use sensors. In order to guarantee the long term functionality of these devices, two topics should be addressed: the variability of the electrical behavior with the manufacturing process and the functionality of the involved e-textiles after washing cycles. In this sense, only a few works can be found in the literature focused on the electrical behavior of e-textile after washing cycles [8–10]. These previous publications suggest that the electrical behavior of e-textile is modified after several washing cycles. In order to delve in depth in this topic, a capacitive

embroidered textile moisture sensor is presented and a full characterization of its response was carried out, taking into account the manufacturing variability and the washing cycles.

The remainder of the paper is organized as follows. Section 2 describes the Material and methods where the textile sensor layout is defined and the measurement set-up as well as the washing cycle's procedures are described. In Section 3 the experimental results are shown and discussed. Finally, in Section 4 the conclusions are summarized.

2. Materials and Methods

The proposed moisture sensor is based on a capacitive embroidered interdigitated structure whose dimensions are depicted in Figure 1. In this structure, the capacitive sensor performance depends on the geometry (i.e., number of fingers, size, and distant between fingers) and the substrate material permittivity. If a hygroscope material is used as a substrate, the permittivity of the substrate will be modified under the presence of water molecules. This mechanism gives the sensing capability to the proposed devices.

A commercial Shieldex 117/17 dtex 2-ply was chosen as a conductive yarn in order to embroider the interdigitated structures on a high hygroscope substrate. Specifically, a cotton substrate with a thickness (h) of 0.43 mm was chosen. A Singer Futura XL-550 embroidery machine (Singer Corporation, La Vergne, TN, USA) with a satin fill stitch pattern was selected in order to achieve a homogeneous yarn distribution over the sensor surface. With this configuration, the embroidery machine dimension resolution was 100 µm.

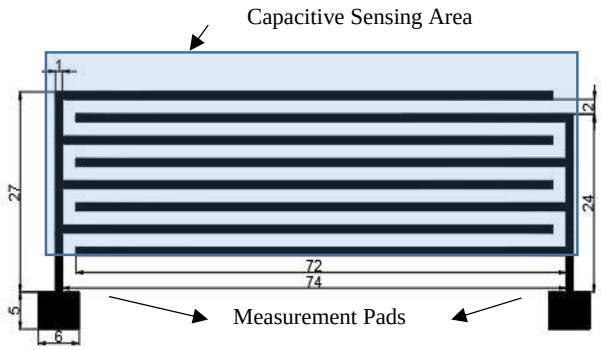

Figure 1. Layout and dimension detail of the proposed moisture sensor (in mm). The bottom squares correspond to the characterization pads, and the capacitive sensing area corresponds to the interdigitated area.

In order to characterize the sensor behavior, the device was tested in a CCK-25/48 Dycometal climatic chamber (Dycomental Equipos S.L., Viladecans, Spain), and the sensor impedance was measured by means of an external Rohde & Schwarz HM8118 LCR meter (Rohde & Schwarz, Munich, Germany). The LCR and sensor connection was done through a feed cable hole on the climatic chamber chassis. An image of the experimental setup and the embroidered sensor are shown in Figure 2.

(**a**) (**b**)

Figure 2. Image of the experimental setup. (**a**) CCK-25/48 Dycometal (**b**) Embroidered capacitive sensor.

The sensor impedance was measured in a frequency range from 20 Hz to 20 kHz in a 25% to 65% relative humidity environment, meanwhile, the temperature remained constant at 20 °C. In order to guarantee and analyze the reproducibility, ten different samples were characterized and analyzed at 200 Hz, and the average and standard deviation was used as a figure of merit.

Finally, in order to evaluate the impact of washing cycles on the electrical behavior, the electrical impedance was measured before and after putting the samples into the washing cycles. For this process, the selected soap and the washing machine were used according to the standard requirements defined on the UNE-EN ISO 6330:2012. A neutral ECE-Color Detergent ISO 105-C06 soap (Testgewebe Gmbh, Brüggen, Germany) was used and 1 kg of support fabric was used in every wash (Figure 3). A washing machine (Balay T5609, BSH Electrodomesticos, Zaragoza, Spain) was configured at 1000 rpm and temperature of 40 °C, and 1% by weight of soap (i.e., 10 g) was introduced in the washing machine.

Figure 3. Image of the experimental Balay T5609 washing machine and the support fabric for washing cycles (inset).

3. Results and Discussion

Figure 4 shows the measured sensor impedances when the moisture is increased from 25% to 65% for four different test frequencies. It is observed that the impedance module of the sensor is reduced when the environmental moisture increases. This fact confirms the functionality of the proposed structure as a moisture sensor. The measured phase impedance of the sensor is negative in all the studied frequency ranges, denoting that for low relative humidity, the sensor has a capacitive behavior, as expected. However, for higher relative humidity concentrations, the sensor tends to be resistive. The reason of this behavior is the hydrophilic property of the cotton. Indeed, when the relative humidity increases, the cotton substrate absorbs water, and the electrical permittivity of the substrate increases. As a result, the impedance of the sensor is reduced. In particular, for the 200 Hz test signal, the sensor impedance module decreases from 127 MΩ to 9.08 MΩ when the moisture increases from 25% to 65%. For the same moisture range, the phase impedance increases from $-76.92°$ to $-22.38°$.

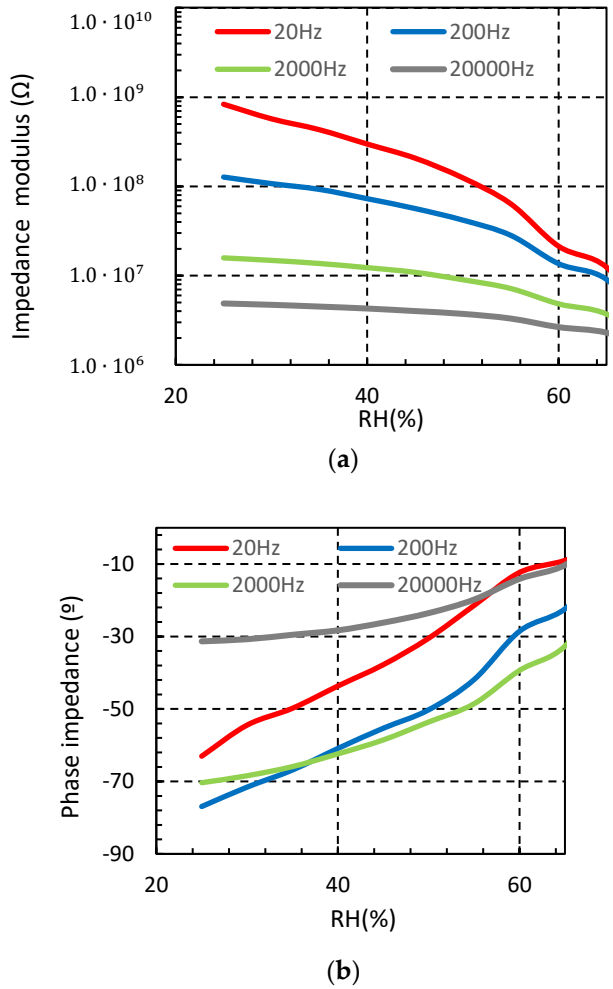

Figure 4. Measured sensor impedance from 25% to 65% relative humidity (RH) at different frequencies (T = 20 °C) (**a**) impedance modulus (**b**) impedance phase.

3.1. Manufacturing Variability

Once the functionality of the proposed sensor to measure the ambient moisture was demonstrated, the reproducibility of this sensor was evaluated in order to know the impact of manufacturing variability on its performance. In this analysis, the previous sensor capacitor structure was used, and the electrical impedance of ten samples was measured from 25% to 65% relative humidity (RH) at 200 Hz with a 95% confidence interval.

Figure 5 shows the measured module and phase impedance at 200 Hz, where the red line represents the average measured impedance with a 95% confidence interval error, continuous black line depicts the linear regression for the average value, and the dotted line and dashed lines represent the linear regression for +9% confidence interval and 95% confidence interval, respectively. The linear regression equations are also shown in the graph. From this data, a linear dependence behavior is observed with the moisture. However, due to the manufacturing variability, the static sensor characteristic shows a clear variability. Table 1 summarizes the dispersion measured on the sensitivity and zero shift parameter of the sensor impedance. In particular, the sensitivity of the sensor impedance module has a value of 2.97 MΩ/%RH ± 7%, meanwhile the average zero shift is 193.8 MΩ ± 10%. Meanwhile, the value of the sensor impedance phase achieves a sensitivity value of 1.272°/%RH ± 7.3% and the zero shift a value of −111° ± 0.9%.

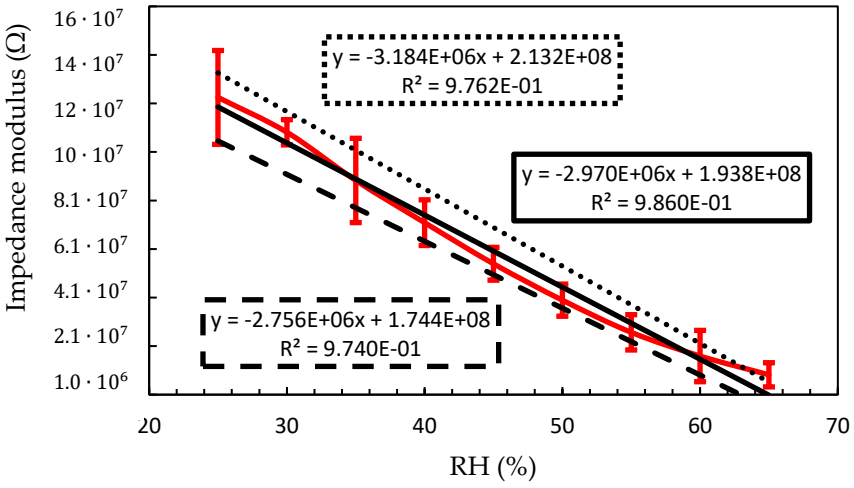

(a)

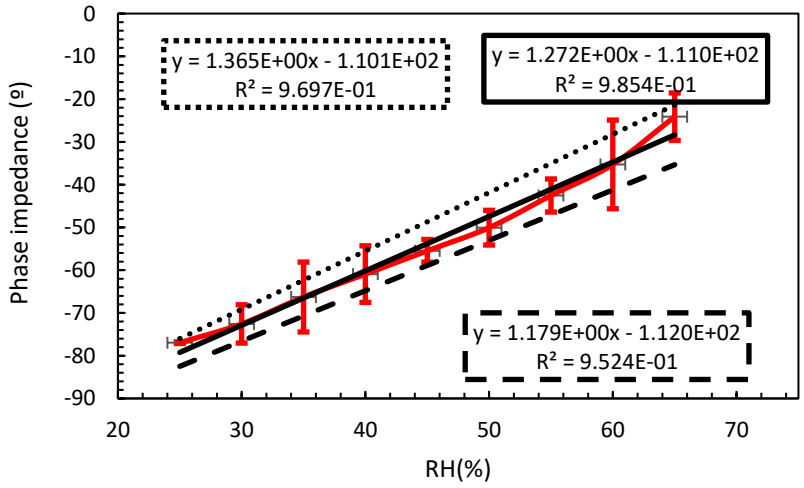

(b)

Figure 5. Sensor impedance at 200 Hz with a 95% of confidence interval. Red line represents the average measured impedance with 95% confidence interval error, continuous black line represents the linear regression for the average value, and the dotted and dashed lines represent the linear regression for +9% confidence interval and −95% of confidence interval, respectively. The linear regression equations are also shown in the graph. (**a**) impedance modulus (**b**) impedance phase.

Table 1. Sensor impedance properties with process variability for 95% interval of confidence.

Impedance Modulus				**Impedance Phase**			
	min	**mean**	**max**		**min**	**mean**	**max**
Sensitivity $\left(\frac{M\Omega}{\%RH}\right)$	−3.184	−2.97	−2.756	**Sensitivity** $\left(\frac{^\circ}{\%RH}\right)$	1.179	1.272	1.365
Zero shift $(M\Omega)$	174.4	193.8	213.2	**Zero shift** $(^\circ)$	−112	−111	−110

From the previous dispersion values, it is possible to determine the expected error on module and phase impedance due to manufacturing variability. The results are depicted in Figure 6. A maximum error lower than 6% on the moisture measurement was obtained. It should be noted that the error decreased with the moisture when the impedance modulus was measured. Meanwhile the phase error

increased with the moisture. According with this behavior, and in order to reduce the error up 4% on the moisture measurement, for moisture values lower than 40% RH, the impedance phase should be used. However, for higher moisture values, the moisture value should be obtained from the impedance module measurement.

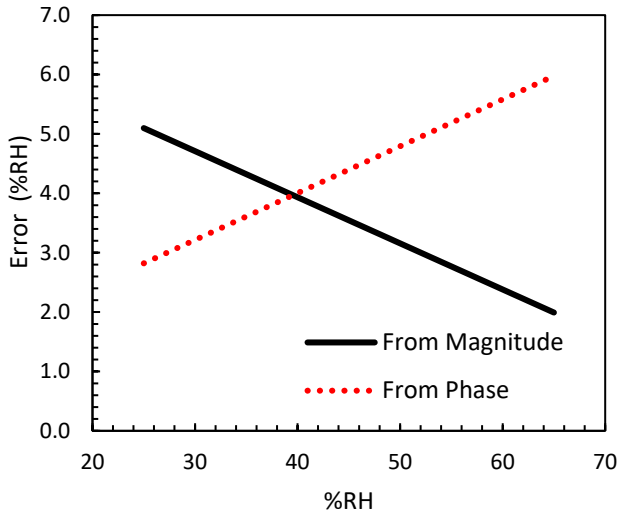

Figure 6. Error of relative humidity at 200 Hz due to the manufacturing variability. The errors were obtained from the magnitude and phase impedance measurement of the sensor.

3.2. Washing Cycles

In order to assure the success of e-textiles in real applications, these products should guarantee their functionality after the washing process. At this point, the electrical behavior of the proposed interdigitated textile sensor was evaluated after applying a washing process. Figure 7 shows the sensor impedance module and impedance phase without washing (continuous line), after applying one conventional washing cycles (dash-dot line) and after applying two washing cycles (dash-line). The linear regression for each case and the corresponding equation are also shown.

It was observed that after applying the washing cycles, the impedance module increased for all moisture values whereas the impedance phase was reduced. This behavior points out that after washing cycles the capacitance behavior of the proposed sensor decreased, meanwhile the resistance increased. A small significant difference was observed between one and two washing cycles. This fact is explained by the commercial fabrics' manufacturing process. In order to guarantee the distributions, the textiles are subjected to a specific antibacterial treatment. After washing, this treatment disappears, and this explains the reason of the similar electrical impedance after one and two washing cycles.

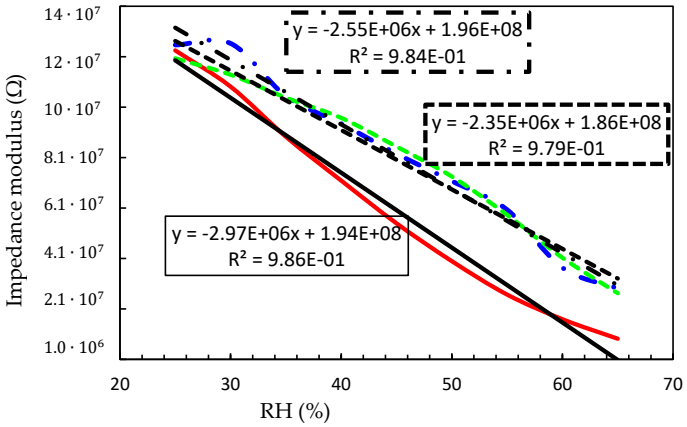

(**a**) Module impedance.

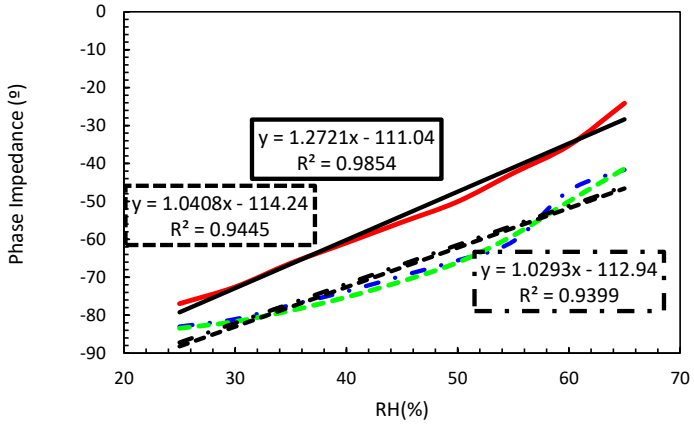

(**b**) Phase impedance.

Figure 7. Effect of washing cycles on the impedance at 200Hz. Before washing (continues line), after one washing cycle (dot-dash line), and after two washing cycle (dash line). The linear regression for each case and the equations are also show.

Table 2 summarizes the impact of washing cycles on sensor behavior. A clear difference before and after washing was observed. After the first washing, impedance module sensitivity was reduced by 14.14%, meanwhile, the zero drift was shifted just 1%. However, after the second washing cycle, only an additional 7.8% of reduction was observed, which represents a reduction of 20.88% with regard to unwashed samples. With respect to the impedance phase, almost no differences were observed between one or two washings. After washing the sensitivity was reduced between 18–19% and the offset about 2% in both cases. As previously mentioned, the used fabric has an antibacterial treatment that modifies its dielectric properties. In fact, this antibacterial treatment consists of an increase in the electrical conductivity of the fabric. Therefore, before washing, the treatment makes the sensor more conductive but, when the sensor was washed, this treatment was deleted, decreasing the conductivity of the fabric and therefore increasing the sensor impedance.

Table 2. Relation between the parameters measured and the relative humidity.

	Module				Phase			
Impedance	**Sensitivity** ($\frac{M\Omega}{\%RH}$)	**ΔS%**	**Zero Shift** $M\Omega$	**ΔZs %**	**Sensitivity** ($\frac{^\circ}{\%RH}$)	**ΔS %**	**Zero Shift** °	**ΔZs %**
No-wash	−2.97		194		1.272		−111.04	
1 wash	−2.55	−14.14	196	1.03%	1.029	−19.1	−112.94	1.71
2 washes	−2.35	−20.88	186	4.12%	1.041	−18.16	−114.24	2.88

4. Conclusions

In this work, an interdigitated embroidered textile sensor was proposed and the manufacturing variability and washing impact were characterized. The sensors were embroidered over a cotton substrate with a commercial Shieldex 117/17 dtex 2 yarn. The measured results demonstrate experimentally the usefulness of the proposed sensors at the kHz range to develop wearable applications over textile materials for moisture measurement. Due to the manufacturing variability process, an error lower that 6% on the RH measurement was obtained. However, this error can be reduced up to 4% when both the module and phase impedance of the sensor are measured. The washing process of the textile sensor also impacted the electrical behavior, mainly after the first washing cycle, when the treatment of the fabrics disappeared, this effect was mainly observed as a reduction on the sensor sensitivity. In any case, the devices kept some of their sensing capabilities.

Author Contributions: Investigation, M.M.-E. and R.F.-G.; Methodology, M.M.-E. and B.M.; Writing-Original Draft Preparation, R.F.-G.; Writing-Review & Editing, I.G.; Supervision, R.F.-G. and I.G.

Funding: This research was funded by the Spanish -MINECO grant number TEC2016-79465-R.

Conflicts of Interest: The authors declare no conflict of interest.

References

1. Barber, E.J.W. *Prehistoric Textiles: The Development of Cloth in the Neolithic and Bronze Ages with Special Reference to the Aegean*; Princeton University Press: Princeton, NJ, USA, 1991.
2. Castano, L.M.; Flatau, A.B. Smart fabric sensors and e-textile technologies: A review. *Smart Mater. Struct.* **2014**, *23*, 053001. [CrossRef]
3. Tsolis, A.; Whittow, W.G.; Alexandridis, A.A.; Vardaxoglou, J.Y.C. Embroidery and Related Manufacturing Techniques for Wearable Antennas: Challenges and Opportunities. *Electronics* **2014**, *3*, 314–338. [CrossRef]
4. Tessarolo, M.; Gualandi, I.; Fraboni, B. Recent Progress in Wearable Fully Textile Chemical Sensors. *Adv. Mater. Technol.* **2018**, *3*, 1700310. [CrossRef]
5. Saenz-Cogollo, J.; Pau, M.; Fraboni, B.; Bonfiglio, A. Pressure Mapping Mat for Tele-Home Care Applications. *Sensors* **2016**, *16*, 365. [CrossRef] [PubMed]
6. Wu, J.; Qiu, C.; Wang, Y.; Zhao, R.; Cai, Z.; Zhao, X. Human Limb Motion Detection with Novel Flexible Capacitive Angle Sensor Based on Conductive Textile. *Electronics* **2018**, *7*, 192. [CrossRef]
7. Tartare, G.; Zeng, X.; Koehl, L. Development of a wearable system for monitoring the firefighter's physiological state. In Proceedings of the 2018 IEEE Industrial Cyber-Physical Systems (ICPS), Saint Petersburg, Russia, 15–18 May 2018; pp. 561–566.
8. Fu, Y.Y.; Chan, Y.L.; Yang, M.H.; Chan, Y.C.; Virkki, J.; Björninen, T.; Sydänheimo, L.; Ukkonen, L. Experimental Study on the Washing Durability of Electro-Textile UHF RFID Tags. *IEEE Antennas Wirel. Propag. Lett.* **2015**, *14*, 466–469. [CrossRef]
9. Cao, R.; Pu, X.; Du, X.; Yang, W.; Wang, J.; Guo, H.; Zhao, S.; Yuan, Z.; Zhang, C.; Li, C. Screen-Printed Washable Electronic Textiles as Self-Powered Touch/Gesture Tribo-Sensors for Intelligent Human–Machine Interaction. *ACS Nano* **2018**, *12*, 5190–5196. [CrossRef] [PubMed]
10. Ryan, J.D.; Mengistie, D.A.; Gabrielsson, R.; Lund, A.; Müller, C. Machine-Washable PEDOT:PSS Dyed Silk Yarns for Electronic Textiles. *ACS Appl. Mater. Interfaces* **2017**, *9*, 9045–9050. [CrossRef] [PubMed]

© 2018 by the authors. Licensee MDPI, Basel, Switzerland. This article is an open access article distributed under the terms and conditions of the Creative Commons Attribution (CC BY) license (http://creativecommons.org/licenses/by/4.0/).

Paper C

Martínez-Estrada, M., Moradi, B., Fernández-Garcia, R., & Gil, I. (2019). Impact of conductive yarns on an embroidery textile moisture sensor. Sensors (Switzerland), 19(5), 1–10. https://doi.org/10.3390/s19051004

sensors

MDPI

Article

Impact of Conductive Yarns on an Embroidery Textile Moisture Sensor †

Marc Martínez-Estrada, Bahareh Moradi, Raúl Fernández-Garcia * and Ignacio Gil

Department of Electronic Engineering, Universitat Politècnica de Catalunya, 08222 Terrassa, Spain; marc.martinez.estrada@upc.edu (M.M.-E.); bahareh.moradi@upc.edu (B.M.); ignasi.gil@upc.edu (I.G.)

* Correspondence: raul.fernandez-garcia@upc.edu; Tel.: +34-937-398-089

† This paper is an extended version of our paper published in: Martínez-Estrada, M.; Moradi, B.; Fernández-Garcia, R.; Gil, I.; Embroidery Textile Moisture Sensor. In Proceedings of the Eurosensors 2018 Conference, Graz, Austria, 9–12 September 2018.

Received: 31 January 2019; Accepted: 20 February 2019; Published: 27 February 2019

Abstract: In this work, two embroidered textile moisture sensors are characterized with three different conductive yarns. The sensors are based on a capacitive interdigitated structure embroidered on a cotton substrate with an embroidered conductor yarn. The performance comparison of three different type of conductive yarns has been addressed. In order to evaluate the sensor sensitivity, the impedance of the sensor has been measured by means of an LCR meter from 20 Hz to 20 kHz on a climatic chamber with a sweep of the relative humidity from 30% to 65% at 20 °C. The experimental results show a clear and controllable dependence of the sensor impedance with the relative humidity and the chosen conductor yarns. This dependence points out the optimum conductive yarn to be used to develop wearable applications for moisture measurement.

Keywords: sensor; e-textile; embroidery; moisture; capacitive

1. Introduction

Nowadays, there is a huge demand on the research and development of wearable sensors for biological sensing applications [1,2] like health monitoring, physical training [3], emergency rescue service and law-enforcement [4]. In order to develop these sensors, fabric substrates have been revealed as a natural and convenient choice in the development of wearable electronic applications due to the fact that humans have been covering their body with fabrics for thousands of years. The integration of these sensors over textiles can be carried out by means of several techniques, such as inkjet printing, screen printing, stamp transfer, electrospinning and dip coating [5]. Among all the textile techniques, embroidery has been revealed as one of the most effective techniques to implement wearable sensors. This fact is due to the availability of the manufacturing technology (industrial embroidery machines), the efficient exploitation of the expensive specialized conductive threads and the repeatability of the involved geometries and layouts [6].

The development of moisture sensors for wearable applications over textiles and outfits is a current research topic. This field has been investigated using different methodologies such as carbon nanotubes (CNT) [7], ink-jet technology [8], knitted fabric [9], screen printing [10] and embroidery [10,11]. Most of the papers in the literature are focused on moisture sensors over textiles for humidity ranges higher than 60% RH whereas no effective impact for moisture lower than 60% RH was observed [7,8]. In this paper, a comparison of the electrical properties of the embroidered sensor over cotton substrate with several types of conductive yarns are analysed and assessed in the range of 30% RH to 65% RH. This is a practical moisture range from the point of view of the human body and it has not been deeply

investigated in the literature. In addition, the full characterization and electrical modelling has been carried out.

The remainder of the paper is organized as follows. Section 2 describes the material and methods including the conductive yarns used, the textile sensor layout and its implementation as well as the measurement set-up. In Section 3, the experimental results are shown and discussed. Finally, in Section 4, the conclusions are summarized.

2. Materials and Methods

The proposed moisture sensor is based on a capacitive embroidered interdigitated structure whose dimensions are depicted in Figure 1. Three different conductive yarns are used to evaluate the behaviour of each yarn. Firstly, a commercial Shieldex 117/17 dtex 2-ply has been chosen. This yarn is made of polyamide (PA) coated with pure silver. Secondly, two commercial Bekaert yarn have been chosen. These yarns are made of stainless steel (SS) in mix with polyester (PES) or cotton (CO). One of the Bekaert yarns is made by polyester (80%) and stainless steel (20%). The other Bekaert yarn is made by a mix of cotton (80%) and stainless steel (20%) [12]. Furthermore, these yarns, Shieldex and Bekaert, are manufactured by using different techniques. Shieldex yarn is made by a coating of pure silver in the surface of the PA filament (Figure 2a). The Bekaert yarns are made by mixing fibers of different materials (cotton and polyester with stainless steel) at the beginning of the process to manufacture the yarn (Figure 2b). The most important properties for the aforementioned yarns are summarized in Table 1.

Table 1. Most important properties about the yarns.

Properties	Shieldex	Bekaert (PES-SS)	Bekaert (CO-SS)
Density(tex)	11.7/2	20/2	20/2
Linear resistance (Ω/cm)	<30	50	35–70
Thread type	Twisted Multifilament	Ring yarn	Ring yarn

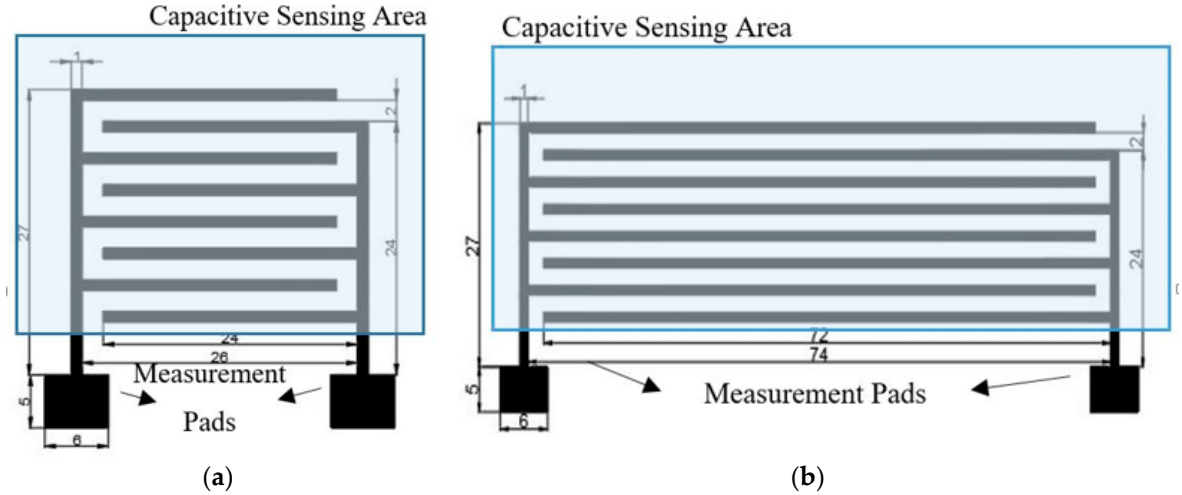

(**a**) (**b**)

Figure 1. Layout and dimension detail of the proposed moisture sensor (in mm): (**a**) short sensor; (**b**) long sensor. The bottom squares correspond to the characterization pads.

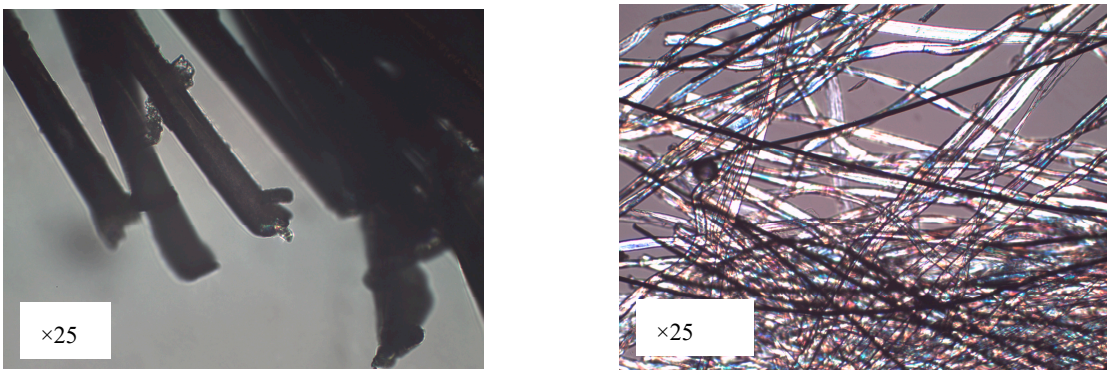

(**a**) (**b**)

Figure 2. Microscope image of the used conductive yarns (**a**) Shieldex: this yarn is made of polyamide (PA) (inner) coated with pure silver (outer); (**b**) Bekaert: This yarn is made by mixing fibers (white fibers) of cotton with stainless steel (black fibers).

The considered conductive yarns are used in order to embroider the interdigitated structures on a high hygroscope substrate. In these cases, the permittivity of the substrate will be modified under the presence of water molecules. This mechanism allows achieving the sensing capability of the proposed devices. Specifically, a cotton substrate with a thickness (h) of 0.43 mm has been chosen. A Singer Futura XL-550 embroidery machine with a satin fill stitch pattern has been selected in order to achieve a homogeneous yarn distribution over the sensor surface.

In order to experimentally compare the sensors' behaviour, the implemented devices have been tested in a CCK-25/48 Dycometal climatic chamber and the sensors impedances have been measured by means of an external Rohde & Schwarz HM8118 LCR meter. An image of the experimental setup is shown in Figure 3.

Figure 3. Image of the experimental setup.

The sensors impedances have been measured from 20 Hz to 20 kHz in a 30% to 65% range of relative humidity environment, whereas the temperature has remained constant at 20 °C.

3. Results and Discussion

Figure 4 shows the measured sensor impedance of the sensor embroidered with Shieldex when the moisture is swept from 30% to 65% for four different test frequencies. It is observed that the impedance module of the sensor is reduced when the environmental moisture increases, which confirms the functionality of the proposed structure as a moisture sensor. The measured phase impedance of the sensor denotes that for low relative humidity the sensor has a capacitive behaviour, as expected. Moreover, for higher relative humidity concentration the sensor tends to be resistive. The reason for

this behaviour is the hydrophilic property of the cotton. Indeed, when the relative humidity increases, the cotton substrate absorbs water and the electrical permittivity of the substrate increases. As a result, the impedance of the sensor is reduced.

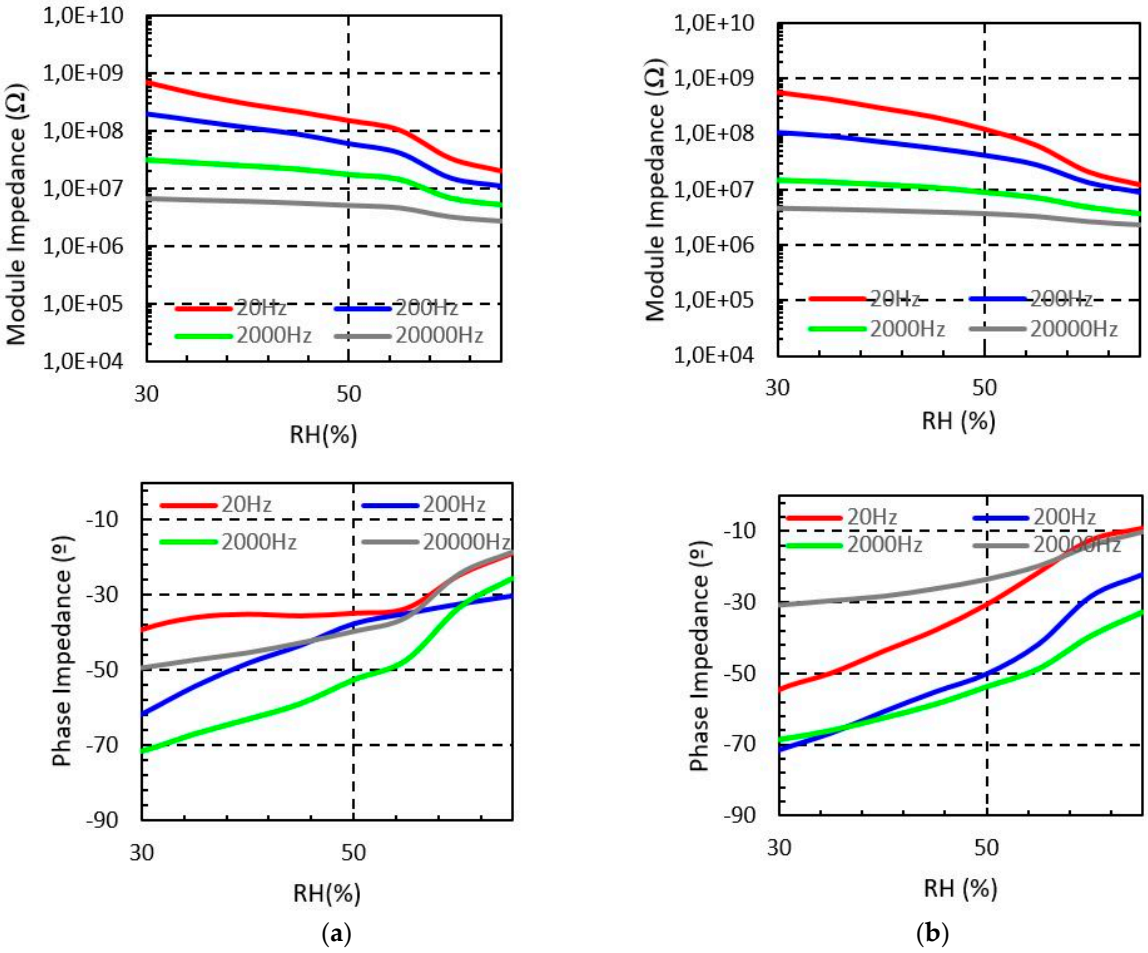

Figure 4. Measured Shieldex sensors impedance from 30% to 65% RH at different frequencies (T = 20 °C). (**a**) Short sensor impedance (**b**) Long sensor impedance.

Long and short sensors show similar behaviour with the relative moisture. However, as it is expected, the impedance of the longer sensor (Figure 4b) is lower than the impedance of the short device (Figure 4a). In particular, for the 20 Hz test signal, the short sensor impedance decreases from 0.7 GΩ to 20.4 MΩ when the moisture increases from 30% to 65%, whereas, for the long sensor device it decreases from 0.57 GΩ to 12.5 MΩ for the same moisture range.

Figures 5 and 6 show the measured impedance of the sensor embroidered with Bekaert PES-SS and Bekaert CO-SS, respectively. In all cases, it is observed that the sensor impedance module is reduced when the moisture increases, as we observed for the Shieldex yarn. However, both PES-SS and CO-SS show a significant impedance module reduction compared to Shieldex yarn, in all cases. In particular, for PES-SS at 20 Hz test, the impedance module decreases from 0.12 GΩ to 0.92 MΩ. In the case of the long sensor, the range decreases from 27 MΩ to 0.47 MΩ, whereas for CO-SS these values decrease from 0.13 GΩ to 4.2 MΩ and from 23.7 MΩ to 0.37 MΩ for the short and long sensor, respectively. The explanation for these differences between the Shieldex and Bekaert yarns is based on the electrical conductivity of the yarn, which depends on the conductive materials but also of the fabrication process. The non-conductive material of the yarn (i.e., polyester or cotton) does not have any significant impact on this behaviour.

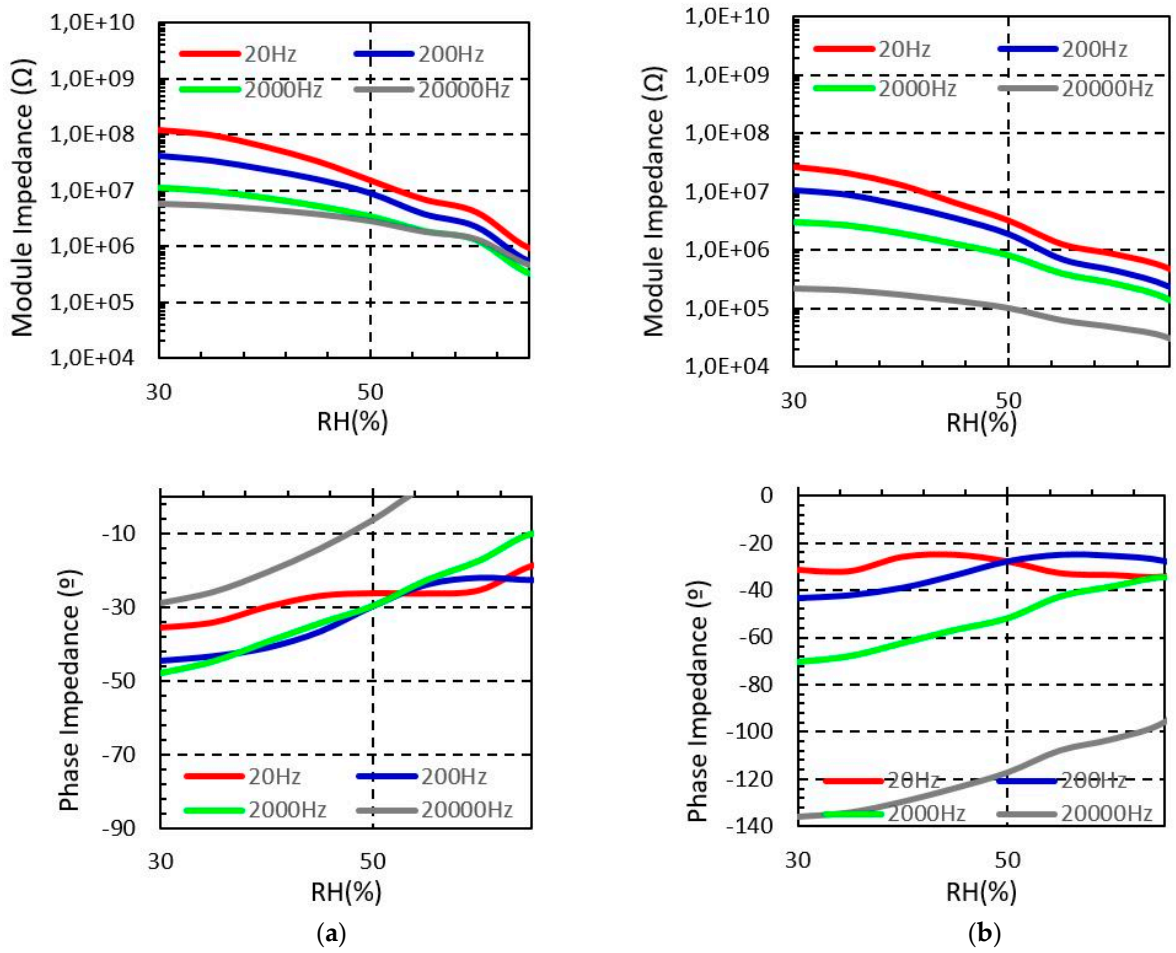

Figure 5. Measured Bekaert (PES-SS) sensors impedance from 30% to 65% RH at different frequencies (T = 20 °C). (**a**) Short sensor impedance (**b**) Long sensor impedance.

It should be noticed that the obtained impedance values at the low frequency range are too high in order to develop a portable device based on the proposed sensor. These wearable devices are typically based on a single integrated circuit, such as the Texas Instrument AD5933 impedance converter [13]. Nevertheless, using the proposed sensor in the range of kHz allows obtaining impedances in the range of a MΩ. In these cases, the impedance values can be measured with those integrated circuits.

For comparison, in Table 2, the impedance range values at 2 kHz are summarized. Again, it is observed that for the same parameters of size, the sensors embroidered with Bekaert yarn had almost three times less module impedance than the Shieldex sensors. The difference should be due to the differences in the fabrication of each yarn. Bekaert yarns are made by fibres, whereas, Shieldex is made by coating a filament with silver. Another hypothesis consists of the fact that the Bekaert yarns can retain more moisture on their surface, and this moisture will decrease most effectively the values of impedance than in the other study case.

Table 2. Measured sensors module impedances ranges at 2 kHz.

Sensor	Shieldex	Bekaert (PES-SS)	Bekaert (CO-SS)
Short	31.2-5.18 MΩ	11.3-0.32 MΩ	12.6-0.85 MΩ
Long	14.8-3.71 MΩ	2.98-0.14 MΩ	3.62-0.19 MΩ

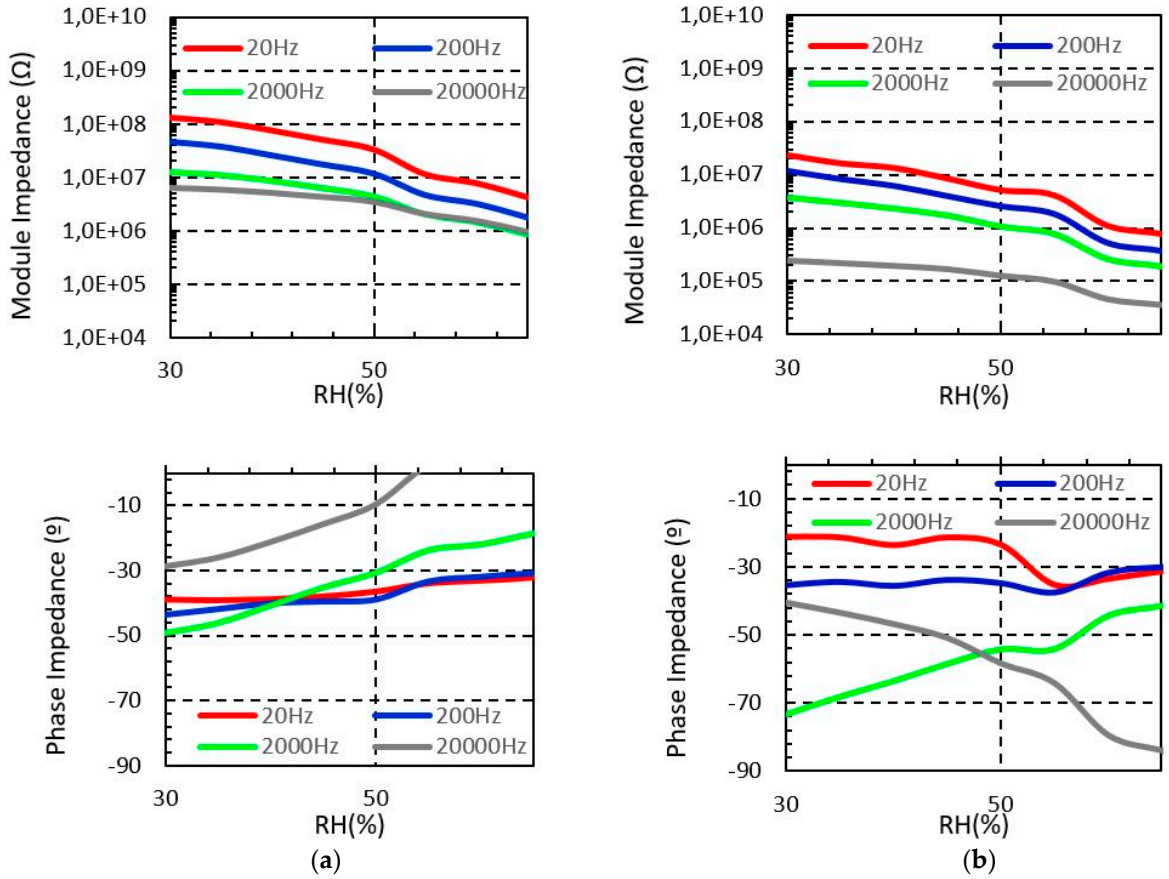

Figure 6. Measured Bekaert (CO-SS) sensors impedance from 30% to 65% RH at different frequencies (T = 20 °C). (**a**) Short sensor impedance (**b**) Long sensor impedance.

If we focus on the electrical model according to the measured behaviour of the proposed sensors at 2 kHz, they can be modelled as a RC parallel lumped model (Figure 7b), where the R and C values are moisture dependent. The C represents the capacitance and R the current leakage of the interdigitated structure.

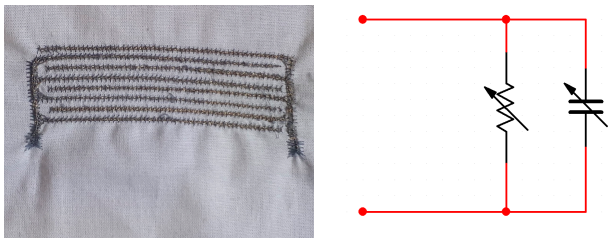

Figure 7. Proposed long sensor: (**a**) physical implementation and (**b**) electrical model.

From Figures 8–10, the R and C dependence from 30% to 65% RH at 2 kHz is shown for both short and long sensors with Shieldex, Bekaert PES-SS and Bekaert CO-SS yarn, respectively. It can be observed that when the moisture level increases the capacitance is increased, whereas the resistance is reduced in all cases. It should be pointed out that the sensor based on Bekaert yarn shows a higher sensitivity with the moisture than the Shieldex yarn. This effect can be due to the moisture impact of the electrical properties of the yarn. Tables 2 and 3 summarise the resistance and capacitance values of the electrical model when the moisture is swept from 30% to 65. The Bekaert yarns have a larger range of resistance value than the Shieldex sensors. However, between the Bekaert sensors it is not observed

a relevant difference. Specifically, the resistance of Shieldex short sensor is reduced about 39%, whereas for Bekaert PES-SS and Bekaert CO-SS the reduction achieves 95.7% and 90.2%, respectively when the moisture is swept from 30% to 65% (Table 2). For the same moisture range, the capacitance increases about one order of magnitude (×10) for Shieldex yarn and about two order of magnitude (×100) for Bekaert PES-SS and Bekaert CO-SS (Table 3). This key fact points out that Bekaert yarns are more sensitive to develop moisture sensors, increasing the overall sensor sensitivity. It should be pointed out that for all conductive yarns and sensors a clear sensitivity change is produced around 55 % RH.

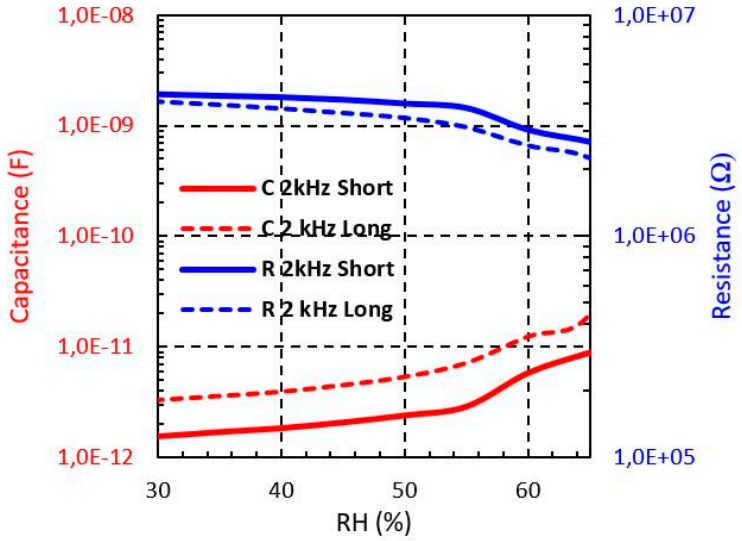

Figure 8. Measured Shieldex sensors impedance from 30% to 65% RH at different frequencies.

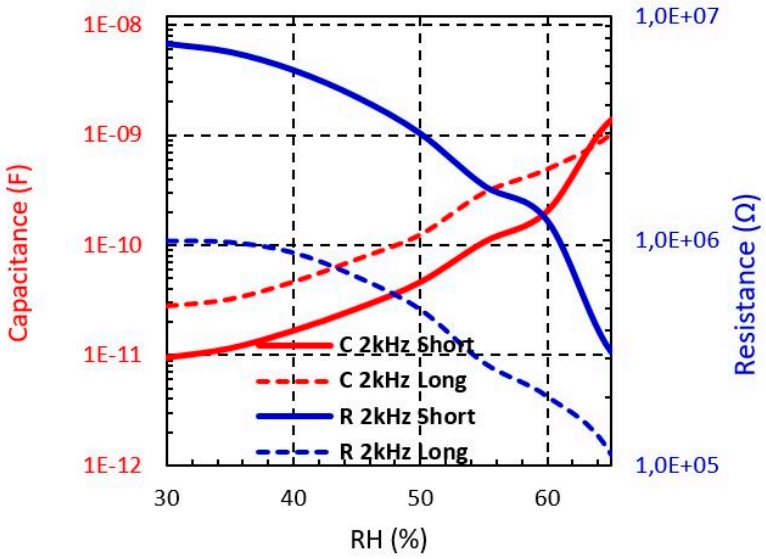

Figure 9. Measured Bekaert (PES-SS) sensors impedance from 30% to 65% RH at different frequencies.

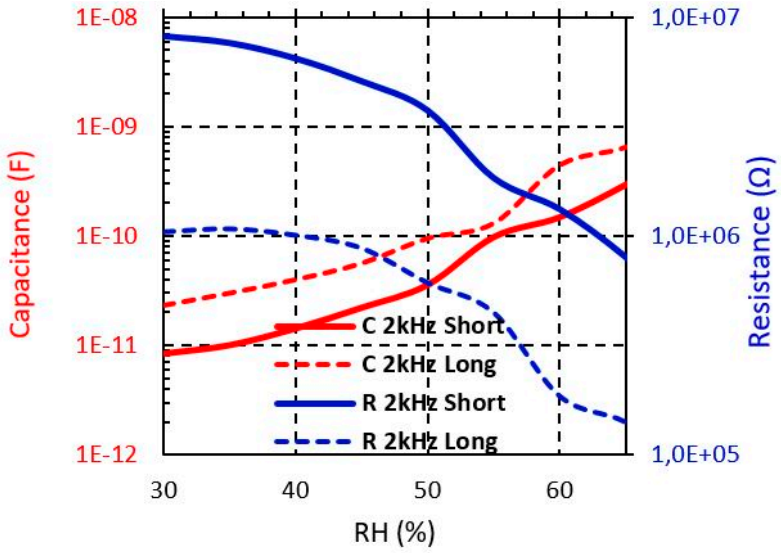

Figure 10. Measured Bekaert (CO-SS) sensors impedance from 30% to 65% RH at different frequencies.

Table 3. Measured sensors resistance ranges at 2 kHz.

Sensor	Shieldex	Bekaert (PES-SS)	Bekaert (CO-SS)
Short	4.42-2.68 MΩ	7.57-0.32 MΩ	8.22-0.8 MΩ
Long	4.17-2.26 MΩ	0.99-0.11 MΩ	1.04-0.14 MΩ

In the following Tables 3 and 4 the values of resistance and capacitance for the studied sensors.

Table 4. Measured sensors capacitance ranges at 2 kHz.

Sensor	Shieldex	Bekaert (PES-SS)	Bekaert (CO-SS)
Short	1.56-8.84 pF	9.48 pF-1.37 nF	8.37 pF-0.29 nF
Long	3.3-19.4 pF	28.3 pF-1.02 nF	23 pF-0.65 nF

4. Conclusions

In this work, two interdigitated embroidered textile sensors have been proposed and characterized. The sensors have been embroidered over a cotton substrate with a commercial Shieldex 117/17 dtex 2 yarn, a commercial Bekaert (PES-SS) and Bekaert (CO-SS) 20/2 Tex. The measured results show that the sensor under analysis can be modelled by means of an RC parallel lumped circuit, where the R and C value are dependent on the moisture level. Particularly, a capacitance sensitivity at 2 kHz for short sensors of 0.21 pF/% RH, 38.87 pF/% RH and 8.05 pF/% RH is measured for Shieldex, PES-SS, CO-SS, respectively, whereas the resistance sensitivity is -49.7 kΩ/% RH, -207 kΩ/% RH and -212 kΩ/% RH. These results demonstrate experimentally the usefulness of the proposed sensors to achieve wearable moisture effective sensors for human body monitoring. In addition, the study points out that the Bekaert yarn PES-SS is preferred to increase the moisture sensitivity performance.

Author Contributions: Investigation, M.M.-E. and B.M.; Methodology, R.F.-G.; Writing-Original Draft Preparation, R.F.-G.; Writing-Review & Editing, I.G.

Funding: This work was supported by the Spanish -MINECO Project TEC2016-79465-R.

Conflicts of Interest: The authors declare no conflict of interest.

References

1. Matzeu, G.; Florea, L.; Diamond, D. Advances in wearable chemical sensor design for monitoring biological fluids. *Sensors Actuators B Chem.* **2015**, *211*, 403–418. [CrossRef]
2. Wang, S.; Gong, L.; Shang, Z.; Ding, L.; Yin, G.; Jiang, W.; Gong, X.; Xuan, S. Novel Safeguarding Tactile e-Skins for Monitoring Human Motion Based on SST/PDMS-AgNW-PET Hybrid Structures. *Adv. Funct. Mater.* **2018**, *1707538*, 28. [CrossRef]
3. Wu, J.-F.; Qiu, C.; Wang, Y.; Zhao, R.; Cai, Z.-P.; Zhao, X.-G.; He, S.-S.; Wang, F.; Wang, Q.; Li, J.-Q. Human Limb Motion Detection with Novel Flexible Capacitive Angle Sensor Based on Conductive Textile. *Electronics* **2018**, *7*, 192. [CrossRef]
4. Tartare, G.; Zeng, X.; Koehl, L. Development of a wearable system for monitoring the firefighter's physiological state. In Proceedings of the 2018 IEEE Industrial Cyber-Physical Systems (ICPS), Saint-Petersburg, Russia, 15–18 May 2018; pp. 561–566.
5. Tessarolo, M.; Gualandi, I.; Fraboni, B. Recent Progress in Wearable Fully Textile Chemical Sensors. *Adv. Mater. Technol.* **2018**, *3*, 1700310. [CrossRef]
6. Castano, L.M.; Flatau, A.B. Flatau, Smart fabric sensors and e-textile technologies: A review. *Smart Mater. Struct.* **2014**, *23*, 053001. [CrossRef]
7. Zhou, G.; Byun, J.-H.; Oh, Y.; Jung, B.-M.; Cha, H.-J.; Seong, D.-G.; Um, M.-K.; Hyum, S.; Chou, T.-W. Highly Sensitive Wearable Textile-Based Humidity Sensor Made of High-Strength, Single-Walled Carbon Nanotube/Poly(vinyl alcohol) Filaments. *ACS Appl. Mater. Interfaces* **2017**, *9*, 4788–4797. [CrossRef] [PubMed]
8. Weremczuk, J.; Tarapata, G.; Jachowicz, R. Humidity Sensor Printed on Textile with Use of Ink-Jet Technology. *Procedia Eng.* **2012**, *47*, 1366–1369. [CrossRef]
9. Jakubas, A.; Lada-Tondyra, E.; Nowak, M. Textile sensors used in smart clothing to monitor the vital functions of young children. In Proceedings of the 2017 Progress in Applied Electrical Engineering (PAEE), Koscielisko, Poland, 25–30 June 2017; pp. 1–4.
10. Grethe, T.; Borczyk, S.; Plenkmann, K.; Normann, M.; Rabe, M.; Schwarz-Pfeiffer, A. Textile humidity sensors. In Proceedings of the 2018 Symposium on Design, Test, Integration & Packaging of MEMS and MOEMS (DTIP), Rome, Italy, 22–25 May 2018; pp. 1–3.
11. Soukup, R.; Hamacek, A.; Mracek, L.; Reboun, J. Textile based temperature and humidity sensor elements for healthcare applications. In Proceedings of the 2014 37th International Spring Seminar on Electronics Technology, Dresden, Germany, 7–11 May 2014; pp. 407–411.
12. Agcayazi, T.; Yokus, M.A.; Gordon, M.; Ghosh, T.; Bozkurt, A. A stitched textile-based capacitive respiration sensor. In Proceedings of the 16th IEEE Sensors Conference, Glasgow, UK, 29 October–1 November 2017; pp. 1074–1076.
13. A. Devices, AD5933 1 MSPS, 12-Bit Impedance Converter, Network Analyzer. Available online: http://www.analog.com/media/en/technical-documentation/data-sheets/AD5933.pdf (accessed on 4 July 2018).

© 2019 by the authors. Licensee MDPI, Basel, Switzerland. This article is an open access article distributed under the terms and conditions of the Creative Commons Attribution (CC BY) license (http://creativecommons.org/licenses/by/4.0/).

Paper D

Martínez-Estrada, M., Fernández-García, R., & Gil, I. (2021). Experimental analysis of fabric substrate on a moisture sensor. Journal of the Textile Institute, 112(6), 881–886. https://doi.org/10.1080/00405000.2020.1783781

The Journal of The Textile Institute

ISSN: (Print) (Online) Journal homepage: https://www.tandfonline.com/loi/tjti20

Experimental analysis of fabric substrate on a moisture sensor

Marc Martínez-Estrada, Raúl Fernández-García & Ignacio Gil

To cite this article: Marc Martínez-Estrada, Raúl Fernández-García & Ignacio Gil (2021) Experimental analysis of fabric substrate on a moisture sensor, The Journal of The Textile Institute, 112:6, 881-886, DOI: 10.1080/00405000.2020.1783781

To link to this article: https://doi.org/10.1080/00405000.2020.1783781

Published online: 25 Jun 2020.

Submit your article to this journal

Article views: 178

View related articles

View Crossmark data

Full Terms & Conditions of access and use can be found at
https://www.tandfonline.com/action/journalInformation?journalCode=tjti20

Note from: Servei de Biblioteques, Publicacions i Arxius de la UPC

Pages 187 to 192 of the thesis which contain this article are available on the publisher's website:

- Martínez-Estrada, M., Fernández-García, R., & Gil, I. (2021). Experimental analysis of fabric substrate on a moisture sensor. *The Journal of The Textile Institute,* 112(6), 881–886. https://doi.org/10.1080/00405000.2020.1783781

Paper E

Martínez-Estrada, M., Ventura, H., Gil, I., & Fernández-García, R. (2022). A Full Textile Capacitive Woven Sensor. Advanced Materials Technologies, 2200284. https://doi.org/10.1002/ADMT.202200284

ADVANCED MATERIALS TECHNOLOGIES
www.advmattechnol.de

A Full Textile Capacitive Woven Sensor

Marc Martínez-Estrada, Heura Ventura, Ignacio Gil, and Raúl Fernández-García*

In this paper, a full textile capacitive woven sensor integrated over a textile substrate is presented. The sensor consists in an interdigitated capacitance prepared to measure moisture and/or presence detection. In order to evaluate the sensor response to moisture, capacitance has been measured by means of an LCR meter from 20 Hz to 20 kHz in a climatic chamber with a swept of the relative humidity (RH) from 30% to 90% at 20 °C. Subsequently, presence response is evaluated measuring the capacitance of the woven sensor meanwhile a person is sitting down and getting up. The woven sensor results demonstrate its functionality over moisture measurement where sensor capacitance changes from a minimum of 9.74 pF at 30% RH to a maximum of 2.31 uF at 90% RH. The presence detection is also demonstrated, which makes the capacitance variation change from a 10% of capacitance variation when the chair is empty, to a capacitance variation of 170% when a person is sitting on it. The adaptation of the weaving process to accomplish a fully integrated sensor provides a better repeatability than previous embroidered sensors and opens a door to being commercially produced.

1. Introduction

Smart textiles and wearable devices are being developed everyday by researchers with the objective of substitute standard electronic components. People have an increasing interest obtaining information about their health, the world around them and the interactions with others during their daily life. To achieve this, on-body sensors are the most commonly used technology at present, and they can be found in fields as healthcare applications,[1,2] physical training,[3] emergency rescue service, and law-enforcement.[4] Nevertheless, smart textile developments are leading to the appearance of new applications beyond on-body sensors such as gas detection,[5] ballistics,[6] or structural deflection detection.[7] Latest advances are introducing energy harvesting methods on textile sensors to obtain power from other source, which typically are batteries.[8,9]

Although sensors integrated on clothes are the core field nowadays, new ways to use the technology of integrated sensor on textile are taking importance on current research. Fabrics are used in many applications that are not related to personal clothing. Some of these fields are automotive industry, home clothing, agriculture, building materials, maritime industry, and more.[7,10] Applied textile technology to produce smart textiles provides an increase of the product's value used in those fields, which companies could use to launch new products. Smart textiles could provide tools to be used on unexpected applications, such as using the new textile materials and standard electronic devices to add functionalities to the fabrics as humidity or presence detection.[11] Some advantages of integrated textile sensors are the capability to cover longer areas than standard sensors with lower cost, fewer requirements than electronic components, or the ability to monitor physical or chemical stimuli without significantly affecting the structure of the fabric.

Integration methods to produce textile sensor are also a research field over the world, where it can be found a wide variety of methods used. There are chemical oriented methods as the layer by layer self-assembled method,[12] integration by electromagnetic fields (electrospinning)[13] and methods that use the textiles processes to introduce the sensor as embroidery or woven manufacture methods.

Embroidery has been demonstrated over different researches, as the most cost-effective technique for prototyping and low-scale production, due to its fast prototyping and cost of the needed machinery. Previous works[14–16] on capacitive interdigitated sensor were made using embroidery as integration method. However, when the textile sensors are prepared for being used in health care applications, low-scale production could be a drawback. Woven fabrics are known to be produced in large-scale production with lower cost than embroidery. In addition, woven technology could produce textile sensor fully integrated and non-touch-sensitive.[17] Woven electronic textiles are also a growing research field, which have been increasing in the last years.[18,19] Weaving technique provides better results for the integration of the textile sensor, maintaining the textile properties of the substrate.

The humidity has been a crucial factor in hospitals or nursing homes over the years. Injuries related to the long

M. Martínez-Estrada, I. Gil, R. Fernández-García
Department of Electronical Engineering
Universitat Politécnica de Catalunya
Terrassa, Spain
E-mail: marc.martinez.estrada@upc.edu
H. Ventura
Departament de Ciéncia i Enginyeria de Materials – Textile Engineering Section
Universitat Politécnica de Catalunya
Terrassa, Spain

The ORCID identification number(s) for the author(s) of this article can be found under https://doi.org/10.1002/admt.202200284.

© 2022 The Authors. Advanced Materials Technologies published by Wiley-VCH GmbH. This is an open access article under the terms of the Creative Commons Attribution-NonCommercial-NoDerivs License, which permits use and distribution in any medium, provided the original work is properly cited, the use is non-commercial and no modifications or adaptations are made.

DOI: 10.1002/admt.202200284

Check for updates
2365709x, 0, Downloaded from https://onlinelibrary.wiley.com/doi/10.1002/admt.202200284 by Readcube (Labtiva Inc.), Wiley Online Library on [11/12/2022]. See the Terms and Conditions (https://onlinelibrary.wiley.com/terms-and-conditions) on Wiley Online Library for rules of use; OA articles are governed by the applicable Creative Commons License

2365709x, 0, Downloaded from https://onlinelibrary.wiley.com/doi/10.1002/admt.202200284 by Readcube (Labtiva Inc.), Wiley Online Library on [11/12/2022]. See the Terms and Conditions (https://onlinelibrary.wiley.com/terms-and-conditions) on Wiley Online Library for rules of use; OA articles are governed by the applicable Creative Commons License

exposures of the patient to the humidity could be minimized having a close control on the humidity state. The staff has many patients to care about, and a system to monitor humidity, providing information in real time could be crucial for improving the attendance. A system to respond that necessity was presented in previous works by the author.[16] To improve the previous system, a textile sensor is produced by weaving process to obtain a better touch feeling, large scale production, and lower production cost.

Furthermore, several applications can be also developed, such as presence detector, using the same sensor. It could be done installing the sensor on the seat textiles. Force Sensitive Resistor(FSR)[20] is the actual technology used on the car seats to detect the presence and send the signal to a microcontroller that activates the seat alarm if the seat belt is not attached and the person is sitting on the seat. Depending on the pressure that actuates on the FSR the resistance variation is higher or lower. Hence, they do not detect the difference between a person or a heavy object. For example, when a bag is disposed on a seat, if the threshold is exceeded the alarm starts ringing. Pressure woven sensors[21] could be the natural textile substitute to FSR sensors in car seats. The woven capacitive sensor presented in this work could avoid the problem presented as example.

In this paper, to demonstrate the viability of the woven technologies to integrate interdigitated sensor on fabrics, a full textile capacitive woven sensor to measure humidity and presence is evaluated. The woven sensor is presented as an improvement of the previous reported embroidered sensors providing a higher degree of integration, more comfort for the user and facilitate large-scale integration of the textile sensor.

2. Experimental Section

The proposed woven sensor is based on an interdigitated structure. **Figure 1** shows the layout and dimensions of the sensor. The sensor was woven on a Dornier LWV8/J weaving machine moved by a Jacquard Stäubli LX1600B, which is shown in **Figure 2**. The

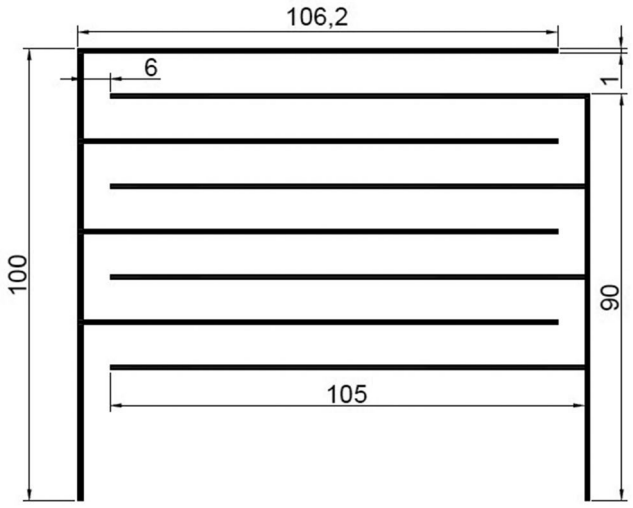

Figure 1. Dimensions of woven sensor in mm.

Figure 2. Dornier LWV8/J weaving machine moved by a Jacquard Stäubli LX1600B.

woven machine was prepared with a warp beam formed by 100% cotton yarns. Weft yarn was composed by a cotton/polyester yarn (35/65%). These materials formed the substrate where the sensor is integrated. The substrate has a hydrophilic nature, which means that the water particles in the air could be absorbed by the substrate changing its electrical permittivity.

2.1. Manufacturing Process

The weaving process is the method used to manufacture a fabric through a sequential introduction of a horizontal yarn (weft yarn) between vertical yarns (warp yarns) that come from a beam. To configure the structure of the final fabric, the warp yarns were moved up or down by a Jacquard system corresponding to the position required for the weave. Consecutively for each Jacquard position, a weft yarn was inserted between the warp yarns, causing the link between them and producing the fabric sensor.

Warp beam was prepared with high-cost process and only a few companies of the zone have the machinery need. The weft yarns were prepared in a yarn rack and connected to one of the six introduction yarn systems that our weaving machine had. As it can be observed, **Figure 3** shows the weaving process scheme. The method of the introduction of the weft yarn varied depending on the specific technology. In Figure 3, it can be observed as a flying shuttle, which is the hand-made system. In the case of the Dornier LWV8/J weaving machine, an insertion by air pressure was used.

In order to weave the sensor two different conductive yarns were used. One of them was a commercial Shieldex 117/17 2-ply(S), which was a silver 99% coating covering a polyamide filament. The second yarn used was a Bekaert 20/2 Tex (B) polyester mixed with stainless steel fibers with a proportion of 60/40%, respectively, which was produced by ring yarn procedure. The yarns had different properties; on one hand, Shieldex yarn had more tensile resistance and lower electrical resistance. On the other hand, Bekaert yarn was more comfortable and lighter. Properties of conductive and non-conductive yarns used are presented on **Table 1**.

© 2022 The Authors. Advanced Materials Technologies published by Wiley-VCH GmbH

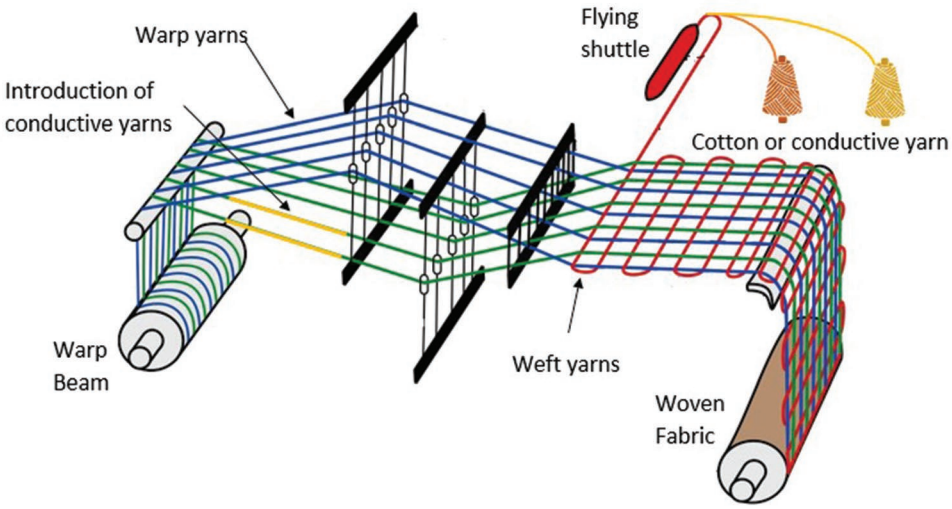

Figure 3. Weave process scheme.

To weave the sensor, the conductive yarns should be introduced on the warp and weft. Preparing a new warp beam is unfeasible due to the cost and the machinery need. Instead of it, warp single yarns are being partial substituted by hand. In Figure 3, it is shown where the yarns are substituted. The process followed was to cut the initial cotton warp yarn on the beam and knot a portion of conductive yarn to both ends of the initial warp yarn, which is represented as yellow yarns in the figure. This process is repeated for each substitution.

Regarding the manufacture process of the sensors with Shieldex yarn, 12 individual yarns of the warp were substituted by Shieldex conductive yarns. These yarns formed two vertical lines along the woven fabric, which were the lines that connected the different horizontal lines. Afterward, Shieldex conductive yarn was introduced on the weft system to proceed with the weave process of the fabric. The same methodology was performed with the Bekaert yarn. As a result, two types of sensors were obtained. Sensors produced with warp and weft yarn from Shieldex were defined as USTS, and sensors made with warp and weft yarn from Bekaert were defined as UBTB. The resulting fabric from the process counts with 40 yarns cm^{-1} in warp direction, 26 yarns cm^{-1} in weft direction and a mass per surface of 292 \texg m^{-2}.

2.2. Sensor Characterization

The proposed woven textile sensor was characterized with relative humidity and evaluated as a presence sensor. **Figure 4** shows the two woven sensors.

Table 1. Properties for the yarns used on the research.

Properties	Shieldex(S)	Bekaert(B)	Warp (CO)	Warp (CO/PES)
Density (tex)	11.7/2	20/2	19/2	24/2
Linear R(Ω cm^{-1})	30	50	–	–
Thread type	Twisted multifil.	Ring yarn	Ring yarn	Ring yarn

With regard to the humidity characterization, the sensor was introduced into a CCK-25/48 Dycometal climatic chamber to observe the behavior facing a swept from 30% to 90% of relative humidity and temperature has remained constant at 20 °C. To obtain the optimal behavior of the sensor, it is maintained 5 min at the initial relative humidity. This time was used to balance the relative humidity with the humidity that remained into the substrate, avoiding hysteresis during the measurements. The temperature was fixed due to at hospitals and nursing homes, the temperature is controlled. During this test, the capacitance was measured all over the swept by means of an external Rohde & Schwarz HM8118 LCR meter. The test was performed three times for each sensor. At the end, 9 groups of values were obtained for each type.

To check the sensor behavior as presence sensor, it was placed over a chair. A person, whose weight was 70 kg, sat down on the chair while the capacitance values were recapped, the actions duration was 10 s and it was repeated four times. Additionally, 3 cycles of the presence test were repeated for a 4,6,10, and 15 kg bag, covering the sensor to demonstrate that the sensor is able to distinguish between a person and an object. The sensor capacitance had been measured from 20 Hz to 2 kHz.

The sensor operation principle is based on the permittivity (ε_{RH}) change, which can be produced by a change in the humidity (humidity sensor) or a change on the contact material (presence sensor). The equation that describes the total series capacitance of an interdigital capacitor can be written as follows:[22]

$$C_{RH} = \frac{\varepsilon_{RH} \cdot 10^{-3}}{18\pi} \frac{K(k)}{K'(k)} \cdot l \cdot (N-1)\,(pF) \tag{1}$$

$$\frac{K(k)}{K'(k)} = \frac{\pi}{ln \times 2\dfrac{1+\sqrt{k'}}{1-\sqrt{k'}}} \tag{2}$$

$$k = \tan^2\left(\frac{a\pi}{4b}\right) \tag{3}$$

© 2022 The Authors. Advanced Materials Technologies published by Wiley-VCH GmbH

2365709x, 0, Downloaded from https://onlinelibrary.wiley.com/doi/10.1002/admt.202200284 by Readcube (Labtiva Inc.), Wiley Online Library on [11/12/2022]. See the Terms and Conditions (https://onlinelibrary.wiley.com/terms-and-conditions) on Wiley Online Library for rules of use; OA articles are governed by the applicable Creative Commons License

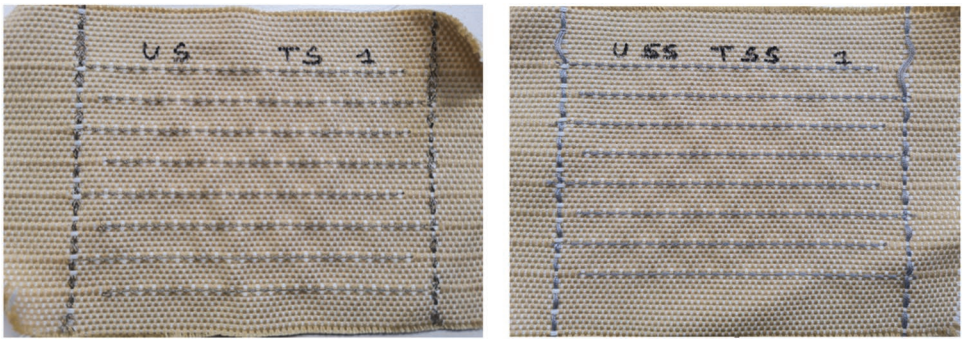

Figure 4. Textile woven sensor.

$$a = \frac{W}{2} \tag{4}$$

$$k' = \sqrt{1-k^2} \tag{5}$$

$$b = \frac{W+S}{2} \tag{6}$$

where l is the length of the fingers in microns, N is the number of fingers, (ε_{RH}) is the parameter that suffers changes with moisture level or when a person is touching the textile sensor.

3. Results and Discussion

3.1. Humidity Sensor

In order to validate the sensor behavior, the capacitance of the sensor at 20 Hz was evaluated. **Figure 5** shows the sensor capacitance against humidity response for the USTS and UBTB sensors. It is shown how the logarithm of the capacitance ($Y = log_{10}(C)$), where C is the capacitance in Farads, increases as the relative humidity increases for both sensors. The measurement range presented for USTS sensorson Figure 5a starts at –11.01 (9.74 pF) at 30% of relative humidity and develop till –5.79 (2.31 μ F) at 90% of relative humidity.

On Figure 5b can be observed the behavior of the UBTB sensors. The Bekaert yarns show good stability around the swept in relative humidity. The measured capacity range goes from –10.97 (11.9 pF) at 30% of relative humidity and grows till –6.42 (0.3 μ F) at 90% of relative humidity.

Linear regression is evaluated for each sensor logarithmic capacitive values. Linear regression follows the equation:

$$log_{10}(C) = a \cdot \mathrm{HR} + b \tag{7}$$

where HR refers to the relative humidity value on percentage. On **Table 2**, values from linear regression are displayed.

Linear regression evaluation provides the sensitivity of each sensor, which is the slope of the line. Linear regression shows that UBTB has a lower slope and its $62 \times 10^6 \mathrm{Sm}^{-1}$ is higher, being more linear than USTS sensor and matching better with its equation.

USTS has the highest dispersion between 75% to 85%, the standard deviation values go from 4.3% to 5.5% regarding the average value. Being the highest standard deviation point on 75% of relative humidity with a value of 5.5%. Instead, UBTB standard deviation values are more stable. There are not as big differences as for USTS values. The highest standard deviation values are on 80% and 85% of relative humidity with a value of 2.5% and 2.9%, respectively, regarding the average value.

The differences between these materials could be explained by their electrical properties. On one hand, the range of values is wider on the USTS due to the silver conductivity. Silver is more conductive ($[1.28-1.32] \times 10^6 \mathrm{Sm}^{-1}$) and it has lower resistivity than stainless steel ($log(C)(\mathrm{RH})^{-1}$). On the other hand, UBTB has a lower standard deviation than USTS. The fact that stainless steel yarns are made by

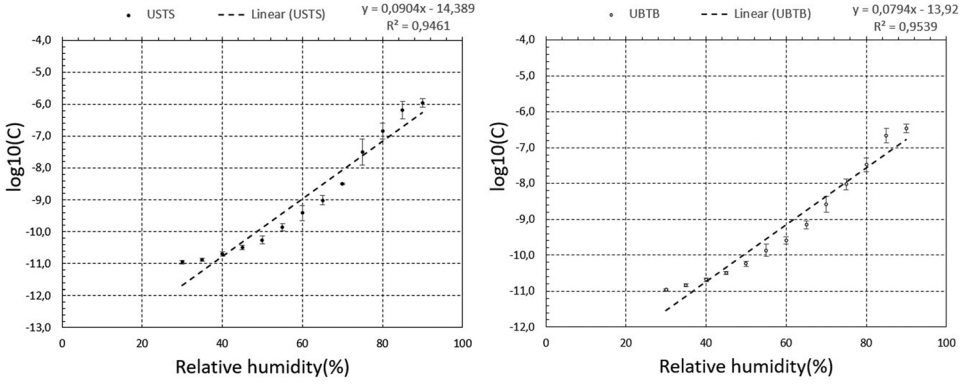

Figure 5. Relative humidity response for woven sensors.

© 2022 The Authors. Advanced Materials Technologies published by Wiley-VCH GmbH

2365709x, 0, Downloaded from https://onlinelibrary.wiley.com/doi/10.1002/admt.202200284 by Readcube (Labtiva Inc.), Wiley Online Library on [11/12/2022]. See the Terms and Conditions (https://onlinelibrary.wiley.com/terms-and-conditions) on Wiley Online Library for rules of use; OA articles are governed by the applicable Creative Commons License

Table 2. Properties for the yarns tested.

Sensor	Linear Regression	R^2
USTS	0,0904· HR-14,389	0,9461
UBTB	0,0794· HR-13,92	0,9539

ring yarn process, which is the same method as the common yarns used on the substrate, could have better behavior when the yarn is woven.

Data presented can be compared to previous works to confirm the expectations about the weaving sensor. In **Table 3** embroidery data acquired in previous works[14,15] are compared with the data obtained. It is observed how the weaving process decreases the standard deviation in comparison with the sensors. Embroidery presents, on average, a 2.1% on standard deviation, considering three different sensors and repetitive test. Meanwhile, woven sensor has a 1.34% of standard deviation on average. As a result, this process produces sensors with higher repeatability and with less dispersion. Sensitivity is also modified from embroidery to weaving. The sensitivity has an increase of 0.0168 $log(C)(RH)^{-1}$ for woven sensor.

A comparison with other sensors on the literature is done in **Table 4**. As it can be seen, woven technology performed as well as the other interdigital sensors. These results demonstrate its functionality as humidity sensor and the possibility to provide the value of relative humidity measured. The woven sensor provides better capacitance values with less dispersion compared with the embroidered integration method. Humidity applications that need large-scale production could be satisfied with the woven sensor presented.

3.2. Presence Sensor

The second part of the Experimental Section presents the characteristics of the woven sensor as a presence detector. As explained in section 2, a presence test is performed to evaluate the sensor feasibility to be used as presence detector. A person sat down over the woven sensor (occupied state) and stand up (void state) 4 consecutive times. It was done in periods of 10 seconds. **Figure 6** shows the capacity shifts results of the test for USTS and UBTB. USTS is represented as a continuous line, meanwhile, UBTB is represented as a dashed line.

As it can be observed, the response of USTS after a person is sitting on the sensor is a significant increase on the capacitance, which is maintained at a high state till the person got up. After a person occupied the place and got up, the sensor presents a slight increase in its void state. Sensor void state values are between 0% and 15% of capacity variation, meanwhile sensor occupied values are between 100% and 170% of their initial capacitance value.

Table 3. Comparison between technologies.

Technology	Sensitivity $log(C)(RH)^{-1}$	Standard deviation (average(%))	Improvement %
Embroidery	0.0736	2.1	–
Weaving	0.0904	1.34	36.2%

Table 4. Comparison with other interdigital humidity sensor. In this case, the impedance sensitivity is used to be able to compare with other sensors.

Reference	Sensitivity $log(Z)(RH)^{-1}$	Working Range %RH	Size H × W(mm)	Integration Technology
This work	0.0673	30-90	100 × 106.2	woven
[23]	0.0559	20-90	4.25 × 4.25	drop-coated
[15]	0.0535	25-80	27 × 74	embroidered
[24]	0.0804	40-90	150 × 220	embroidered

The UBTB sensor presents a good response when presence is detected. The void values are similar to USTS, being around 0% to 15% of capacity variation. In this case, the sensor increases its values to 120–170% of capacity variation.

The behavior of the sensor has been evaluated when a heavy object is placed on it, such as a shopping bag. Specifically, a bag with 4,6,10, and 15 kg was tested, as shown in **Figure 7**. The capacitance values showed an increase to a maximum of 20% of capacitance, similar capacitance values than previous void states. The capacitance remains constant between 15% and 20% values in all the different load cases, when the bag is placed over the sensor. Different loads do not present significant capacitance values, which means that the sensor variation is due to the textile of the bag, which has a different permittivity. It is demonstrated that the sensor is capable to differentiate between a bag and a person.

Both sensors present and increase of their capacitance when the place is occupied. Void state and object occupation are clearly differentiated from a person occupied state. As a result, the woven sensor demonstrates its functionality on presence detection, and it opens a door to continue this research line. The adaptability of the woven capacitive sensor is demonstrated along the paper, showing that it can be used as a humidity detection sensor and also as a presence sensor with good performance.

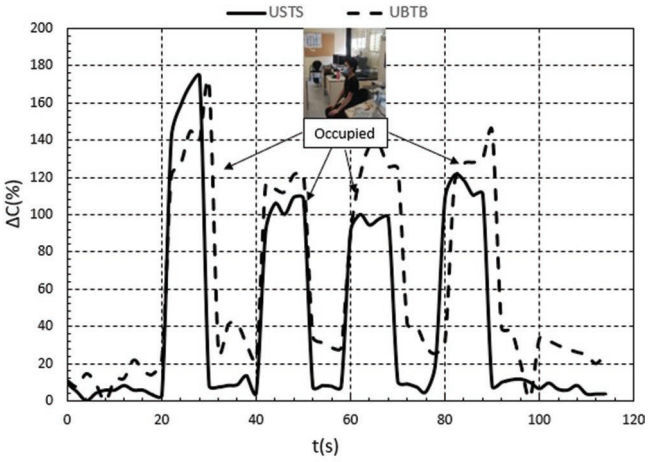

Figure 6. Capacity shift, in percentage, during presence detector test.

© 2022 The Authors. Advanced Materials Technologies published by Wiley-VCH GmbH

2365709x, 0, Downloaded from https://onlinelibrary.wiley.com/doi/10.1002/admt.202200284 by Readcube (Labtiva Inc.), Wiley Online Library on [11/12/2022]. See the Terms and Conditions (https://onlinelibrary.wiley.com/terms-and-conditions) on Wiley Online Library for rules of use; OA articles are governed by the applicable Creative Commons License

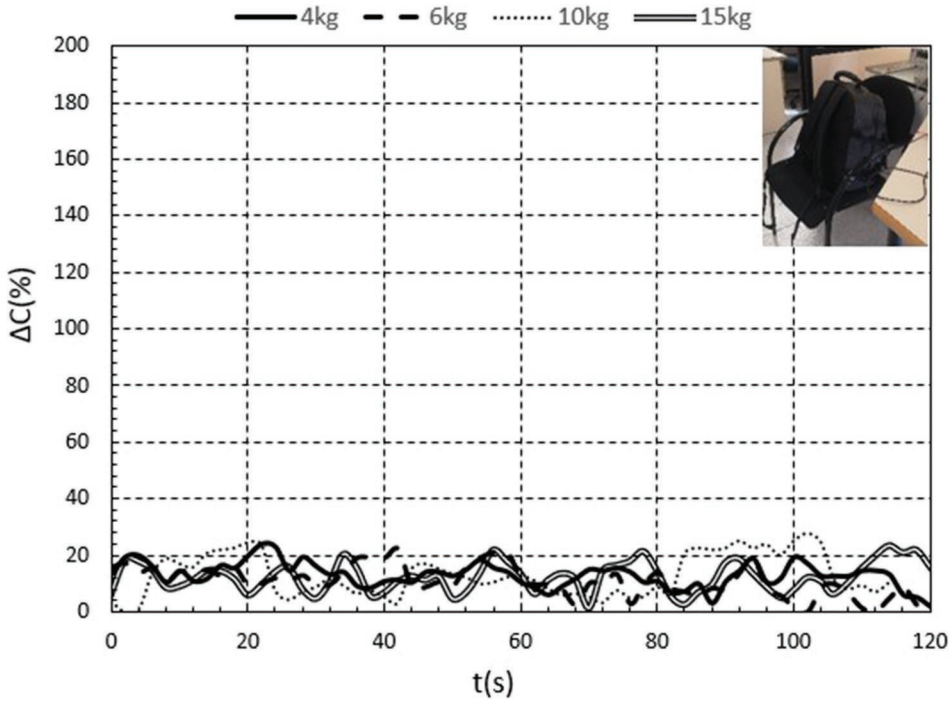

Figure 7. Capacity shift, in percentage, during load test.

4. Conclusions

A woven sensor was presented and its work-ability on the relative humidity measurement and the presence detection was demonstrated. Sensor behavior to measure humidity demonstrates the functionality of the sensor application with a high repeatability and large-scale production option, due to the weaving process. Capacitive values increase directly with humidity and a linear dependence with lower standard deviation comparing with embroidery technique is achieved. Presence detection test results demonstrate its usability, providing clear values for occupied and void situations, which should make ease to apply to new applications. Results encourage researchers to continue with the presence detection sensor for future works. The adaptation of the previous works to a new manufacturing procedure has provided a new way to produce the sensor with lower standard deviation and better textile properties. The woven technology expands the applications where the textile capacitive sensor can be applied where previously properties, as the touch feel, were a drawback. The most important objective achieved along this work is the complete integration of the sensor into the fabric, encouraging to use them without bothering the user.

Acknowledgements

This work was supported by Spanish Government-MINECO under Project TEC2016-79465-R and AGAUR-UPC(2020 FI-B 00028). Agencia de Gestión de Ayudas Universitarias y de Investigación, Generalitat de Catalunya.

Conflict of Interest

The authors declare no conflict of interest.

Data Availability Statement

Research data are not shared.

Keywords

humidity, presence, sensor, smart-textile, textile, woven

Received: February 22, 2022
Revised: July 10, 2022
Published online:

[1] R. R. Rajanna, N. Sriraam, P. R. Vittal, U. Arun, *IEEE Sens. J.* **2020**, *20*, 1573.
[2] J. Cai, M. Du, Z. Li, *Adv. Mater. Technol.* **2022**, *5*, 2101182.
[3] M. Lou, I. Abdalla, M. Zhu, X. Wei, J. Yu, Z. Li, B. Ding, *ACS Appl. Mater. Interfaces* **2020**, *12*, 19965.
[4] G. Tartare, X. Zeng, L. Koehl, in *Proceedings - 2018 IEEE Industrial Cyber-Physical Systems, ICPS 2018*, IEEE, ISBN 9781538665312 **2018**, pp. 561–566.
[5] S. H. Lee, W. Eom, H. Shin, R. B. Ambade, J. H. Bang, H. W. Kim, T. H. Han, *ACS Appl. Mater. Interfaces* **2020**, *12*, 10434.
[6] F. Seng, D. Hackney, T. Goode, A. Noevere, A. Hammond, I. Velasco, K. Peters, M. Pankow, S. Schultz, *International Journal of Impact Engineering* **2021**, *150*, 103800.
[7] P. Hofmann, A. Walch, S. Arnold-Keifer, S. K. Selvarayan, G. T. Gresser, *Composites, Part A* **2019**, *126*, 105603.

© 2022 The Authors. Advanced Materials Technologies published by Wiley-VCH GmbH

2365709x, 0, Downloaded from https://onlinelibrary.wiley.com/doi/10.1002/admt.202200284 by Readcube (Labtiva Inc.), Wiley Online Library on [11/12/2022]. See the Terms and Conditions (https://onlinelibrary.wiley.com/terms-and-conditions) on Wiley Online Library for rules of use; OA articles are governed by the applicable Creative Commons License

[8] D. Zhang, Z. Xu, Z. Yang, X. Song, *Nano Energy* **2020**, *67*.
[9] D. Zhang, L. Yu, D. Wang, Y. Yang, Q. Mi, J. Zhang, *ACS Nano* **2021**, *15*, 2911.
[10] A. Kefal, I. E. Tabrizi, M. Yildiz, A. Tessler, *Mechanical Systems and Signal Processing* **2021**, *152*, 107486.
[11] T. Agcayazi, J. Tabor, M. McKnight, I. Martin, T. K. Ghosh, A. Bozkurt, *Adv. Mater. Technol.* **2020**, *5*.
[12] D. Zhang, D. Wang, P. Li, X. Zhou, X. Zong, G. Dong, *Sens. Actuators, B* **2018**, *255*, 1869.
[13] D. Wang, D. Zhang, P. Li, Z. Yang, Q. Mi, L. Yu, *Nano-Micro Lett.* **2021**, *13*.
[14] M. Martinez, B. Moradi, R. Fernandez-Garcia, I. Gil, *Sensors* **2018**, *18*, 3824.
[15] M. Martínez-Estrada, B. Moradi, R. Fernández-Garcia, I. Gil, *Sensors (Switzerland)* **2019**, *19*, 1.
[16] M. Martínez-Estrada, R. Fernández-García, I. Gil, *J. Text. Inst.* **2021**, *112*, 881.
[17] Z. Zhao, Q. Huang, C. Yan, Y. Liu, X. Zeng, X. Wei, Y. Hu, Z. Zheng, *Nano Energy* **2020**, *70*, 104528.
[18] H. Y. Song, J. H. Lee, D. Kang, H. Cho, H. S. Cho, J. W. Lee, Y. J. Lee, *J. Text. Inst.* **2010**, *101*, 758.
[19] T. Kuroda, H. Takahashi, A. Masuda, *Wearable Sensors* **2021**, 249.
[20] Interlink Technologies, FSR 402 Data Sheet, Technical report **2013**, http://www.interlinkelectronics.com/FSR402short.php.
[21] G. Kim, C. C. Vu, J. Kim, *Appl. Sci. (Switzerland)* **2020**, *10*.
[22] A. M. Khan, H. V. Manjunath Reddy, R. S. Beeresha, *International Journal of Research in Engineering and Technology* **1994**, *05*, 273.
[23] P. G. Su, X. H. Lee, *Sens. Actuators, B* **2018**, *269*, 110.
[24] M. E. Marc, G. Ignacio, F. G. Raul, *IEEE Sens. J.* **2021**, *21*, 26234.

© 2022 The Authors. Advanced Materials Technologies published by Wiley-VCH GmbH

2365709x, 0, Downloaded from https://onlinelibrary.wiley.com/doi/10.1002/admt.202200284 by Readcube (Labtiva Inc.), Wiley Online Library on [11/12/2022]. See the Terms and Conditions (https://onlinelibrary.wiley.com/terms-and-conditions) on Wiley Online Library for rules of use; OA articles are governed by the applicable Creative Commons License

Paper F

Martínez-Estrada, Marc; Ventura, Heura; Gil, Ignacio; Fernández-García, R. (2022). Experimental abrasion analysis of textile capacitive sensor. 21st World Textile Conference, 1–4. https://doi.org/10.34658/9878366741751

AUTEX 2022 Conference Proceedings 978-83-66741-xx-x © Lodz University of Technology, 2022

DOI: 10.34658/xxxxxxxxx

EXPERIMENTAL ABRASION ANALYSIS OF TEXTILE CAPACITIVE SENSORS

Marc Martínez-Estrada[1(*)], Heura Ventura[2], Ignacio Gil[1], Raúl Fernandez-Garcia[1]
[1] Department of Electronic Engineering, Universitat Politecnica de Catalunya; Terrassa, Spain
[2] Departament de Ciencia i Enginyeria de Materials - Textile Engineering Section,
Universitat Politecnica de Catalunya; Terrassa, Spain
(*) *Email:* marc.martinez.estrada@upc.edu

ABSTRACT

This paper presents an experimental abrasion analysis of textile capacitive sensors based on Martindale test. The textile sensor is manufactured with a well-known woven technology where some yarns are replaced by electrical conductive yarn. Specifically, two types of conductive yarns were used to compare the abrasion behaviour respect to conventional fabrics and the impact of abrasion on sensors functionality. The results show that the integration of conductive yarn on fabric don't reduce the fabric lifetime and moreover the sensing behaviour remains unalterable during the lifetime of the textile.

KEYWORDS

Smart-textile, sensor, textile, woven, abrasion, Martindale.

MATERIALS AND METHODS

The sensors under test are based on an interdigitated structure manufactured by means of woven technology, which improves the usability and comfort, when in contact with human skin, in comparison with another textile technology previously used, such us embroidered [1]. The sensor is manufactured with a combination of electrical conductive and non-conductive yarns. To produce the sensor, a Dornier LWV8/J 71 weaving machine moved by a Jacquard Stäubli LX1600B was set up to produce plain weave fabric. Warps beam were formed by 100% cotton yarns and weft yarns were polyester/cotton yarns produced with a proportion of 35/65%, respectively (Figure 1).

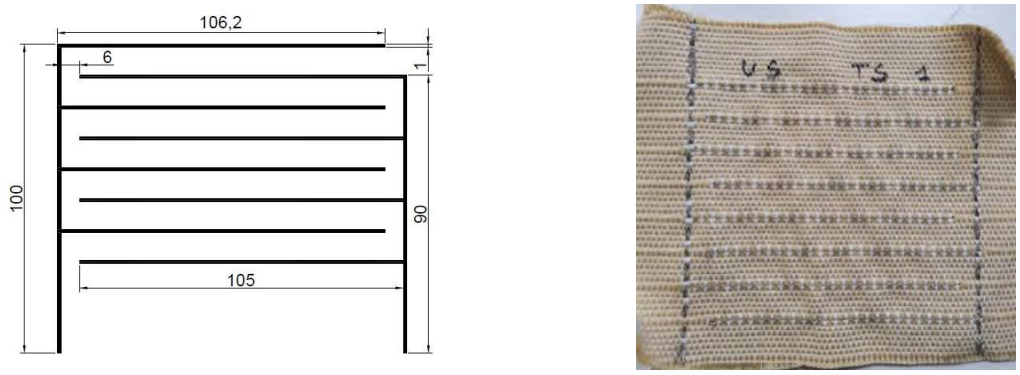

a) Sensor dimensions (mm) b) Sensor manufactured prototype

Figure 1. Interdigital geometry.

© 2022 by the authors. This article is an open access article distributed under the terms and conditions of the Creative Commons Attribution (CC-BY) license (http://creativecommons.org/licenses/by/4.0/)

To integrate the sensor on the plain weave structure, two type of conductive yarns were used and analysed during the process; Shieldex 117/17 2-ply and Bekaert 20/2 Tex. Each yarn was produced by different processes. Shieldex yarn is based on a silver coating covering a polyamide filament, whereas Bekaert yarn was produced by mixing polyester and stainless-steel fibres with a 60/40% proportion, respectively.

To analyse the impact of abrasion on sensor functionality, Martindale abrasion test was performed with the manufactured sensors (Figure 2). The test consists on the abrasion of the fabric under test against a normalized abrasive fabric. The force applied during the movement is determined by the EN ISO 12947-2:2016 [2], which determines that for upholstery fabric the weight used is (795±7) g. The movement performed by Martindale follows a Lissajous curve pattern. The fabric physical state and the properties of the measured conductive yarn are verified periodically after each step of the Martindale test, Table 1. The test is finished when more than three yarns are broken or conductive yarns lost completely their electrical continuity (i.e. resistance lower than 50 Ω).

Table 1. Frequency of Martindale evaluations steps from standard EN ISO 12947-2:2016.

Interval (nº cycles)	Martindale evaluation step (nº cycles)
1000-6000	1000
6000-20000	2000
20000-50000	5000
+50000	10000

Figure 2. Martindale machine performing a test.

Three different samples are prepared for the Martindale test: the substrate fabric without any conductive yarns, using conductive Bekaert yarns and using conductive Shieldex yarns integrated on it. The electrical conductivity of the conductive yarn was evaluated with a Multimeter Tenma 88 72-7730A after each Martindale evaluation step. The section of fabric under test is taken from the middle part of the sensor and consists of a circular section with diameter of 38 mm as shown in Figure 3.

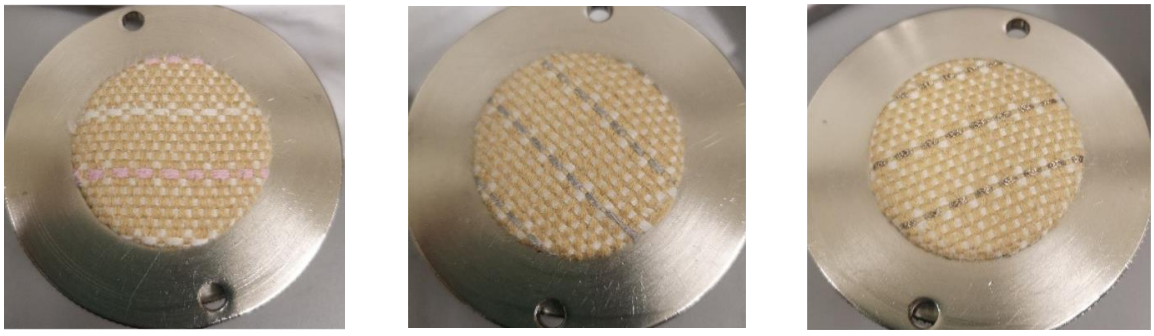

a) b) c)

Figure 3. Samples initial state: a) non-conductive sample, b) Bekaert, c) Shieldex.

RESULTS AND DISCUSSION

During the first Martindale interval (up to 6000 cycles), the samples do not show any alteration, the electrical properties remain constant and the physical aspect do not have signs of wear out. However, at the end of the second Martindale interval (i.e. 20000 cycles) some wear out effects are observed (Figure 4). Specifically, the sample with normal yarns presents pilling which is not observed on the samples with the conductive yarn. From the electrical point of view, the conductive yarns do not lose their electrical continuity.

a) b) c)

Figure 4. Samples after 20.000 cycles: a) non-conductive sample, b) Bekaert, c) Shieldex.

At the third Martindale interval the conductive samples do not lose the continuity up to 35.000 cycle. However, after 40.000 cycle the electrical continuity is lost. Figure 5 shows the state of the samples after 40.000 cycles. It is observed an important wear out; the samples show pilling around all the surface. Broken yarns can be found on non-conductive sample but not on both conductive samples.

a) b) c)

Figure 5. Samples after 40.000 cycles: a) non-conductive sample, b) Bekaert, c) Shieldex.

With regard to electrical properties, both electrical samples decrease the electrical conductivity. However, this reduction on the electrical conductivity is not the same on each sample. In Bekaert the resistance increases from 16 Ω/cm up to 120 Ω/cm whereas in Shieldex it increases from 0.7 Ω/cm up to 200 Ω/cm. Results are summarized in Table 2.

Table 2. Comparison between electrical properties before and after the Martindale test.

	Bekaert		**Shieldex**	
	Initial	**35k cycles**	**Initial**	**35k cycles**
Resistance (Ω/cm)	16	<120	0.7	<200

The resistance rise on Bekaert yarn can be due to loss of weight which includes some conductive fibres (stainless-steel fibres). In case of Shieldex yarn, the resistance rise is due to the loss of silver coating. Despite of the resistance rise, it should be notice that sensor preserves its functionality.

CONCLUSION

Martindale test was performed to analyse the abrasion effects on woven textile capacitive sensors with two type of conductive yarns. The results show that the integration of conductive yarn reduces the pilling effect on the fabric. Moreover, any yarn is broken on conductive sample up to 40000 cycle, meanwhile some broken yarns are observed on non-conductive yarns. The electrical properties are being affected by the abrasion on conductive samples. Depending on the conductive yarn manufacture process, the electrical resistance increases after applying the abrasion test. In case of Bekaert yarns, the resistance increases due to the loss of conductive fibres and in case of Shieldex it is due to silver coating reduction. In both cases, however, the functionality of the sensor is preserved. This fact denotes that the integration of conductive yarn on fabrics do not affect negatively on the fabric properties and guarantees the sensor functionality during the fabric lifetime. The properties described denote the possibility to use the sensors into applications as upholstery where previously abrasion resistance could be a drawback.

ACKNOWLEDGMENT

This work was supported by Spanish Government-MINECO under Project TEC2016-232 79465-R and AGAUR-UPC (2020 FI-B 00028).

REFERENCES

[1] Marc, M. E., Ignacio, G., & Raul, F. G. (2021). A smart textile system to detect urine leakage. *IEEE Sensors Journal*, *21*(23), 26234–126242. https://doi.org/10.1109/JSEN.2021.3080824.
[2] Textiles, Determination of the abrasion resistance of fabrics by the Martindale method. Part 2: Determination of specimen breakdown (EN ISO 12947-2:2016).

Paper G

Marc, M. E., Ignacio, G., & Raul, F. G. (2021). A Smart Textile System to Detect Urine Leakage. IEEE Sensors Journal, 21(23), 26234–26242. https://doi.org/10.1109/JSEN.2021.3080824

Note from: Servei de Biblioteques, Publicacions i Arxius de la UPC

Pages 207 to 217 of the thesis which contain this article are available on the publisher's website:

M. -E. Marc, G. Ignacio and F. -G. Raúl, "A Smart Textile System to Detect Urine Leakage," in *IEEE Sensors Journal*, vol. 21, no. 23, pp. 26234-26242, 1 Dec.1, 2021, doi: 10.1109/JSEN.2021.3080824.
https://ieeexplore.ieee.org/document/9432850

Paper H

Martínez-Estrada, Marc, Vuohijoki. Tiina, Poberznik. Anja, Shaikh. Asif, Virkki. Johanna, Gil. Ignacio, and Fernández-García. Raúl. (2022). A smart chair to monitor sitting posture by capacitive textile sensors. **Submitted to IEEE Sensors Journal**

A smart chair to monitor sitting posture by capacitive textile sensors.

Martínez-Estrada. Marc, Vuohijoki. Tiina, Poberznik. Anja, Shaikh. Asif, Virkki. Johanna, Gil. Ignacio, and Fernández-García. Raúl

***Abstract*— In this paper a smart office chair with movable textile sensors to monitor sitting position during the workday is presented. The system consists of a presence textile capacitive sensor with different levels of activation with a signal conditioning device. The proposed system has been integrated into an office chair to detect postures that could provoke musculoskeletal disorders or discomfort. The microcontroller measures the capacitance by means of cycle count and provides the position information in real time. The information could be analysed to set up warnings to prevent incorrect postures or the necessity to move. Five participants assumed a series of postures, and the results showed the workability of the proposed smart chair. The chair could be provided as a new tool to companies, hospitals, or other institutions to detect incorrect postures and monitor postures of people with reduced mobility. This tool can optimise control procedures or prevent occupational risks.**

***Index Terms*— office chair, smart textile, embroidery, sensor, textile, presence.**

I. Introduction

In sedentary occupations such as office work, prolonged static sitting poses a health risk for developing musculoskeletal disorders, cardiovascular, metabolic and cognitive issues [1], [2]. A good workstation consists of suitable furniture and (technical) equipment, optimal lighting, good air quality and diminished noise disturbances [3]. Adjusting the workstation and chair setup to ergonomically optimal positioning may reduce musculoskeletal risks for pain and discomfort of the lower back, elbows, fingers, and legs [4].]. The literature often suggests an optimal office sitting posture where one should sit straight, yet following the natural spinal curvature, with feet flat on the floor, hips as far back in the chair as possible and knees in line with the hips. Elbows should be flexed at 90 degrees at the side of your body, shoulders relaxed, and wrists in a neutral position. The monitor should be directly in front at arm's length, with the top of the screen at eye level to prevent neck strain [3], [5].

However, there has been some controversy in the literature regarding the most ideal sitting posture or whether it even exists. The long-standing belief of sitting 'as upright as possible' has been slowly replaced by the concept of 'dynamic' or 'active sitting' where sitting positions are changed as often as possible [6], [7]. Yet again, a literature review [8] suggests that there is no ideal sitting posture, and for preventing low back pain one should sit with preferred lumbar lordosis and, in addition, move regularly. Frequent position changes for office workers, which include working in standing position and moving regularly, are usually recommended by ergonomics experts and physiotherapists to avoid work-related discomfort and injuries [9].

People have adopted their own ways of sitting that are natural and comfortable for them, and the same sitting posture that feels good to someone might feel uncomfortable to another. In fact, eight main sitting postures have been identified in the literature [10], [11]: upright sitting; slumped sitting; leaning forward; leaning backward; leaning left; leaning right; right leg crossed; and left leg crossed. Often the users are not aware of the postures that they have adopted [12].

Ergonomic office chairs have been designed to help achieve optimal posture with their shape, adjustable height, armrests, adjustable reclining backrest and additional lumbar spine support [3]. Users, however, do not utilize all the adjustments, and thus do not use the office chair in the most optimal ergonomic way [12], either due to lack of knowledge or simply their habitual sitting positions. A feedback system integrated into the chair may help tackle this issue and guide the user towards a more optimal sitting posture.

A feedback system should be designed to be naturally integrated into the chair. Ergonomic chairs are commonly covered with textiles, which could be the ideal substrate to

This paragraph of the first footnote will contain the date on which you submitted your paper for review. It will also contain support information, including sponsor and financial support acknowledgment. For example, "This work was supported in part by the U.S. Department of Commerce under Grant BS123456."

Martinez-Estrada, Marc; Gil, Ignacio and Fernández-García, Raúl are with Universitat Politècnica de Catalunya, ESEIAAT, 08222 SPAIN (e-mail: marc.martinez.estrada@upc.edu).

Shaikh, Asif; Vuohijoki, Tiina and Virkki, Johanna are with Faculty of Medicine and Health Technology, Tampere University (Hervanta Campus), 33720 Tampere, Finland.

Poberznik, Anja; Faculty of Technology, Satakunta University of Applied Sciences, 28130 Pori, Finland.

integrate sensors on. Capacitive textile sensors provide the opportunity to obtain direct sensing, which could not be obtained with common electronic sensors. Electronic sensors would have to be installed into the chair foam, which could affect the user's comfort and make replacement of the sensors difficult; therefore, this solution would be unfeasible for the feedback system. Chair upholstery is easier to replace if the textile sensors fail.

The most important characteristics of capacitive textile sensors are the flexibility, low cost, low impact on the user, comfortable feel , and applicability in different fabrics and wearables. In healthcare applications, capacitive textile sensors are showing comparable results to common electronics, such as those that measure blood flow [13], or pH [13], or that monitor breath [14], sweat [15], urine leakage, humidity [16] or motion[17].

To integrate the sensors into the chair fabric, there are plenty of textile processes used at the present time. Nevertheless, to produce a system that accomplishes the requirements, i.e. fast prototyping and low-cost production, the embroidery method has been selected. Embroidery is commonly used in commercial garments and furniture and is thus well known to people, which is an asset when designing unobtrusive technology.

To produce a capacitive textile sensor, it is necessary to use conductive yarn, which is nowadays being commercialized by some yarn companies, such as Shieldex [18] or Bekaert [19]. These yarns have conductive properties, which allow integrating a sensor within, but also textile properties, which are derived from the manufacturing process to be unnoticeable by the user.

The works of [20]–[23] analysed some feedback systems on office chairs. One of these works revised [21] an office chair with electronic distance sensors and pressure sensors for real-time posture classification. The distance sensors were installed on the chair's back; meanwhile, the pressure sensors were installed on the seat. The chair was capable of obtaining information about people's sitting positions. This information was taken and analysed to classify the positions automatically by a neuronal network (machine learning). The ergonomic chair with the Internet of Things (IoT) presented on [20] is also designed with a common electronic force sensor. Despite the fact that they could obtain more information from the force sensor, they are only distinguishing between pressure detected or not. In this case, the capacitive textile sensor presented in this work could substitute for the electronic sensors, using only one kind of sensor with a single type of data which can contain information about distance and pressure.

To obtain the data from the capacitive textile sensors, a microcontroller is connected to the sensors. The microcontroller analyses and organizes the data of different textile sensors to store it and then send it to a database or visualization software. These real-time data provide an information source which reacts when it detects a bad position that could provoke disorders and notifies the user to take preventive actions. This feedback system could be provided as a tool to companies to promote their workers' health, or to hospitals to improve the wheelchairs usability and their attention to people with reduced mobility.

As the related work shows, the embroidered sensors have potential in tracking physical factors. A case study with embroidered capacitive sensors that aims to track body positions from an office chair is presented next.

II. Materials and methods

A. Office chair preparation

The locations of the sensors were identified to correspond to the most optimal sitting ergonomics as identified in the previous section. The smart chair and the sensor distribution are shown in Figure 1. The sensors are positioned in the spots on the chair where the user's body comes into contact with the chair.

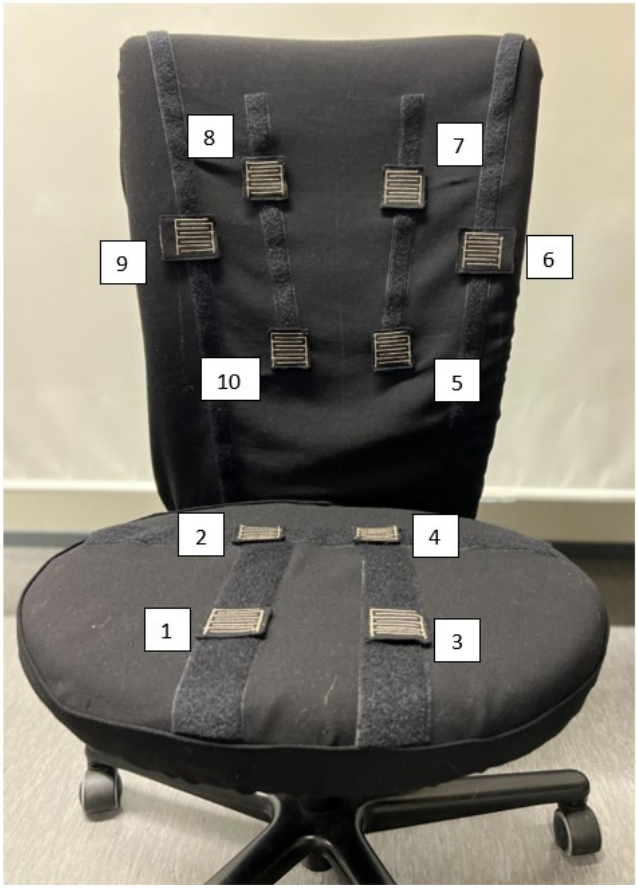

Fig. 1: Smart chair with sensor distribution and number identification.

The following sensor locations were identified: i) bilaterally on the lower back (to promote straight posture with the hips as far back in the chair as possible); ii) bilaterally on the upper back just beneath the shoulder blades to promote the user's contact with the backrest of the chair and to prevent slumped sitting and forward lean posture; iii) bilaterally on the sides of the mid-back to prevent excessive leaning to the side; and iv) bilaterally on the buttocks and on the back of the thighs to ensure contact with the seat and to discourage crossing the legs.

To detect the user's sitting position on the chair, ten interdigitated capacitive embroidered sensors were produced. The interdigitated pattern can be observed in Figure 2.

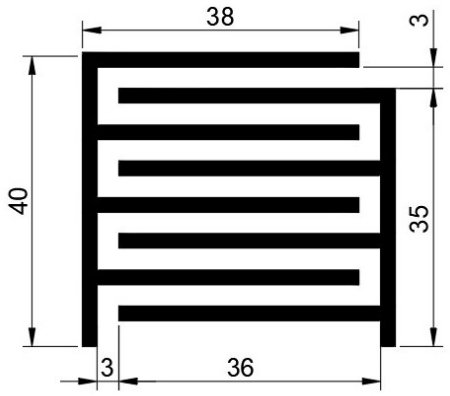

Fig. 2: Interdigitated sensor geometry (dimensions in mm).

The decision to use an interdigital structure was made due to two conditions: the capacitive sensor integrated in one layer and the response obtained by this well-known structure. Capacitance value is determined by the dimensions of the pattern and properties of the materials around them. Because the sensor is going to be used to distinguish between certain position circumstances, dimension parameters acquire higher importance than other parameters. Dimensions should be big enough to characterise different sitting positions and levels of body proximity, but not so big that the capacitive value derived experiments cause an excessive increase or occupy too much space. Bigger sensors could produce misunderstandings in position distinction. To obtain an approximation for the capacitance of each sensor, the dimensions are determined by the following equations [24].

$$C_{RH} = \frac{\varepsilon_{RH} 10^{-3}}{18\pi} \frac{K(k)}{K'(k)} l(N-1)(pF) \tag{1}$$

$$\frac{K(k)}{K'(k)} = \frac{\pi}{ln2\frac{1+\sqrt{k'}}{1-\sqrt{k'}}} \tag{2}$$

$$k = tan^2(\frac{a\pi}{4b}) \tag{3}$$

$$a = \frac{W}{2} \tag{4}$$

$$k' = \sqrt{1-k^2} \tag{5}$$

$$b = \frac{W+S}{2} \tag{6}$$

Where l is in microns $(10^{-3}mm)$, N is the number of fingers and ε_{RH} is the effective dielectric constant of the material substrate, W finger width and S space between fingers. The result obtained is the capacitance of the interdigital sensor in pF.

After obtaining this balance, the sensor was embroidered on a Husqvarna Viking Designer Ruby Royale sewing machine. The pattern was designed in Autocad and introduced as a JPEG file in the embroidery machine software. The embroidery parameters, such as stitch density or embroidery pattern, were selected at this stage. A Shieldex 110/34 dtex 2-ply conductive yarn [18] was inserted as top thread during the embroidering process. A common cotton yarn with a similar density was inserted from the bottom. The final substrate used was a 100% wool crepe fabric. To embroider the sensor on the substrate, a support non-woven fabric was used to avoid movement during the manufacturing process. The support fabric can be removed afterwards by being diluted in water. The final presence textile capacitive sensor (PreCaTex), embroidered, can be observed in Figure 3.

(a) Top side of the sensor

(b) Bottom side of the sensor

Fig. 3: PreCaTex sensor embroidered with the Husqvarna Viking Designer Ruby Royale.

A commonly available office chair without the armrests was used for this prototype. The chair was covered with 100% wool crepe fabric to create a surface to which the sensors would be attached. Sensor attachment was designed to be movable. People are individually shaped and sized, and due to these facts, the prototype needs to be adjustable to the user's attributes.

There are several options for attaching the PreCaTex sensors to be movable, such as attaching them to the cover, using the magnets to hold them in the right location or utilising Velcro, which allows easy relocation of the sensor. We decided to use the last mentioned.

Most of the sensors were sewn individually, and to add possibilities to inspect the optimal locations, a couple of sensors were sewn in sets of twos. The embroidered fabric would be face-up on the office chair. The Velcro fabric (hook side) would cover the bottom of the sensor flap, thus connecting to the Velcro (loop side) placed on the cover.

The embroidered sensor pieces were cut to suitable sizes, i.e., 5.5 cm * 5.0 cm, and each sensor piece's sidelines were folded to the reverse side, then pinned and as last neatened with hand-basted stitching. Afterwards, the Velcro was cut to same size pieces as the front ones, 5.5 cm * 5.0 cm , that match the embroidered pieces, and then sewn together with top stitching. Figure 4 shows the ready-made sensor.

Fig. 4: Ready-made sensor from both sides.

B. Test procedure

To gather the data from the PreCaTex sensors, a microcontroller is used. Each individual sensor is connected to the microcontroller, which is in charge of measuring the capacitance of the sensor. To evaluate the data from the PreCaTex sensor, a cycle count method is used (Figure 5). Two microcontroller pins are required, as the send pin and receive pin. These pins are connected with a $10M\Omega$ resistance between them. On the receive pin side is connected one sensor electrode to measure the tension. The measurement process starts setting up a tension of 5V in the send pin. Then the current goes through the resistance and starts charging the sensor capacitor. Each cycle the microcontroller programming compares the tension measured in the received pin with the sensor in the send pin. If there is no match between them, the software increases the cycle count by one and starts a new cycle. Each cycle that the program evaluates the receive pin to compare it with the send pin is counted as a new cycle. When the sensor capacitor is fully charged, the receive pin gets the 5V and the program stops counting the cycles. The cycles counted are used as the value of the sensor. This measurement process is performed for each sensor constantly.

The measurement methodology explained provides the opportunity to obtain information which could be used to distinguish between levels of pressure. These different levels of pressure are expected due to the body weight distribution. The more pressure applied with the body, the higher the capacitive value the sensor will take. The capacitive sensor value variation is related to the distance between the sensor surface and the person's skin. This distance has a minimum value, which is found where maximum pressure is applied

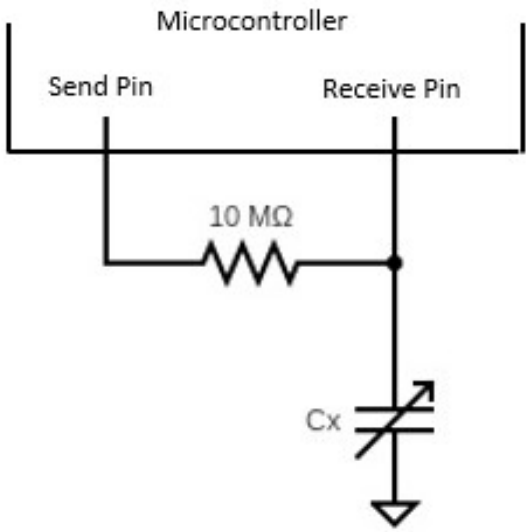

Fig. 5: Measurement circuit of each individual sensor.

on the sensor surface and the clothes in contact with it are compressed. In the following table different levels of activation are presented.

Sensor levels	Surrounding detection	Contact	Close contact (pressure)	Close contact (high pressure)
Cycle count	±500	±1000	±1500	±2000

TABLE I: Levels of activation of the sensor depending on the cycle count.

The first sensor level that indicates contact between the sensor and the body is marked with a red dashed line in each figure in the Results section.

As this was an initial proof of concept, the number of participants was relatively small. For future studies the statistical data from PreCaTex sensors operativity would be searched more thoroughly. The five volunteer participants took part in the technical evaluation. All the measurements were taken in office settings, and the researcher adjusted the chair height to meet each participant's individual fit, meaning that the participant's feet were in contact with the floor and the participant's buttock area was located as close to the back of the chair as possible. Researchers asked the participants to focus on exaggerated positions to obtain accurate data from the capacitive sensor. The capacitive sensors were confirmed to meet the desired locations corresponding to the participant's physical markers. In other words, the upper sensors met the scapula (shoulder blade), and the seat's sensors meet the ischium bones (the bottom bones that touch the seat) and both thighs. There were only slight changes made to the capacitive sensor locations between the measured participants.

The position measurement process was focused on the evaluation of eight sitting positions. The positions selected included the optimal sitting position for work, which is defined by the ergonomic studies [3], [5], and other common sitting

positions found in related work [20], [21]. Additional common sitting positions were included in the process. These positions are presented in Figure 6.

The pre-selected measurement positions were explained and demonstrated by the researcher and practised by participants before the official measurement.

People sitting in the same positions could have different responses from the system regarding different sizes, pressure and clothes. The aim was to demonstrate that the capacitive sensor is capable of monitoring the sitting position and evaluating it.

Fig. 6: Measured sitting positions during the smart chair test.

III. Results and Discussion

To obtain data from the smart chair, five people with various body heights and weights were selected to participate. Participants' clothing was homogeneous. They were dressed in different kinds of jeans and shirts or T-shirts. Homogeneous clothing is expected to decrease the variability of the sensor values during the measurement and facilitate the analysis of the measurement.

The smart chair was prepared to obtain data from different positions for each person. PreCaTex sensors were placed and connected to the microcontroller. During the test, different levels of activation were expected (as mentioned in Section 2).

The smart chair data are presented for each position in a figure, which includes the value for every participant for that particular position. Values for each PreCaTex sensor were compared between the participants. The values for general and individual characteristics of each position and participant were analysed.

A. The ergonomic posture

Firstly, participants were asked to assume the ergonomic posture. This is the position that should not provoke disorder risk or tension all over the body. Data from the ergonomic position are shown in Figure 7.

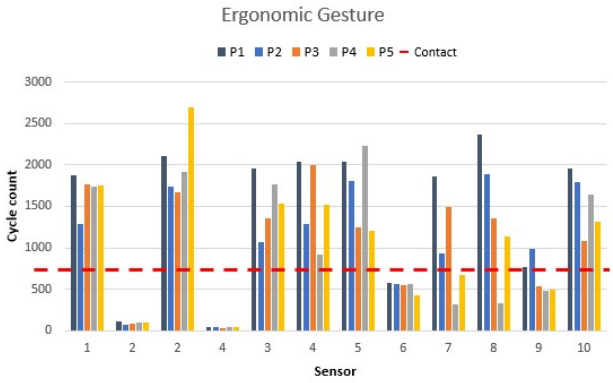

Fig. 7: The ergonomic posture sensor values as shown in Figure 6a.

The data from the ergonomic position for all five participants were compared. The buttock position was monitored by sensors 1 to 4. The four sensors were activated during the ergonomic position, acquiring values around 1000 cycles.

The position of the legs could increase or decrease the value. A sensor value lower than 1000 indicates that the legs could be displaced from the sensor.

The level of activating the backrest sensors depended on how the participants had their upper and lower back positioned on the chair. The graph shows that side sensors 6 and 9 are not reaching the red dashed line, which indicates that the sensor is detecting the body's proximity but is not in contact with the sensor.

Participant 4 did not activate upper back sensors (7 and 8) which may indicate that their back curvature did not permit them to be close enough to the sensor. For the remaining participants this sensor value was activated and reached the dashed line.

Three participants (2, 4 and 5) showed a noticeable asymmetrical distribution to the right. The differences observed for the sensor values were calculated as $\Delta S = (S2 - S4)$. The result provided an estimation of how much more pressure was applied to the right side. Participant 2 had a $\Delta S = 456$, participant 4 had a $\Delta S = 152$ and participant 5 had a $\Delta S = 1170$ which was the highest asymmetrical value observed. However, participant 3 showed an asymmetrical position to the left. The value $\Delta S = -325$ was obtained. The negative value indicates that the higher value was obtained in sensor 4, which corresponds to the left side.

B. Right and left leg crossed

Consecutively, right leg crossed, and left leg crossed were analysed. These are common positions used by office workers to provide distension to their bodies. First, participants were asked to cross their right leg over the left leg. Right leg sensor values are shown in Figure 8.

During the measurement of this position, values close to 0 or lower than 500 were expected on the right edge seat sensor

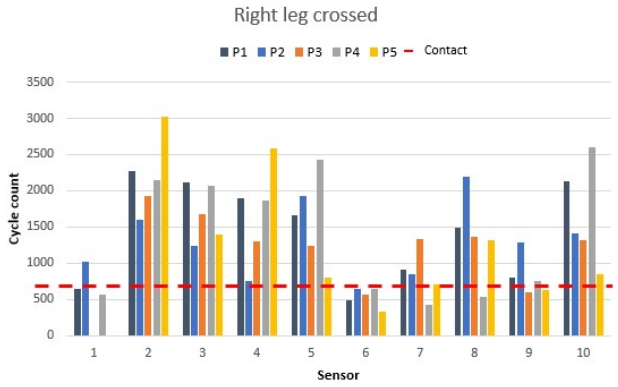

Fig. 8: Right leg crossed sensor values as shown in Figure 6b.

(sensor 1) which was the sensor in contact with the right leg. Four participants, all but participant 2, matched this condition and showed how the pressure remained only in the left edge seat sensor (sensor 3). Participant 2 increased the pressure in sensors 8 and 9, which corresponds to right side upper back and side middle back. The upper back sensor (sensor 8) increased its value of 308 cycles due to the pressure, and the ide middle back (sensor 9) showed an increase of 306 cycles. Participant 4 held all the pressure change on the lower back sensor (sensor 10). The increase of 946 cycles indicates that the pressure applied changed the level of detection of the sensor to the close contact high pressure. Participant 1's right leg movement caused a decrease of the pressure on their high back, which is displayed on the high backrest sensors (sensors 8 and 9).

To view when the leg crossed changed from left to right, the pressure redistribution can be observed in Figure 9.

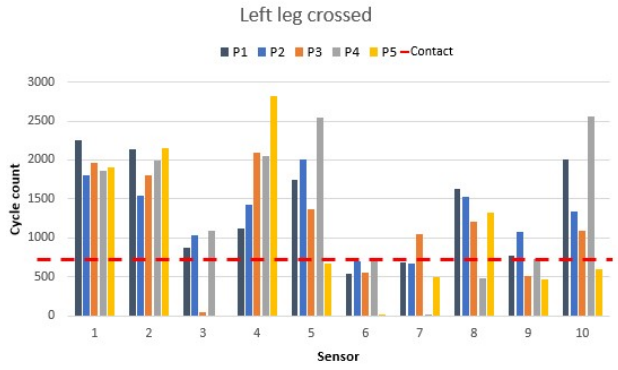

Fig. 9: Left leg crossed sensor values as shown in Figure 6c.

The most noticeable change is provoked by the leg change. The right edge seat sensor (sensor 1) reaches the value that had during ergonomic position. However, the left edge seat sensor (sensor 3) values decrease due to the left leg movement. As in the previous situation, the values in sensor 3 decrease lower than the 1000 cycle count. Participants 1, 2 and 3 show values close to the detection line; their flexibility or leg size do not let them detach enough the leg from the sensor. Backside back seat sensor values reach a higher value when the leg from the side is crossed, which is due to the increase of contact or pressure during the movement. This fact is more observed in the values of the participant 5 in both positions. During right leg crossed, the sensor 2 value increased to 331 cycle counts, but for the left leg situation, the cycle count increased to 1290.

Left backrest sensor values exchange some pressure with the right backrest sensors. This pressure change is noticeable in sensor 5. Participant 4's left low-mid backrest sensors (sensors 6 and 7) decrease significantly during movement, especially sensor 6 with a 0-count cycle.

The crossed leg position shows how the smart chair could monitor the movement and detect pressure distribution depending on which leg is crossed.

C. Detachment from the backrest

The movement of detaching the back from the seat is performed by workers when they are doing tasks under pressure or focussing too much on the screen they are working on. Position values are shown in Figure 10.

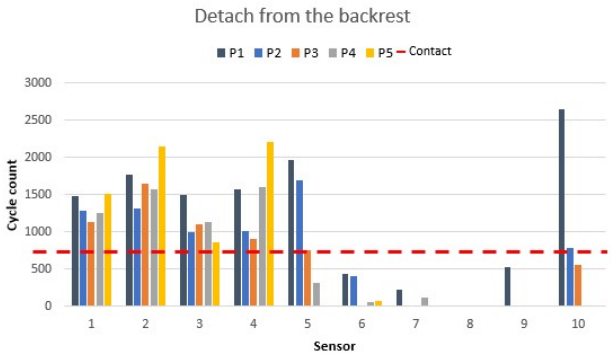

Fig. 10: Detach from the backrest sensor values as shown in Figure 6d.

The movement of detaching the back starting from the ergonomic position shows how the high backrest sensors (7 and 8) and side backrest sensors (6 and 9) are deactivated because of the back movement to the front. Values of the low backrest sensors 5 and 10 depend on the back movement and if the back is detached when the movement is performed. Here we can observe that participants 1, 2 and 3 did not move their lower backs as much as participants 4 and 5, who moved their backs away from the backrest in this position.

Seat sensor values are similar to the ergonomic position values, but some pressure change is observed.

D. Sitting on the edge of the chair

Sitting on the edge of the chair is one of the positions that some people take when sitting for a short time or just before standing up. The values for this position are presented in Figure 11. This position has activated only the edge seat sensors, 1 and 3. The rest of the sensors are not activated. This position should be defined in the microcontroller with a clock, which would activate an alarm if there were no change in 10 seconds.

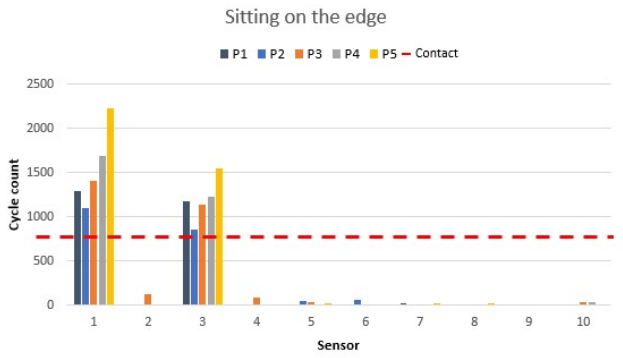

Fig. 11: Sitting on the edge of the chair sensor values as shown in Figure 6e.

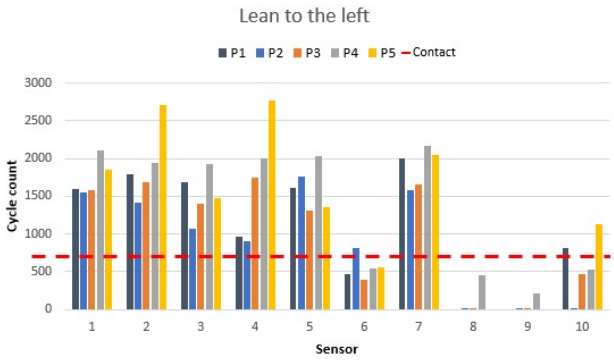

Fig. 13: Left leaning sensor values as shown in Figure 6g.

E. Right and left leaning

Right and left leaning can happen if a person is about to fall off a chair or if the sitting position is very asymmetrical. Thus, two leaning side situations were measured. Firstly, the values for a person lean to the right are presented in Figure 12 .

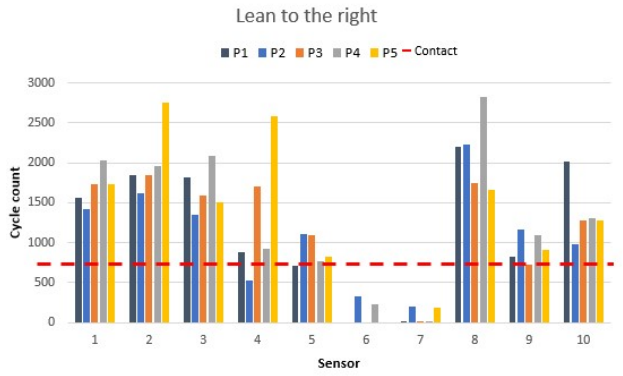

Fig. 12: Right leaning sensor values as shown in Figure 6f.

When the participants leaned to the right side, sensors 6 and 7 were deactivated; their values go close to 0 cycle count. The values of sensor 9 (mid backrest side sensor) increased due to the body lean to the right. The increase observed is from 200 to 500 cycle count for each participant. Sensor 8 displayed an increase in the value between 200-500 cycle count, which is the consequence of all the pressure lying on the right side of the chair. In participant 4, sensor 8 displayed the biggest increase, which means 2500 cycle count more, because the participant was unable to push their back close enough to the sensor when in the ergonomic position.

Following the procedure, the participants leaned to the left, and sensor responses were the opposite of the previous position. The sensor values for left leaning are shown in Figure 13.

Sensors 8 and 9 are deactivated due to the movement to the left. Sensor 6 and 7, which were off previously, now are activated. Some of the data taken show that sensor 10 experiences some value decrease, and in the meantime, sensor 5 increases the values due to the leaning, which results in all the participant having values higher than 1000 (contact detection). Seat sensors are not experiencing value changes during the movement of the leaning to the sides. For both leaning situations, though, detection is demonstrated. Leaning detection could be more useful in other smart chair applications, such as a wheelchair, where people with mobility disorders need to be monitored to avoid harm. Another application could be the detection of hyperactivity in kids. In these potential applications, feedback is essential for the smart chair to be useful.

F. Sitting on the edge and leaning the body back

This position is usually adopted by tired workers in an office situation. In this position, the lower back is detached from the backrest and moved forward while the upper back stays in contact with the chair. The back is thus not fully supported by the chair's backrest and remains curved. These characteristics are observed in Figure 14 .

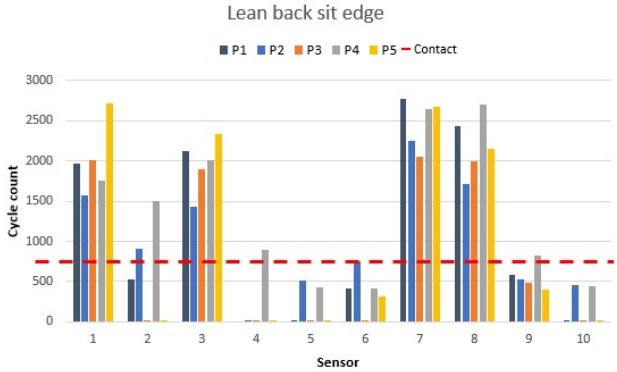

Fig. 14: Sitting on the edge and leaning the body back sensor values as shown in Figure 6h.

Sensors 1 and 3 from the seat and 7 and 8 from the backrest are the ones activated during this position. Sensor 2 is detecting body weight over it in some cases due to the position taken by the person during the measurement. A clear pattern is observed when this position is taken.

The values of 1, 3, 7 and 8 are at their higher points, which indicates higher pressure on them than in previous positions.

Furthermore, the value difference between the sensors activated and the rest of the sensors is noticeable. The rest of the sensors show values from 0 to 500 cycle count, which correspond to sensor deactivation or body detection close by but not in contact.

From the results obtained, it is demonstrated that the chair permits differentiation between different sitting positions and different levels of contact indicating proximity, contact, close contact or high pressure on contact. The chair provides a tool to correct the position, to detect an asymmetrical gesture or monitor movement behaviour. The information obtained by the smart chair may be useful in prevention of low back pain or musculoskeletal disorders while sitting for a long time. The programming of the microcontroller at this stage focuses on the ability to notify the user to change the sitting position or to stand up and move, in order to prevent musculoskeletal disorders.

Future work would be the complete integration of the sensor into the upholstery of the chair and different kinds of integration depending on the applications, such as wheelchairs or school chairs. Also, the alarm system needs to be studied according to the ergonomics studies. Maximum sitting time, detecting the incorrect sitting position and correcting it, and notifying the user to stand up and move should be improved in the future. The measurement tests should be accompanied by video or images to obtain more precise information for analysis of the sitting positions.

IV. Conclusion

In this paper we presented a detailed description of the initial prototype of an office chair with presence capacitive textile sensors (PreCaTex) detecting the user's movement and positioning. The PreCaTex sensor can identify four levels of proximity and contact of the body; two of them are close contact detection. Real-time data provide perfect information to the microcontroller to prepare warnings for the user, such as movement need or poor position taken. It is essential to note the sensors' low-cost and relatively effortless fabrication with a commercial embroidery machine. However, as this study was to proof of concept and tests were made in laboratory conditions, we still have many unanswered questions about the chair's viability in real-life-use. Nevertheless, after more thorough investigation of the sensors' features, we might be able to adopt this fabrication method to create applications to serve, for example, people with disabilities or impairments. If a similar kind of covering were placed on a wheelchair, it could help identify those body parts that are easily exposed to redundant pressure and insidiously cause skin traumas and discomfort.

V. Acknowledgment

This work was supported by The Academy of Finland (decisions 332168 and 337861) and The Ministry of Education and Culture, Finland (Tekos project). Also it is supported by the *Agencia Estatal de Investigación* under the project PID2021-124288OB-I00 and AGAURUPC(2020 FI-B 00028).

References

[1] R. Baker, P. Coenen, E. Howie, A. Williamson, and L. Straker, "The short term musculoskeletal and cognitive effects of prolonged sitting during office computer work," *International Journal of Environmental Research and Public Health*, vol. 15, no. 8, 2018, ISSN: 16604601. DOI: 10.3390/ijerph15081678.

[2] S. Celik, K. Celik, E. Dirimese, N. Tasdemir, T. Arik, and Büyükkara, "Determinación del dolor en el sistema musculoesquelético informado por oficinistas y los factores de riesgo del dolor," *International Journal of Occupational Medicine and Environmental Health*, vol. 31, no. 1, pp. 91–111, 2018, ISSN: 1896494X.

[3] L. Dimberg, J. G. Laestadius, S. Ross, and I. Dimberg, "Send Orders for Reprints to reprints@benthamscience.ae The Changing Face of Office Ergonomics," *The Ergonomics Open Journal*, vol. 8, pp. 38–56, 2015. [Online]. Available: https://benthamopen.com/contents/pdf/TOERGJ/TOERGJ-8-38.pdf.

[4] M. M. Robertson and M. J. O'Neill, "Reducing musculoskeletal discomfort: Effects of an office ergonomics workplace and training intervention," *International Journal of Occupational Safety and Ergonomics*, vol. 9, no. 4, pp. 491–502, 2003, ISSN: 10803548. DOI: 10.1080/10803548.2003.11076585.

[5] S. Arora, K. Subhash, K. Tanna, and D. Girish, "Are You Sitting Correctly? What Research Say's: A Review Paper 1," vol. 514, no. 4, pp. 132–140, 2021.

[6] R. K. Lueder, "Seat comfort: a review of the construct in the office environment.," eng, *Human factors*, vol. 25, no. 6, pp. 701–711, 1983, ISSN: 0018-7208 (Print). DOI: 10.1177/001872088302500607.

[7] J. H. van Dieën, M. P. de Looze, and V Hermans, "Effects of dynamic office chairs on trunk kinematics, trunk extensor EMG and spinal shrinkage.," eng, *Ergonomics*, vol. 44, no. 7, pp. 739–750, 2001, ISSN: 0014-0139 (Print). DOI: 10.1080/00140130120297.

[8] J. Pynt, J. Higgs, and M. Mackey, "Seeking the optimal posture of the seated lumbar spine," *https://doi.org/10.1080/09593980151143228*, vol. 17, no. 1, 2009, ISSN: 09593985. DOI: 10.1080/09593980151143228. [Online]. Available: https://www.tandfonline.com/doi/abs/10.1080/09593980151143228.

[9] *Office Ergonomics - Environment, Health and Safety*. [Online]. Available: https://ehs.unc.edu/workplace-safety/ergonomics/office/ (visited on 07/26/2022).

[10] A. Schrempf, G. Schossleitner, T. Minarik, M. Haller, and S. Gross, *PostureCare - Towards a novel system for posture monitoring and guidance*. IFAC, 2011, vol. 44, pp. 593–598, ISBN: 9783902661937. DOI: 10.3182/20110828-6-IT-1002.02987. [Online]. Available: http://dx.doi.org/10.3182/20110828-6-IT-1002.02987.

[11] M. Huang, I. Gibson, and R. Yang, "Smart Chair for Monitoring of Sitting Behavior," *KnE Engineering*, vol. 2, no. 2, p. 274, 2017. DOI: 10.18502/keg.v2i2.626.

[12] R. H. Goossens, M. P. Netten, and B. Van Der Doelen, "An office chair to influence the sitting behavior of office workers," *Work*, vol. 41, no. SUPPL.1, pp. 2086–2088, 2012, ISSN: 10519815. DOI: 10.3233/WOR-2012-0435-2086.

[13] S. Nasiri and M. R. Khosravani, "Progress and challenges in fabrication of wearable sensors for health monitoring," *Sensors and Actuators, A: Physical*, vol. 312, p. 112 105, 2020, ISSN: 09244247. DOI: 10.1016/j.sna.2020.112105. [Online]. Available: https://doi.org/10.1016/j.sna.2020.112105.

[14] C. M. Yang, T. L. Yang, C. C. Wu, *et al.*, "Textile-based capacitive sensor for a wireless wearable breath monitoring system," *Digest of Technical Papers - IEEE International Conference on Consumer Electronics*, pp. 232–233, 2014, ISSN: 0747668X. DOI: 10.1109/ICCE.2014.6775985.

[15] A. Bhide, S. Muthukumar, and S. Prasad, "CLASP (Continuous lifestyle awareness through sweat platform): A novel sensor for simultaneous detection of alcohol and glucose from passive perspired sweat," *Biosensors and Bioelectronics*, vol. 117, no. June, pp. 537–545, 2018, ISSN: 18734235. DOI: 10.1016/j.bios.2018.06.065. [Online]. Available: https://doi.org/10.1016/j.bios.2018.06.065.

[16] M. Martinez-Estrada, I. Gil, and R. Fernandez-Garcia, "A Smart Textile System to Detect Urine Leakage," *IEEE Sensors Journal*, vol. 21, no. 23, pp. 26 234–26 242, 2021, ISSN: 15581748. DOI: 10.1109/JSEN.2021.3080824.

[17] J. Tabor, T. Agcayazi, A. Fleming, *et al.*, "Textile-Based Pressure Sensors for Monitoring Prosthetic-Socket Interfaces," *IEEE Sensors Journal*, vol. 21, no. 7, pp. 9413–9422, 2021, ISSN: 15581748. DOI: 10.1109/JSEN.2021.3053434.

[18] Shieldex-Statex, "Shieldex 110/34 dtex 2-ply conductive yarn," *Technical data sheet*, vol. 123, no. May, pp. 98–99, 2005.

[19] Bekinox-Bekaert, "Highly electrically conductive spun yarn for anti-static textiles," *Technical data sheet*,

[20] B. Prueksanusak, P. Rujivipatand, and K. Wongpatikaseree, "An Ergonomic Chair with Internet of Thing Technology using SVM," *TIMES-iCON 2019 - 2019 4th Technology Innovation Management and Engineering Science International Conference*, 2019. DOI: 10.1109/TIMES-iCON47539.2019.9024488.

[21] H. Jeong and W. Park, "Developing and Evaluating a Mixed Sensor Smart Chair System for Real-Time Posture Classification: Combining Pressure and Distance Sensors," *IEEE Journal of Biomedical and Health Informatics*, vol. 25, no. 5, pp. 1805–1813, 2021, ISSN: 21682208. DOI: 10.1109/JBHI.2020.3030096.

[22] J. Liu, "Development of an Intelligent Office Chair by Combining Vibrotactile and Visual Feedbacks," *Journal of Physics: Conference Series*, vol. 1877, no. 1, pp. 5–10, 2021, ISSN: 17426596. DOI: 10.1088/1742-6596/1877/1/012015.

[23] A. R. Anwary, M. Vassallo, and H. Bouchachia, "Monitoring of Prolonged and Asymmetrical Posture to Improve Sitting Behavior," *2020 International Conference on Data Analytics for Business and Industry: Way Towards a Sustainable Economy, ICDABI 2020*, 2020. DOI: 10.1109/ICDABI51230.2020.9325598.

[24] M. R. H. V. Beeresha R S, A M Khan, "Design and Optimization of Interdigited Capacitors," *International Journal of Research in Engineering and Technology*, vol. 05, no. 21, pp. 273–277, 1994.

Martínez-Estrada. Marc received the B.Eng degree in Industrial Technologies and M. degree in Industrial Engineering specialised on Textile technologies from the Universitat Politecnica de Catalunya(ESEIAAT), Terrassa(Barcelona) in 2016 and 2018. In 2018 he starts the Ph.D. degree in Electronic Engineering at Universitat Politecnica de Catalunya, which is focused on Smart textiles. From 2015 to 2016 he worked for FirstVision, as a product designer in charge of the design and development of the product, where he starts to introduce himself in the smart textile technology. From 2018 to 2020, he was part-time Assistant Professor in electronics with the Department of Electronics Engineering at Universitat Politecnica de Catalunya. At 2020 he gets a grant for the recruitment of new research staff from AGAUR (FI-2020) and being contracted by the university as a full-time researcher. Mr. Martinez-Estrada is author of 10 papers in international journals and conferences. He is starting his career as a researcher and focus on his Ph.D. in capacitive sensors integrated on textile substrates that can be helpful for healthcare applications.

Vuohijoki. Tiina received a Bachelor's degree in Nursing and Health Care and specialisation of Public Health Nursing at the Saimaa University of Applied Sciences in 2011. She has taken the degree of Master of Health Care in Degree Programme in Welfare Technology in Satakunta University of Applied Sciences in 2021. Currently she is full-time researcher in Tampere University and proceeds her Ph.D. studies focusing on supporting participation and social inclusion through intelligent clothing. Her personal interests are in agile development and interdisciplinary project management.

Poberznik. Anja received a Bachelor's degree in General linguistics and Slovakian language and literature at the University of Ljubljana in 2012, and a Bachelor degree in Physiotherapy at Satakunta University of Applied Sciences in 2018. Since 2018 she has been working as a researcher at RD centre RoboAI at the Satakunta University of Applied Sciences in Pori, Finland. Her main areas of interests are exoskeleton research, welfare technology usability and user experience studies.

Shaikh, Asif received B.E degree in mechanical engineering from Dr. Bamu University, Aurangabad, in 2014 and the M.Tech degree in robotics engineering with major in robotics and automation from Mumbai University, Mumbai, India, in 2018.He is currently pursuing Ph.D. degree in smart clothing at Tampere University, Tampere, Finland. His research areas includes human-technology interaction based on textiles, RFID system, wearables, IoT and RFID antennas.

Virkki, Johanna Dr. Virkki is an Associate Professor at the Faculty of Information Technology and Communication Sciences at Tampere University, Finland, where she leads Intelligent Clothing Research Group. Her current research interests include augmentative and alternative communication, smart clothing, and radio frequency identification.

Gil.Ignacio was born in 1978 in Barcelona, Spain. He received degrees in physics and electronics engineering in 2000 and 2003, and then his PhD in 2007 from the Universitat Autònoma de Barcelona, Spain. From 2003 to 2008 he was assistant professor in electronics and a researcher with the RF-Microwave Group in the Electronic Engineering Department, Universitat Autonòma de Barcelona, Spain. From 2006 to 2008 he worked for EPSON Europe Electronics GmbH where he developed high-performance integrated RF CMOS circuits, transceivers and system design. In 2008 he joined the Electronic Engineering Department, Universitat Politècnica de Catalunya (UPC), Spain, as lecturer and researcher. Since 2011 he is associate professor at UPC. Since 2012 he is also a collaborator at Universitat Oberta de Catalunya (UOC), Spain.

He has been involved in 12 research projects (3 as principal researcher) in different research activities including passive and active RF and microwave devices and circuits, metamaterials, EMC and smart textile electronics. From 2012-2014 he served as Chairman of the Spanish IEEE EMC Chapter. In 2017 he was academic visitor at Loughborough University (UK) in the Wireless Communications Research Group. Since 2019 he is Deputy Director of International Relations at ESEIAAT (UPC).

Dr. Gil is co-author of more than 150 scientific publications and 17 patents. He has been awarded the Duran Farell de Investigación Tecnológica (2006) and the patent award from SEIKO EPSON Corporation (2010). Dr. Gil has been visiting professor in different Universities: New Jersey Institute of Technology (USA), Limerick University (Ireland), Loughborough University (UK), Shaoxing University (China) and Polytechnic University of Tirana (Albania).

Fernández-García, Raúl. received the B.Eng. degree in telecommunications and M.Eng degree in electronics from the Universitat Politecnica de Catalunya, Barcelona, in 1997 and 1999, respectively. In 2007 he received the Ph.D. degree from the Universitat Autonoma de Barcelona. From 1998 to 2001, he worked for Sony Spain, as Radiofrequency Engineer, where he developed analog and digital TV tuners. From 2001 to 2007, he was part-time Assistant Professor in electronics with the Department of Electronics Engineering, Universitat Autonoma de Barcelona. Funded by the European Marie Curie Program, he worked on devices and circuits reliability at IMEC (Belgium) between 2005 and 2006. From 2008 to 2011, he was full-time Assistant Professor in the Department of Electronics Engineering, Universitat Politecnica de Catalunya. At present he is Associate Professor at the same department.

Dr. Fernandez-Garcia is author or a co-author of more than 110 papers in international journals and conferences. He was the recipient of Best Paper Awards at IPFA 2007. His current scientific interest is focused on wearable sensor development for sport and health applications.